



## Faculté de Pharmacie

Ecole Doctorale en Sciences Pharmaceutiques

### **Stabilization and development of sustained-release formulations of protein/antibody for subcutaneous delivery**

**Sarah Marquette**

Thèse présentée en vue de l'obtention du grade de Docteur en Sciences  
Biomédicales et Pharmaceutiques

**Promoteur(s) et co-promoteur(s) éventuel(s) :**

Prof. Karim AMIGHI (Promoteur)  
Prof. Ass. Jonathan GOOLE (Co-promoteur)

**Composition du jury:**

Prof. Jean-Michel KAUFFMANN (Président),  
Prof. Ingrid LANGER  
Prof. Bieke DEJAEGER  
Prof. David VERMIJLEN  
Prof. Elias FATTAL (Université de Paris Sud)  
Prof. Rita VANBEVER (Université Catholique de Louvain)

Au terme de ce travail, je souhaite adresser mes sincères remerciements à toutes les personnes qui ont contribué à sa réalisation et ont permis par leur soutien et leurs conseils, de le mener à bien.

Je tiens à remercier UCB-Pharma pour m'avoir permis de réaliser ce projet et plus particulièrement Domenico Fanara et Laurence Denis.

Je remercie aussi tous mes collègues et plus spécialement Katia, Michaël, Jan et Claude pour leur aide et leur bonne humeur.

Je remercie particulièrement Monsieur le Professeur Karim Amighi de m'avoir accueillie comme doctorante dans son laboratoire.

Je remercie également très chaleureusement Jonathan Goole, Professeur assistant et Ingrid Langers, Professeur de pharmacologie, pour m'avoir épaulé tout au long de ce travail.

Ce travail n'aurait pu voir le jour sans la participation financière de la région wallonne, que je tiens à remercier vivement.

Mes sincères remerciements s'adressent à Mesdames et Messieurs les Membres du Comité d'accompagnement ainsi qu'à Mesdames et Messieurs les Membres du Jury qui me font l'honneur de juger ce mémoire.

Je remercie mes amis et ma famille pour leur soutien constant.

Finalement, je remercie mon mari, Valéry pour son soutien et son écoute ainsi que mes grandes filles Margot et Manon qui sont pour moi un encouragement constant.

Sarah Marquette

---

**Table of Contents**

LIST OF ABBREVIATIONS.....	7
ABSTRACT.....	10
RÉSUMÉ.....	12
INTRODUCTION PART.....	14
1 INTRODUCTION.....	14
2 OBJECTIVE OF THE PROJECT.....	17
3 CHALLENGES OF THE PROJECT.....	18
BIBLIOGRAPHIC PART.....	19
1 ANTIBODY STRUCTURE.....	19
1.1 The structure of a typical antibody molecule.....	19
1.2 Anti-TNF alpha antibody.....	22
2 STABILIZATION OF PROTEINS AND ANTIBODIES.....	23
2.1 Antibody instability.....	23
2.2 Antibody stabilization and formulations.....	31
3 CONTROLLED RELEASE FORMULATIONS.....	37
3.1 Controlled-delivery/depot technologies.....	37
MATERIALS & METHODS.....	48
1 MATERIALS.....	48
1.1 General description of materials.....	48
1.2 Drug model molecules.....	50
1.3 Poly (lactide-co-glycolide) copolymer.....	50
2 MANUFACTURING METHODS.....	53
2.1 Preparation of antibody solutions.....	53
2.2 Spray-drying process.....	53
2.3 Preparation techniques of the drug-loaded PLGA MS.....	56
2.4 Preparation of the placebo PLGA microspheres.....	60
3 ANALYTICAL METHODS.....	60
3.1 Antibody characterization.....	60
3.2 Encapsulation efficiency and drug loading evaluation.....	67
3.3 Dissolution study.....	67
3.4 Particle size and morphology characterization.....	68
3.5 Residual moisture content.....	69
3.6 Residual solvent content.....	69
3.7 Thermogravimetric analysis.....	70
3.8 Differential scanning calorimetry.....	70
3.9 X-ray powder diffraction (XRPD).....	71

3.10	Gel permeation chromatography.....	71
3.11	Freeze-drying microscopy .....	71
3.12	Syringeability / injectability study .....	72
3.13	Statistical analysis.....	72
4	<i>IN VIVO</i> EVALUATIONS .....	73
4.1	Preliminary pK study on CDP571 solutions (IV).....	73
4.2	pK study on CDP571 loaded PLGA MS (SC).....	73
4.3	pK analysis.....	74
4.4	Histological study .....	75
	EXPERIMENTAL APPROACH.....	76
	EXPERIMENTAL PART.....	79
	SELECTION OF THE TYPE OF ENCAPSULATION PROCESS SUITABLE FOR ANTIBODY .....	80
1	INTRODUCTION .....	80
2	RESULTS AND DISCUSSION .....	80
2.1	Stabilization of IgG solution formulation.....	80
2.2	W/o/w versus s/o/w to be selected as the encapsulation processes - selection of the organic solvent.....	86
2.3	Encapsulation method (s/o/w versus s/o spray-drying) .....	89
3	CONCLUSION.....	93
	DEVELOPMENT OF A SUITABLE SPRAY-DRYING PROCESS FOR THE PRODUCTION OF SOLID ANTIBODY MICROPARTICLES FOR THE SUBSEQUENT S/O/W ENCAPSULATION PROCESS (IMMUNOGLOBULIN G AS MODEL MOLECULE) .....	94
1	INTRODUCTION .....	94
2	STATISTICAL MODELING OF THE SPRAY-DRYING PROCESS.....	94
2.1	Introduction.....	94
2.2	Results and discussion .....	96
2.3	Conclusion: .....	100
	ENCAPSULATION OF IMMUNOGLOBULIN G, AS MODEL MOLECULE, BY SOLID- IN-OIL-IN-WATER: EFFECT OF PROCESS PARAMETERS ON MICROSPHERES PROPERTIES * .....	102
1	INTRODUCTION .....	102
2	RESULTS AND DISCUSSION.....	104
2.1	Influence of the investigated parameters on particle size distribution and morphology of the MS .....	104
2.2	Influence of the investigated parameters on the actual drug loading of the MS..	107
2.3	Influence of the investigated parameters on the EE% of the MS .....	109
2.4	Influence of the investigated parameters on the burst effect of microspheres.....	111

---

2.5	Influence of the investigated parameters on IgG stability during the encapsulation process and dissolution .....	114
2.6	Factor selection .....	116
3	CONCLUSION.....	117
APPLICATION AND EVALUATION OF THE SPRAY-DRYING PROCESS TO A FULL LENGTH ANTIBODY (ANTI-TNF ALPHA) IN ORDER TO PREPARE SUBSEQUENT ENCAPSULATION .....		
1	INTRODUCTION .....	118
2	SPRAY-DRIED FORMULATION DEVELOPMENT FOR ANTI-TNF-ALPHA ANTIBODY .....	118
2.1	Results and discussion .....	119
3	CONCLUSION.....	126
DEVELOPMENT OF FULL LENGTH ANTIBODY (ANTI-TNF ALPHA) LOADED PLGA MICROSPHERES USING THE SOLID-IN-OIL-IN-WATER ENCAPSULATION METHOD .....		
1	INTRODUCTION .....	127
2	SELECTIONS OF FORMULATIONS .....	127
2.1	Results and discussion .....	127
2.2	CONCLUSION.....	135
3	SELECTION OF PLGA POLYMER.....	135
3.1	Results and discussion .....	136
3.2	Conclusion .....	144
4	EVALUATION OF ADDITION OF BASIC ADDITIVES.....	144
4.1	Results and discussion .....	146
4.2	Conclusion .....	152
5	DEVELOPMENT OF A FREEZE-DRIED PRODUCT .....	152
5.1	Results and discussion .....	154
5.2	CONCLUSION.....	167
STABILITY STUDY OF A FULL-LENGTH ANTIBODY (ANTI-TNF ALPHA) LOADED PLGA MICROSPHERES * .....		
1	INTRODUCTION .....	169
2	RESULTS AND DISCUSSION .....	169
2.1	Particle size and morphology of the MS.....	169
2.2	Polymorphic state – glass transition temperature and enthalpy of relaxation .....	174
2.3	Drug content.....	176
2.4	HMWS/LMWS and activity evaluation.....	177
2.5	Dissolution test.....	181
3	CONCLUSION.....	183
PK STUDY IN RATS OF FULL-LENGTH ANTIBODY (ANTI-TNF ALPHA) LOADED PLGA MICROSPHERES.....		
		184

Table of contents

---

1	INTRODUCTION .....	184
2	RESULTS AND DISCUSSION .....	184
2.1	pK data of the anti-TNF alpha MAb <i>in vivo</i> studies .....	184
2.2	Anti-TNF alpha activity evaluation .....	188
2.3	Histological studies.....	191
3	CONCLUSION.....	192
	GENERAL CONCLUSION AND PERSPECTIVES .....	194
	REFERENCES .....	198
	APPENDIX.....	208

---

**LIST OF ABBREVIATIONS**

(M)Ab(s)	(Monoclonal) antibody (antibodies)
ANOVA	Analysis of variance
Asp	Aspartic acid
ATR	Attenuated total reflectance
AUC	Area under the concentration - time curve
BCA	Bicinchonimic acid
BS	buffered saline
CL	Elimination of the drug from the body expressed as the volume of blood cleared of drug per unit time
$C_{\max}$	maximum plasma concentration
DDS	Drug delivery system
DLS	Dynamic light scattering
DoE	Design of experiment
DSC	Differential scanning calorimetry
e.g.	Exempli gratia (“for example”)
$EC_{50}$	Half maximum effective concentration
EE%	Encapsulation efficiency
ELISA	Enzyme – linked immunosorbent assay
EMA	European Medical Agency
EtAc	Ethyl acetate
Fab	Fragment antigen-binding
Fc	Crystallizable fragment
FDA	Food and Drug Administration

---

FDM	Freeze – drying microscope
FT-IR	Fourier – transform infrared spectroscopy
G	Gauge
GPC	Gel permeation chromatography
HMWS	High molecular weight species
IgG	Immunoglobulin G
Inlet T°	inlet temperature
IV	Intravenous
kDa	Kilo Dalton
LMWS	Low molecular weight species
MC	Methylene chloride
MS	Microsphere(s)
Mw	Molecular weight
NBE	New biological entity
Outlet T°	outlet temperature
PB	Phosphate buffer
PEG	Polyethylene glycol
PGA	poly-glycolide
pI	Isoelectric point
pK	Pharmacokinetic
PLA	poly-lactide acid
PLGA	Poly(D,L-lactide-co-glycolide acid)
PVA	Polyvinyl alcohol
PVP	Polyvinyl pyrrolidone

---

RH	Relative humidity
RPM	Revolution per minute
RT	Room temperature
s	Standard deviation
s/o (/w)	Solid-in-oil (-in-water)
SAX	Strong anion exchange chromatography
SC	Subcutaneous
SD	spray-dried
SEC	Size exclusion (high-performance liquid) chromatography
SEM	Scanning electron microscopy
$T_{1/2}$	Half-life
$T_c$	Collapse temperature
$T_{eut}$	Eutectic temperature
$T_g$	Glass transition temperature
$T_m$	Melting temperature
$T_{max}$	Maximum time to peak concentration
TNF	Tumor necrosis factor
w/o/w	water-in-oil-in-water
$\eta$	viscosity

---

## ABSTRACT

This project aimed at developing a drug delivery system (DDS) able to enhance the stability and residence time *in vivo* of antibodies (Abs). The system will deliver drug by the subcutaneous route (SC), while ensuring accurate control of the drug release and the resulting plasmatic level. This technology platform will allow to reduce frequency of injection, potentially decrease side effects and maintain high concentration of Abs which will improve life of patient having chronic disease such as autoimmune and inflammatory disease.

Biodegradable synthetic polymer-based formulations (polylactide-co-glycolide (PLGA)) were selected as carriers for encapsulated Abs. This was because they offer good protection for the Abs and allow sustained release of the Abs for a controlled period of time. After the evaluation of different encapsulation methods such as the water-oil-in-water (w/o/w) and the solid-in-oil-in-water (s/o/w) processes, the encapsulation of the Ab in solid state (s/o/w) appeared to be more appropriate for producing Ab-loaded PLGA microspheres (MS). It allowed us to maintain the Ab in a monomeric conformation and to avoid the formation of insoluble aggregates mainly present at the water/oil interface. The first part of the project was the optimization of both the method for producing the Ab solid particles (spray-drying process) and the encapsulation of these Ab solid particles into the polymeric MS (s/o/w process) by design of experiment (DoE). These optimizations were carried out using a bovine polyclonal immunoglobulin G (IgG) as model molecule. In further optimization of the spray-drying process by (DoE), aqueous Ab solutions were spray-dried using a mini Spray-Dryer assembly with a 0.7 mm spray nozzle. In accordance with the particle size ( $d(0.5) \sim 5 \mu\text{m}$ ), the stability (no loss of monomer measured by size exclusion chromatography (SEC) and the yield of the spray-drying process ( $> 60\% \text{ w/w}$ ), the process parameters were set of follow: 3 mL/min as liquid feed flow rate,  $130^\circ\text{C} / 75^\circ\text{C}$  as inlet temperature (inlet  $T^\circ$ ) / outlet temperature (outlet  $T^\circ$ ), 800 L/h as atomization flow rate and  $30 \text{ m}^3/\text{h}$  as drying air flow rate. For the s/o/w, the methylene chloride (MC) commonly used for an encapsulation process was replaced by ethyl acetate (EtAc), which was considered as a more suitable organic solvent in terms of both environmental and human safety. The effects of several processes and formulation factors were evaluated on IgG:PLGA MS properties such as: particle size distribution, drug loading, IgG stability, and encapsulation efficiency (EE%). Several formulations and processing parameters were also statistically identified as critical to get

reproducible process (e.g. the PLGA concentration, the volume of the external phase, the emulsification rate, and the quantity of IgG microparticles). The optimized encapsulation method of the IgG has shown a drug loading of up to 6 % (w/w) and an encapsulation efficiency of up to 60 % (w/w) while preserving the integrity of the encapsulated antibody. The produced MS were characterized by a  $d(0.9)$  lower than 110  $\mu\text{m}$  and showed burst effect lower than 50 % (w/w). In the second part of the project, the optimized spray-drying and s/o/w processes developed with the IgG were applied to a humanized anti-tumor necrosis factor (TNF) alpha MAb to confirm the preservation of the MAb activity during these processes. The selected s/o/w method allowed us to produce MAb-loaded PLGA MS with an appropriate release profile up to 6 weeks and MAb stability. In order to maintain the Abs' activity, both during encapsulation and dissolution, the addition of a stabilizer such as trehalose appeared to be crucial, as did the selection of the PLGA. It was demonstrated that the use of a PLGA characterized by a 75:25 lactide:glycolide (e.g. Resomer<sup>®</sup> RG755S) ratio decreased the formation of low molecular weight species during dissolution, which led to preserve Abs activity through its release from the delivery system. Furthermore, the release profile was adjusted according to the type of polymer and its concentration. E.g. 10 % w/v RG755S allowed Ab MS with a release time of 6 weeks to be obtained. The optimization of both the formulation and the encapsulation process allowed maximum 13 % w/w Ab-loaded MS to be produced. It was demonstrated that the Ab-loaded PLGA MS were stable when stored at 5°C for up to 12 weeks and that the selection of the appropriate type of PLGA was critical to assuring the stability of the system. The better stability observed when using a PLGA characterized by a 75:25 lactide:glycolide ratio was attributed to its slower degradation rate. Finally, the sustained release of Ab from the developed MS and the preservation of its activity was confirmed *in vivo* in a pharmacokinetic (pK) study realized in rats. In conclusion, the application of the concept of entrapment into a polymer matrix for stabilization and sustained release of biological compounds was demonstrated through this work.

---

## RÉSUMÉ

Ce projet a pour but de développer un système de délivrance de médicament capable d'augmenter la stabilité et le temps de résidence *in vivo* des anticorps. Ce système sera administré par voie sous-cutanée et permettra un control précis de la libération du produit et de son niveau plasmatique. Cette plateforme technologique nous permettra de réduire la fréquence d'injection, de réduire potentiellement les effets secondaires et de maintenir des concentrations élevées en anticorps tout en améliorant la vie des patients atteints de maladies chroniques auto-immunes ou inflammatoires. Les formulations à base de polymères synthétiques, biodégradables (PLGA) ont été sélectionnés comme véhicules pour encapsuler les anticorps. Ils offrent en effet une bonne protection pour les anticorps and permettent une libération contrôlée de ceux-ci pendant une période définie. Après l'évaluation de différents méthodes d'encapsulation tels que les procédés d'eau-dans-huile-dans-eau (w/o/w) et solide-dans-huile-dans-eau (s/o/w), l'encapsulation des anticorps sous forme solide apparaissait plus appropriée pour produire des microsphères de polymère chargées en anticorps. Cette technique nous permettait de maintenir l'anticorps sous sa forme monomérique et d'éviter la formation d'agrégats insolubles qui apparaissaient principalement à l'interface eau/huile. La première partie du projet a été d'optimiser à la fois la méthode nous permettant d'obtenir les anticorps sous forme de particules solides (spray-drying) et la méthode d'encapsulation de ces particules d'anticorps dans les microsphères de polymères. Cela a été réalisé par des plans d'expérience en utilisant une IgG bovine polyclonale comme molécule modèle. Durant l'optimisation du procédé de spray-drying, les solutions aqueuses d'anticorps ont été atomisées en utilisant le mini Spray-Dryer assemblé avec une buse de pulvérisation d'un diamètre de 0.7 mm. En accord avec la taille particulaire ( $d(0.5) \sim 5 \mu\text{m}$ ), la stabilité (absence de perte en monomère mesurée par chromatographie d'exclusion de taille et le rendement d'atomisation ( $> 60 \% \text{ w/w}$ ), les paramètres d'atomisation ont été fixés: 3 mL/min pour le débit de liquide, 130°C /75°C pour la température d'entrée / température de sortie, 800 L/h pour le débit d'air d'atomisation et 30 m<sup>3</sup>/h pour le débit d'air de séchage. Pour le s/o/w, le dichlorométhane communément utilisé dans les procédés d'encapsulation a été remplacé par l'acétate d'éthyle qui est considéré comme un meilleure solvant organique en terme d'environnement et de sécurité. Les effets de plusieurs paramètres de fabrication ou de formulation ont été évalués sur les propriétés des microsphères polymériques

d'anticorps (distribution de taille particulière, taux de charge en anticorps, stabilité de l'anticorps et efficacité d'encapsulation). Plusieurs paramètres de fabrication et de formulation ont été statistiquement identifiés comme critiques pour obtenir un procédé reproductible (par exemple. La concentration en PLGA, le volume de phase externe, la vitesse d'émulsification et la quantité d'anticorps). La méthode d'encapsulation ainsi optimisée permettait d'obtenir un taux de charge jusqu'à 6% (w/w) avec une efficacité d'encapsulation jusqu'à 60 % (w/w) tout en préservant l'intégrité de l'anticorps encapsulé. Les microsphères produites étaient caractérisées par un  $d(0.9)$  inférieur à 110  $\mu\text{m}$  et montraient une libération après 24 h inférieure à 50 % (w/w). Dans la seconde partie du projet, les procédés d'atomisation et d'encapsulation développés avec l'IgG ont été appliqués à un anticorps monoclonal anti-TNF alpha humanisé pour confirmer la conservation de l'activité de l'anticorps pendant ces procédés. La méthode s/o/w sélectionnée permettait de produire des microsphères de PLGA chargées en anticorps avec un profil de libération jusqu'à 6 semaines et un maintien de la stabilité de l'actif. Afin de maintenir l'activité de l'anticorps, à la fois pendant le procédé d'encapsulation et pendant la libération, l'ajout d'un stabilisant tel que le tréhalose est apparu crucial ainsi que le choix du type de PLGA. Il a été démontré que l'utilisation du PLGA caractérisé par un ratio lactide :glycolide de 75 :25 (par exemple, Resomer<sup>®</sup> RG755S) diminuait la formation d'espèces de faible poids moléculaire pendant la dissolution. Cela contribuait à préserver l'activité de l'anticorps durant la libération à partir des microsphères. De plus, le profil de libération était modulé en fonction du type de polymère et de sa concentration. Par exemple, l'utilisation d'une solution à 10 % w/v RG755S conduisait à la production de microsphères d'anticorps avec un temps de libération sur 6 semaines. L'optimisation de la formulation et du procédé d'encapsulation a permis de produire des microsphères avec des taux de charge en anticorps de maximum 13 % w/w. Il a été démontré que ces microsphères, stockées à 5°C, étaient stables jusqu'à 12 semaines et que la sélection du type de PLGA était critique pour assurer la stabilité du système. La meilleure stabilité a été obtenue en utilisant le PLGA caractérisé par un ratio lactide :glycolide de 75 :25. Cela a été attribué à sa plus faible vitesse de dégradation. Enfin, la libération contrôlée de l'anticorps à partir de ces microsphères et la conservation de son activité ont été confirmées *in vivo* lors d'une étude pharmacocinétique réalisée chez le rat. En conclusion, ce travail a permis de démontrer l'application du concept d' « emprisonnement » des composés biologiques dans des matrices polymériques afin de les stabiliser et contrôler leur libération.

## INTRODUCTION PART

### 1 INTRODUCTION

Currently, peptide-, protein- or Ab-based therapeutics are administered by injection, a painful process associated with low patient compliancy. A number of noninvasive strategies have been explored for the delivery of large molecules, including: inhalation (intranasal and pulmonary), transdermal delivery (across the skin), or the oral route via the gastrointestinal tract (GIT; oral–enteric). However, each of these routes has limitations such as poor bioavailability, risk of concomitant pathogen uptake, abnormal lung function with extended use or difficulty of administering a controlled dosage.

Nowadays, the most common method of protein delivery is through the parenteral routes, mainly via intravenous (IV), SC or intramuscular injections. Although parenteral injection of proteins increases their bioavailability effectively, rapid clearance from the bloodstream through renal filtration and proteolysis shortens their half-lives *in vivo*. Therefore, frequent injections are required to maintain the drug concentration within the therapeutic window. This frequent injection often causes patient discomfort, lack of compliancy and increase in cost of treatment due to its requirement for trained medical personnel. These drawbacks prompted the development of sustained-release systems designed to sustain the therapeutic effect(s) *in vivo* [1, 2].

Injectable biotherapeutics could improve the compliancy of the patients through novel formulations or delivery systems. The current industrial strategy for developing improved injectable systems focuses on technologies and formulations that promise to reduce injection frequency and consequently enhance the quality of life of the patient [3].

In addition, the success of a formulation depends on the ability of the protein to keep its native structure and activity during preparation and delivery as well as during shipping and long-term storage of the formulation [4]. During the development of formulations of proteins or Ab-based materials, there is a series of technical challenges for maintaining sufficient stability and sometimes at particularly high concentrations. Therefore, the development of new DDS is essential.

---

The number of therapeutic MAbs which are currently in development has increased dramatically over the past few years. There are 43 therapeutic MAbs approved or in review in both the European Union and the United States of America [5]. Their pharmacological activity is highly specific and commonly leads to minimal side effects. MAbs are now established as targeted therapies for malignancies, transplant rejection, autoimmune and infectious diseases, as well as a range of new indications. However, administration of MAbs carries the risk of immune reactions such as acute anaphylaxis, serum sickness and the generation of antibodies. In addition, there are numerous adverse effects of mAbs that are related to their specific targets, including infections and cancer, autoimmune disease, and organ-specific adverse events such as cardiotoxicity [6]. MAbs may also be conjugated to other therapeutic compounds or radioisotopes to increase the efficacy of a drug to a target site, reducing its potential systemic side effects, or for specific diagnostic purposes, respectively. Nowadays, fewer immunogenic human MAbs are available but they are still prone to a variety of physical and chemical degradation pathways. Nevertheless, MAbs seem to be more stable than other proteins [7, 8]. MAbs are characterized by relatively high molecular weight (Mw) (150 kilo Daltons (kDa)). However, engineered Ab fragments are much smaller (50 kDa) than intact full-length MAb and are characterized by different systemic distribution and plasmatic clearance [9]. Fragmentation of Ab results in altered physiochemical features of the full-size MAbs [10]. Compared to full-size antibodies Fab' fragments present certain advantages, including higher mobility and penetration into tissues inaccessible to full-size MAbs, ability to bind antigen monovalently and lack of fragment crystallizable (Fc) region-mediated functions such as antibody-dependent cell mediated cytotoxicity or complement-dependent cytotoxicity [11]. Antibody fragments may prove easier and less costly to manufacture due to the lack of glycosylation and relatively small size, which permits use of prokaryotic expression systems. The main drawback for the use of Fab's in clinical applications is associated with their short half-life *in vivo*, which is a consequence of no longer having the Fc region (1 day as the typical half-life of Ab fragment to up to several weeks half-life for a full-size Ab (e.g. 21 days for the IgG) [12]. Indeed, the Fc domain serves to both stabilize full-size Ab and allow FcRn-mediated recycling. Several strategies are developed to extend the half-life of fragments, including conjugation to proteins such as PEGylation (PEG = poly-ethylene glycol), which was applied to the FDA approved anti-TNF $\alpha$  Fab, certolizumab pegol (Cimzia<sup>®</sup>).

---

However, biomanufacturing advantages of fragment production may be lost if PEGylation is required because the process can prove expensive and technically challenging.

Pharmaceutical companies have numerous new biological entities (NBE) in the pipeline. Consequently, the route of administration for these new biological drugs is considered as a serious concern for pharmaceutical development. Despite the therapeutic potential of these new molecules, their use could be limited or even abandoned by the fact that they currently cannot be stabilized or be administered with an acceptable half-life. It is specially the case for the Fab' Ab. Issues related to identifying stable formulations, such as high concentration formulations that might reduce the volume of Ab administrations, have arisen in the move from intravenous infusions to the realm of subcutaneous injection strategies [9].

Therefore, the development of a controlled-release stable formulation for the administration of proteins or MAbs, through the subcutaneous route represents an interesting alternative.

Sustained-release technologies focus on slowing the rate of release of the therapeutic protein to maintain a steady plasma drug level in the therapeutic range. These technologies either attempt to manipulate the physical state of the protein, for example, through crystallization, amorphous precipitation or gelation, or utilize polymers or lipids to entrap and slow the release of the protein.

One approach to overcoming potential issues related to undesirable degradation has been the entrapment of these drugs into a carrier system [13]. Encapsulation protects the drugs against degradation *in vitro* and *in vivo*. Different drug delivery systems can be explored, such as MS, hydrogels, liposomes, solid lipid nanoparticles or emulsions.

During this project, polymer-based formulations were selected as carriers for encapsulated MAb. This system should be able to stabilize the drugs *in vivo* as well as during storage, to properly sustain the release of the incorporated MAb and to maintain a suitable therapeutic concentration. It is especially interesting for fragments which present a lower plasmatic half-life than the corresponding full-size Ab.

The developed system is based on biodegradable synthetic polymers offering a good protection for the MAb and allowing a sustained release of the MAb for a controlled period of time. PLGA was preferred as it is already approved for human drug delivery by the US Food and Drug

---

Administration (FDA) and the European Medical Agency (EMA) [14]. IgG was used as a model to validate the concept of the developed formulation because they present high molecular weight and a similar structure to MAbs. Extrapolation to a full-length humanized Ab anti-TNF alpha (CDP571) and a Fab' fragment anti-TNF alpha were investigated further.

## 2 OBJECTIVE OF THE PROJECT

The aim of this project was to stabilize and develop a sustained release formations for biological compounds and more specially for Abs and fragments. Microparticulate polymer-based formulations were selected as the preferred technical approach. The encapsulation method had to maintain the native structure of the biological compound and so preserve its biological activity. On the other hand, the process had to achieve sufficient drug loading ( $> 20\%$  w/w) into the MS to allow administration of the therapeutic doses ( $> 100$  mg/mL). The target release profile had to reach a time greater than that observed with typical biological formulations in solution (i.e.  $> 1$  month). UCB-Pharma would achieve release time to 3 - 6 months if the drug loading content allows it. The dissolution profile of the drug had to demonstrate sustained release. Thus, the effects of peaks and valleys in plasma curves had to be avoided *in vivo* by providing a continuous and regular supply of drug. Finally, the delivery system had to be administered subcutaneously through accepted needles ( $> 22$  gauges (G)).

This project aimed at building a DDS able to enhance the stability and the residence time *in vivo* of MAbs delivered by the subcutaneous route, while ensuring accurate control of the drug release and the resulting plasmatic level. By reducing the number of injections, decreasing the side effects, e.g. by reducing the high peak concentrations of bolus injections, or achieving stable long-term concentrations in the therapeutical interval, this project should make it easier and more convenient to take medication for many chronic disease such as autoimmune and inflammatory diseases, cancer and osteoporosis.

This development project was realized in collaboration with an industrial partner, UCB-Pharma and funded by the Walloon Region. UCB-Pharma has numerous NBE in its growing pipeline. Consequently the administration route for these new biological drugs is considered as a serious concern for the pharmaceutical development. Despite the enormous therapeutic potential of these new molecules, their use could be limited or even abandoned by the fact that they currently

---

cannot be stabilized or be administered with an acceptable half-life. UCB-Pharma and the project partner are therefore willing to explore and develop highly effective formulations with prolonged release properties for some of its new therapeutic molecules. This is considered as a real breakthrough for business development as patient compliance would be dramatically improved, and as it opens new horizons to market sales.

### **3 CHALLENGES OF THE PROJECT**

The proposed strategy for the administration of the MAbs was faced to several challenges and had to meet the following criteria:

- The DDS had to be sufficiently loaded with MAb to achieve the desired dose.
- The DDS had to be biocompatible and biodegradable. They had to be non-cytotoxic, well-tolerated and could not bring about any immunogenic effect.
- The release rate of the MAbs from the DDS had to be appropriate for ensuring the desired drug plasmatic concentration level. This could be achieved by finely tailoring both the polymer properties.
- The DDS had to stabilize the MAb while maintaining its *in vivo* release for at least one month with minimal burst effect.
- The manufacturing yields had to be high enough for economic viability.
- The degradation products of the polymer should not affect the stability of the protein nor induce any *in vivo* toxicity.
- The degradation of the drug had to be limited in the final product and during the formulation process.

The main challenge was to develop a robust sustained release formulation which can provide a platform for a large number of MAb (or Fragment).

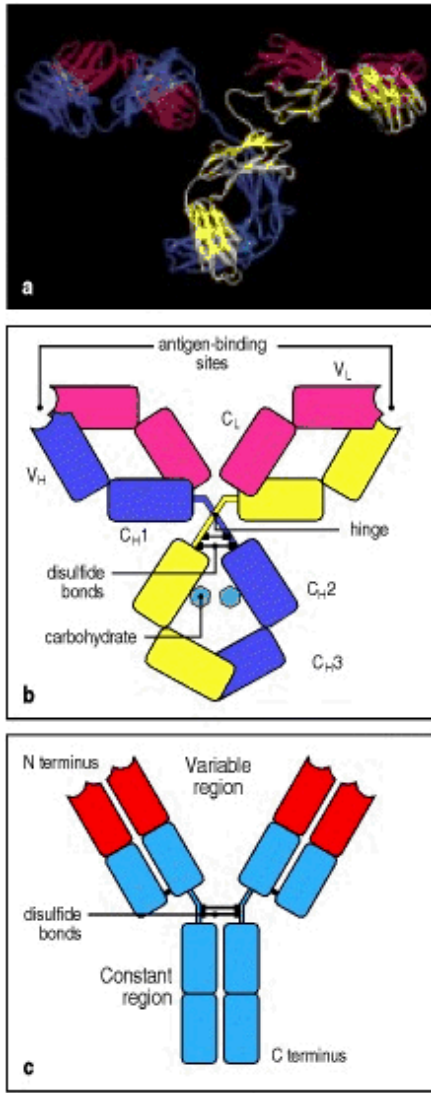
## **BIBLIOGRAPHIC PART**

### **1 ANTIBODY STRUCTURE**

#### **1.1 The structure of a typical antibody molecule**

Ab molecules are roughly Y-shaped molecules consisting of three equal-sized portions, loosely connected by a flexible tether. All Abs are constructed in the same way, from paired heavy and light polypeptide chains. The generic term “immunoglobulin” is used for all such proteins. Within this general category, there are five main heavy-chain classes or isotypes of immunoglobulins (IgM, IgD, IgG, IgA and IgE) which can be distinguished by their C regions. The general structural features of all the isotypes are similar and IgG, which is the most abundant isotype in plasma, could be considered as a typical Ab molecule.

IgG antibodies are large molecules, having a Mw of approximately 150 kDa and composed of two different kinds of polypeptide chain. One, of approximately 50 kDa, is termed the heavy or H chain, and the other, of 25 kDa, is termed the light or L chain. Each IgG molecule consists of two heavy chains and two light chains. The two heavy chains are linked to each other by disulfide bonds and each heavy chain is linked to a light chain by a disulfide bond. In any given immunoglobulin molecule, both the heavy chains and both the light chains are similar, giving an Ab molecule two identical antigen-binding sites and thus the ability to bind two identical structures simultaneously. The possession of two antigen-binding sites allows the Ab molecules to cross-link antigens and to bind them much more stably.



Three schematic representations of Ab structure are shown in Figure 1.

Figure 1 (a) illustrates a ribbon diagram based on the X-ray crystallographic structure of an IgG antibody, showing the course of the backbones of the polypeptide chains. Three globular regions form a Y. The two antigen-binding sites are at the tips of the arms, which are tethered to the trunk of the Y by a flexible hinge region. A schematic representation of the structure is given in

Figure 1 (b), illustrating the four-chain composition and the separate domains comprising each chain.

Figure 1 (c) shows a simplified schematic representation of an Ab molecule.

Each of the four chains has a variable (V) region at its amino terminus, which contributes to the antigen-binding site, and a constant (C) region, which determines the isotype. The isotype of the heavy chain determines the functional properties of the Ab [15].

**Figure 1: Structure of an antibody molecule [16]**

The amino acid sequences of many heavy and light chains of immunoglobulins have been determined and revealed two important features of Ab molecules. First, each chain consists of a series of similar, although not identical, sequences, each about 110 amino acids long. Each of these repeats corresponds to a discrete, compactly folded region of protein structure known as a protein domain. The light chain is made up of two such immunoglobulin domains, whereas the heavy chain of the IgG contains four [8].

The second important feature revealed by comparisons of amino acid sequences is that the amino-terminal sequences of both the heavy and light chains greatly change between different Abs. The variability in sequence is limited to approximately the first 110 amino acids,

corresponding to the first domain, whereas the remaining domains are constant between immunoglobulin chains of the same isotype. The amino-terminal variable or V domains of the heavy and light chains (VH and VL, respectively) together make up the V region of the Ab forming the antigen-binding regions (Fab) and confer on it the ability to bind a specific antigen. The constant domains (C domains) of the heavy and light chains (CH and CL, respectively) make up the C region forming the Fc (fragment crystallizable) regions [8].

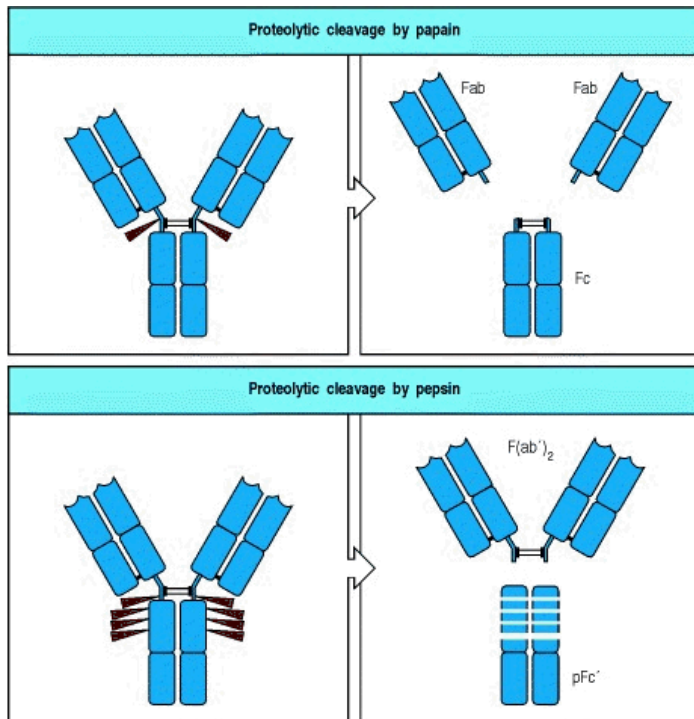


**Figure 2: Partial digestion of Y-shaped IgG molecule with proteases [15]**

Proteolytic enzymes (proteases) that cleave polypeptide sequences were used to dissect the structure of Ab molecules. Limited digestion with the protease papain cleaves the N-terminal side of the disulfide bonds and generates two identical Fab fragments containing the antigen-binding activity and one Fc fragment (Figure 2).

The Fab fragments (50 kDa) correspond to the couple of identical arms of the Ab molecule, which contain the complete light chains paired with both the VH and CH1 domains of the heavy chains. The other fragment contains no antigen-binding activity but was originally observed to crystallize readily, and for this reason was named the Fc fragment [8]. Treatment with pepsin cleaves the C-terminal side of the disulfide bonds (Figure 2). This produces a fragment, the

F(ab')<sub>2</sub> fragment, in which the two antigen-binding arms of the Ab molecule remain linked. The F(ab')<sub>2</sub> fragment has exactly the same antigen-binding characteristics as the original Ab but is unable to interact with any effector molecule. It is thus of potential value in therapeutic applications of Abs. The reduction of F(ab')<sub>2</sub> produces two Fab'.

The Ab' secondary structure is formed as the polypeptide chains form anti-parallel  $\beta$ -sheets. These beta-sheets are the major type of secondary structure in IgGs and are roughly 70 % of their content, as measured by FTIR [8].

## **1.2 Anti-TNF alpha antibody**

TNF alpha is a member of the TNF / TNFR cytokine superfamily. The term “cytokine” refers to a set of (glycosylated (or not) polypeptide) molecules involved in signaling in the immune response. In common with other TNF cytokine family members, TNF alpha is involved in maintenance and homeostasis of the immune system, inflammation and host defense. TNF alpha is an inflammatory cytokine produced by macrophages/monocytes during acute inflammation and is responsible for a diverse range of signaling events within cells, leading to necrosis or apoptosis. This protein is also important for resistance to infection and cancers. However, it is now clear that TNF alpha is involved in pathological processes such as chronic inflammation, autoimmunity and, in apparent contradiction to its name, malignant disease. TNF promotes the inflammatory response, which may cause several clinical issues associated with autoimmune disorders such as rheumatoid arthritis, ankylosing spondylitis, Crohn's disease, psoriasis, hidradenitis suppurativa and refractory asthma [17, 18].

Its central role in the inflammation processes has led to the development of TNF alpha antagonists as effective therapies for both rheumatoid arthritis and inflammatory bowel disease. This inhibition can be achieved with MAbs such as infliximab (Remicade<sup>®</sup>), adalimumab (Humira<sup>®</sup>), certolizumab pegol (Cimzia<sup>®</sup>) and golimumab (Simponi<sup>®</sup>) [24]. A human anti-TNF full-length Ab was used as a model during this project.

## **2 STABILIZATION OF PROTEINS AND ANTIBODIES**

### **2.1 Antibody instability**

Abs, like other proteins, are prone to a variety of physical and chemical degradation pathways, although Abs, on average, seem to be more stable than other proteins. Their tendency to generate degradation compounds mainly depends on their individual sequence, isoelectric point (pI) and hydrophobicity [8, 19]. Multiple degradation pathways can occur at the same time, and the degradation mechanism may change depending on the stress conditions. These degradation pathways are divided into two major categories: physical and chemical instabilities [9].

#### **2.1.1 Physical instability**

The pI of a protein is defined as the pH at which the molecule is globally neutral (or has a net zero charge). Theoretically, the pI is the pH at which a protein is the most chemically stable. However, due to a reduced surface charge, the molecule is physically unstable resulting to an agglomeration. Indeed, the reduced physical stability can be explained by considering the zeta potential of colloidal systems. The zeta potential may be described as the measure of the global charge on the molecule plus the adsorbed counter-ions from the solution. It represents the apparent ability of the protein to repel other like-charged protein molecules. As the zeta potential approaches zero (where the solution pH is equal to the pI), the ability of the protein molecule to repel a neighboring protein molecule is negligible, encouraging physical degradations of the protein, including conformational changes (denaturation), undesirable adsorption to surfaces, denaturation, precipitation and aggregation [8, 20].

##### **a. Conformational changes (denaturation)**

Any change in the protein structure, whether at the secondary, tertiary or quaternary levels, is considered as a denaturation issue [20].

Denaturation of proteins may occur at increased temperatures, through pH changes, or after the addition of salts, surfactants (especially ionic) and organic solvents. Also, physical forces such as shear stress, agitation, pressure and interfacial tension at hydrophobic interfaces may cause conformational changes in a protein. Compared with other proteins, Abs seem to be more

resistant to thermal stress. They may not melt completely until temperature is raised above 70°C, while most other proteins melt below this temperature [8].

Specific protein folding is required to interact with the biological target. Therefore, denaturation usually results in protein inactivation. However, under some conditions, denaturation can be reversible, allowing the protein to refold back to its native state. In this state, it is assumed that the native and denatured, or non-native, states are in a dynamic equilibrium.

## **b. Aggregation**

### **1) Definition and mechanism of protein aggregation**

Many definitions are given in the literature for the term “protein aggregation”. “Protein aggregates” are defined as protein species of higher molecular weight (HMWS) such as “oligomers” or “multimers”, instead of the desired defined species (e.g. a monomer). Aggregates are thus a universal term for all kinds of non-further-defined multimeric species that are formed by covalent bonds or noncovalent interactions [21].

Protein aggregates are usually categorized on the basis of different considerations, divided as follows [20, 22]:

- a. by type of bond: noncovalent aggregates, formed via weak forces such as Van der Waals interactions, hydrogen bonding, hydrophobic and electrostatic interactions versus covalent aggregates, resulting from a chemical bond between the two constituent species;
- b. by reversibility: reversible versus irreversible aggregates;
- c. by size: small soluble aggregates (oligomers), large oligomers ( $\geq 10$  nm), aggregates in the diameter range from 20 nm to 1  $\mu$ m, insoluble particles in the 1 – 25  $\mu$ m range or larger insoluble particles visible to the eye;
- d. by protein conformation: aggregates with a predominantly native structure versus aggregates with a predominantly non-native structure.

Pathologic protein aggregates are the cause of more than 20 different diseases in humans, e.g., Alzheimer’s disease, Parkinson’s disease and prion diseases [23]. Accordingly, the presence of a large percentage of aggregates in a protein medicine is unacceptable. Avoiding protein aggregation contributes to the preservation of the required biological function.

The presence of aggregates in pharmaceutical preparations is typically undesirable due to the potential for unwanted immunogenicity, altered pharmacokinetics, changed potency or undesirable toxicity. Immunoglobulin aggregates could cause serious renal failure and anaphylactoid reactions such as headache, fever and chills. Therefore, the aggregate level in commercial intravenous immunoglobulin products is limited to less than 5 %, based on the World Health Organization (WHO) standards [8]. However, this level can be adjusted on a case by case basis.

Several mechanisms were proposed to describe the formation of aggregates based on the kinetics of assembly (Figure 3). The model starts with a partial unfolding state of the native protein.

Partial unfolding allows the association of monomers through exposure of previously inaccessible residues. It should be noted that they are models which does not start with partial unfolding but due to colloidal instability foster aggregation between monomers in their native state. There are a variety of protein aggregation pathways, which may differ between proteins and result in different states. A protein may undergo various aggregation pathways depending on the environmental conditions and stress. The initial state of a protein prone to subsequent aggregation may be constituted by its native structure, by a degraded or modified structure, by a partially unfolded structure or by its fully unfolded state [23].

The aggregation process can be described as a scheme (Figure 3), where proteins form reversible unfolding intermediates, which then form reversible unfolded proteins or irreversible/reversible aggregates.



**Figure 3: Model illustrating protein aggregation under native conditions [24]**

The process from N to A can be considered as the nucleation step, which is usually rate limiting; in other words, the aggregation process is nucleation-dependent [24].

## **2) Induction factors causing protein aggregation**

Aggregates can be easily produced both in liquid and solid states under a variety of conditions, including variations in temperature, freezing and/or thawing, mechanical stress such as shaking, stirring, and pumping and formulation [8, 21]. Moreover, as partially unfolded protein molecules are part of the native state, aggregation can occur under no stress conditions during the storage.

### **a. Temperature**

In contrast to the other types of intermolecular interactions, hydrophobic interactions increase when the temperature increases. Higher temperature has an effect on the conformation of polypeptide chains at the level of its quaternary, tertiary and secondary structure, and can lead to temperature-induced unfolding that promotes aggregation. A measure for the thermal stability of a protein is the melting temperature ( $T_m$ ), which is the temperature at which 50% of protein molecules are unfolded during a thermal unfolding transition. On the other hand, increased temperatures accelerate chemical reactions such as oxidation and deamidation of biopharmaceuticals, which could lead to aggregation [22].

### **b. Freezing and thawing**

During the freezing process, complex physical and chemical changes may appear. During the early stage of the freeze drying process, the water in a formulation forms ice, which may cause cryoconcentration of the protein and solutes. Moreover, the pH may vary due to the crystallization of the buffer components. This increase in protein and excipient concentrations may result in insolubility. Interactions of the protein at the ice/solution interfaces can induce denaturation issues [25].

### **c. Mechanical stress**

Mechanical stress, such as stirring, pumping, shearing and shaking during manufacturing and transport is described as causing aggregation. These types of stress could induce interfacial effects, cavitation forces and local increase of the temperature [22].

### d. Protein concentration

Increasing the concentration of Abs often increases the aggregation tendency. The formation of aggregates occurs by at least bimolecular interaction of molecules and thus, this reaction is considered to be concentration-dependent.

At high concentrations of protein, the macromolecular crowding effect may appear. This is the effect of high total volume occupancy by macromolecular solutes on the behavior of each macromolecular species in that solution. According to this excluded volume theory, self-assembly and potential aggregation may be favored. At the same time, unfolding, which is a prerequisite for many aggregation reactions, may be reduced. The crowding effect can accelerate the folding process since a compact folded protein occupies less volume than an unfolded protein [26]. However, crowding can reduce the yield of correctly folded protein by increasing protein aggregation [27].

On the other hand, a decrease in protein concentration via dilution may affect the aggregate content since aggregates formed by weak reversible interaction can dissociate as the protein concentration decreases.

### e. Solvent and surface effects

Changes to the solution environment of a protein (e.g. pH, ionic strength, buffer species, excipients and contact materials) could affect the physical stability of Abs. The pH alters the number and distribution of charges on the protein surface and may affect the physical stability of Abs. Both the nature and the amount of excipients in the solvent may also have an impact on the aggregation behavior. For instance, the ability of the surfactants such as polysorbates to stabilize a protein against aggregation was shown to depend on the protein - surfactant ratio [21].

It should be mentioned that the use of organic solvent is commonly required for encapsulation of drug into PLGA MS. Clearly, not all organic solvents are equivalent and properties such as solvent hydrophobicity, hydrogen-bonding capacity and miscibility in water have profound influence on the structural integrity and activity of proteins [28]. Proteins in hydrophobic solvents are thought to retain their native structure as a result of kinetic trapping, which results from stronger hydrogen bonding between the protein atoms and a more rigid structure in the

absence of water. In hydrophobic water-immiscible solvents, any water that might be present will tend to stay at the protein surface because of the hydrophilic nature of the protein surface. Conversely, polar solvents that can easily strip water from the surface of the protein and compete strongly for hydrogen bonds between protein atoms (e.g. dimethyl sulfoxide, dimethylformamide, formamide) usually denature the structure to a largely unfolded state. Alcohols have some hydrophilic component, but are only moderate competitors for amide hydrogen bonds. They tend to disrupt tertiary structure and leave secondary structure interactions largely undisturbed.

### **2.1.2 Chemical instability**

Chemical degradation of proteins refers to modifications involving covalent bonds [19, 20, 8]. The major chemical degradation pathways in an Ab include cross-linking, deamidation, oxidation, and fragmentation [8].

#### **a. Deamidation**

Ab deamidation is extensively reported in the literature [8]. Storage, both in liquid or solid states, can easily generate large amounts of deamidated products.

Deamidation in Abs is mainly occurring via the Asparagine (Asn) and Glutamine (Gln) leading to an intermediate which is a succinimide (Figure 4 ) [9]. This chemical reaction may occur through direct hydrolysis of the side chain, amide linkage (Figure 4 a) or, more commonly, by succinimide formation (Figure 4 b). Deamidation has been reported over a wide range of pH, but is typically faster at neutral and alkaline pH [19].

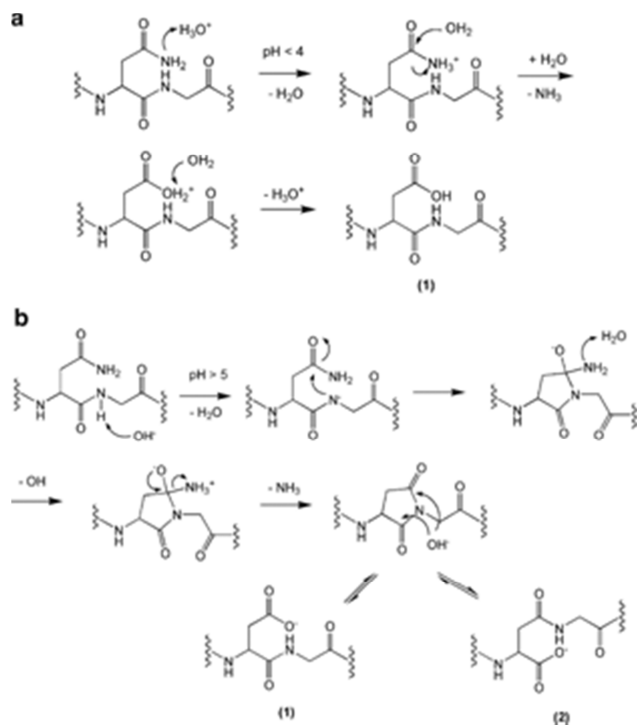


**Figure 4: (a) Deamidation mechanisms, as established in aqueous solution. Mechanisms for both acid (a) and base (b) catalysis are shown. (1)—Aspartic acid (Asp) degradation product. (2)—iso-Asp degradation product [29]**

Deamidation issues decreases the pH of the solution/suspension due to formation of additional carboxylic acid groups. Initial detection of deamidation in Ab preparations is typically identified by differences in charge distribution or content using methods such as isoelectric focusing or high-performance cation-exchange chromatography. Deamidation of asparagine is usually associated with other chemical rearrangements which lead to the formation of isoaspartic acid (iso-Asp) [30].

Nevertheless, deamidation does not result in a decrease in potency. However, it can affect potency through the introduction of an unfavorable negative charge, particularly when deamidation occurs in the binding regions.

### **b. Oxidation**

Although oxidation is not as prevalent as deamidation, it can easily occur during storage of Abs [8]. Due to their thiol groups, both methionine and cysteine residues are frequently a site of oxidation in biotherapeutics [9].

### **c. Disulfide formation and exchange**

Disulfide bond formation is probably the most common cross-linking pathway, leading to chemical aggregation. Disulfide bond exchange between cysteine residues may lead to an altered three-dimensional structure and a subsequent loss of activity [19].

In addition, disulfide scission or reduction occurs when cysteine is oxidized. The thiolate group may exchange a current disulfide bridge with a new bond, which is referred to as disulfide exchange [20].

### **d. Fragmentation and amide bond hydrolysis**

It is widely recognized that peptide bonds around Asp are more sensitive to hydrolysis [20]. In this case, an intermolecular cyclization of aspartic acid cleaves the peptide bond before or after the Asp residue. Asp residues bonded to proline and glycine are especially susceptible to cleavage under acidic conditions [8].

In PLGA formulations, acid catalyzed amide bond cleavage is a common source of protein chemical instability [29]. The extent of protein chain cleavage in PLGA matrices depends on the microenvironment pH of the PLGA matrix as the reaction is not observed above the  $pK_a$  of the aspartic acid side-chain ( $pK_a = 3.9$ ). Thus, chain cleavage at Asp in PLGA requires the accumulation of PLGA hydrolysis acidic compounds.

Fragmentation of a full-length Ab into smaller fragments (low molecular weight species (LMWS)) dramatically affects their physiological function [9]. Fragmentation issues may appear at each step of the fabrication/production of a formulated Ab (e.g. acidic or basic treatment, thermal treatment, freeze-thaw or storage).

Molecular sizing methods, such as sodium dodecyl sulphate polyacrylamide gel electrophoresis (SDS-PAGE) and SEC can be used to evaluate the fragmentation of an Ab.

### **e. Acylation**

Recent studies have reported that acylation issues may appear between proteins and the ester bonds of PLGA derivatives [29]. This reaction is promoted by a nucleophilic attack of a primary amine on the carboxyl carbon, producing a tetrahedral intermediate that is cleaved during the molecular rearrangement to produce the acylated protein.

## **2.2 Antibody stabilization and formulations**

Hands-on experience has shown that there is no general stabilization approach for proteins. A customized formulation needs to be developed for each peptide [19].

Protein stabilization can be achieved by internal and external stabilization [16]. Internal protein stabilization is a modification in the amino acid sequence that results in an increase in the stabilizing forces without changing the overall conformation. The external stabilization can be done by selecting proper parameters to produce a suitable formulation.

### **2.2.1 Liquid formulations**

Usually, liquid dosage forms are preferred due to their ease of administration and their low cost manufacturing process [8, 9]. However, liquid Ab formulations are more susceptible to instability [9]. The protein is generally more stable in the solid state than in the liquid state. This stability is believed to be related to protein mobility [31]. Protein movement is restricted in the dry state, substantially limiting the influence of the surroundings on the protein. The main cause of instability in liquid is water, which is involved in oxidation, deamidation and fragmentation reactions. When dispersed or solubilized in water, the hydrophobic surfaces of a protein are exposed to water and try to find a lower energy state by non-native protein-protein interactions, which lead to protein aggregation [32].

#### **a. Effect of protein concentration**

Protein concentration plays a significant role in formulation stability. Indeed, the risk of aggregation is increased with increasing protein concentration. Moreover, the viscosity is increased, leading to injection issues [32].

Since the half maximum effective concentration ( $EC_{50}$ ) value (used as a measure of a drug's potency) of Ab is often 10 –1 000 times higher than for other proteins, such as hormones and cytokines, a relatively large amount of Ab needs to be administered to achieve the therapeutic effect. Concentration-dependent protein aggregation appeared to be the greatest challenge in the development of high-concentration protein formulations.

#### **b. Effect of formulation pH and buffering agents**

Formulating a protein at its pI could lead to protein-protein interaction likely to result in aggregation. Moreover, a basic or acidic formulation pH has led to deamidation [32]. Both the type and concentration of a buffering agent may affect the stability of a protein [8]. One of these agents is histidine, which is characterized by a pKa of pH 6.0, which makes it a potential candidate for buffering the pH in weak acid condition.

#### **c. Effect of formulation excipients/stabilizers**

Generally, excipients are effective in protecting the physical stability of an Ab. A wide variety of excipients is used to improve the stability of pharmaceutical proteins (Table 1). Polyols, sugars, salts and amino acids or polymers can be used as stabilizers. Polyols (i.e. sorbitol and mannitol) and sugars (i.e. sucrose and trehalose) are often used to stabilize proteins and avoid their aggregation by contributing to increasing the  $T_m$  of Ab [8]. They can also protect the proteins from chemical processes such as oxidation degradation [33]. Generally, stabilization effect increases with increasing concentration of additives. The salts present in the formulations through buffers also increase the stability of proteins in solution [34]. They are not effective in the dry state [35]. The aggregation issues may be limited by the addition of ionic or non-ionic surfactants. Such agents stabilize the interfaces by reducing the surface tension. Moreover, surfactants reduce the adsorption of low concentration proteins onto the container surface but also at the liquid surface due to the interface with hydrophobic environment.. Polysorbates are commonly used surfactants reducing aggregation generated by temperature or agitation stress. It is important to note that the optimum performance is shown at low concentration (0.01 - 0.05 % w/v) and that, at high concentration (e.g. 1 % w/v), they can lead to protein denaturation [9]. Amino acids are reported as increasing the thermal stability of proteins. Aspartic acid, glutamic acid, glycine, arginine, lysine and histidine are used to reduce aggregation.

**Table 1: Pharmaceutical excipients commonly used in protein formulations [36]**

Category	Examples	General comments
Buffering agents	Citrate, acetate, histidine, phosphate	Control and maintain pH
Amino acids	Histidine (Hist), arginine, proline, glycine	Specific interactions with protein Antioxidant (Hist, Met) Buffering agents
Osmolytes	Sucrose, trehalose, sorbitol, glycine, proline, glutamate	Stabilize proteins against environmental stress (temperature, dehydration)
Sugars and carbohydrates	Sucrose, trehalose, sorbitol, mannitol, glucose, lactose	Protein stabilizer in liquid and lyophilized states Tonicifying agents
Proteins and polymers	Human serum albumin (HAS), gelatin, PVP, PLGA, PEG	Competitive inhibitor of protein adsorption Lyophilization bulking agents Drug delivery vehicles
Salts	Sodium chloride, potassium chloride, sodium sulfate	Tonicifying agents, Stabilizing or destabilizing effects on protein, especially with anions
Surfactants	Polysorbate 20/80, poloxamer 188/407	Competitive inhibitor of protein adsorption Competitive inhibitor of protein surface denaturation
Chelatants and anti-oxydants	EDTA, amino acids (Hist, Met)	Bind metal ions Free radical scavengers
Preservatives	Ascorbic acid, benzyl alcohol, phenol	Prevent microbial growth in multi-dose formulations
Specific ligands	Metals, ligands, amino acids, polyanions	Binds protein and stabilize native conformation against stress induced unfolding Binding may also affect protein's conformational stability

The involvement of water in mechanisms for stabilization may explain the stabilization effects of co-solvents such as the excluded volume effect [35].

The mechanism of preferential exclusion and its relevance for the stabilization of proteins in solution was found and explained by Arakawa and Timasheff et al. [37]. This mechanism is used to explain the effect of polymers on both the stability and the solubility of a protein. Briefly, the concept is that in solution, highly hydrated solubilized molecules compete with a protein for water, creating an “exclusion zone” around the protein where the other solutes are statistically and sterically excluded to a certain extent. Any molecules that are larger than water are excluded from the vicinity of protein surface (Figure 5). Therefore, the excluded volume effect stabilizes the compact native structure of the protein; conformations of protein that provide the system with a larger exclusion volume (like unfolded, less condensed conformations) are unfavorable and will be reduced [38].

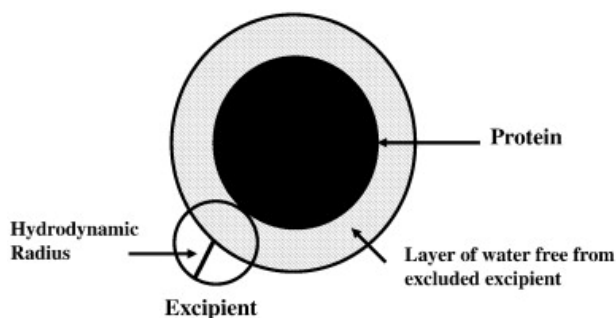


**Figure 5: Schematic illustration of the excluded volume effect. The protein is represented by the black circle and the excipient by the white circle. The striped area represents the layer of water free from the excluded excipient [35]**

### 2.2.2 Lyophilized formulations

Freeze-drying, also known as lyophilization, is a dehydration process. It works by freezing material and then reducing the surrounding pressure to allow the frozen water in the material to sublime directly from the solid phase to the gas phase [38]. Lyophilization can reduce the impact of water on Ab drug formulations [8]. The basic principal behind all drying-based stabilization methods is the removal of water and its replacement by suitable excipients. Nevertheless, relevant stress is applied to a protein during freezing and drying. Commonly, Abs are recognized to be more robust to freeze drying than other proteins [9].

#### a. Effect of the excipients on the freeze-drying process

In order to obtain a homogenous cake after lyophilization, a bulking and/or a cryoprotective agent should be added to the formulation. Although they are characterized by poor stabilizing

properties, both mannitol and glycine are commonly used as bulking agents due to their ability to crystallize during the freeze-drying process. To increase the stability of the lyophilized protein, cryoprotectants, such as sugars or surfactants, may be added to create a preferential exclusion phenomenon.

Improved native-like structure and reduction of aggregation issues can be obtained by incorporating a carbohydrate excipient (e.g. cryoprotectants and lyoprotectants) to meet the hydrogen bonding requirements on the protein surface, suggesting a critical role for non-water molecules to act as placeholders for water molecules during drying and in the dry state. Carbohydrates are favored as freeze-drying excipients since they are chemically innocuous and can be easily vitrified during freezing. Sucrose and trehalose were shown to form amorphous masses at very low temperatures [39]. These sugars are known to vitrify at a specific temperature, denoted as  $T_g'$  (glass transition temperature). Lyophilized formulations containing trehalose have been found to show a lower tendency to generate aggregates of Ab than those with sucrose.

It has been suggested that a molar lyoprotectant:protein ratio of 300:1 or greater should be used to achieve a significant effect on the stabilization of the corresponding protein. However, as the excipients can affect the tonicity of the lyophilized products, its relative amount should be carefully controlled [38].

### **b. Effect of formulation pH and buffering agents**

In addition to the nature of the buffering agents, the pH of the initial liquid formulation can affect the stability of the lyophilized product. Moreover, it should be noted that some buffering agents, such as sodium phosphate, may induce significant modification of pH due to a selective crystallization process during lyophilization.

### **c. Effect of protein concentration**

Usually, a high concentration of protein increases the protein's stability during the lyophilization process. However, Abs do not seem to follow this trend and many Abs were shown to be less stable at high concentrations [8].

#### **d. Effect of moisture content**

It is commonly accepted that the higher the moisture content of a lyophilized product, the higher the rate of degradation during the storage. Several studies discussed in Wang's review have shown that a residual water content ranging from 1 to 8 % w/w allows an optimal stabilization of the lyophilized Ab [8]. Indeed, a higher moisture content is known to increase both aggregation and Asn deamidation and isomerization issues.

#### **2.2.3 Spray-dried formulations**

In addition to the liquid and lyophilized dosage forms on the market, other processes such as spray-drying have been reported to stabilize Ab-containing dosage forms.

The spray-drying process is an efficient way of preparing solid dosage forms. As the solution is nebulized into small droplets before drying, the overall surface is dramatically increased, allowing an efficient evaporation of the solvent. Spray-drying may be an alternative method to lyophilization for removing water from Ab formulations. Moreover, the resulting material (spray-dried (SD) material) is a fine powder. An application for dry protein particles is the production of parenteral protein depots based on polymer matrices, where the protein has to be finely dispersed in a non-solvent solution of the polymer [38].

Protein aggregation during the process seems to be the main challenge. However, the addition of appropriate excipients could minimize aggregation issues. They should be able to achieve good water replacement in the dried state by closely surrounding protein molecules with a sufficient amount of saccharides or other excipients that are able to remain in an amorphous state and provide enough hydrogen bonds per surface area. As observed for lyophilization, sugars and polyols were reported to reduce aggregation during this drying process. The molecular ratio that is needed to obtain a significant inhibition of aggregation seems to be similar to that used in lyophilized formulations (e.g. 300:1 to 500:1 for trehalose:protein). The addition of mannitol also reduced aggregation, but only up to a molar ratio of 200:1. A higher ratio resulted in crystallization, which had a detrimental effect on protein stability [38].

### 3 CONTROLLED RELEASE FORMULATIONS

Administration of an injectable sustained-release drug delivery system usually increases the compliancy of patient by reducing the number of injections. It also decreases potential side effects (e.g. by reducing the so-called peak-and-trough effect) and can allow long-term local delivery. Such systems represent an attractive alternative to the conventional formulations containing proteins, in which the macromolecule is usually either lyophilized, in suspension or in an aqueous solution.

Numerous methods exist for enhancing the residence time *in vivo* of biotherapeutics. Such methods are commonly classified into three categories: (1) plasma persistence technologies, (2) controlled-payout/depot technologies and (3) device-assisted protein delivery technologies. The controlled delivery technologies are described in detail in the next section [2].

#### 3.1 Controlled-delivery/depot technologies

Controlled-release systems have been extensively investigated for proteins in the past two decades [4]. Little work has been conducted in this area for Abs, partly due to their relatively long plasma half-lives compared with other proteins [8]. Fab' compounds characterized by a shorter half-life should be good candidates.

These sustained-release technologies focus on slowing the apparent rate of absorption of the biotherapeutics from a subcutaneous site of injection with the goal of maintaining a steady plasma drug level. These technologies attempt either to manipulate the physical state of the protein, e.g. through crystallization, amorphous precipitation or gelation, or utilize polymers/lipids to entrap and slow down the release of the protein. Controlled delivery of proteins can be obtained with different DDSs, e.g. MS, hydrogels, liposomes, solid lipid micro- or nanoparticles and emulsions [40]. This project was focused on the polymer-based delivery systems described further on.

##### 3.1.1 Polymer-based formulations

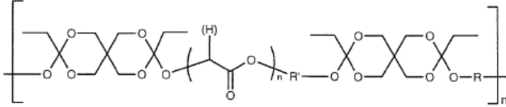
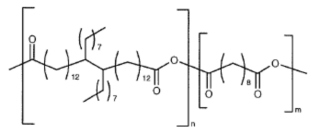
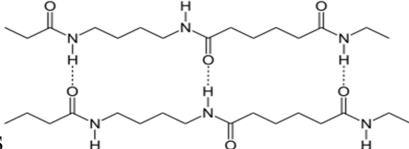
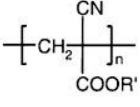
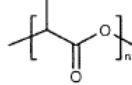
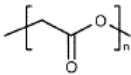
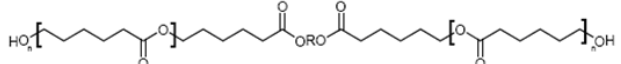
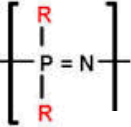
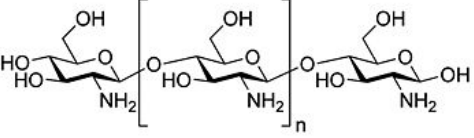
Polymer-based formulations are predicated on the principle of protein entrapment and controlled release through diffusion and polymer degradation. The duration of the release is governed by the nature of the polymer.

### **a. Microspheres and nanoparticles**

Proteins can be encapsulated into MS that act as protein carriers. Micro- and nanoparticles are produced from a number of nondegradable and degradable polymers, of both synthetic and natural origin. Particles that are 1 – 1 000  $\mu\text{m}$  in diameter are generally considered to be microparticles, whereas particles of 1 – 1 000 nm in diameter are nanoparticles.

In the micro- and nanocapsules, a distinct polymer membrane surrounds a vesicular space that contains the drug. The micro- and nanospheres consist of a homogenous spherical matrix wherein the drug is dispersed. Because nondegradable materials increase the risks of toxicity and potential persistence in the body, micro- and nanoparticles are generally made from biodegradable polymers. Injectable biodegradable and biocompatible polymeric particles could be used both to protect MAbs from *in vivo* degradation and to control their release after administration. A variety of synthetic and naturally occurring polymers have been intensively studied over the past 30 years, which include the natural and synthetic ones ([Table 2](#)).

**Table 2: Classification of biodegradable polymers [41]**

<p>Synthetic</p>	<div style="text-align: center;">  <p>Polyorthoesters <span style="margin-left: 150px;">POE IV</span></p> </div> <div style="text-align: center;">  <p>Polyamides</p> </div> <div style="text-align: center;">  <p>Polyamides</p> </div> <div style="text-align: center;">  <p>Polyalkylcyanoacrylates</p> </div> <div style="display: flex; justify-content: space-around; align-items: center;"> <div style="text-align: center;">  <p>Poly(lactic acid)</p> </div> <div style="text-align: center;">  <p>Poly(glycolic acid)</p> </div> </div> <div style="text-align: center;"> <p>Polyesters (lactides/glycolides)</p>  <p>Polycaprolactone</p> </div> <div style="text-align: center;">  <p>Polyphosphazenes</p> </div>
<p>Naturals</p>	<p>Proteins (albumin, globulin, gelatin, collagene, casein)          Polysaccharides as hydrophilic polymers (Starch, cellulose, chitosan, dextran, alginic acid, hyaluronic acid)</p> <div style="text-align: center;">  <p>= chitosan</p> </div>

Synthetic biodegradable polymers have been increasingly used in drug delivery systems as they are more stable than natural polymers. Thermoplastic aliphatic poly(esters) derivatives, such as poly-lactide (PLA), poly-glycolide (PGA) and especially PLGA, have generated tremendous interest due to their excellent biocompatibility and biodegradability (Table 2). PLGA undergoes hydrolysis to produce the original monomers, lactic and glycolic acids. Both monomers are easily metabolized *in vivo* through the citric acid cycle. Various polymeric DDSs such as MS, microcapsules, nanoparticles, pellets, implants and films are produced using PLGA for the delivery of a variety of drugs [42]. Since the body effectively metabolizes the two monomers, there is minimal systemic toxicity associated with the use of PLGA for drug delivery or biomaterial applications. PLGA are approved by the FDA and the EMA for human drug delivery [14]. Several products based on PLGA microparticles are currently on the market (Table 3) [3]. No PLGA-based protein delivery system has reached the market, with the exception of Nutropin Depot<sup>®</sup> (a depot formulation of human growth hormone) by Genentech. However, this latter was withdrawn from the market a few years after launch for economic reasons.

**Table 3: Examples of marketed products produced with biodegradable MS [41, 43, 44]**

Product name	Active ingredient	Company	Release period	Application
Lupron Depot <sup>®</sup>	Leuprolide acetate	Abott	1, 3 or 4 months	Prostate cancer
Prostap <sup>®</sup>	Leuprolide acetate	Takeda	1 or 3 months	Prostate cancer
Nutropin Depot <sup>®</sup>	Growth hormone	Genetech- Alkermes	1 or 2 months	Pediatric growth hormone deficiency
Suprecur <sup>®</sup> MP	Buserelin acetate	Aventis	1 month	Prostate cancer
Decapeptyl <sup>®</sup>	Triptorelin pamoate	Debiopharm - Ipsen	1 month	Prostate cancer
Sandostatin LAR <sup>®</sup> Depot	Octreotide acetate	Novartis	1 month	GH suppression Anti-cancer Acromegaly
Somatuline <sup>®</sup> LA	Lanreotide	Ipsen	14 days	Acromegaly
Trelstar <sup>™</sup> Depot	Triptorelin pamoate	Pfizer	1 month	Prostate cancer
Arestin <sup>®</sup>	Minocycline	Orapharma	2 weeks	Periodontal disease
Risperidal <sup>®</sup> Consta <sup>™</sup>	Risperidone	Johnson & Johnson	2 weeks	Antipsychotic
Zoladex <sup>®</sup>	Goserelin acetate	I.C.I.C - AstraZeneca	1 or 3 months	Prostate cancer
Vivitrol <sup>®</sup>	Naltrexone	Alkermes	1 month	Alcohol and opioid dependence
Posilac <sup>®</sup>	Recombinant bovine somatotropin	Eli Lilly	2 weeks	Milk production in cattle

During each common preparation process for drug-loaded PLGA MS, each critical step can be the cause of drug degradation (Figure 6). The limited success of peptide-loaded MS and implants based on PLA or PLGA can be explained by the fragile three-dimensional macromolecular structure of proteins, which makes them susceptible to a variety of chemical and physical degradation pathways during manufacturing, storage and release [9].

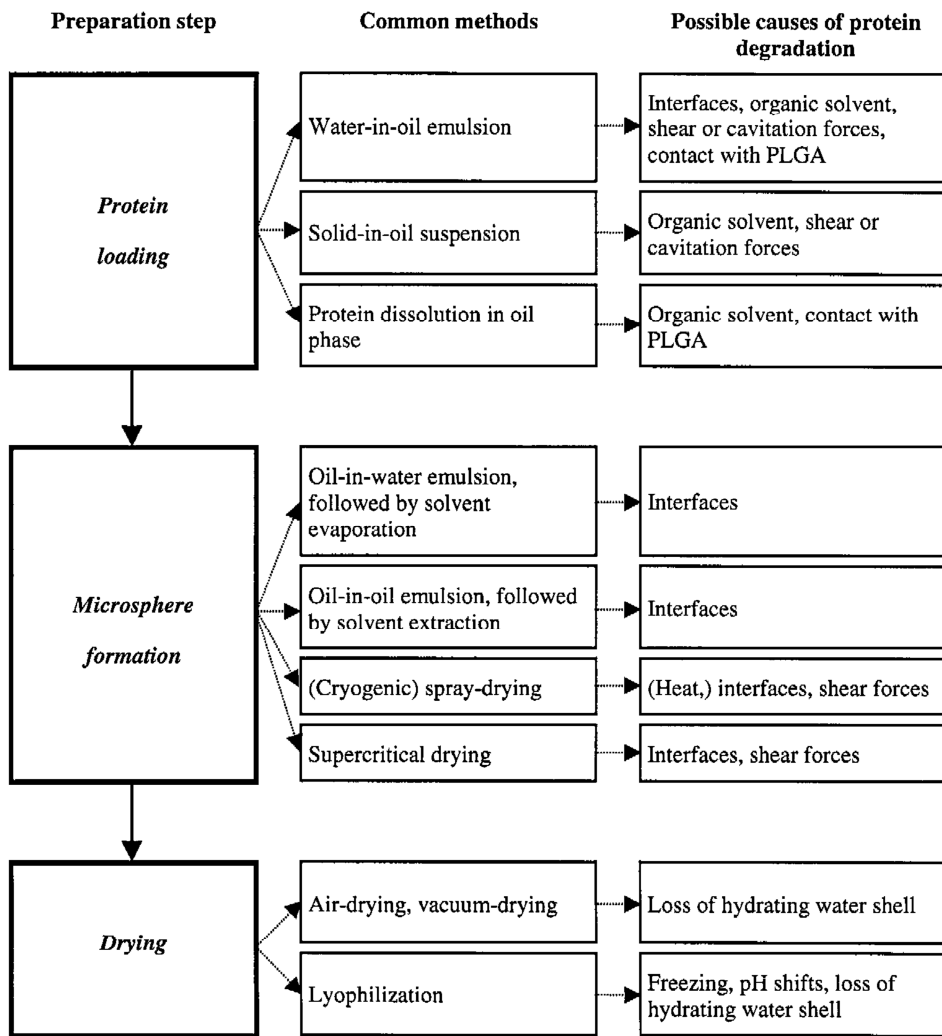


**Figure 6: Critical steps in encapsulation processes [45]**

As illustrated in Table 4 , different approaches to protect Ab against degradation are feasible at each step of the encapsulation process and during the release from the delivery system and the storage, such as the addition of polyol, surfactant, and the reduction of agitation time.

**Table 4: Approaches to Protect Microencapsulated Proteins against Stress Factors During Preparation, Storage, and Release [45]**

<b>Stage</b>	<b>Stress factor</b>	<b>Stabilization approach</b>	<b>Stabilization mechanism</b>
Preparation	Water/organic solvent interfaces	Add sugars, polyols, PEG  Increase protein loading  Add other proteins  Avoid emulsification, use non-aqueous process  Pre-encapsulate protein in hydrophilic core	Increase of Gibbs free energy of unfolding, shielding from interfaces by preferential hydration  Reduction of interface/protein ratio Competition for interfaces  Absence of water/organic solvent interfaces  Shielding from interfaces
Preparation	Protein-PLGA contacts	Add other proteins Pre-encapsulate protein in hydrophilic core Hydrophobic ion pairing	Competition for PLGA Shielding from PLGA Shielding from PLGA
Preparation	Shear	Add surfactants  Reduce homogenization time  Avoid sonication, use other homogenization method	Competition for interfaces  Minimized exposure to shear  Absence of cavitation stress
Preparation	Drying	Add lyoprotectants  Avoid lyophilization, use other drying method	Increase of Gibbs free energy of unfolding, water substitution  Absence of freezing step
Storage	Moisture	Reduce residual solvent level	Minimized mobility and water-induced degradation
	Dehydration	Add lyoprotectants	Increase of Gibbs free energy of unfolding, water substitution

Stage	Stress factor	Stabilization approach	Stabilization mechanism
Release	Acidification Protein-PLGA contacts	Add basic compounds Add other proteins Add surfactants Add sugars	Buffering Competition for PLGA Shielding from PLGA Increase of Gibbs free energy of unfolding, shielding from PLGA by preferential hydration

In addition to protein degradation, other drawbacks are associated with the formulation of MS. One of them is the initial burst and the incomplete release of the encapsulated protein [4]. Normally, the proteins are released from the MS due to a combination of diffusion through the polymer matrix and the degradation of the particle itself. There is also usually an initial release (called “burst effect”) of the protein adsorbed on the surface of the particle. The degradation profile of the polymer that determines diffusion depends on polymer attributes such as individual polymer molecular weights, copolymer type and ratios, and their resulting glass transition temperature, crystallinity and hydrophilicity [46].

Another drawback is linked to the hydrolysis of polymer and the formation of glycolic and lactic acid molecules, resulting to an acidic microenvironment. Consequently, the incorporated proteins face a completely altered microenvironment. In particular, the significant pH-drop that results is identified as a cause for protein unfolding, aggregation and chemical degradation [3, 29, 47, 48, 49]. Other disadvantages of the microencapsulation technology include a relatively low loading capacity for proteins [50].

However, the application of MS DDSs includes challenges with formulation and manufacturing as well as the requirement of large gauge needles (18 G-21 G) for the delivery of the suspension, which can induce considerable pain upon injection. That induces that (a) the processing techniques, for producing drug loaded microparticles, require precise control of size and surface morphology of the microparticles formed, (b) the produced MS have to be physically stable and (c) the suspension of the polymeric microparticles has to be homogeneous.

Another feature of PLGA microparticle preparations is their potential recognition by immune elements and their capacity to stimulate immunization against incorporated proteins. Hydrophobic microparticles were reported to incite local inflammation at subcutaneous injection

sites [9, 49]. It poses a serious concern for therapeutic protein delivery. Indeed, the subcutaneous implantation of MS may cause severe tissue responses, including acute and chronic inflammation reactions, undesired immune reactions and fibrosis. These inflammatory reactions can affect and even prevent formulations' functionality [51]. However, polymeric MS and delivery systems can be successful Ab formulations if administered to the appropriate sites, using certain types of polymers or preparing MS or polymeric formulations by methods that are more protective of the Ab. Resorbable polymers such as PLGA that show less potential to induce inflammation might be used to deliver Abs in a sustained manner.

### **Examples of available technologies**

Alkermes' Prolease technology has used PLGA MS to control the release of human growth hormone [52]. The MS are injected as a suspension into the body and the entrapped protein is released through a particle hydration process followed by the dissolution of the drug, the diffusion of the drug through pores in the particles and subsequent polymer erosion. The aim of the current project is to apply this kind of technology to either MAbs or Fabs.

PROMAXX MS (Epic Therapeutics) can bypass the use of solvents [9]. The MS are prepared by combining water-soluble polymers (e.g. PEG, Poloxamer, PVP, etc.) and the aqueous solution of Ab. The decrease in the initial temperature leads to the precipitation of the protein into MS. This technology has appeared attractive for biotherapeutic applications.

In addition, the use of biodegradable MS is intensively described in the literature for proteins delivery as shown in the review article of Sinha and Trehan [41].

### **b. In situ polymer precipitation/gelation**

Implantation of solid devices or viscous devices can be associated with significant pain. For this reason, another approach to creating an injectable sustained-release system is to form it *in situ*. These formulations are injected as a liquid using a small-bore needle and solidify in the body.

One way to achieve this is by injecting a solution of polymer such as PLGA in an acceptable organic solvent. The dilution into the aqueous environment *in vivo* results in the polymer's precipitation and encapsulation of the active compound within the formed matrix. The AtriGel® technology, as an example, is based on PLGA and/or poly (D, L-lactide-co-ε-caprolactone) dissolved in a non-toxic solvent, N-methyl-2- pyrrolidone [50].

A further option for generating an injectable formulation formed *in situ* is to use polymers that undergo a physical change on a certain trigger. The triggers of temperature or external light have mainly been investigated. Thermogels are amphiphilic copolymers that are water-soluble at room temperature and, when properly constructed and used at the proper concentration, form gels at body temperature. Incorporation of proteins into thermogels involves dissolving and injecting the protein in the aqueous solution of the thermogel, which leads to preserving the integrity of the sensitive proteins. The ReGel™ technology, for example, is currently being used in a clinical trial for intratumoral Paclitaxel administration: Oncogel®. A triblock copolymer based on poly(ethylene glycol) and PLGA presents *in situ* gelification due to the physiological temperature, with a sustained release for up to 6 weeks [50, 53].

From a manufacturer's point of view, *in situ* formation of a delivery system is an attractive approach as it eliminates the need for a relatively demanding process of microencapsulation. However, the level of protein incorporation and potential burst effect needs to be considered [50]. The MS system appears more suitable for MAb and Fab requiring a high drug load and controlled burst effect.

### **c. Hydrogel**

Hydrogels are polymeric networks with a three-dimensional configuration capable of absorbing high amounts of water or biological fluids. Their tendency to absorb water is attributed to the presence of hydrophilic groups such as  $-\text{OH}$ ,  $-\text{CONH}-$ ,  $-\text{CONH}_2$ ,  $-\text{COOH}$  and  $-\text{SO}_3\text{H}$  in polymers forming hydrogel structures. In contrast, polymeric networks of hydrophobic characteristics (e.g., PLA or PLGA) have limited water-absorbing capacities [54].

High water content imparts a unique property to hydrogels, which, while macroscopically solids, behave like aqueous solutions on a microscopic scale. As a result, the diffusion of molecular species, including water-soluble proteins, within a hydrogel is limited only by their size with respect to the space between individual cross-linked polymer elements. Hydrogels have been created from a variety of polymers, including collagen, gelatin, fibrin, hyaluronic acid, alginate, chitosan and dextran. In addition to natural polymers, hydrogels made from synthetic polymers have also been investigated, including those based on poly(ethylene oxide), poly-(acrylic acid) and poly(vinyl alcohol). Because of their high water content, it is often difficult to control the rate of release of agents from hydrogels which appears shorter than with hydrophobic polymers.

Several challenges remain to improve the clinical applicability of hydrogels for drug delivery [55]. One set of major challenges relates to improving the ease of clinical usage. E.g. Designing physical gelators which gel at lower polymer concentrations and at more precise gelation temperatures would reduce the risk of premature gelation inside the needle upon injection. There are also challenges in expanding the types of kinetic release profiles which can be achieved using hydrogels. Extending the duration of release would be useful in many applications and could allow hydrogels to supplant hydrophobic systems for long-term release applications. There is a need for improvement in the delivery sensitive molecules such as proteins, antibodies which can readily be deactivated or unfolded by interactions with the hydrogel delivery vehicle. A review of the development stage of various hydrogels is summarized in the article of Arti Vashist and co-authors [56].

## MATERIALS & METHODS

### 1 MATERIALS

#### 1.1 General description of materials

**Table 5: Materials used during this project**

<b>Material</b>	<b>Functions</b>	<b>Suppliers</b>
Polyclonal bovine IgG	Biotherapeutic drug model	Equitech-Bio Inc. (Kerrville, USA)
Anti-TNF MAb (CDP571)	Biotherapeutic drug model	UCB-Celltech (Slough, UK)
Anti-TNF Fab'	Biotherapeutic drug model	UCB-Pharma (Bulle, Suisse)
PLGA ( <a href="#">Table 6</a> )	Biodegradable polymer (Poly (lactic-co-glycolic acid) used for sustained release formulations	Boehringer Ingelheim (Ingelheim, Germany)
PEG-PLGA ( <a href="#">Table 7</a> )	Biodegradable polymer used for sustained release formulations	Boehringer Ingelheim (Ingelheim, Germany)
Mannitol	Polyol used as stabilizer for Ab solution  cryoprotectants for freeze-drying process	Sigma-Aldrich (Diegem, Belgium)
L-histidine	Amino acid used as Ab stabilizer for solution and SD formulations  buffer agent pH 5.0 and 6.0	Sigma-Aldrich (Diegem, Belgium)
Trehalose	Sugar used as Ab stabilizer for SD formulations and freeze-drying process	Sigma-Aldrich (Diegem, Belgium)
Sucrose	Sugar used as cryoprotectants and lyoprotectants for freeze-drying process	Sigma-Aldrich (Diegem, Belgium)

L-proline, L-arginine, L-serine	Amino acid used as stabilizer for Ab solution	Sigma-Aldrich (Diegem, Belgium)
Tween 20, Tween 80	Surfactant used as stabilizer for Ab solution	Sigma-Aldrich (Diegem, Belgium)
Pluronic F68	Surfactant used as stabilizer for Ab solution	Sigma-Aldrich (Diegem, Belgium)
PEG4000	Polymer used as stabilizer for Ab solution	Sigma-Aldrich (Diegem, Belgium)
NaCl	Salt used as stabilizer for Ab solution	Sigma-Aldrich (Diegem, Belgium)
Sodium phosphate monobasic Sodium phosphate dibasic	Buffer agent pH 7.0 and 7.4	Sigma-Aldrich (Diegem, Belgium)
Phosphate buffer (PB) pH 7.4 Gibco <sup>®</sup>	Buffer agent pH 7.4	Invitrogen (Gent, Belgium)
Glycine	Amino acid used as buffering agent pH 5.0	Sigma-Aldrich (Diegem, Belgium)
Polyvinyl pyrrolidone (PVP)	Surfactant used during the encapsulation processes	Sigma-Aldrich (Diegem, Belgium)
Polyvinyl alcohol (PVA)	Surfactant used during the encapsulation processes	Sigma-Aldrich (Diegem, Belgium)
Ethyl acetate (EtAc)	Organic solvent used during the encapsulation processes	Sigma-Aldrich (Diegem, Belgium)
Methylene chloride (MC)	Organic solvent used for encapsulation processes	Merck (Darmstadt, Germany)
Amicon 15 or 30 KDa Mw cut-off membranes	Filtration devices	Millipore (Billerica, USA)
Vivacell 100 30 KDa Mw cut-off membranes	Filtration devices	Sartorius (Goettingen, Germany)
Steriflip-GP, 0.22 $\mu$ m	Filtration devices	Millipore (Billerica, USA)

## **1.2 Drug model molecules**

### **1.2.1 Bovine immunoglobulin G (IgG)**

At the early stage of the project, a polyclonal full-length IgG from bovine serum was used as a model molecule for screening encapsulation processes and formulations. The IgG was supplied by Equitech-Bio Inc. (Kerrville, US) in the form of lyophilized powder. The IgG tested formulations are summarized in [Table 37](#) and [Table 39](#) in appendix.

### **1.2.2 Humanized full length anti-human TNF alpha antibody**

After determining the most suitable process of encapsulation, a full length anti-human TNF alpha Ab (called CDP571; Mw 150 kDa) was tested for further evaluating the activity of the drug after the manufacture of MS. It was received from UCB-Pharma (Slough, UK) at 18 mg/mL in an aqueous solution 0.27 M glycine, 1 % maltose (w/v) pH 5.0 buffer. The CDP571 tested formulations are summarized in [Table 41](#), [Table 42](#) and [Table 43](#).

### **1.2.3 Antibody fragment - anti-human TNF alpha (Fab')**

Finally, the developed process was applied to an Ab fragment. The Fab' was supplied by UCB-Pharma S.A. (Slough, UK) in acetate buffer pH 4.5 at 20 mg/mL.

## **1.3 Poly (lactide-co-glycolide) copolymer**

PLGA supplied by Boehringer Ingelheim (Ingelheim, Germany) were used as the biodegradable polymer. PLGA is a biodegradable and biocompatible copolymer made of two monomers, which are lactic acid and glycolic acid ([Figure 7](#)). During polymerization, the successive monomeric units are linked together in PLGA by ester linkages, thus yielding linear, aliphatic polyester. The ratio of the monomers and the molecular weight set both the identity and the properties of the copolymer. Depending on the ratio of lactide to glycolide used for the polymerization, different forms of PLGA can be obtained. These are usually identified in regard to the monomers' ratio. For instance, PLGA 75:25 means the polymer is made of 75 % lactic acid and 25 % glycolic acid.

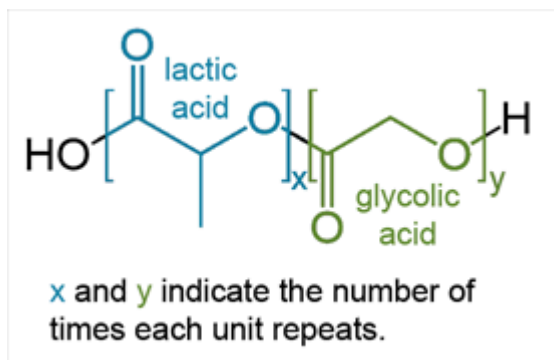


**Figure 7: PLGA structure**

PLGA are also characterized by their inherent viscosity ( $\eta$ ) which is related to their  $M_w$  and their  $T_g$ . All tested PLGA derivatives are amorphous and show a  $T_g$  ranged between 40 and 60°C.

PLGA can be dissolved by a wide range of common solvents, including chlorinated solvents, tetrahydrofuran, acetone or EtAc. PLGA is degraded by hydrolysis of its ester linkages in the presence of water. It has been shown that the rate of PLGA derivatives is related to the ratio of the monomers. Commonly, the higher the percentage of lactide units, the longer the polymer lasts before degrading in the presence of water [57]. As PLGA are made up of acidic monomers, its degradation may result in a build-up of acidic products. An acidic microenvironment and an accelerated degradation inside large specimens of PLGA are well-documented [58, 47]. Upon exposure to either aqueous solution or vapor, the ester carbon is subject to nucleophilic attack by water. Hydrolysis proceeds via a tetrahedral intermediate, producing both a primary alcohol and a carboxylic acid. The accumulation of carboxylic acid hydrolysis products in PLGA matrices results in autocatalysis of the hydrolysis reaction [29].

The PLGA copolymers were supplied from Boehringer Ingelheim (Ingelheim, Germany). Copolymers of PEG-PLGA from Boehringer Ingelheim (Ingelheim, Germany) were also tested.

The characteristics of the evaluated PLGA and PEG-PLGA are summarized in [Table 6](#) and [Table 7](#).

**Table 6: Characteristics of evaluated PLGA**

<b>PLGA</b>	<b>Lactide to glycolide ratio</b>	<b>Inherent <math>\eta</math> (0.1% in MC, 25°C) (dL/g)</b>	<b>Mw (KDa)</b>	<b>T<sub>g</sub> (°C)</b>
Resomer® RG502	50:50	0.16 - 0.24	7 - 17	42 - 46
Resomer® RG504	50:50	0.45 - 0.6	38 - 54	46 - 50
Resomer® RG505	50:50	0.61 - 0.74	54 - 69	48 - 52
Resomer® RG755S	75:25	0.50 - 0.70	54 - 69	48 - 52

**Table 7: Characteristics of evaluated PEG-PLGA**

<b>PEG-PLGA</b>	<b>Lactide to glycolide ratio</b>	<b>PEG 5 kDa part (%)</b>
RGP d 5055	50:50	3 - 7
RGP d 50105	50:50	8 - 12
RGP d 50155	50:50	13 - 17

## **2 MANUFACTURING METHODS**

### **2.1 Preparation of antibody solutions**

#### **2.1.1 Bovine IgG solutions (IgG)**

The bovine IgG solutions were prepared by dissolving an appropriate amount of lyophilized IgG powder into the appropriate formulation solution.

#### **2.1.2 Anti-TNF alpha solution (CDP571)**

All the CDP571 solutions were prepared from the initial CDP571 formulation solution containing 18 mg/mL MAb in an aqueous solution of 0.27 M glycine and 1 % maltose (w/v) at pH 5.0.

The CDP571 formulation solutions were prepared by buffer exchange using appropriate centrifugal filter devices, such as the Vivacell 100 30 KDa Mw Co membranes (Sartorius, Goettingen, Germany) or the Amicon 15 or 30 KDa Mw Co membranes (Millipore, USA). The initial CDP571 solution was transferred into the appropriate formulation solution by sequential dilution and concentration by centrifugation at 3500 g. The final MAb solutions were filtered on 0.22 µm membranes using the Steritop™ or Steriflip® filter Units (Millipore, Billerica, USA) before further processing.

### **2.2 Spray-drying process**

Spray drying is a widely-applied method for converting aqueous or organic solutions, emulsions, dispersion and suspensions into dry powder. A spray-dryer ([Figure 8](#)) atomizes a liquid feed into fine droplets and evaporates the solvent or water by means of a hot drying gas. Typically, a nozzle is used to form droplets in a range of 20 to 180 microns in size [59].

A complete spray-drying process consists of a sequence of 4 steps: (1) feed preparation; (2) atomization and hot gas contact; (3) evaporation, particle shape formation and drying; and (4) separation of the dried product from the gas and discharge.

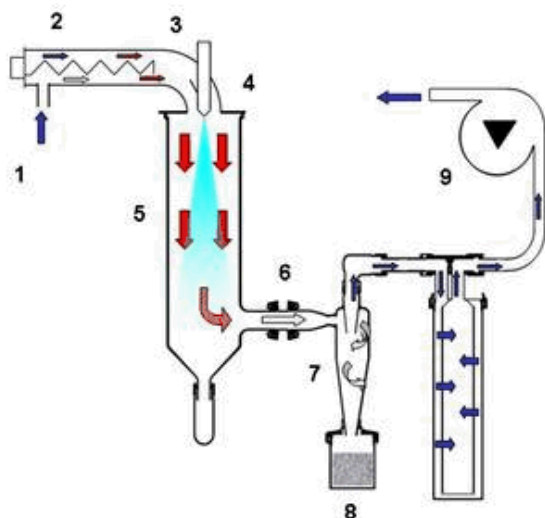


**Figure 8: scheme of a spray-drier with air intake (1), heating (2), temperature sensor at air entry point (3), two-fluid nozzle (4), flow-stabilized entry into the drying chamber (5), temperature sensor at air exit point (6), cyclone for the separation of the product from the air stream (7), collection vessel for finished product (8) and aspirator (9)**

During the preparation of Ab microparticles and encapsulation of Ab in PLGA MS, the following mini Spray-Dryers (Büchi) were used as a laboratory scale system.

- A mini Spray-Dryer B-190 from Büchi (Büchi Labortechnik, Flawil, Switzerland) used at the ULB, laboratory of Pharmaceutics and Biopharmaceutics. This spray-dryer can be equipped with a refrigerated atomization chamber, which was used to control the outlet temperature during the spray-drying process. The nozzle could also be refrigerated by circulating cold water into the double chamber (Figure 9).
- A mini Spray-Dryer B-290 from Büchi used at the ULB, laboratory of Pharmaceutics and Biopharmaceutics.
- A mini Spray-Dryer B-290 equipped with a Büchi Inert Loop B-295 (as a solvent condenser) used at the UCB-Pharma, Preformulation department.



**Figure 9:** Büchi - mini Spray-Dryer B290

For the encapsulation of the Ab in solid state into the PLGA MS, Ab microparticles need to be produced with reduced particle size, thus following a preliminary particle size reduction process such as high pressure homogenization or spray-drying. It was estimated that a particle size ratio (Ab microparticles compared to PLGA MS) of about 1/10 is required to be able to encapsulated Ab into polymer MS efficiently. Aqueous Ab solutions were spray-dried after buffer exchange or dissolution of the lyophilized powder in an aqueous buffer at variable concentrations. Excipients such as sugars, polyols, surfactants and PEG were added to stabilize the Ab during the spray-drying process. Process parameters such as inlet temperature, outlet temperature, atomization pressure, flow rate and aspiration were controlled during the process.

In further optimization of the spray-drying process by DoE, aqueous Ab solutions were spray-dried using a mini Spray-Dryer assembly with a 0.7 mm spray nozzle. The inlet T° and the liquid flow rate were set at 130°C and 3 mL/min, respectively. The drying air flow rate was fixed at 30 m<sup>3</sup>/h and the atomization flow rate was set at 800 L/h. The resulting outlet T° was 80°C.

## 2.3 Preparation techniques of the drug-loaded PLGA MS

Several methods for encapsulating Ab into PLGA MS were investigated. These methods could be classified in two classes, with either Ab in solution or Ab in solid state [60].

### 2.3.1 Double emulsion solvent extraction process

The first method to be evaluated was encapsulation with Ab in solution. The polymer is a lipophilic macromolecule which requires suitable organic solvents, such as MC, to be dissolved properly. As the Ab is mostly amphiphilic and not soluble in the organic solvent used to solubilize the biodegradable polymer, the Ab was dissolved in an aqueous phase and a double emulsion method, w/o/w process was carried out (Figure 10).

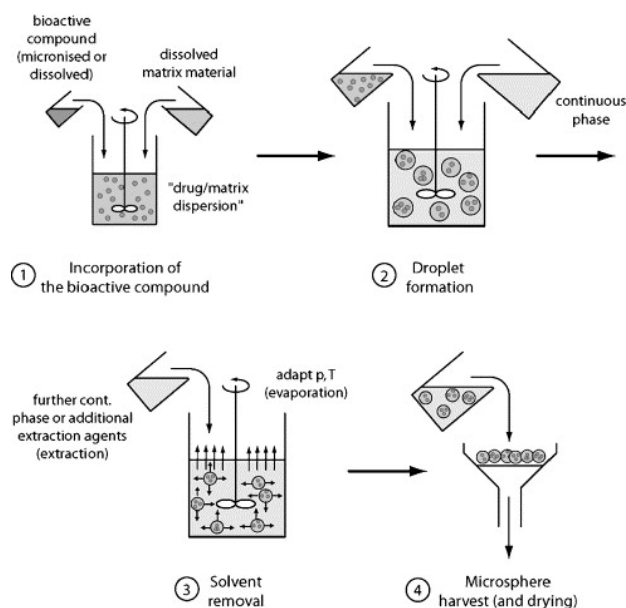


**Figure 10: w/o/w process where bioactive compounds are dissolved [61]**

A PLGA derivative of known Mw was dissolved in a determined volume (5 mL) of organic solvent (e.g. MC or EtAc) under magnetic stirring. Simultaneously, the Ab was dissolved in a fixed volume of buffer ( $W_1 = 1$  mL).  $W_1$  was added drop wise to the organic phase containing PLGA. An Ultra-Turrax<sup>®</sup> apparatus (IKA<sup>®</sup>, Staufen, Germany) was used during the first emulsification step at a selected agitation speed. When the aqueous phase was completely added, the stirring speed (6500 – 24000 rotations per minutes (rpm)) was increased to create a first w/o emulsion, containing fine droplets. After emulsification, the water droplets containing the Ab were entrapped in the polymer-containing organic solvent. The outer aqueous phase,  $W_2$ , was

composed of a known volume of water containing a known amount of surfactant such as PVA or PVP. This w/o emulsion was then transferred into a second aqueous phase (W2), which contains a surfactant, at a fixed agitation speed (250 rpm) to form the final w/o/w double emulsion. The system was left under magnetic stirring at room temperature and atmospheric pressure for 24 hours to allow the evaporation of the organic solvent, which led to the formation of solid particles suspended into the aqueous phase. The MS were recovered by filtration using Whatman ME29 paper filters with a porosity of 3  $\mu\text{m}$  (Whatman, England). The MS collected on the filter were washed a few times with Milli Q water. The filter was then placed under vacuum for 48 hours to dry the MS. The dried MS could then be collected and evaluated [3].

### **2.3.2 Solid-in-oil-in-water - solvent extraction process**

Although a w/o/w emulsion method is frequently used for the production of protein-loaded MS, the protein may lose its activity at the w/o interface. Therefore, a non-denaturing s/o/w emulsion evaporation/extraction technique may be more suitable for therapeutic proteins, because solid-state proteins retain their activity in organic conditions [62]. Indeed, solidified protein microparticles in the s/o/w emulsion may suppress the contact between the protein and the water-oil interface, which is one of the major causes of denaturation.

With encapsulation in the solid state, Ab microparticles had to be produced with an appropriate particle size. Spray-drying was selected as the drying process for the production of micronized Ab particles. It was estimated that a particle size ratio (SD microparticles compared to PLGA MS) of about 1/10 was required to be able to encapsulate the drug into polymer MS efficiently. Usually, needles of 22 - 25 G (inner diameters of 394 – 241  $\mu\text{m}$ ) are used for intravenous infusion, as well as for intramuscular and subcutaneous injections. Therefore, MS characterized by a lower mean diameter than the internal diameter of the needle are preferred (125 - 250  $\mu\text{m}$ ).

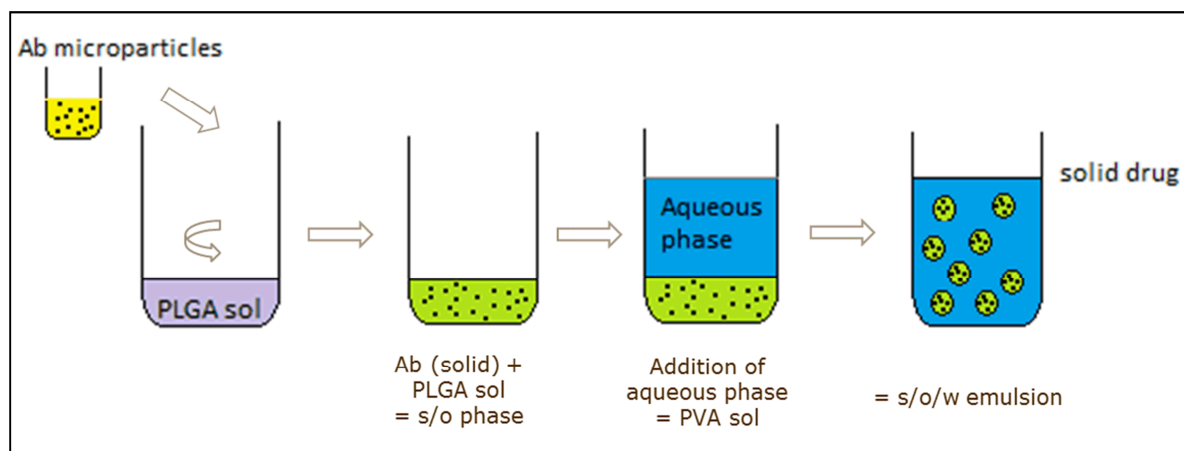


**Figure 11: Encapsulation process of Ab into PLGA MS using the s/o/w method**

PLGA was dissolved in a fixed volume (5 mL) of organic solvent such as MC or EtAc under magnetic stirring at a concentration ranging from 1 – 15 % (w/v) at room temperature (RT) (Figure 11). The solid-in-oil (s/o) dispersion was formed by adding (30 – 150 mg) the SD Ab (SD Ab) powder into the organic solution of PLGA using a T25 digital Ultra-Turrax<sup>®</sup> high-performance disperser equipped with the S25N – 8 G dispersing tool (IKA<sup>®</sup>, Staufen, Germany) set at 13500 rpm for 1 - 2 minutes. This suspension was added to 30 – 100 mL of an aqueous external phase containing 0.1 - 2.0 % (w/v) of a surfactant such as PVA or PVP and maintained under agitation using the Ultra-Turrax<sup>®</sup> stirrer at 3400 - 13500 rpm for 1 – 5 minutes. Finally, the s/o/w emulsion was added into an additional volume of water (100 – 400 mL extraction phase) to produce the final s/o/w emulsion. This emulsion was maintained under magnetic stirring for 30 min – 24 h to allow both the extraction and the evaporation of the organic solvent. The MS were recovered by filtration using nylon filters with a porosity of 0.2  $\mu\text{m}$  (Nylaflo<sup>™</sup>, Pall, Zaventem, Belgium), washed several times with Milli Q water and finally dried [63, 64].

### 2.3.3 Solid-in-oil dispersion spray-drying process

Atomization of Ab suspension in PLGA solution (s/o) is also an interesting alternative (Figure 12).

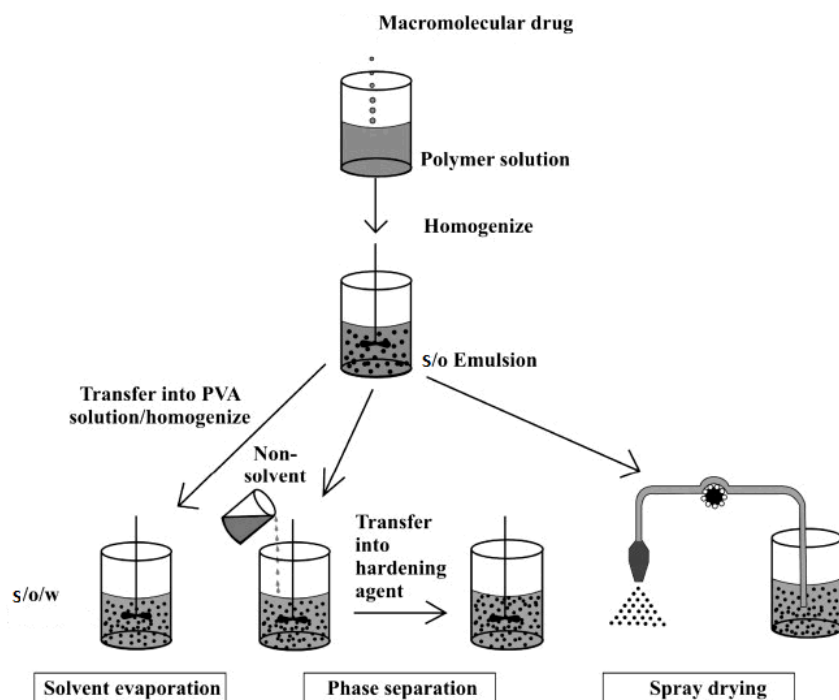


**Figure 12:** s/o/w or s/o spray-drying processes (adapted from [42])

A PLGA derivate characterized by a known molecular weight was dissolved in a known volume of organic solvent such as MC or EtAc under magnetic stirring. A weighed amount of IgG microparticles was dispersed in a known volume of the PLGA solution. This was done as described before using a Ultra-Turrax<sup>®</sup> at a selected agitation speed (V1) for 2 minutes to form an s/o dispersion. This s/o dispersion was then spray-dried in order to remove the organic solvent and form MS by solidification of the polymer with the atomization air flow set at 400 – 800 L/h N<sub>2</sub>, the feed flow rate at 15 – 35 %, the inlet T° at 50 - 85°C and the outlet T° at 25 – 38°C.

### 2.3.4 Drying techniques for the PLGA Microspheres

A final drying was applied to remove water from the PLGA MS.

#### a. Vacuum drying

The filter, previously described for collecting the produced MS, with the collected PLGA MS was placed under vacuum for 48 hours. Then, the PLGA MS were placed under vacuum for 2 hours at 1 mBar.

### **b. Freeze-drying**

Freeze-drying was carried out using a Epsilon 2-6D freeze dryer (Martin Christ, Osterode am Harz, Germany). After the filtration and the washing, the produced MS were put in lyophilization vials (3 mL) and directly resuspended with 1 mL of the aqueous solution containing 0.5 – 5 % w/v lyoprotectant (e.g. trehalose, sucrose). The vials were put directly into liquid nitrogen to freeze the suspension rapidly. The vials were then placed in the freeze dryer, which was previously thermostated at - 40°C. Temperature probes were inserted into the vials before freezing to measure the product temperature during the lyophilization process. The sublimation was carried out at - 35°C ( $< T_g$ ) at  $< 1$  mBar pressure. The secondary drying was performed at 0°C and 0.01 mBar pressure. A final drying was applied for 6 h at 20°C. The produced freeze-dried CDP571-loaded PLGA MS were stored at 2 - 8°C before dosing. Just before administration, the freeze-dried MS were resuspended in an appropriate volume of water to prepare a 15 % (w/v) suspension.

### **2.4 Preparation of the placebo PLGA microspheres**

Placebo MS were prepared following the same manufacturing process described previously but without the dispersion of Ab step (= s/o dispersion).

## **3 ANALYTICAL METHODS**

The physicochemical properties of both the drug and the delivery system were characterized during the project.

### **3.1 Antibody characterization**

Before these biopharmaceuticals enter clinical programs to evaluate their therapeutic potential, they need to be extensively characterized and adequately monitored during and after manufacturing and storage with regard to structural and biological integrity and molecular and biological properties. With recent technological progress, various analytical methods are currently available to characterize biopharmaceuticals better. Molecular weight, conformation, size and shape and extent of aggregation are a few of the physico-chemical properties which should be studied [21].

### 3.1.1 UV–Vis transmission spectroscopy

UV–Vis transmission measurements are used in several assays for the determination of protein concentration, colorimetry, solubility and turbidity [19].

#### a. Protein Concentration – A280

The total CDP571 assay was performed using UV spectrophotometry at 280 nm on a Varian<sup>®</sup> 50 Bio UV/VIS spectrometer equipped with a Solo VPE optical fiber (C Technologies, Inc., Bridgewater, USA) or on a SpectraMax M5 microplate reader (Molecular Devices, Sunnyvale, USA). The concentrations were calculated using the established mass attenuation coefficient ( $\mu = 1.61 \text{ mL/mg.cm}$  for the CDP571) or using a calibration curve plotted as absorbance values vs. known Ab concentrations.

#### b. Total protein assay by BCA (Bicinchoninic acid) colorimetric assay

The evaluation of IgG encapsulated inside MS was performed by total protein assay using the BCA method. This method is not able to provide information on the physicochemical stability of the product. The Pierce protocol “Microplate procedure” was followed [65]. Before dosing IgG inside MS, it was necessary to extract IgG from the MS. For this purpose, a known quantity of MS (5 - 20 mg) was placed in contact with 1 mL of NaOH 0,1 N solution to dissolve the polymer and the protein. The working reagent was prepared by mixing 50 parts of BCA Reagent A (solution containing sodium carbonate, sodium bicarbonate, bicinchoninic acid and sodium tartrate in 0.1 M sodium hydroxide) with 1 part of BCA Reagent B (solution containing 4 % cupric sulfate) (50:1, Reagent A:B). 25  $\mu\text{L}$  of each standard or unknown sample was put into a microplate well (working range 20 – 2000  $\mu\text{g/mL}$ ). 200  $\mu\text{L}$  of the working reagent was added to each well. After 30 seconds mixing on a plate shaker, the plate was covered and incubated at 37°C for 30 minutes. The absorbance was measured at 562 nm on a SpectraMax M5 microplate reader (Molecular Devices, Sunnyvale, USA). A standard curve was prepared by plotting the average 562 nm measurement for each IgG standard vs. its concentration in  $\mu\text{g/mL}$ . This standard curve was used to determine the IgG concentration of each unknown sample.

#### c. Determination of turbidity

Potential insoluble aggregates ( $> 5 \mu\text{m}$ ) were evaluated by measuring the turbidity at 350 nm on the sample solutions on the SpectraMax M5 microplate reader (Molecular Devices, Sunnyvale, USA). Spectra were recorded from 270 to 350 nm with a resolution of 5 nm.

### **3.1.2 Dynamic light scattering**

Dynamic light scattering (DLS), also called Photon correlation spectroscopy, is a useful technique for determining the size distribution of particles in a suspension and detecting small amounts of high molecular weight species in protein samples [66]. The scattered light may allow detection of proteins from sizes of 1 nm to 10  $\mu\text{m}$  [21].

Soluble protein aggregation was evaluated by DLS using a DynaPro plate reader (Wyatt, Santa Barbara, USA). Ten acquisitions of 10 seconds were performed on sample aliquots of 20  $\mu\text{L}$  after 2 minutes centrifugation at 3000 rpm.

### **3.1.3 Fluorescence intensity**

The Ab spectra were recorded on a Gemini EM spectrofluorimeter or a SpectraMax M5 microplate reader (Molecular Devices, Sunnyvale, USA) using a 96 - wells black micro plaque for qualitative evaluation of the tertiary structure. Each spectrum was a measurement performed from 300 to 380 nm with a resolution of 5 nm. The selected wavelength for excitation was set at 280 nm. A fluorescence intensity ratio was calculated at 330 and 340 nm [62]. The increase of this ratio indicated a blue shift (towards to shorter wavelength) of the emission spectrum, most likely resulting from an overall increased hydrophobic environment and/or chemical degradation.

### **3.1.4 Fourier-transform infrared spectroscopy**

Infrared spectroscopy can provide information on the secondary structure of a protein in both aqueous and solid states [19, 67]. Fourier-transform infrared spectroscopy (FT-IR) may determine the amount of chemical degradation in protein formulations.

FT-IR studies were conducted using:

- An Equinox 55 from Brücker (Coventry, UK) equipped with an attenuated total reflectance (ATR) accessory from the “Structure et Fonction des Membranes Biologique” laboratory at the ULB.
- A Spectrum One FT-IR Spectrum equipped with a Perkin ATR rotative press Sampling Accessory from PerkinElmer (Waltham, US)

15  $\mu\text{L}$  of each Ab solution was put on the ATR accessory. The water was removed in airflow before scan recording on the formed film. Scans ( $1800 - 1400 \text{ cm}^{-1}$ ) were collected and averaged to obtain a simple spectrum. All spectra were analyzed in the amide I region ( $1700 - 1600 \text{ cm}^{-1}$ ).

The Euclidean distance was calculated to compare the spectra. According to the Euclidean distance formula, the distance between two points in the plane with coordinates  $(x, y)$  and  $(a, b)$  is given by Equation 1. The source of this formula is in the Pythagorean Theorem [68].

$$\text{Dist}((x, y), (a, b)) = \sqrt{(x - a)^2 + (y - b)^2} \quad \text{(Equation 1)}$$

### 3.1.5 Size exclusion chromatography

SEC is one of the most commonly used analytical methods for the detection and quantification of both the HMWS and the LMWS [21]. Insoluble aggregates are not considered to be measurable by SEC due to potential removal via filtration by the column or by the sample preparation for SEC.

#### a. SEC – IgG

The assay of IgG monomer and evaluation of HMWS and LMWS was achieved using a Hewlett Packard Agilent 1100 HPLC system with UV detector from Agilent Technologies, Inc. (Diegem, Belgium) [69]. A TSK Gel G3000 SWXL 7.8 mm x 30.0 cm column (Tosoh Bioscience GMBH, Stuttgart, Germany) with a TSK Gel Guardcol SWXL 6.0 mm x 4.0 cm guard column (Tosoh Bioscience GMBH) was used with the flow rate set at 0.5 mL/min, the volume of sample injection at 20  $\mu\text{L}$  with a protein concentration range fixed at 25 – 1000  $\mu\text{g}/\text{mL}$  and a wavelength of detection at 280 nm. The mobile phase was composed of a saline 0.05 M PB, pH 7.2.

The SEC data were summarized as the loss of monomer (Equation 2) or expressed as the relative level (%) of HMWS and LMWS.

$$\text{Loss of monomer} = \text{monomer before process} (\%) - \text{monomer after process} (\%) \quad \text{(Equation 2)}$$

#### b. SEC – Full-length MAb anti-TNF alpha (CDP571)

For dissolution studies and encapsulation efficiency evaluations, the evaluation of the MAb monomer and the HMWS and LMWS contents were carried out by SEC using a Hewlett Packard Agilent 1200 equipped with a UV detector (Agilent Technologies, Waldbronn, Germany). A

Zorbax Bioseries GF250 9.4 m length x 250 mm column (Hewlett Packard Analytical, Agilent Technologies, Santa Clara, USA) was used with a flow rate set at 1.0 mL/min, a volume of injection fixed at 50  $\mu$ L and a wavelength fixed at 280 nm. The mobile phase was composed of a 0.2 M PB, pH 7.0. The molecular weight of the detected species was evaluated using the Bio-Rad Gel Filtration Standard, a lyophilized mixture of molecular weight markers ranging from 1350 to 670000 Da (Bio-Rad Laboratories, Hercules, USA).

The concentration of Ab monomer was determined using a calibration curve (from 10 to 2000  $\mu$ g/mL) built with known concentrations of Ab standard solution stored at - 80°C. The blank was removed.

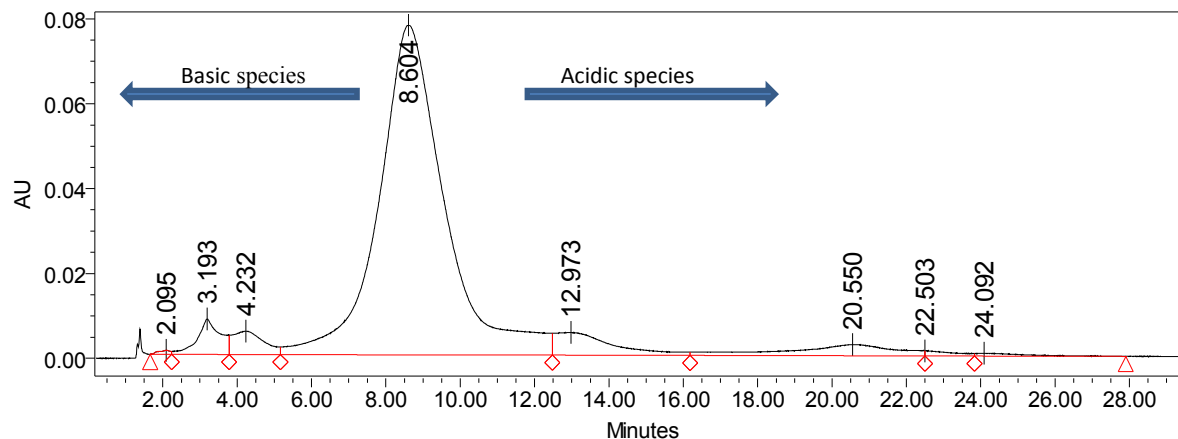
### 3.1.6 Strong anion exchange chromatography – Full length antibody anti-TNF alpha (CDP571)

The quantity of acidic and basic species was determined by strong anion exchange (SAX) chromatography. A Pro-Pac SAX-10 4 x 250 nm column heated to 30°C was used with the flow rate set at 1.0 mL/min, the volume of sample injection at 30  $\mu$ L with a protein concentration range fixed at 25 – 1000  $\mu$ g/mL and the wavelength of detection at 280 nm.

The mobile phases were composed of a 10 mM di-sodium hydrogen PB, pH 7.8 as eluent A, and a 10 mM di-sodium hydrogen PB, 150 mM NaCl, pH 7.8 as eluent B, with the gradient described in [Table 8](#).

**Table 8: SAX gradient**

Time (min)	(%) eluent A	(%) eluent B
0	85	15
1	85	15
40	45	55
42	45	55
44	85	15
54	85	15



- Peaks with a retention time < 8.6 were identified as the basic species.
- The peak with a retention time = 8.6 was identified as the CDP571 main peak.
- Peaks with a retention time > 8.6 were identified as the acidic species.

**Figure 13: Example of an SAX chromatogram for CDP571**

### 3.1.7 Enzyme-linked immunosorbent assay (ELISA test)

The binding capacity and the plasmatic concentration of the MAb was evaluated using an ELISA test developed for human TNF- $\alpha$  and the results were expressed as a percentage of the measured sample concentration determined at 280 nm. In summary, human TNF- $\alpha$  (R&D Systems, Minneapolis, USA) immobilized on a 96-well plate was incubated with samples containing MAb. Bound MAb was then detected using horseradish peroxidase (Cappel, MP Biomedical, Belgium) conjugated goat IgG fraction to a human kappa chain, with the reaction visualized by addition of the chromogenic substrate tetramethylbenzidine (Sigma-Aldrich, Diegem, Belgium). Absorbance values (proportional to the amount of MAb present in the sample) were measured at 450 nm. The standard curve was prepared using the MAb standard solution stored at - 80°C as the reference.

### 3.1.8 Bioassay

#### a. TNF bioassay

The potency of the MAb samples was determined using a bioassay, which was a TNF-alpha cytotoxicity neutralization assay using WEHI 164 cells. After treatment with TNF, the anti-TNF alpha activity of the MAb was evaluated measuring the cell viability with a tetrazolium salt (MTT) assay. This assay is a colorimetric assay for assessing cell viability. The MTT, a yellow tetrazole, is reduced to purple formazan in living cells. A solubilization solution (dimethyl

sulfoxide solution) is added to dissolve the insoluble purple formazan product into a colored solution. The absorbance of this colored solution can be quantified by measuring at 595 nm. The half maximum effective concentrations ( $EC_{50}$ ) values, calculated from the dose-response curves (absorbance vs. concentration), represent the concentration of MAb that induced 50 % of the maximal neutralizing effect observed. The  $EC_{50}$  values were calculated using SoftMax Pro<sup>®</sup> Software (Molecular Devices, Sunnyvale, USA) using a 4 - parameter curve fitting. The MAb standard solution stored at - 80°C was used as the reference. A relative activity was calculated using the anti-TNF MAb reference standard stored at - 80°C considered being 100 % active (Equation 3). The relative potency was also estimated by the SoftMax Pro<sup>®</sup> Software using the parallel line analysis (PLA).

$$\text{Relative activity (\%)} = (EC_{50} \text{ sample}) / (EC_{50} \text{ reference}) \times 100 \quad (\text{Equation 3})$$

#### **b. Reporter gene bioassay**

TNF- $\alpha$  activity and its inhibition by anti-TNF alpha MAb are measured by stimulation of cells carrying a TNF-responding luciferase gene, and quantifying luciferase expression by luminometry [70]. The test procedure involved the use of division-arrested, frozen, ready-to-use TNF alpha-sensitive reporter cells (iLite TNF alpha Reporter Cells, Biomonitor, Ireland) in a bioassay which was able to evaluate the anti-TNF alpha activity using luciferase generated bioluminescence (Bright-Glo Luciferase assay system, Promega, USA). After incubation of the MAb samples with known amount of TNF alpha, the cells were added for quantifying the residual TNF alpha activity. The Dual-Glo<sup>®</sup> Luciferase Reagent (Promega Corporation, Madison, USA) was added directly to the cells. This reagent induces cell lysis and acts as a substrate for luciferase, producing a stable luminescent signal. The luminescence was measured using a SpectraMax M5 (Molecular Devices, Sunnyvale, USA). The increasing concentrations of anti-TNF alpha completely suppressed the luciferase activity in a dose-dependent manner. A 4-parameter curve was constructed and the  $EC_{50}$  was calculated for each sample. A relative activity was calculated using the anti-TNF MAb reference standard stored at - 80°C considered being 100 % active (Equation 3). The relative potency was also estimated by the SoftMax Pro<sup>®</sup> Software using the parallel line analysis (PLA).

### 3.2 Encapsulation efficiency and drug loading evaluation

The drug loading (content) of MAb in the PLGA MS was defined as the percent ratio between the quantified amount of encapsulated MAb and the total amount of MS (Equation 5). The EE % referred to the percent ratio between the amount of MAb encapsulated in the MS compared to the total amount of MAb introduced into the organic phase. The theoretical drug loading content, actual drug loading content, and EE % were calculated from Equation 4, 5, and 6, respectively.

An exact amount of PLGA MS ranging from 5 to 20 mg was placed in contact with 750  $\mu$ L of MC to dissolve the polymer. The MAb was extracted from the MC with 4 volumes of PBS buffer pH 7.4 using 15 minutes of centrifugation at 3000 – 8800 rpm. The aqueous phases were combined and the drug loading, EE %, SEC profile and activity of the MAb were evaluated using the analytical methods described previously.

$$\textit{Theoretical drug loading content} (\%) = \frac{\textit{Weight of feed drug}}{\textit{Weight of feed drug and copolymer}} \times 100 \quad (\text{Equation 4})$$

$$\textit{Actual drug loading content} (\%) = \frac{\textit{weight of actual drug entrapped in microspheres}}{\textit{weight of drug-loaded microspheres}} \times 100 \quad (\text{Equation 5})$$

$$\textit{EE} (\%) = \frac{\textit{Actual drug loading content}}{\textit{Theoretical drug loading content}} \times 100 \quad (\text{Equation 6})$$

### 3.3 Dissolution study

Dissolution profiles of MAb from MAb - PLGA MS were evaluated by adding 1 mL of PBS buffered at pH 7.0 to 30 mg of MS in 2 mL tubes. The tubes were incubated at 37°C and stirred at 600 rpm using a Thermomixer comfort<sup>®</sup> micro tubes mixer (Eppendorf AG, Hamburg, Germany). At a pre-determined time, samples were centrifuged for 15 minutes at 12000 rpm and the supernatant (1 mL) was collected and filtrated on a 0.2  $\mu$ m HDPE Millex filter. The MS were suspended again in 1 mL of fresh PBS solution for further dissolution. The burst effect was calculated as the percentage of MAb released after 24 hours.

The pH of the sample solutions collected during the dissolution was measured with a Hach sensION pH31 micro pH meter (Loveland, USA). The dissolution profiles of different formulations were compared based on the FDA guidance recommended metric that refers to the similarity factor ( $f_2$ ). The dissolution profiles of different formulations were compared based on the FDA guidance recommended metric that refers to the similarity factor ( $f_2$  – Equation 7) to assess whether change occurred during the stability study:

$$f_2 = 50 \log \left\{ \left[ 1 + \frac{1}{n} \sum_{t=1}^n (R_t - T_t)^2 \right]^{-0.5} \times 100 \right\} \quad (\text{Equation 7})$$

where  $R_t$  is the percentage dissolved at each time point for the reference formulation and  $T_t$  is the percentage dissolved at each time point for the test formulation. It was noted that an  $f_2$  value between 50 and 100 suggests that the two dissolution profiles under consideration are similar and indicates a point-point difference of 10 % or less [71].

Several kinetic models based on different mathematical functions, such as zero order, Higuchi and Korsmeyer models, were applied to describe the overall release of MAb from the evaluated dosage for MS [72, 73]. The plotted curves obtained from the evaluated kinetics models described previously were regressed and the corresponding coefficients of determination ( $r$ ) and slopes were computed.

### 3.4 Particle size and morphology characterization

#### 3.4.1 Laser diffraction

Laser diffraction is a technique that measures particle size distributions by measuring the angular variation in intensity of light scattered as a laser beam passes through a dispersed particle sample.

The particle size of the Ab microparticles and PLGA MS was evaluated using a Malvern Mastersizer Hydro 2000 S (Malvern Instruments, Malvern, UK). Ab microparticles were analyzed after dispersion in isopropanol. A refractive index of 1.520 was used as default value. PLGA MS were analyzed, with water as the dispersion medium, using refractive indexes of 1.33 and 1.55 for water and PLGA, respectively. Prior to measurement, each sample was sonicated for 30 seconds after addition of one droplet of Tween 20 to de-aggregate the particles. The particle size distribution was evaluated in terms of the  $d(0.1)$ , the median diameter  $d(0.5)$  and the  $d(0.9)$ ,

which are the diameters below which lie 10 %, 50 % and 90 % of the particles, respectively. The  $D[4, 3]$ , the volume moment mean (De Brouckere mean diameter), was also reported.

### **3.4.2 Scanning Electron Microscopy**

The morphology of the surface and the internal porosity of the polymeric MS were observed using an XL30 ESEM-FEG scanning electron microscope from Philips (Eindhoven, Netherlands) with an environmental chamber. This microscope was equipped with a field emission gun. The images were obtained using secondary electrons (topographic contrast) at an accelerating voltage of 10 kV. To observe the external surfaces, the MS were deposited on an adhesive conductive support (carbon). Sectional views were made and the internal porosity evaluation was carried out after coating the samples in an epoxy resin and cutting and polishing them with a microtome diamond knife [74, 75].

### **3.5 Residual moisture content**

Residual moisture content was determined by Karl-Fischer titration using a Karl-Fischer Headspace 774 oven sample processor (Metrohm, Anvers, Belgium). The samples are automatically transferred into a temperature controlled oven from where the evaporated water is transferred to the titration cell via an applied gas flow. Approximately 15 mg sample was weighed and analyzed by heating to 120°C. 50 mg of Hydranal (4.90 - 5.20 %, 150°C) was used as the calibration standard.

### **3.6 Residual solvent content**

Residual solvent (EtAc) was determined by gas chromatography using an Agilent 6890 N equipped with a flame ionization detector (Agilent Technologies, Santa Clara, USA). A 50 m long x 0.32 mm Fused Silica WCOT (Varian, Agilent Technologies, Santa Clara, USA) was used as the stationary phase. Standard calibration solutions were prepared from an EtAc solution in dimethyl formamide. The samples were prepared by weighing accurately around 20 mg of MS in a 10 mL head space vial and adding exactly 2 mL of dimethyl formamide.

### 3.7 Thermogravimetric analysis

Thermogravimetric analysis was used to measure the residual solvent content and the residual moisture content using a TA instruments Q500 Thermogravimetric Analyzer (US). The samples were stabilized for 15 min at 25°C and then heated from 25°C to 150°C at 10°C/min.

### 3.8 Differential scanning calorimetry

Differential scanning calorimetry (DSC) is a thermal analysis technique that looks at how a material's heat capacity ( $C_p$ ) is changed by temperature [76]. This allows the detection of transitions such as melts, glass transitions and phase changes [77].

During this project, DSC analysis was carried out using a DSC Q2000 (TA instrument, New Castle, USA) and Tzero aluminum hermetic pans with lids at different steps of the encapsulation process:

- On PLGA and dried PLGA MS (5 - 10 mg) it was used to determine the  $T_g$  of the polymer during heating. The DSC was performed by heating the powders from 0°C to 55 - 60°C (cycle 1) at a rate of 10°C/minute. The samples were cooled from 55 - 60°C to 0°C (cycle 2) and heated again from 0°C to 200°C (cycle 3) at the same rate. All  $T_g$  values were reported as the inflexion point of the transition measured during cycle 1 and confirmation obtained during cycle 3, and the enthalpy of relaxation.
- On formulation solutions and corresponding Ab-loaded PLGA MS suspensions (5 – 10 mg) it was used to determine the  $T_g$ , during freezing. All  $T_g$  values were reported, as well as the inflexion point of the transition. The applied DSC cycle is described in [Table 9](#).

**Table 9: DSC cycle for solutions and MS suspensions**

Step	Temperature (°C)	Rate (°C/min)
Cooling	25 → - 60	10
15 minutes equilibrium	60°C	NA
Heating	- 60 → 25	10

### 3.9 X-ray powder diffraction (XRPD)

SD powders and PLGA MS were analyzed by XRPD using a Bruker D8 Advance Cu anode and Lynx Eye detector (Karlsruhe, Germany) with a standard method scan from 4.5° to 50° in 2 $\theta$ , divergence slit 12 mm. The crystallinity was estimated by deducting the surface area of the contribution of the amorphous part from the total surface area.

### 3.10 Gel permeation chromatography

Gel permeation chromatography (GPC) was used to evaluate the Mw of the PLGA during the stability study performed on the MAb - loaded PLGA MS.

The GPC system consisted of a HP 1200 series HPLC (Agilent Technologies, Diegem, Belgium) equipped with a binary pump, an auto sampler, a column oven profile at 40°C and a refractive index detector (RI). Two PLgel 5 micron Mixed C - 300 7.5 mm analytical columns were placed in series (Mw ranging from 200 to 2000000 g/mole) (Varian, Agilent Technologies, Diegem, Belgium) and heated to 40°C. The flow rate was set at 1.0 mL/min and the run time was fixed at 30 minutes. The mobile phase consisted of tetrahydrofuran. The calibration was based on the results achieved using polystyrene standards of known Mw (EasiVial standard PS -M Varian, Agilent Technologies, Diegem, Belgium). The standards were diluted in 1.0 mL of tetrahydrofuran to reach suitable concentrations. The dried samples obtained during the study were dissolved in tetrahydrofuran to provide a final concentration of 1 mg/mL, filtered through a PTFE membrane with porosity of 0.22  $\mu$ m and finally injected into the GPC system.

### 3.11 Freeze-drying microscopy

A Lyostat3 freeze-drying microscope (FDM) (Biopharma Ltd) was used to determine the collapse temperature ( $T_c$ ) and eutectic temperature ( $T_{eut}$ ) of the freeze-dried formulations. 2  $\mu$ L sample solutions were frozen and then dried under vacuum (0.001 mBar) while heated from -

60°C to 20°C. Images were collected during freeze-drying. At  $T_c$  or  $T_{out}$ , samples show the first signs of collapse and continued to dry with poor structure.

### **3.12 Syringeability / injectability study**

To evaluate the flow properties of the PLGA microparticulate system, a syringeability / injectability study was performed. MS were suspended in 1 mL water in a 3 mL-capacity glass vial. The resulting suspension was withdrawn into a syringe and subsequently injected out. In the study, a regular hypodermic disposable plastic syringe and a 23 G needle were employed. The study was realized using Zwick Roell equipment (Zwick GmbH & Co. KG, Ulm, Germany), with a speed set at 360 mm/min. The parameters studied included ease of withdrawal, freedom from clogging and maximum force applied.

### **3.13 Statistical analysis**

DoE is a practical approach for exploring multifactor opportunity spaces. This branch of applied statistics deals with planning, conducting, analyzing and interpreting controlled tests to evaluate the factors that control the value of a parameter or group of parameters. A strategically planned and executed experiment may provide a great deal of information about the effect on a response variable due to one or more factors. These methodical experimentations were applied to reveal or model relationships between factors and responses during this work. The DoEs were designed and analyzed using version 8.0.2 JMP statistical software (SAS, NC, USA). Mathematical models based on these relationships were constructed for the DoE. The prediction fitted model was determined using the least square regression method [78, 79]. An analysis of variance (ANOVA) was performed to validate the statistical model. The effects of the investigated factors were determined using the least square regression method [80, 81]. A statistical hypothesis test was performed to identify the statistically significant effects of the factors. In statistics, a result is called statistically significant if it has been predicted as unlikely to have occurred by chance alone, according to a pre-determined threshold probability, the significance level. In statistical significance testing, JMP used a two-tailed test for computing the statistical significance of a data set.

Statistical hypothesis tests (e.g. Student's t-test) were used to determine whether sets of data were significantly different from each other. Differences were considered significant at  $p < 0.05$ .

## 4 IN VIVO EVALUATIONS

### 4.1 Preliminary pK study on CDP571 solutions (IV)

The plasmatic pK profile of CDP571 was evaluated, at UCB Braine site, in rat after single and repeated IV administration at 10 and 100 mg/kg. The injected formulations were a 5 mg/mL and a 50 mg/mL CDP571 solution containing 0.27 M glycine, 1% maltose (w/v) at pH5.0. The volume of injection was 2 mL/kg. The 12 animals (Sprague Dawley rats from Charles River, France) were allocated to four different groups (n = 3 rats/group) (Table 10).

**Table 10: Experimental protocol of the preliminary pK study**

Groups	ID Rats	Design	Route	Dose (mg/kg)	Day of dosing	Samples	Time points
1	1 - 3	pK rat single	IV	10	1	Plasma	15 min - 1 h - 6 h -24 h - 48 h - D3 - D4 -D5 - D6 - D10
2	4 - 6	pK rat single	IV	100	1	Plasma	
3	7 - 9	pK rat repeated	IV	10	1 and 11	Plasma	15 min - 1 h - 6 h -24 h - 48 h - D3 - D4 -D5 - D6 - <b><u>D10 post second administration on Day 11</u></b>
4	10 - 12	pK rat repeated	IV	100	1 and 11	Plasma	

The first day of administration was considered as Day (D) 1. In groups 3 and 4, the blood samples were collected after the second IV administration on Day 11 and over 10 days after this second administration following the same schedule applied to groups 1 and 2.

### 4.2 pK study on CDP571 loaded PLGA MS (SC)

The plasmatic pK profile of CDP571 was evaluated in rat after single SC administration at 50 mg/kg. A 20 mg/mL CDP571 solution containing trehalose and histidine at pH 6.0, used as a control formulation, was administrated at 2.5 mL/kg. The investigated controlled-release formulations were the CDP571-loaded RG505 and RG755S MS in suspension.

Aqueous CDP571 solutions with a 40 mg/mL CDP571 concentration in ~ 30 % (w/w) trehalose in a 20 mM histidine pH 6.0 buffer prepared as described previously were spray dried. Four batches of CDP571 loaded Resomer<sup>®</sup> RG505 MS and four batches of CDP571-loaded Resomer<sup>®</sup>

RG755S MS were then produced and freeze-dried after resuspension in 1 mL of 0.5 % (w/v) trehalose solution.

The drug loading of the RG505 and RG755S MS was measured to be  $10.0 \pm 0.03$  % (w/w) and  $12.5 \pm 0.2$  % (w/w), respectively (Table 49). Just before administration, the freeze-dried MS were resuspended in an appropriate volume of water to prepare a 15 % (w/v) suspension. The volumes to be administered for dosing at 50 Mab mg/kg were 3.3 mL/kg and 2.7 mL/kg for the RG505 and RG755S MS, respectively.

The corresponding placebo formulations were injected as controls in the opposite side of the same rat.

The 12 animals (Sprague Dawley rats from Charles River, France) were allocated to three different groups (n = 4 rats/group) as summarized in the Table 11.

**Table 11: Experimental protocol of the pK study**

Groups	ID Rats	Design	Route	Dose (mg/kg)	Formulation	Samples	Time points
1	1 - 4	pK rat single	SC	50	Aqueous buffer	Plasma	6 h – 24 h – 48 h and once a week up to 2 months post-dose
2	5 - 8	pK rat single	SC	50	RG505 MS	Plasma	
3	9 - 12	pK rat single	SC	50	RG755S MS	Plasma	

The first day of administration was considered as Day 1. The tested formulations were injected using a 1 mL syringe with a 22 G needle. For each group, the test formulation was injected subcutaneously in the right flank. The respective control placebo was injected subcutaneously in the left flank. At the end of the study, the skin at the injection site (control and test) was collected and prepared for histological examination.

### 4.3 pK analysis

Blood samples (~ 200 µL) were collected on lithium heparin via the tail vein and centrifuged to separate plasma. Plasma samples were stored at - 80°C. The MAb plasmatic concentration was measured by ELISA. pK parameters (area under the concentration - time curve (AUC), elimination of the drug from the body expressed as the volume of blood cleared of drug per unit time (CL), half-life ( $T_{1/2}$ ), maximum plasma concentration ( $C_{max}$ ), maximum time to peak

concentration ( $T_{max}$ ) were calculated based on the concentration-time profiles after IV administration. The pK parameters were calculated by non-compartmental methods using the Phoenix<sup>®</sup> pharmacokinetic software (Certara, St Louis, USA). The AUC was calculated using the trapezoidal rule from zero to the last observed concentration. The  $C_{max}$ , the  $T_{max}$  and the CL were registered from the observed plasma concentration time data.

#### **4.4 Histological study**

Tissue samples from the various rat studies (Table 11) were fixed in 10 % formalin and sections were immersed in paraffin and cut using a microtome [82]. The inflammation effect of the PLGA MS was determined via histological examination using hematoxylin and eosin staining. Placebo solutions injected into the left flank of the group 1 rats (Table 11) were used as a negative control. Photomicrographs of the histology slides were taken and digitally stored using an Olympus microscope (model Ax70, Olympus America, Melville, NY) at a 10× magnification.

## EXPERIMENTAL APPROACH

The aim of this project was to stabilize and develop a sustained release platform for biological compounds. Microparticulate polymer-based formulations were selected as the preferred technical approach. The encapsulation method had to maintain the native structure of the biological compound and so preserve its biological activity. On the other hand, the process had to achieve sufficient drug loading ( $> 20\%$  w/w) into the MS to allow administration of the therapeutic doses ( $> 100$  mg/mL). The target release profile had to reach a time greater than that observed with typical biological formulations in solution (e.g.  $> 1$  month). The dissolution profile of the drug had to demonstrate sustained release. Thus, the effects of peaks and valleys in plasma curves had to be avoided *in vivo* by providing a continuous and regular supply of drug. Finally, the delivery system had to be administered subcutaneously through accepted needles ( $> 22$  G).

Briefly, the selection and the optimization of the encapsulation method were performed using a bovine IgG as model molecule. The preferred method was then applied to an anti-TNF alpha MAb to demonstrate that the process did not affect the properties and biological activity of the drug.

The experimental approach is summarized in [Figure 14](#) and is divided into 7 stages.

1. The first part of the work was to select a suitable encapsulation process for biological compounds. Bovine IgG was used as a model. Three methods described in the literature were tested: the w/o/w, the s/o/w method and spray-drying a s/o dispersion. The s/o/w method was preferred.
2. Following the selection of the s/o/w method, the spray-drying process appeared to be a good technique of producing solidified Ab microparticles characterized by properties appropriate for encapsulation. A screening study was realized in order to optimize the process parameters.
3. The third part of the work aimed at increasing the drug loading, the release time and the stability of the Ab during the encapsulation process and the release of drug from the polymer matrix. The s/o/w process parameters were optimized accordingly thanks to a design of experiment.

4. The optimized encapsulation process developed using bovine IgG was applied to the MAb anti-TNF alpha. To ensure the stability and activity of the MAb, the formulation was adapted. The fourth stage of the experimental part described the development of the SD MAb anti-TNF alpha formulation. The addition of a stabilizer such as trehalose appeared to be essential to guarantee the activity of the MAb during the drying process.
5. The fifth part of the work focused on the choice of Mab formulation and the type of polymer. It appeared that the addition of stabilizer was important for the stability of the MAb but also that the choice of polymer played an important role in both the release time and the stability of the product during release from the MS.
6. A stability study was conducted on two MS formulations to evaluate the influence of the conditions and duration of storage on the activity, content and dissolution profiles of Mab and on the particle size and the morphology of the MS.
7. A pharmacokinetic study was finally carried out on the MAb - loaded polymer-based MS containing the anti TNF alpha MAb. The purpose of this investigation was to study and compare the pharmacokinetic profiles of the MAb obtained from the polymer MS with those obtained after administration of a standard MAb solution.

#### IV. Experimental approach

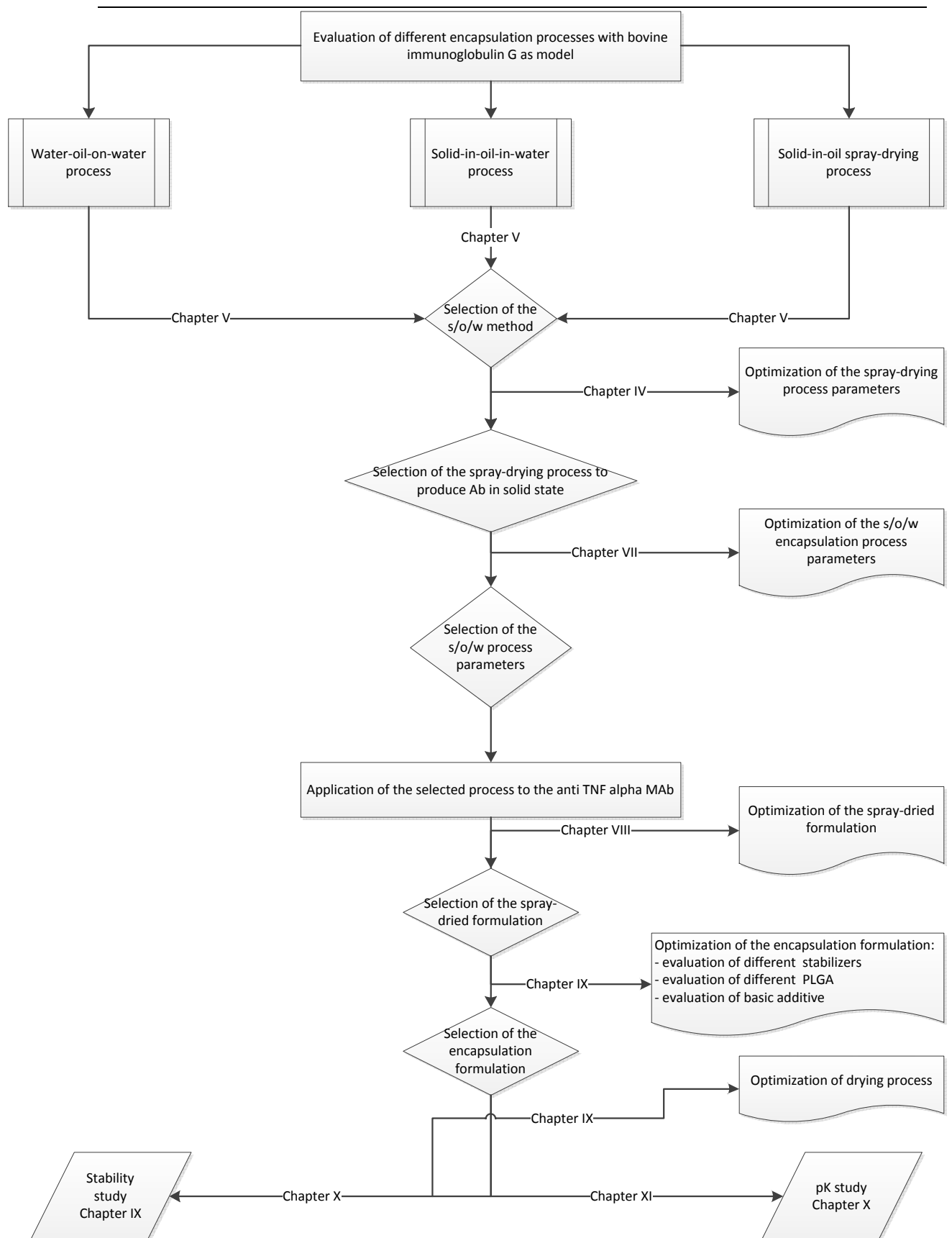


**Figure 14: experimental approach**

## **EXPERIMENTAL PART**

## **SELECTION OF THE TYPE OF ENCAPSULATION PROCESS SUITABLE FOR ANTIBODY**

### **1 INTRODUCTION**

The goal of this study was to select the appropriate manufacturing method for producing Ab-loaded PLGA MS. The IgG was used as a model to validate the concept of the selected encapsulation process and formulations.

Different methods such as the w/o/w, s/o/w and s/o spray-drying processes were evaluated for encapsulating the IgG in PLGA MS.

### **2 RESULTS AND DISCUSSION**

#### **2.1 Stabilization of IgG solution formulation**

During the encapsulation process, chemical degradation and aggregation issues may appear. These are caused in particular by the agitation rate, the air/liquid interface and the oil/water interface.

During a preliminary study, it was observed that a 2 minutes Ultra Turrax<sup>®</sup> stirring at 6500 rpm at RT decreased the percentage of IgG monomer to 78 % when it was dissolved in a 1.2 % w/v aqueous solution. When the IgG was dispersed in solid state in organic solvent, the same agitation conditions seemed to be less stressful, especially when using EtAc, as 95 % of the IgG remained as monomer after dispersion. With regard to these preliminary results, it appeared that the stability of IgG in solution needed to be improved for further encapsulation.

To select the IgG formulation in solution, a screening design was performed by modulating different variables identified from the literature [8, 45, 52]. In particular, the buffering system, the IgG concentration, the NaCl concentration, the type and the concentration of surfactants, the use of a polyol such as mannitol, amino acids and PEG and their concentration were considered as the main parameters to work with. The evaluated formulations are described in [Table 12](#) and [Table 37](#) in appendix. The low and upper levels of the studied factors are summarized in the [Table 12](#). A Plaket-Burman experimental plan was selected with 2 center points (sol IgG 1 and sol IgG 14; [Table 37](#) in appendix) to estimate

the main effects. The plan was then augmented with four additional tests (sol IgG 15 to 18; [Table 37](#) in appendix).

**Table 12** Experimental factors and levels

Factor	Low level	Upper level
Buffer	0.025 M histidine buffer pH 6	0.05 M PB pH 7.2
IgG concentration	1.2 % (w/v)	8.3 % (w/v)
Mannitol concentration	1 % (w/v)	10 % (w/v)
Type of amino acid	L-proline / L-arginine / L-serine	
Amino acid concentration	0.2 %w/v	5 % (w/v)
Type of surfactant	Tween 20	Pluronic F68
Surfactant concentration	0.025 % (w/v)	0.25 % (w/v)
PEG 4000 concentration	0.025 % (w/v)	0.5 % (w/v)
NaCl quantity	50 mM	250 mM

The stability of the IgG in the tested formulations (sol IgG 1 to sol IgG 18) was evaluated by a double emulsion process without the addition of PLGA ([Figure 15](#)). The primary emulsion w/o, the first step of the double emulsion process, was considered as the most stressful step for the IgG as the dissolved Ab was exposed to both the w/o and the liquid/air interfaces.

The subsequent solution was then emulsified with the MC for 2 minutes at 6500 rpm using an Ultra Turrax<sup>®</sup>. 10 mL PB was added to the w/o emulsion and centrifuged for 15 minutes at 4000 rpm [63, 83]. The aqueous fraction containing IgG was withdrawn for further analysis such as SEC and FT-IR. The “after process / before process” recovery of IgG concentration was calculated, providing an indication regarding the level of insoluble aggregates appearing during the emulsification process.

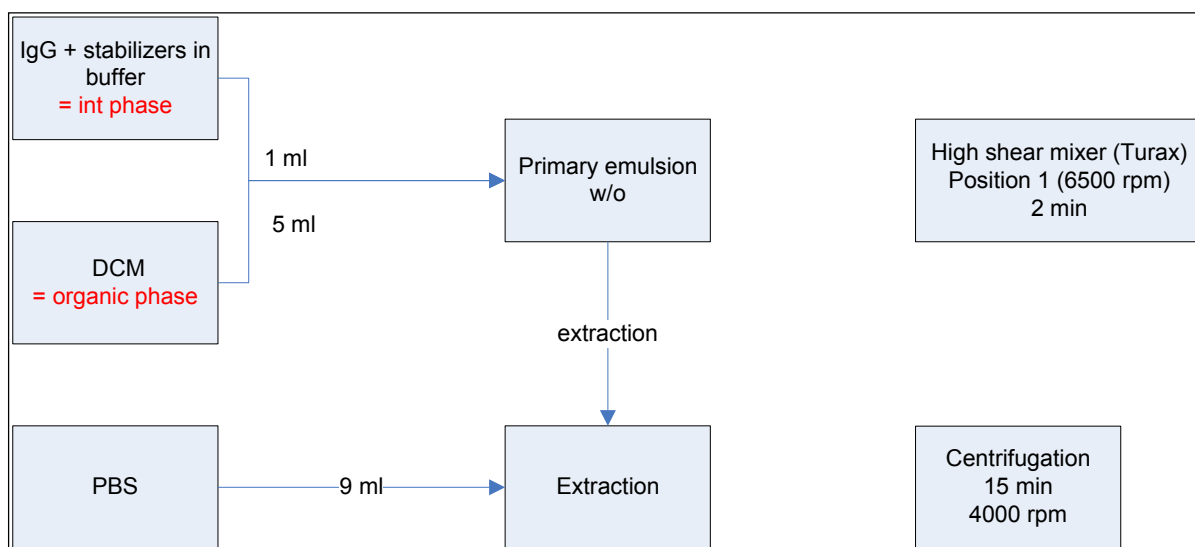


**Figure 15: Method of double emulsion process without PLGA**

### 2.1.1 Results and discussion

During the emulsification process, a precipitation issue was observed at the water/oil interface for all the samples. The “after process/before process” recovery of the IgG concentration, measured by SEC, ranged between 57 and 94 %, reflecting a high tendency to aggregation (Table 13). The highest recoveries ( $\geq 90$  %) were obtained for formulations containing proline and the highest quantity of dissolved IgG solubilized in the aqueous phase.

Due to this aggregation tendency, it was concluded that this type of encapsulation method (w/o/w), requiring an emulsification step (w/o), was not the most appropriate for Ab as a minimum amount of 6 % w/w of monomer was lost during the process.

When FT-IR spectra obtained from solutions collected before and after the emulsification step were compared, significant differences were observed between the formulations. A shift of the maximum absorbance of the amide I peak ( $1640\text{ cm}^{-1}$ ) was observed for some formulations, all containing the lowest quantity of IgG (Figure 16).

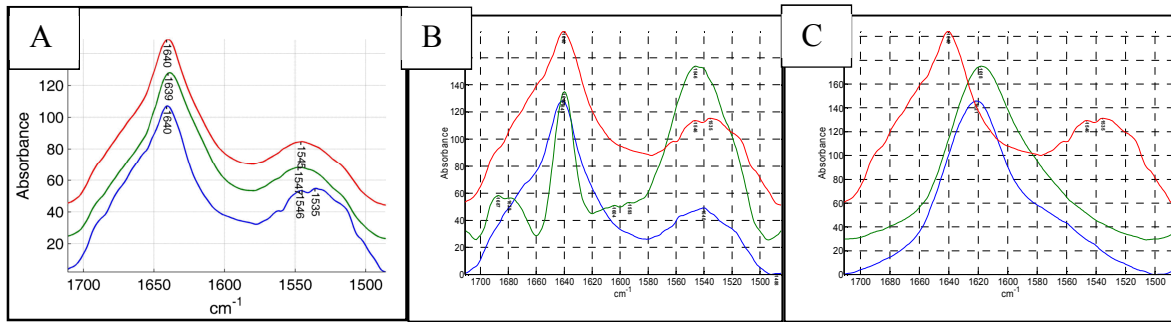


**Figure 16:** FT-IR spectra – sol IgG 8 (A); sol IgG 12 (B); sol IgG 14 (C) with the IgG reference in red, the solutions prior to the simulated encapsulation process in blue and the solutions after the simulated encapsulation process in green

Mostly, as illustrated in [Figure 16 A](#), when comparing the FT-IR spectra of the IgG reference (bovine lyophilized IgG) and the IgG in solution (sol IgG 8) before and after the process, no change was observed in term of intensity and wavelength of the amide I ( $1640\text{ cm}^{-1}$ ) and amide II ( $1545\text{ cm}^{-1}$ ) peaks. This observation led to the conclusion that the secondary structure of the IgG was maintained over the process. In contrast, as illustrated in [Figure 16 \(B\)](#), no significant change was observed between the FT-IR spectra of the IgG reference and the IgG solutions sol IgG 7, 11, 12 and 13 before the process. However, an additional peak and an increase in the intensity of the amide II peak ( $\sim 1545\text{ cm}^{-1}$ ) were observed after the process. Therefore, it seemed that the secondary structure was affected by the encapsulation process. In [Figure 16 \(C\)](#), a shift of the amide I peak ( $\sim 1640\text{ cm}^{-1}$ ) and the disappearance of the amide II peak ( $\sim 1545\text{ cm}^{-1}$ ) were already observed for the IgG solution (sol IgG 14) before the process. The formulation tended to modify the secondary structure. This was also the case for the formulations containing the lowest quantity of IgG with arginine as the amino acid (sol IgG 6 and 9).

In order to compare the FT-IR spectra easily, the Euclidean distance between the evaluated solution before and after the simulated encapsulation process was calculated to evaluate the difference between the spectra ([Table 13](#)). Values from 28 to 660 were observed. The highest values reflected the highest differences in the FT-IR spectra shape before and after the process. The formulations with the lowest IgG concentrations led to the highest Euclidean distance ( $> 150$ ). It appeared that the highest IgG concentration tended to stabilize the IgG.

**Table 13: IgG recovery (SEC) and Euclidian distance (FT-IR) for formulations sol IgG-1 to -18**

<b>Formulation (n=1)</b>	<b>Recovery after/before (%)</b>	<b>FT-IR Euclidian distance before/after</b>
sol IgG 1	72.3	162
sol IgG 2	82.3	79
sol IgG 3	84.6	73.9
sol IgG 4	90.1	94.7
sol IgG 5	80.5	312.1
sol IgG 6	56.7	207.2
sol IgG 7	79.8	113.3
sol IgG 8	83.8	27.7
sol IgG 9	68.8	188.5
sol IgG 10	87.3	86.8
sol IgG 11	82.2	96.3
sol IgG 12	78.5	660.2
sol IgG 13	81.3	99
sol IgG 14	86.3	158.6
sol IgG 15	94.0	109.5
sol IgG 16	85.4	93
sol IgG 17	85.8	83.6
sol IgG 18	89.7	63.3

The statistical analysis was conducted on the recoveries of the IgG concentration and the FT-IR Euclidean distances using JMP8 software ([Figure 17](#)).

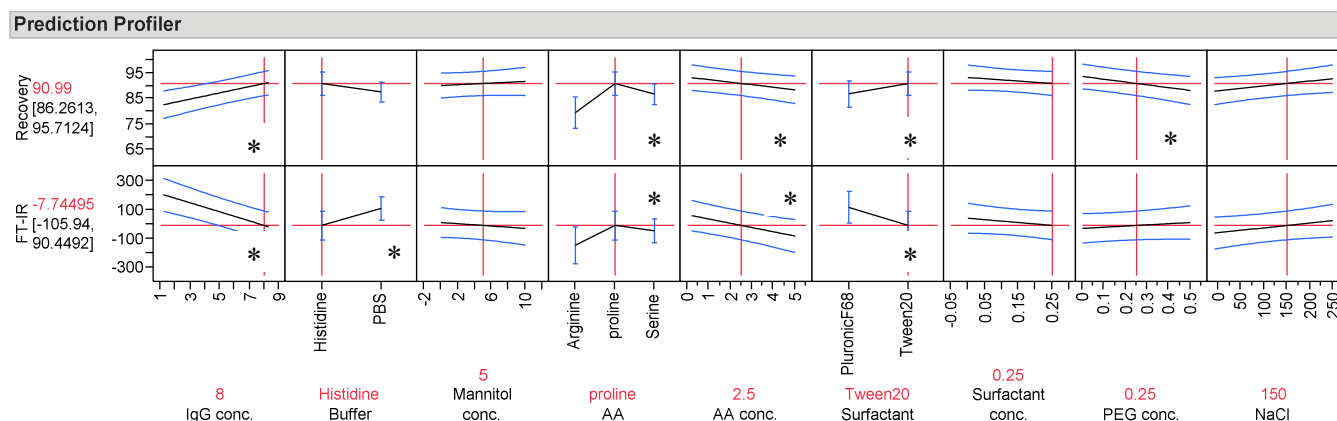


**Figure 17:** Prediction profiler in the optimal conditions (in red) proposed by JMP based on the statistical fitted model constructed by least square fitting and showing the effect of the 9 tested factors on the recovery after/before and the FT-IR Euclidian distance before/after - \* represented the factors with a statistically significant effect (p-value for the test < 0.05; two-tailed test)

The highest effect on the IgG concentration's recovery after/before was observed for the IgG concentration and the type of amino acid (p-value < 0.005). In contrast to arginine with low concentration of IgG (sol IgG 1, 6 and 9), which decreased the recovery, a high IgG concentration and the addition of L-proline improved the recovery value (sol IgG 4, 8, 15, 16, 17 and 18). In addition, a high IgG concentration seemed to improve the stability of the secondary structure. This was reflected in a decrease in the Euclidian distance from before to after when increasing the IgG concentration (p < 0.005). It was concluded that a higher concentration of IgG in solution and the addition of L-proline as stabilizer improved the stability of the solution, which was stressed by the simulated emulsification process. In addition, the addition of polysorbate 20 and the use of histidine contributed to further improving the stability of the IgG as illustrate in the [Figure 17](#).

### 2.1.2 Conclusion

Based on SEC IgG recovery and the FT-IR data and statistical analysis from JMP8, an optimal composition of a formulation suitable for further encapsulation evaluation was determined as 8 % w/v IgG in 0.025 M histidine buffer pH 6.0 solution containing 2.5 % w/v L-proline and 0.25 % w/v polysorbate 20 described as the sol IgG 19 formulation, [Table 37](#) in appendix. The recovery increased occasionally to 95 % and the secondary and the tertiary structures were maintained during the emulsification process. Nevertheless, insoluble aggregation (precipitation at the water – oil interface) was observed during the emulsification

process probably due to the high energy of the w/o interface. Although a w/o/w emulsion method has frequently been used for the preparation of protein-loaded MS, proteins can lose their activity at the w/o interface. Therefore, a non-denaturing solid-in-oil-in-water (s/o/w) emulsion evaporation/extraction technique may be more suitable for therapeutic protein, because solid-state proteins preserve their activity in organic conditions [62, 84, 85]. Therefore, comparison of these two common methods was performed to confirm our hypothesis.

## 2.2 W/o/w versus s/o/w to be selected as the encapsulation processes - selection of the organic solvent

As previously observed, the w/o emulsion led to the precipitation of IgG at the water/oil interface, which led to the loss of monomer. Therefore, the s/o/w method was evaluated and compared to the w/o/w method in terms of IgG stability (SEC profile), particle size of produced MS and loading capacity, evaluated by BCA and SEC.

Both s/o/w and w/o/w were performed using the sol IgG 19 formulation (Table 37 in appendix) selected from the screening design and the IgG microparticles produced by spray-drying from the same IgG formulation solution. The theoretical loading was set at 10 % w/w. Two organic solvents (EtAc and MC) that are commonly used to dissolve PLGA were also evaluated (Table 14).

**Table 14: Experimental process parameters**

<b>Encapsulation process</b>	<b>50:50 PLGA solution</b>
w/o/w	4.6 % w/v in MC
w/o/w	4.6 % w/v in EtAc
s/o/w	4.6 % w/v in MC
s/o/w	4.6 % w/v in EtAc

### 2.2.1 Results and discussion

The produced MS were tested for particle size and encapsulation efficiency (Table 15 and Table 16).

**Table 15: Particle size data of IgG loaded PLGA MS using the formulation IgG 19 at a 10 % w/w theoretical loading**

Test (n = 2)	d(0.1) $\mu\text{m}$	d(0.5) $\mu\text{m}$	d(0.9) $\mu\text{m}$
w/o/w - PLGA in MC	6.2	24.2	94.0
w/o/w - PLGA in EtAc	14.8	31.9	87.9
s/o/w - PLGA in MC	8.5	22.3	60.5
s/o/w - PLGA in EtAc	7.6	29.2	83.2

Both the w/o/w and s/o/w processes provided MS that were characterized by a median diameter d(0, 5) ranging from 22.3 to 31.9  $\mu\text{m}$ . No specific influence of either the organic solvent or the type of process was highlighted. Moreover, the produced MS were spherical with a smooth surface (

Figure 18). However, some donut-like MS were observed.

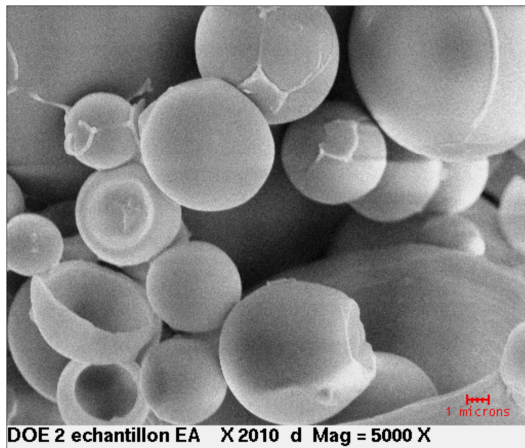


**Figure 18: SEM picture of IgG-loaded PLGA MS produced by w/o/w with PLGA in EtAc solution using the formulation IgG 19 at a 10 % w/w theoretical loading**

The encapsulation efficiency was measured by the BCA method after digestion of the MS with NaOH and by the SEC method after dissolution of the PLGA with MC and extraction of the IgG in the mobile phase. In contrast to the BCA method, which allowed evaluation of the native and the degraded antibody, the SEC method allowed the percentage of IgG in monomer state to be quantified.

**Table 16: Encapsulation data of the IgG loaded PLGA MS using the formulation IgG 19 at a 10 % w/w theoretical loading**

Test (n = 2)	Actual IgG loading (%) (BCA)	Actual IgG loading (%) (SEC)
w/o/w - PLGA in MC	2.7	0
w/o/w - PLGA in EtAc	3.6	1.9
s/o/w - PLGA in MC	2.2	0
s/o/w - PLGA in EtAc	4.9	4.5

When EtAc was used to dissolve PLGA, a IgG loading was measured both by the SEC (1.9 vs. 4.5 % w/w for the w/o/w and s/o/w methods, respectively) and the BCA (3.6 vs. 4.9 % w/w for the w/o/w and s/o/w methods, respectively) methods, which proved the conservation of the monomeric form (Table 16). In contrast, no monomeric IgG peak was observed after SEC evaluation for the IgG-loaded PLGA MS when MC was used to dissolve PLGA. It was concluded that the encapsulation process with IgG dispersed in EtAc was more efficient than encapsulation in MC. In addition, the s/o/w led to a higher loading (4.9 % w/w) than the w/o/w process (3.6 % w/w) as measured by BCA which took into account the IgG total (monomer / HMWS / LMWS).

### 2.2.2 Conclusion

Based on the analytical data, it was decided to select EtAc as the organic solvent. This solvent allowed the monomeric form of IgG to be preserved during the encapsulation process, unlike with MC. In addition, the s/o/w method was preferred for encapsulating the IgG. Indeed, this method led to higher loading than the w/o/w method. Moreover, in contrast to the w/o/w process, which led to aggregation issues at the w/o interface, the s/o dispersion in EtAc was found to preserve the IgG monomer. In addition, the encapsulation of the IgG in its solid

form allowed a higher drug loading than that obtained with the w/o/w process, which required a high concentration of the antibody.

### 2.3 Encapsulation method (s/o/w versus s/o spray-drying)

The Ab can be encapsulated in solid state using different processes. One of them is the spray-drying of a s/o dispersion containing the Ab in an organic solution of polymer.

#### 2.3.1 Optimization of the spray-drying process as method to produce PLGA MS

Before working with Ab, the critical spray-drying process parameters had to be identified to avoid any physical issues during the preparation of the MS. Indeed, during the atomization of an s/o dispersion, some issues can arise such as a large particle size distribution of the SD material or powder sticking onto the spray-dryer. Pre-formulation evaluation was performed on an EtAc solution of PLGA (4.6 % w/v) without the antibody. The mini Spray-dryer B-190 was equipped with a refrigerated atomization chamber and the nozzle was refrigerated by circulating cold water in the double chamber. The morphology of the produced MS was evaluated by SEM.

The lower and the upper-levels of the factors tested in the DoE (atomization air flow, feed flow rate, inlet T°, outlet T° and nozzle cooling) were defined based on the literature and knowledge of PLGA characteristics such as the T<sub>g</sub> (Table 17). The drying air flow rate was set constant at 35 m<sup>3</sup>/h.

**Table 17: Experimental factors and levels**

Factor	Lower level	Upper level
Atomization air flow (L/h N <sub>2</sub> )	400	800
Feed flow rate (%)	15 % (4.5 mL/min)	35 % (10.5 mL/min)
Inlet T° (°C)	50	85
Outlet T° (°C)	25	38
Nozzle cooling	Yes	No

The fractional factorial design, 5 factors at 2 levels was designed to estimate the main effects (resolution III) of the tested factors (Table 17). 8 tests were performed with 2 x 2 repeated center points (tests 1 to 12, Table 18). Five tests (tests 13 to 17, Table 18) were added to

confirm the model. In order to quantify the response, values from 1 (used when both the absence of filament and a small particle size distribution was observed) to 17 (used when both aggregation issues and the presence of filaments were observed) were arbitrarily attributed to the produced MS. The ranking of MS from 1 to 17 was used as the response and was analyzed with JMP8 statistical software (Table 18). The prediction model of the investigated factors on the ranking was determined using the least square regression method [78, 79]. An ANOVA was performed to evaluate the statistical model.

### a. Results and Discussion

The selection of the process parameters appeared to be crucial for the physical aspect of the produced MS. Figure 19 shows two extreme types of the PLGA particles produced. The particles in (A) produced with a 400 L/h N<sub>2</sub> atomization air flow, 15 % flow rate (4.5 mL/min), 85°C inlet T°, 38°C outlet T° and nozzle cooling presented a large number of polymer filaments and a non-spherical shape. The particles in (B) appeared much more spherical, without presence of any filament. They were prepared with 800 L/h N<sub>2</sub> atomization air flow, 35 % feed flow rate, 50°C inlet T° and 25°C outlet T°.

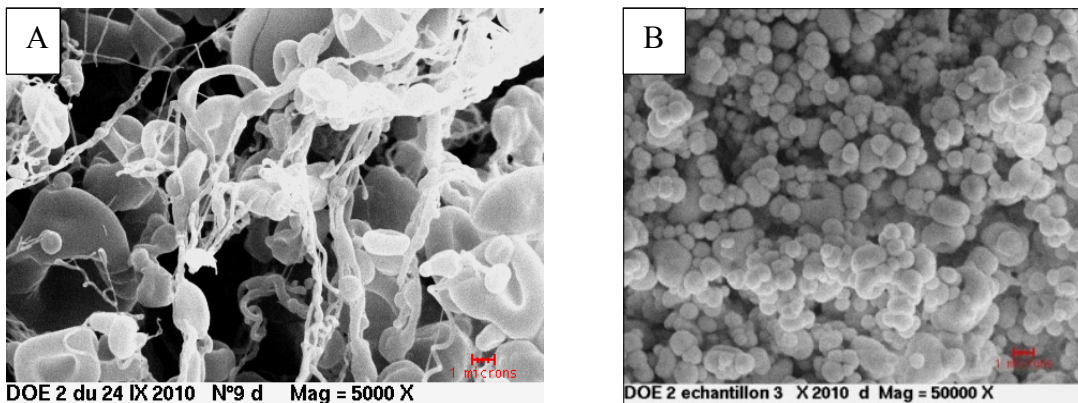


**Figure 19 : SEM pictures of SD PLGA microparticles: (A) test 9 and (B) test 15**

It was shown that working at high temperatures (inlet T° = 85°C and outlet T° = 38°C) increased the ranking to higher values (on a scale from 1 to 17) of the SD formulations ( $p < 0.005$ ) and thus led to the formation of polymer filaments and a large particle size distribution due to collapsed particles (Table 18). In contrast, working at low inlet and outlet temperatures led to microparticles with a spherical shape. This observation may be explained by the  $T_g$  of the PLGA, which is around 50°C. It was concluded that the inlet T° had to be sufficiently

high to allow solvent evaporation but not too high to prevent destruction of the polymer. The outlet T° had to be kept below the T<sub>g</sub> of the polymer.

**Table 18: Spray-drying process parameters and ranking values of the PLGA MS (test 1 to 17)**

Test (n=1)	atomization air flow (L/h)	flow rate (%)	inlet T° (°C)	outlet T° (°C)	nozzle cooling	ranking
1	800	35	50	38	yes	16
2	400	15	50	38	no	17
3	600	25	67	31	yes	9
4	600	25	67	31	yes	10
5	400	35	85	25	yes	11
6	400	35	50	25	no	7
7	800	15	85	25	no	13
8	600	25	67	31	no	14
9	400	15	85	38	yes	15
10	600	25	67.5	31	no	12
11	800	35	85	38	no	5
12	800	15	50	25	yes	4
13	800	15	50	25	yes	3
14	800	15	50	25	no	2
15	800	35	50	25	no	1
16	400	35	50	25	no	6
17	400	15	50	25	no	8

It was observed that working at the lowest atomization air flow rate (400 L/h N<sub>2</sub>) led to the formation of filaments. In contrast, an atomization air flow set at a higher value (800 L/h N<sub>2</sub>) seemed to avoid the polymer sticking and lead to spherical particles. It was concluded that the shear force between the gas and the liquid, applied for a atomization air flow rate set at 400 L/h N<sub>2</sub>, was insufficient to break up the liquid filament into droplets, which led to incomplete formation of particles and agglomerates.

### **b. Conclusion**

Based on the results obtained during the pre-formulation study, the impact of process parameters on the physical aspect of PLGA microparticles produced by spray-drying was clearly highlighted. By selecting optimized parameters, it was possible to obtain PLGA

microparticles without polymer filaments and with a suitable particle size distribution (Table 19).

**Table 19: Selected process parameters for spray-drying of PLGA solution**

Factor	Level
Atomization air flow rate	800 L/h N <sub>2</sub>
Flow rate	15 % (4.5 mL/min)
Inlet T°	50°C
Outlet T°	25°C
Nozzle cooling	No

### 2.3.2 s/o dispersion spray-drying process

After the selection of the spray-drying process parameters (Table 19), the s/o dispersion spray-drying process was evaluated as a method for producing IgG-loaded PLGA MS using a 4.6 % w/v PLGA (Resomer<sup>®</sup> RG504) solution in EtAc. This study was conducted using standard SD IgG formulation (SD IgG 1, Table 38 in appendix) containing 30 % w/w mannitol with regard to the amount of IgG in 20 mM histidine buffer pH 6.0 to highlight the effect of the process parameters. The theoretical loading was set at 10 % w/w.

#### a. Results and discussion

The loading that was evaluated on the MS before washing was similar to that given by the data observed for the s/o/w process (4.9 % w/v) (Table 20). However, IgG could have been adsorbed at the surface of the MS and only be partially encapsulated inside the MS. In order to quantify the IgG that was properly encapsulated, an appropriate amount of IgG:PLGA MS was washed with a 0.1% w/v poloxamer F68 solution.

**Table 20: Encapsulation data**

Formulation	Theoretical loading (%)	Loading % (BCA) (n = 2)
before washing	10.1	4.5 – 4.8
after washing	10.1	1.3 - 1.8

A significant decrease in the loading was observed after washing (Table 20). It was concluded that the IgG was not completely encapsulated inside the MS. These observations

have already been described by by F. Quaglia [86]. The authors found that the production of MS from an *s/o* formulation was not effective to achieve an effective loading of the peptide within the polymeric matrix. This may be explained by sedimentation of the suspension inside the feeding tube before the liquid reaches the nozzle of the spray-drying apparatus [86].

#### **b. Conclusion**

It seemed that the IgG was not properly encapsulated inside the MS using the *s/o* spray-drying process. Therefore, it was decided to not investigate this encapsulation process.

### **3 CONCLUSION**

Various studies conducted under this project demonstrated that it was possible to encapsulate IgG into MS of biodegradable polymers. These studies were performed with IgG in solid state and from solution formulations.

From the early results, encapsulation in solid form seemed to be favorable to maintaining the native form of IgG.

The type of solvent (MC vs. EtAc) was also found to be an important factor for the stability and encapsulation efficiency.

Both the spray-drying and the *s/o/w* processes require further optimization to better understand the impact of the process parameters on the properties of the Ab microparticles and the Ab PLGA MS, respectively.

## **DEVELOPMENT OF A SUITABLE SPRAY-DRYING PROCESS FOR THE PRODUCTION OF SOLID ANTIBODY MICROPARTICLES FOR THE SUBSEQUENT S/O/W ENCAPSULATION PROCESS (IMMUNOGLOBULIN G AS MODEL MOLECULE)**

### **1 INTRODUCTION**

As previously mentioned, the encapsulation of the Ab in solid state was demonstrated to be more suitable for avoiding degradation because solid-state proteins preserve their activity in organic conditions. This chapter describes the optimization study conducted on the spray-drying process to improve properties of the Ab microparticles such as stability and particle size. The aim of this study was to produce Ab SD particles characterized by a particle size small enough (for further encapsulation into the PLGA MS. As mentioned previously, it was estimated that a particle size ratio (SD microparticles compared to PLGA MS) of about 1/10 was required to be able to encapsulated the drug into polymer MS efficiently. The particle size of the Ab SD particles had to be below 10  $\mu\text{m}$  (preferably 5 – 6  $\mu\text{m}$ ) as the PLGA MS characterized by a lower mean diameter than the internal diameter of the needle are preferred (125 - 250  $\mu\text{m}$ ).

### **2 STATISTICAL MODELING OF THE SPRAY-DRYING PROCESS**

#### **2.1 Introduction**

A study was performed to evaluate the effects of the total solid content and the process variables on the characteristics of the SD model molecule. Parameters, such as the inlet  $T^\circ$ , the liquid flow rate or gas spray flow and the concentration of protein might affect the rate of droplet evaporation and influence the particle size distribution.

This study was conducted using a standard IgG solutions with 3 different total solid contents (15, 27.5 and 40 mg/mL) and containing 30 % w/w mannitol with regard to the amount of IgG in 20 mM histidine buffer pH 6.0 to highlight the effect of the process parameters (SD IgG (formulations 1 to 3); [Table 38](#) in appendix). The selected formulation sol IgG 19 ([Table](#)

VI. Development of a suitable spray-drying process for the production of solid antibody microparticles for the subsequent s/o/w encapsulation process (immunoglobulin G as model molecule)

37 in appendix) could be used but a simple standard formulation containing only the mannitol as stabilizer was preferred to evaluate the process parameters. The process variables explored were: (a) the inlet T° (100 - 140°C), (b) the liquid feed flow rate (3 - 5 mL/min), (c) the gas spray flow (atomization flow rate) (400 – 800 L/h N<sub>2</sub>) and (d) the total solid concentration (15 – 40 mg/mL) on a lab-scale spray-dryer (Buchi Mini Spray-drier B290). The volume of liquid spray-dried was set at 20 mL as it was previously demonstrated that this did not influence the properties of the SD IgG (data not shown) and the aspiration setting was set at 85 % (100 % = 35 m<sup>3</sup>/h). A D-optimal experimental plan with one center point was designed to evaluate the main effects and the interaction effects of the 4 tested factors (Table 21). An ANOVA was performed to evaluate the statistical fitted model (least square fitting).

**Table 21: Spray-drying process parameters (a) inlet T°, (b) liquid feed flow rate, (c) gas spray flow and (d) total solid concentration and yield of spray-drying , d(0.5), residual water content (KF) and IgG monomer loss (SEC) observed for the evaluated SD IgG (test 1 to 12)**

Test	SD IgG	a (°C)	b (mL/min)	c (L/h)	d (mg/ml)	Yield (%)	d(0.5) (µm)	KF (%)	IgG monomer loss (%)	Outlet T° (°C)
T1 SD IgG	SD IgG 3	140	5	400	40	30.7	8.6	8.4	-10.1	80.0
T2 SD IgG	SD IgG 1	100	5	800	15	42.5	8.9	10.3	-3.2	52.0
T3 SD IgG	SD IgG 1	140	3	800	15	62.5	7.0	8.8	-9.8	85.0
T4 SD IgG	SD IgG 3	100	3	400	40	29.3	8.7	8.5	-11.7	68.0
T5 SD IgG	SD IgG 2	120	4.6	600	27.5	62.7	5.7	9.5	7.1	65.0
T6 SD IgG	SD IgG 1	100	5	400	15	18.5	8.0	10.9	-4.9	54.0
T7 SD IgG	SD IgG 1	100	3	400	15	33.8	7.3	9.4	-5.7	66.0
T8 SD IgG	SD IgG 3	100	3	800	40	49.0	6.3	7.4	-7.4	65.0
T9 SD IgG	SD IgG 3	140	3	800	40	65.6	5.6	6.1	-14.0	83.0
T10 SD IgG	SD IgG 1	140	3	400	15	35.3	9.1	9.4	-10.4	88.0
T11 SD IgG	SD IgG 3	100	5	800	40	63.0	6.3	9.7	-7.1	55.0
T12 SD IgG	SD IgG 1	140	5	800	15	55.6	3.1	8.9	-4.8	71.0

## 2.2 Results and discussion

### Yield of the spray-drying process (%)

The yield was calculated as weight of collected powder to total solid content in the liquid feed. The yield did not exceed 70 % w/w. The loss of material during the process was explained by the fact that many of the smallest particles were not recovered in the lab-scale apparatus. This was because they were not efficiently deposited in the cyclone because their low mass caused them to be drawn up into the filter bag. However, the low quantity of total solid content (< 1 g) led also to low process yields. The lowest yields (< 40 % w/w) were obtained with the lowest atomization flow rate (400 L/h) (T1 SD IgG, T4 SD IgG T6 SD IgG, T7 SD IgG and T10 SD IgG) (Table 21). The statistical analysis demonstrated the statistical effect of the atomization flow rate on the yield, with a  $p < 0.003$  (Figure 23).

It was observed that the type of stabilizer added to the IgG solution could affect the yield. For example, when sorbitol was used, the yield was significantly lower ( $p = 0.0421$ ) than with mannitol or trehalose ( $13.9 \pm 7.9$  %,  $54.9 \pm 10.9$  % and  $56.0 \pm 22.4$  % for sorbitol, trehalose and mannitol, respectively) (data not shown). A sticky powder was obtained when sorbitol was used. Indeed, sorbitol was characterized by a lower melting point ( $95^{\circ}\text{C}$ ) than that of mannitol ( $166^{\circ}\text{C}$ ) and trehalose ( $203^{\circ}\text{C}$ ). In contrast, when using either trehalose or mannitol, deposition of the powder on the walls of the spray tower was relatively limited. Therefore, the loss of material was mainly due to fine particles passing through the cyclone into the exhaust air.

### Size characteristics of the SD IgG microparticles

The T1, T4, T6, T7 and T10 SD IgGs produced with the lowest atomization flow rate (400 L/h  $\text{N}_2$ ) led to SD microparticles with high particle sizes ( $d(0.5)$  ranging between 7.3 and 9.1  $\mu\text{m}$ , respectively). The decrease in the median particle size (e.g. 5.6  $\mu\text{m}$  and 3.1  $\mu\text{m}$  for the T9 and T12 SD IgG, respectively), which was observed for higher atomization flow rates, was explained by the higher energy provided for fluid dispersion, resulting in smaller droplets, and accordingly, in smaller dried particles. It was concluded that an atomization flow rate set at a higher value (600 - 800 L/h) was necessary for producing particles with appropriate size ( $\sim 5 - 6 \mu\text{m}$ ) (Figure 23).

VI. Development of a suitable spray-drying process for the production of solid antibody microparticles for the subsequent s/o/w encapsulation process (immunoglobulin G as model molecule)

It was also observed that sorbitol significantly increased the  $d(0.5)$  of the SD particles ( $p = 0.0315$ ). The average of  $d(0.5)$  was  $19.4 \pm 3.0 \mu\text{m}$  when sorbitol was used as stabilizer. This could be linked to the lower  $T_m$  of the sorbitol ( $95^\circ\text{C}$ ), leading to agglomeration of particles during the drying step. It was also seen that trehalose gave similar particle size than mannitol ( $d(0.5) = 8.3 \mu\text{m}$ ).

The SEMs of the SD powders showed, irrespective of the process parameters, a smooth particle surface. During the drying process the particle formation underwent indentation and resulted in donutshaped particles (Figure 20). It was in agreement with the morphology of SD anti-IgE monoclonal antibody/lactose (60:40) [87]. These authors showed that, if the drying rate increased via increasing outlet  $T^\circ$  (from  $36 - 52^\circ\text{C}$ ), the particle shape changed from spherical to donutshape. In this study, the outlet  $T^\circ$  was measured above  $70^\circ\text{C}$  which confirmed the deformation of the dried particles at this high outlet  $T^\circ$ .

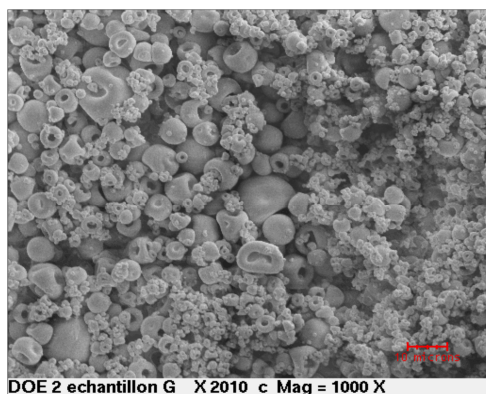


**Figure 20:** SEM picture of SD IgG (T4 SD IgG)

### **Residual moisture of the SD IgG microparticles (%)**

The T2 and T6 SD IgG produced using the lowest inlet  $T^\circ$  ( $100^\circ\text{C}$ ), and the highest liquid flow rate ( $5 \text{ mL}/\text{min}$ ) resulted in the SD microparticles with the highest residual water content ( $> 10 \% \text{ w}/\text{w}$ ). In contrast, when the inlet  $T^\circ$  was set at  $140^\circ\text{C}$ , the solid concentration at  $40 \text{ mg}/\text{mL}$  and the liquid flow rate at  $3 \text{ mL}/\text{min}$  (T9 SD IgG), the water content decreased to  $6.1 \% \text{ w}/\text{w}$ . A clear correlation was highlighted between the residual water and the inlet temperature ( $p = 0.0337$ ), the solid content ( $p = 0.0055$ ) and the liquid flow rate ( $p = 0.0160$ ) (Figure 23). As could be expected, the residual water decreased when the inlet temperature

was increased. This decrease was explained by the higher water evaporation capacity. In contrast, increasing the liquid flow rate required more energy to evaporate the droplets into solid particles, resulting in a decrease in the outlet T°. As a result, the difference between the inlet T° and the outlet T° was greater, leading in a greater amount of residual moisture. Because the proportion of water decreased when the solid content increased, this change led to lower residual water content in the final product.

### **IgG Monomer loss after the spray-drying process (%)**

It was less evident to highlight the relationship between the loss of monomer and the process parameters. Indeed, as already observed during a previous study (data not shown), the quantity of soluble aggregates evaluated by SEC was lower after the spray-drying than before as reflected by a negative loss of IgG monomer ([Table 21](#)).

In contrast to the literature describing the formation of HMWS during the spray-drying of Abs, a decrease in the level of HMWS was measured by SEC and identified as polyaggregates (a decrease from 0.9 to 1.4 %) and dimers (a decrease from 0.3 to 6 %) was observed with all the tested formulations after spray-drying [88, 89, 90, 91].

In addition, no significant change in either the secondary or the tertiary structures was observed after spray-drying as the product was exposed to high temperatures for a very short period of time ([Figure 21](#) and [Figure 22](#)).

VI. Development of a suitable spray-drying process for the production of solid antibody microparticles for the subsequent s/o/w encapsulation process (immunoglobulin G as model molecule)

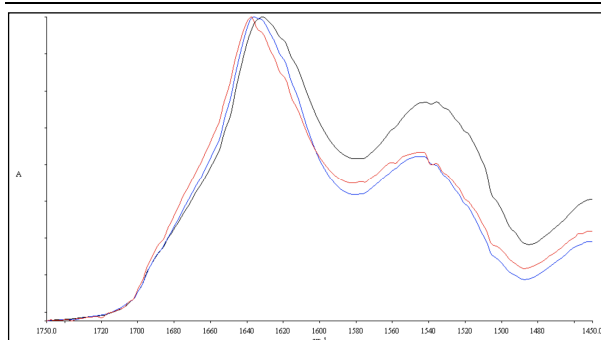


**Figure 21:** Comparison of FT-IR spectra, with the IgG solution before spray-drying in red; the IgG powder after spray-drying in blue; the IgG solution reconstituted from IgG powder after spray-drying in black (T4 SD IgG)

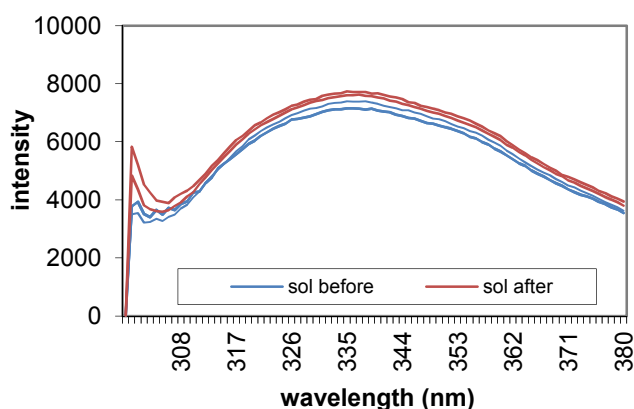


**Figure 22:** Comparison of IFR spectra from 300 to 380 nm, with the IgG solution before spray-drying in blue and the IgG solution reconstituted from IgG powder after spray-drying in red (T4 SD IgG)

### Crystallinity (%)

The produced microparticles were amorphous regardless of the parameters. However, it was previously observed that a lower solid content (5 mg/mL) led to crystallization of the mannitol (data not shown).

A statistical model was constructed for the spray-drying process of the Ab. The prediction profiler shows the effects of the tested parameters on the evaluated responses (Figure 23). It was possible to predict the responses depending of the fixed parameters (in red) which were confirmed on two batches (data not shown).

VI. Development of a suitable spray-drying process for the production of solid antibody microparticles for the subsequent s/o/w encapsulation process (immunoglobulin G as model molecule)

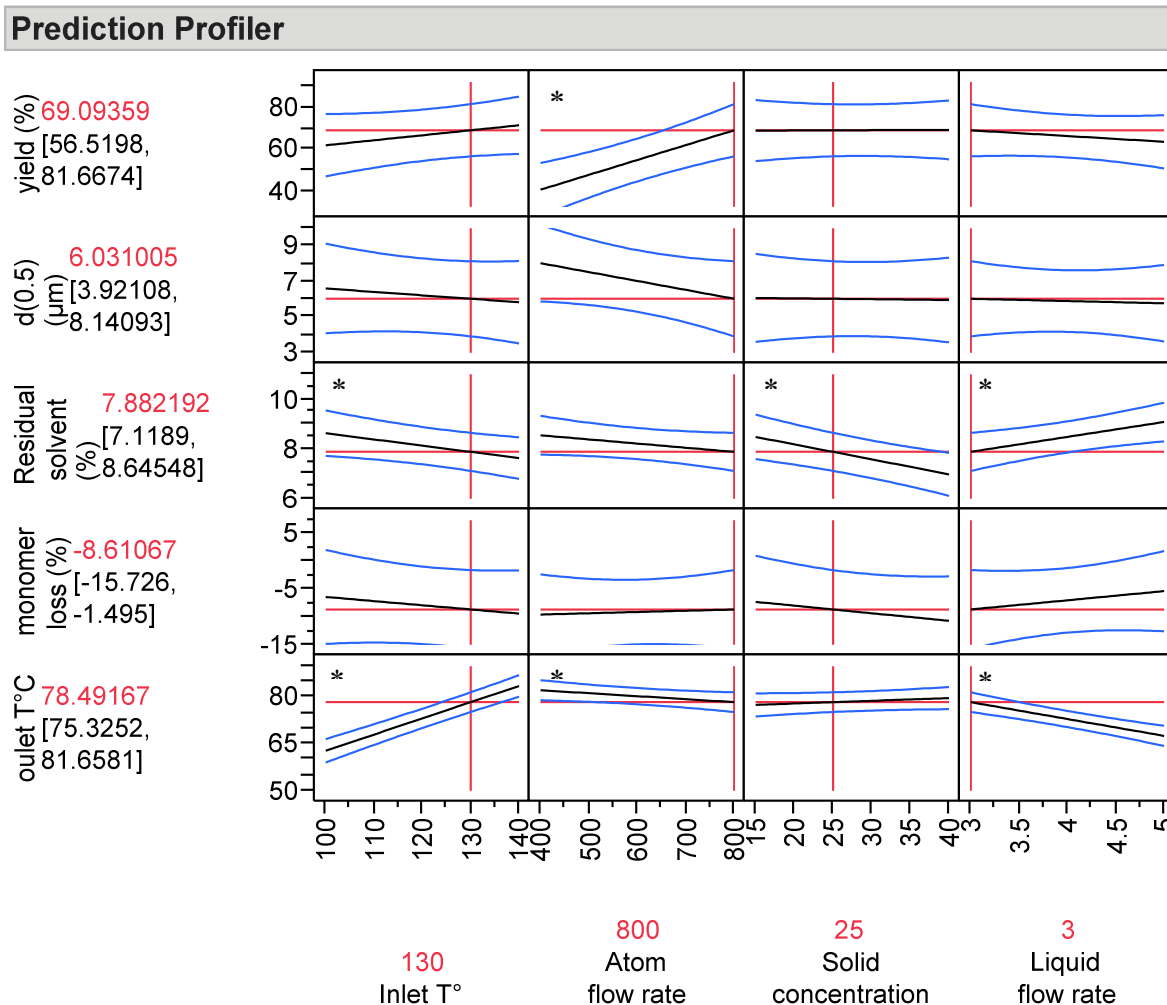


**Figure 23:** Prediction profiler in the optimal conditions (in red) proposed by JMP based on the statistical fitted model constructed by least square fitting and showing the effect of the tested factors (inlet T°, atomization flow rate, solid concentration and liquid flow rate) on the yield, the d (0.5), the residual water content, the IgG monomer loss and the outlet T°- \* represented the factors with a statistically significant effect (p-value for the test < 0.05; two-tailed test)

### 2.3 Conclusion:

In accordance with the particle size ( $d(0.5) \sim 5 \mu\text{m}$ ), the stability (no loss of monomer) and the yield ( $> 60 \%$  w/w), the process parameters were set as follows: liquid flow rate, 3 mL/min; inlet T°, 130°C; atomization air flow, 800 L/h; aspiration setting, 85 %; solid concentration, 25 mg/mL, with a 70:30 Ab:stabilizer ratio (formulation SD IgG 4, Table 38 in appendix).

VI. Development of a suitable spray-drying process for the production of solid antibody microparticles for the subsequent s/o/w encapsulation process (immunoglobulin G as model molecule)

---

Addition of a surfactant such as polysorbates (Polysorbate 20 or 80), Pluronic F68 or PEG 8000 was evaluated for spray-drying but without any improvement on the characteristics of the produced microparticles in term of particle size, stability, residual solvent or yield.

## ENCAPSULATION OF IMMUNOGLOBULIN G, AS MODEL MOLECULE, BY SOLID-IN-OIL-IN-WATER: EFFECT OF PROCESS PARAMETERS ON MICROSPHERES PROPERTIES \*

\* adapted from [64]

### 1 INTRODUCTION

This study aimed at validating the concept of encapsulating antibodies into a stabilizing formulation based on biodegradable PLGA MS, with a high efficiency of encapsulation.

Several factors could influence the properties of MS produced by a solvent evaporation process (Figure 24). A DoE was conducted to study the effects of the critical parameters (such as polymer, solvent, surfactant, quantity of drug and agitation rate) in the s/o/w encapsulation process [92].

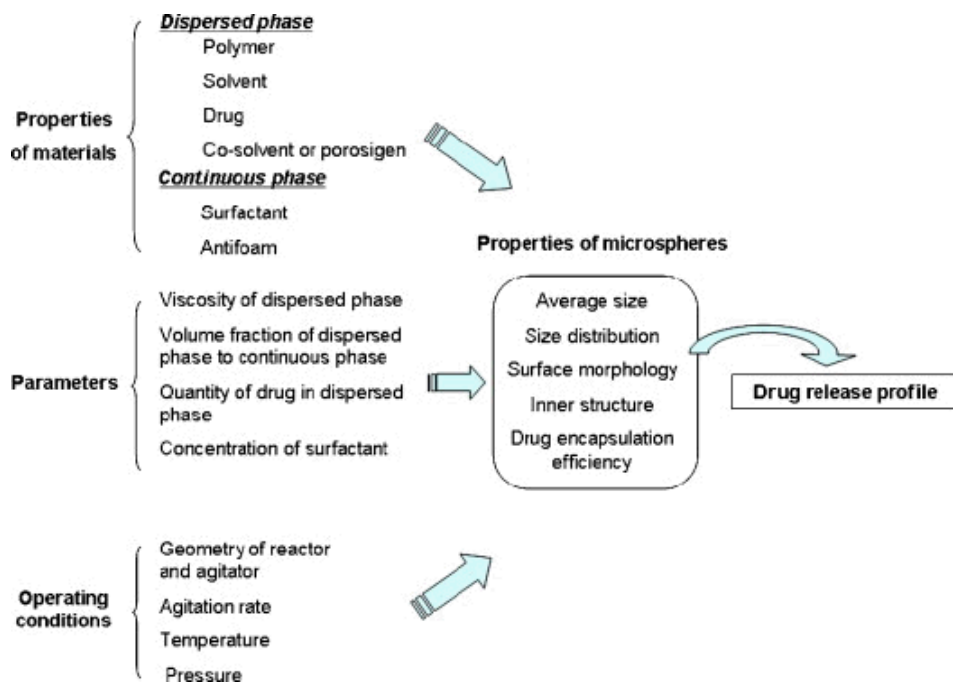


Figure 24: Schematic of the factors influencing the properties of MS [92]

The aqueous IgG solution (SD IgG 4; Table 38 in appendix) was spray-dried. The SD IgG was encapsulated into Resomer<sup>®</sup> RG504 using the s/o/w method with the range of parameters defined by the design of experiment.

The main effects of the process and MS formulation variables in the s/o/w encapsulation process were evaluated. The factors studied were: the PLGA concentration in the organic phase, the stabilizer concentration in the external phase, the volume of the external phase, the s/o/w emulsification time, the s/o/w emulsification rate, the volume of the extraction phase, the type of external phase stabilizer and the quantity of the SD IgG (Table 22). The selected outputs were the particle size, the drug loading, the encapsulation efficiency, the dissolution profile, the stability of the IgG over the encapsulation process and the dissolution profile of the antibody. The experimental plan was constructed step-by-step. The DoE (= fractional factorial design with 7 factors at 2 levels, resolution III) was first designed to estimate the main effects of the first seven factors (factors ID a to g, Table 22). Eight formulations were performed with 3 repeated center points (formulations MS IgG-1 to MS IgG-11, Table 39 in appendix). Based on the statistical analysis of this plan, the levels of 4 factors of the 7 factors (factors ID b, c, f and g) were fixed. The DoE was augmented by 15 additional formulations (MS IgG-12 to MS IgG-26, Table 39 in appendix) and an additional factor was study (SD IgG quantity, factor ID h, Table 22). Finally, the experimental plan was completed by 8 formulations (MS IgG-27 to MS IgG-34, Table 39 in appendix) to obtain a full factorial design at 2 levels with 4 factors (factors ID a, d, e and h, Table 22).

**Table 22: Experimental design - experimental factors and their level**

Factor ID	Factor	Lower-level (-1)	Upper-level (+1)
a	PLGA concentration (% w/v)	1	15
b	Stabilizer concentration (% w/v)	0.1	2
c	Volume of the external phase (mL)	30	100
d	Emulsification time (min)	1	5
e	Emulsification speed (rpm)	3 400	13 500
f	Volume of the extraction phase (mL)	100	400
g	Type of external phase stabilizer	PVA	PVP
h	SD IgG quantity (mg)	30	100

The effects of the investigated parameters on the outputs were determined using the least square regression method [78, 79]. An ANOVA was performed to validate the statistical fitted model and identify the statistical significant effects of the evaluated factors.

## 2 RESULTS AND DISCUSSION

The effects of the studied factors defined in the DoE were evaluated on different output characteristics, taking into account the data from all of the formulations produced (Figure 33). The results of the tested formulations are summarized in the Table 40 in appendix.

### 2.1 Influence of the investigated parameters on particle size distribution and morphology of the MS

In order to be injected, the targeted mean diameter of the microparticles should be no higher than 125  $\mu\text{m}$ . The MS formulations produced from a high PLGA concentration of 10 % (w/v) and the lowest emulsification rate (3400 rpm) were characterized by a D [4, 3] higher than 200  $\mu\text{m}$  (Figure 25). The smallest IgG:PLGA MS (D [4,3] < 20  $\mu\text{m}$ ) were produced using the highest emulsification rate (13500 rpm) with a 1 % (w/v) PLGA concentration. Both the emulsification rate and the PLGA concentration presented a significant effect on the volumetric mean diameter of the IgG:PLGA MS ( $p < 0.001$ ) (Figure 33). An increase in the polymer concentration led to an increase in the D [4, 3], especially from 1 to 10 % w/v. This effect could be attributed to the increase in the viscosity of the organic phase, which affected the shearing efficiency. In addition, due to an increase in the polymer concentration, the frequency of collisions during the emulsification and the polymer solidification might have increased, resulting in the aggregation of semi-solid particles and leading to an increase in particle size [78, 93].

VII. Encapsulation of immunoglobulin G by solid-in-oil-in-water: effect of process parameters on microspheres properties

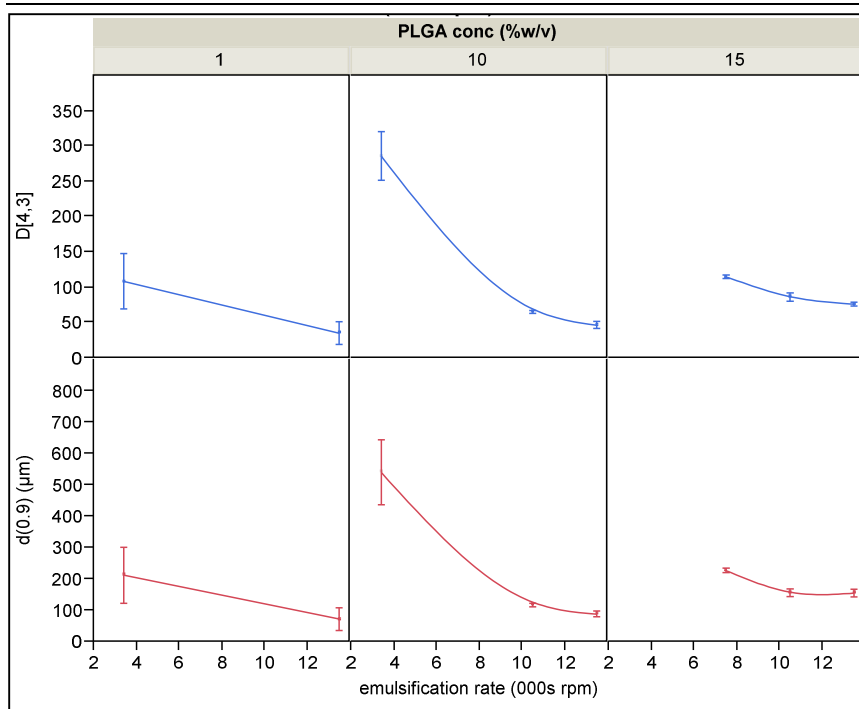


**Figure 25** Influence of emulsification rate (from 3400 to 13500 rpm) on the D [4,3] and the d(0,9) of IgG-loaded PLGA MS produced at different PLGA concentrations (1, 10 and 15 % w/v). This figure shows the mean values and the standard deviations of particle size versus emulsification rate by PLGA concentration. A smoothed curve (obtained by cubic spline) was added to the graph for clarity.

Li and co-workers [92] observed that an increase in the emulsification rate led to a significant decrease in the mean diameter of the MS. The highest emulsification rate (13500 rpm) was thus selected to provide sufficient energy to produce MS with an appropriate particle size ( $d(0,9) < 125 \mu\text{m}$ ). When using a 10 % (w/v) PLGA concentration, the  $d(0,9)$  value was  $92 \pm 28 \mu\text{m}$ . However, with a 15 % (w/v) PLGA concentration, it was not possible to produce microparticles with an appropriate particle size distribution, even at 13500 rpm, which produced MS with an average  $d(0,9)$  of  $156 \pm 24 \mu\text{m}$ .

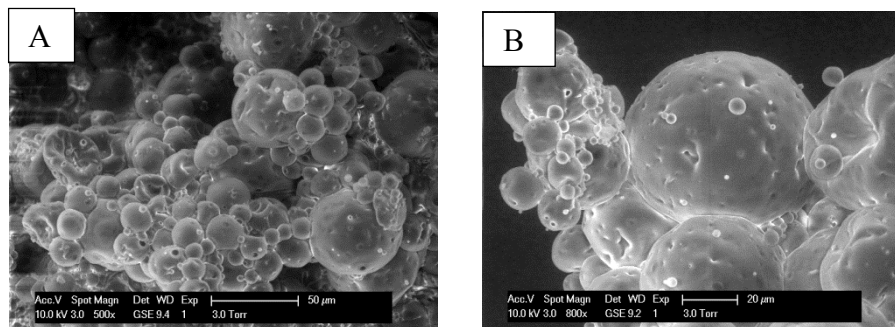
The presence of a stabilizer, such as PVA or PVP, in the external phase stabilized the emulsion droplets against coalescence. Mao and Yang observed that the stabilization effect was the greatest at higher PVA or PVP concentrations (0.05 – 1 % (w/v)) and led to a decrease in the D [4,3] of the MS [75, 94]. However, in our study, the stabilizer concentration in the external water phase did not have a significant effect on the volumetric mean diameter (Figure 33). It was

concluded that, in our case, the concentration of the stabilizer in the external water phase within the evaluated range (0.1 – 2 % w/v) did not influence the particle size of the produced MS.

PVA is the most commonly used emulsifier because it contributes to producing relatively homogeneous particles with a smaller size [95]. We confirmed that PVA was more efficient for decreasing the volumetric mean diameter than PVP (Figure 33).

The morphology of the produced MS using 100 mg of SD IgG, a 10 % w/v PLGA concentration solution and 1 minute of emulsification at a rate of 13500 rpm in 100 mL of external phase containing 1 % w/v PVA and 400 mL of extraction phase (MS IgG-25, Table 40 in appendix) was visualized by SEM. Most of the MS produced were spherical. However, some agglomerates and irregular MS were observed (Figure 26 A and B). Agglomeration issues may be explained by a fast precipitation of the PLGA during the encapsulation process. Li and co-workers described that the MS could not be properly formed, due to the miscibility of EtAc in water, which is 4.5 times higher than that of MC [92, 96]. As a result, the sudden extraction of a large volume of EtAc from the dispersed phase into the aqueous phase might lead to the precipitation of the polymer into fibre-like agglomerates and irregular MS. To avoid immediate hardening of the MS, the addition of a small volume of aqueous solution (30 mL) was evaluated. However, in our study, no correlation was observed between the volume of the external phase and the particle size. In an other hand, the MS appeared porous (Figure 26 A and B). It was reported in the article of L. Al hausley et co-authors that the morphology of particles depended on the operating conditions [78]. The number of pores were correlated with the volume of organic phase, the duration of agitation and with the quantity of polymer. The fast removal of the organic solvent caused by increase of the polymer amount or the increase of the external aqueous phase could cause a local explosion inside the polymer droplets leading to the formation of porous structure and coarse surface. The use of EtAc, as organic solvent, which contributed to increase the solvent removal kinetics, could facilitated the formulation of porous structure. It was also reported that MS with high drug loading were more porous and have more irregular shape [92]. This resultant over-porous surface might lead to a loss of drug. Finally, it has been described that the s/o/w process conducted to the formation of more porous MS compared to the double emulsion process (w/o/w) [63]. It was explained by the solid protein leaching out of the emulsion.

Surface porosity



Internal morphology

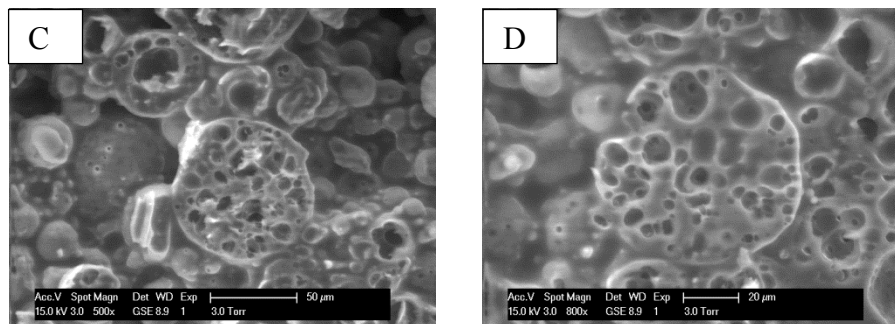


**Figure 26: Scanning electron micrographs of IgG-loaded PLGA MS (MS IgG-25, Table 40 in appendix): Surface porosity at (A) magnification 500x and (B) magnification 800x, and internal morphology after cross-section at (C) magnification 500x and (D) magnification 800x.**

On the other hand, as water is characterized by a solubility of 3.3 % (v/v) at room temperature in EtAc, the solidified polymeric MS could absorb water during the vacuum drying process. MS may therefore soften due to both residual EtAc and migration of water into the MS [97].

## 2.2 Influence of the investigated parameters on the actual drug loading of the MS

A number of factors influenced the drug loading of the MS: the PLGA concentration of the organic solution, the volume of the external phase, the emulsification rate and the quantity of SD IgG dispersed in the organic phase (Figure 33).

For a similar volume of external phase (100 mL), the mean drug loading values were  $2.6 \pm 0.8$  % and  $5.1 \pm 1.0$  % using 30 mg and 100 mg SD IgG, respectively (Figure 27). The drug loading significantly increased when increasing the amount of IgG (2.6 % vs. 5.1 % w/w with 30 and 100 mg SD IgG, respectively).

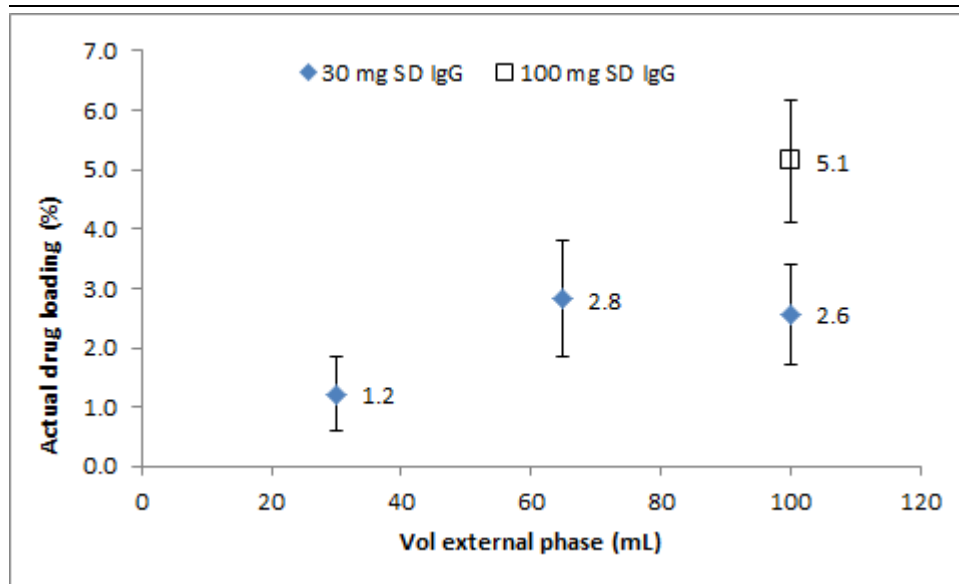


**Figure 27** Influence of the volume of external phase (30, 65 and 100 mL) on the actual drug loading of IgG-loaded PLGA MS produced at different SD IgG quantities (30 and 100 mg). This figure shows the mean values and the standard deviations of drug loading versus volume of external phase by SD IgG quantity.

When the concentration of PLGA increased, the drug loading decreased. It was logically linked to the decrease of the theoretical drug loading as expressed in the equation 4 (page 67).

The effect of the theoretical drug loading was evaluated (data not shown). It was suggested that the drug loading increased with the increase in the theoretical drug loading. However, at a low PLGA concentration (1% w/v), the increase in the theoretical drug loading did not increase the resultant drug loading, probably due to the limited drug entrapment capability of the polymer matrix. Therefore, the SD IgG/PLGA ratio was found to be a critical parameter [98].

The impact of the volume of the external phase was also evaluated. The lowest drug loading values were obtained with formulations that were produced using 30 mL of external phase and 30 mg of SD IgG. The MS with a drug loading higher than 4 % (w/w) were produced using 100 mL of external phase and more than 30 mg of SD IgG (Figure 27). The positive effect of increasing the volume from 30 mL to 65 mL on the increased drug loading was explained by a faster precipitation of the polymer in a larger volume of water, which led to a decrease in the loss of IgG during the solidification of the MS. The increase in the volume of the external aqueous phase from 30 to 65 mL allowed the immediate dissolution of the organic phase into the aqueous

solution. It was noticed that no improvement was observed by increasing the volume to 100 mL (when both the amount of SD IgG and of polymer remained constant).

In contrast, an increase in the emulsification rate seemed to decrease the drug loading, which was attributed to the particle size reduction (Figure 33). It was considered that it was easier to encapsulate the solid IgG small microparticles into larger MS. In addition, a smaller particle size contributed to a higher surface area, which might lead to an increase in the dissolution and loss of IgG into the aqueous phase.

In addition, an increase in the emulsification time tended to decrease the actual drug loading. This decrease was attributed to a longer exposure time during the solidification phase, which might contribute to a higher loss of IgG in the aqueous phase (data not shown).

### 2.3 Influence of the investigated parameters on the EE% of the MS

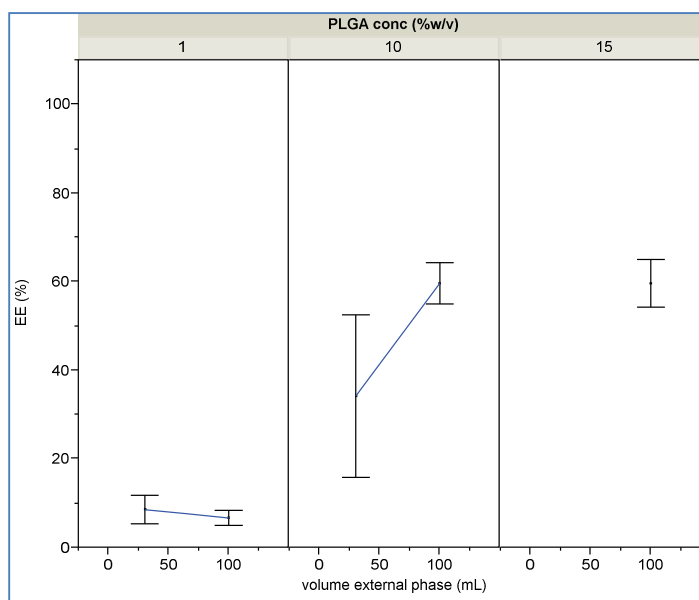


**Figure 28** Influence of volume of external phase (from 30 to 100 mL) on the EE% of IgG-loaded PLGA MS produced at different PLGA concentrations (1, 10 and 15 %). This figure shows the mean values and the standard deviations of EE% versus the volume of the external phase by PLGA concentration.

The lowest EE% was obtained using 1 % (w/v) PLGA solution (which did not exceed 11.8 % (w/w)) (Figure 28). This result may be explained by the limited drug entrapment ability of the

polymer matrix. In contrast, the MS characterized by the highest EE% were produced with at least 10% (w/w) PLGA and 100 mL of external phase. As confirmed by a p value < 0.0001 (Figure 33), the PLGA concentration had a highly significant effect on the EE%. The EE% significantly increased with an increase in the concentration of the polymer [99, 100, 101]. At high concentrations of PLGA, the polymer precipitated faster at the surface of the dispersed phase as less organic solvent was available, reducing drug diffusion into the aqueous phase. The high concentration of PLGA also increased the viscosity of the organic solution, which delayed the drug diffusion throughout the polymer matrix [102].

In addition, the influence of the volume of the external phase was significant ( $p < 0.05$ ) (Figure 33); its increase led to an increased EE%. In contrast, Al Haushey and co-workers found that when using MC as the organic solvent (as opposed to EtAc, as used in this study), the increase in the volume of the external phase had a negative impact on the EE% of bovine serum albumin MS produced by the w/o/w encapsulation method [78]. This was explained by the formation of a porous structure resulting from the faster removal of the organic solvent. In our study, the use of EtAc, which presented a higher aqueous solubility than MC, accelerated the solidification of the polymer, increasing the EE% as a consequence.

This observation was confirmed in some studies in which a higher EE% was observed using a co-solvent system [100, 103]. The increase in the affinity of the solvent system for the continuous phase that resulted from adding a co-solvent allowed fast extraction of the solvent into the continuous phase, which led to higher EE%. In addition, the positive effect of the larger volume of external phase led to a higher concentration gradient between the organic and the aqueous phase, leading to fast solidification of the MS. However, as previously explained, when the aqueous phase increased, the MS hardened quickly and formed irregular precipitates.

An increase in the amount of SD IgG led to a decrease in the EE% (Figure 33), contrary to that reported in the literature indicating that increasing the quantity of drug improved the EE% [92]. It was assumed that the loss of drug into the continuous phase was constant whatever the initial quantity dispersed in the PLGA organic solution. Therefore, the EE% increased when the amount of drug was increased. However, in our study, the EE% decreased when the amount of the theoretical drug loading reached a critical value higher than 10 % (w/w) (data not shown). It was also concluded that a high drug loading increased the risk of drug leakage due to the limited

space inside the MS [92]. It should be noticed that Mao and co-workers observed that no significant difference in the EE% was found for a theoretical drug loading from 1 to 5 % (w/w) for fluorescein isothiocyanate - dextran-loaded PLGA MS [75]. The EE% decreased considerably (below 10 % (w/w)) when the theoretical drug loading was increased to more than 20 % (w/w) and when using a 1 % (w/v) PLGA concentration. A higher theoretical drug loading caused a higher drug concentration in the emulsion. This increase in the gradient of concentration led to a loss of drug into the aqueous phase [75]. Therefore, it was concluded that a minimum value of 10% (w/v) PLGA concentration was needed to allow an efficient encapsulation of the added IgG microparticles. The IgG/PLGA ratio was therefore a key factor in maintaining the entrapment capacity of the polymer matrix.

In addition, the emulsification rate led to a decrease in both the drug loading and the EE% (Figure 33). This could be related to the effect of the particle size on the EE%. Indeed, as previously mentioned, it could be assumed that it was easier to encapsulate small solid IgG microparticles into larger MS.

An increase in the emulsification time tended to decrease the EE%. As previously mentioned, a longer exposure time during the solidification phase might contribute to increasing the loss of IgG in the aqueous phase, giving the IgG more opportunity to escape to the external aqueous phase.

## **2.4 Influence of the investigated parameters on the burst effect of microspheres**

As shown in Figure 33, the PLGA concentration had a high impact on the burst effect. The formulations produced with 1 % (w/v) PLGA were characterized by the highest burst values. Increasing the concentration of PLGA from 1 to 15% (w/v) led to a decrease in the burst effect (= released % after 24h of dissolution) (Figure 29, from  $92.6 \pm 3.5$  % (w/w),  $77.3 \pm 6.0$  % (w/w),  $45.9 \pm 14.7$  % (w/w) and  $29.5 \pm 6.2$  % (w/w) for 1 %, 5.5 %, 10 % and 15 % (w/v) PLGA concentrations, respectively). In addition, with a minimal concentration of 10 % w/v PLGA, a controlled release of the IgG was observed after the initial burst effect for up to 6 weeks (Figure 29).

VII. Encapsulation of immunoglobulin G by solid-in-oil-in-water: effect of process parameters on microspheres properties

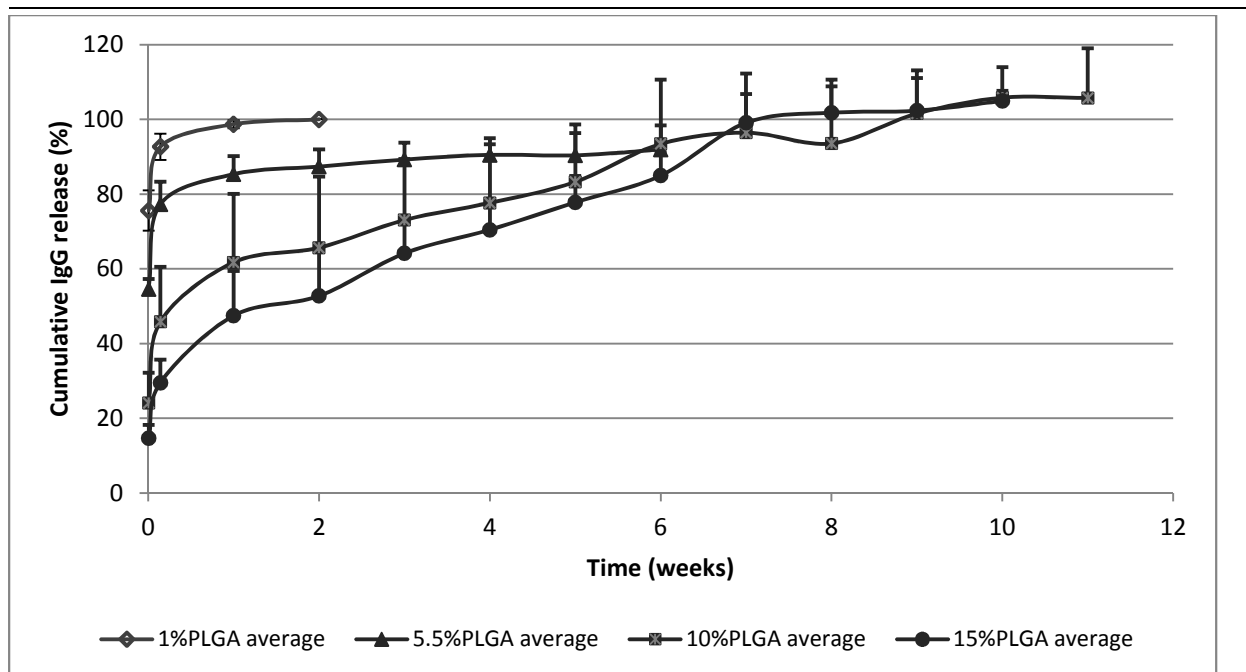


**Figure 29** Influence of the PLGA concentration (from 1 % to 15 % w/v) on the IgG release profile from IgG-loaded PLGA MS: mean dissolution and standard deviation curve of MS produced with (◇) 1 % PLGA solution (n = 3), (Δ) 5.5 % PLGA solution (n = 3), (■) 10 % PLGA solution (n = 16) and (○) 15 % PLGA solution (n = 9).

The statistical analysis confirmed the highly significant effect of the PLGA concentration on the burst effect ( $p < 0.0001$ ). As described by Mao, a higher PLGA concentration might decrease internal matrix porosity by avoiding fast water penetration during dissolution and thereby slowing down the release of the loaded drug and the burst effect [75]. Luan confirmed that a high porosity linked to a low PLGA concentration led to a rapid penetration of the liquid, resulting in a high initial burst effect [104].

It has been reported that the burst effect could be influenced by the volume of the external phase. Indeed, the surface of the MS became porous as the volume of the external phase increased. In contrast, the internal porosity of the MS slightly decreased as the volume decreased. It was observed that an increase in the quantity of SD IgG tended to increase the burst effect. Comparing formulations produced with the same concentration of PLGA (10 and 15 % w/v), the burst effect increased when increasing the amount of SD IgG from 75 to 100 mg (Figure 30). It was linked to a higher quantity of IgG at the surface of the MS [104].

VII. Encapsulation of immunoglobulin G by solid-in-oil-in-water: effect of process parameters on microspheres properties

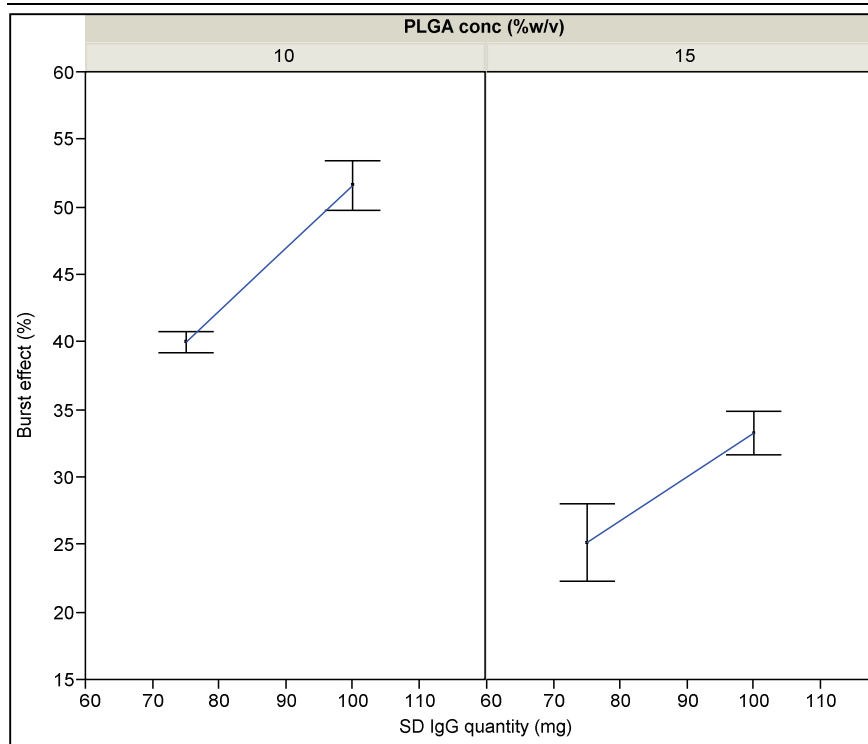


**Figure 30** Influence of the SD IgG quantity (from 75 to 100 mg) on the burst effect of the IgG-loaded PLGA MS produced with 10 or 15 % w/v PLGA concentration. This figure shows the mean values and the standard deviations of the burst effect versus SD IgG quantity by PLGA concentration.

As described in the literature, the release of IgG from the PLGA MS was governed by diffusion through pores and by erosion of the polymeric matrix at later stages [105]. Incomplete release of the active ingredient may be observed. This incomplete release can be attributed to various factors such as the affinity of the drug for the polymer, resulting in drug adsorption, or to instability issues occurring during the dissolution [106]. At later stages, when PLGA started to be degraded, non-specific adsorption, covalent and non-covalent aggregation and denaturation of the MAb could occur. In our study, no incomplete release was observed on MS produced with 10 and 15 % w/v PLGA concentration which confirmed the absence of irreversible IgG interactions with the co-polymer. (Figure 29).

## 2.5 Influence of the investigated parameters on IgG stability during the encapsulation process and dissolution

The stability of the IgG incorporated in the MS was evaluated by SEC during the encapsulation process and the dissolution test.

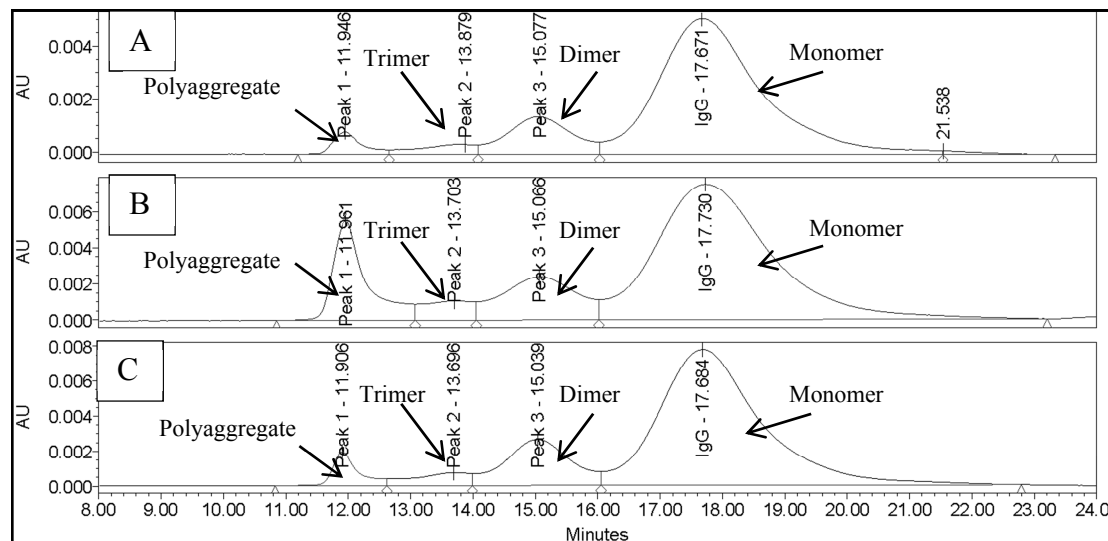


**Figure 31** SEC chromatograms of IgG samples eluted as four species: monomer (17.7 min), dimer (15.1 min), trimer (13.7 min) and polyaggregate (11.9 min) - (A) IgG after 1h time point dissolution of 5.5 % w/v PLGA MS, (B) IgG after 1h time point dissolution of 1 % w/v PLGA MS, (C) IgG in solution (non-encapsulated lyophilized IgG).

Figure 31 shows the chromatograms of the non-encapsulated IgG and the IgG released after 1h of dissolution of the produced MS using 1 % and 5.5 % (w/v) PLGA solutions. The main peak (retention time = 17.7 minutes) was identified as the IgG monomer. The peaks characterized by lower retention times (e.g. 15.1, 13.7 and 11.9 minutes) were identified as dimer, trimer and higher oligomers, respectively. An increase in the % area of the aggregation peak corresponding to soluble polyaggregates (retention time = 11.9 minutes) was observed without modification of the retention time after 1 h for the MS produced using 1 % (w/v) PLGA solution (Figure 31– B). An average loss of 20 % (w/w) monomer linked to this increase in aggregation level was calculated on the produced formulations using a 1 % (w/v) PLGA concentration. In contrast, with the exception of one formulation, which presented a high loss of percent of monomer (data

not shown), no increase in the aggregation level was observed for formulations produced using higher PLGA concentrations.

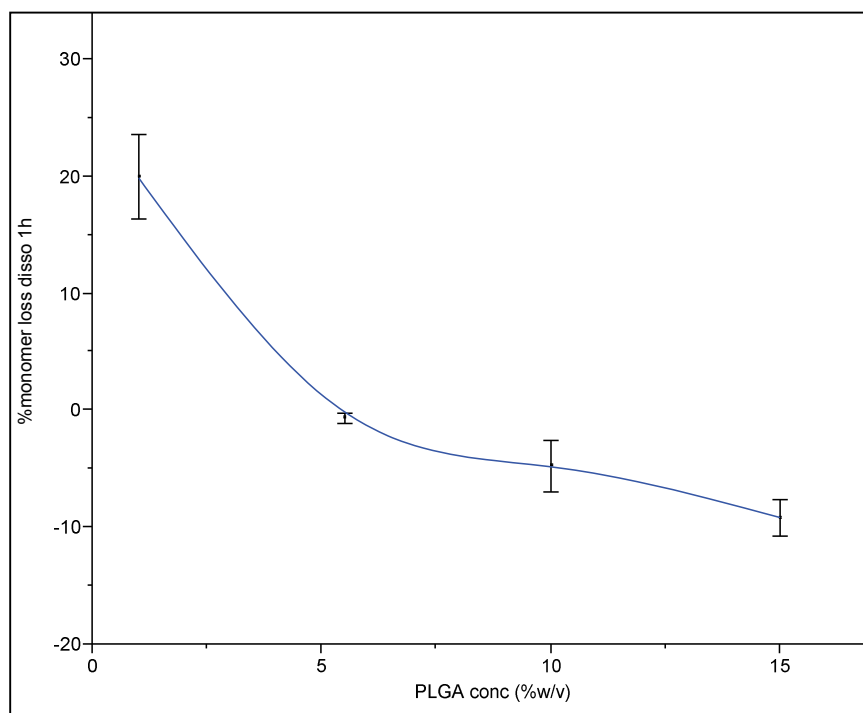


**Figure 32** Influence of the PLGA concentrations (from 1 to 15 % w/v) on the loss of IgG monomer after 1h dissolution (% w/w) of IgG-loaded PLGA MS. This figure shows the mean values and the standard deviations of loss of IgG monomer versus PLGA concentration. A smoothed curve (obtained by cubic spline) was added to the graph for clarity

The effect of the PLGA concentration on IgG stability during the encapsulation process and release was statistically significant ( $p < 0.001$ ) (Figure 33).

This stability improvement observed during the encapsulation process using higher PLGA concentrations was attributed to the faster hardening of the MS, which may have a protective effect on the entrapped IgG. The encapsulated IgG was protected against organic solvent, which could affect the stability of the IgG. The effect of the volume of the external phase on the stability improvement was also attributed to the faster hardening of the MS when using a higher aqueous volume.

An increase in the emulsification time and the emulsification rate might lead to an increase in the aggregation level due to higher energy applied to the IgG. It has been demonstrated that protein degradation might occur during mechanical shearing. Such applied forces increase the risk of

protein adsorption at the air/water interfaces, which promotes hydrophobic interactions leading to aggregation [106].

## 2.6 Factor selection

All the effects of the different studied factors observed on the evaluated responses are summarized in Figure 33 .

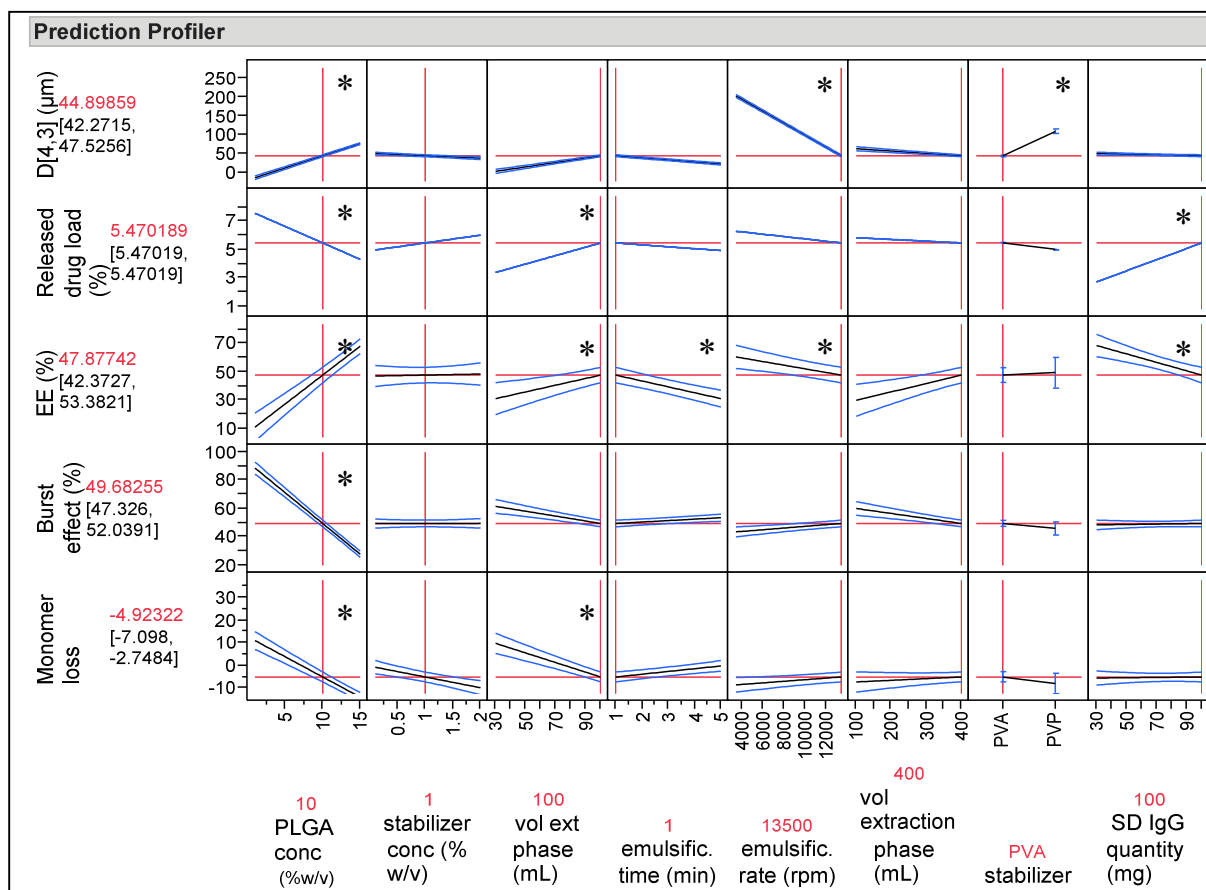


**Figure 33** Prediction profiler in the optimal conditions (in red) proposed by JMP based on the statistical fitted model constructed by least square fitting and showing the effect of the tested factors - \* represented the factors with a statistically significant effect (p-value for the test < 0.05; two-tailed test)

Based on this study, the concentration of PLGA appeared to be one of the most critical factors in the s/o/w process for encapsulating IgG in PLGA MS. Indeed, it was observed that the concentration of PLGA greatly influenced the particle size distribution of the produced MS, the drug loading, the EE%, the release profile and the stability of the IgG during the encapsulation process and its release.

Therefore, it was decided to produce the MS with a PLGA concentration of 10 % (w/v) to obtain a high viscosity in the organic phase, a faster solidification of the MS and a low porosity. Regarding the nature of the stabilizer, it was decided to select PVA, which is the most widely-described stabilizer in the literature for the production of PLGA MS and which tends to decrease their particle size. The PVA was used at 1 % (w/v) in the external phase to stabilize the microdroplets during the emulsification process.

The emulsification time was fixed at 1 minute to reduce the loss of IgG into the aqueous phase and to limit the risk of aggregation related to longer shearing times. The volume of the extraction phase was fixed at 400 mL to allow maximal extraction of the organic solvent.

It should be noted that our study allowed the s/o/w manufacturing process to be modeled, providing good statistical prediction models. This was confirmed by comparing the characteristics of the IgG-loaded PLGA MS predicted by the statistical model and the results obtained with the formulations produced using the selected settings (data not shown).

### **3 CONCLUSION**

It was demonstrated that the s/o/w encapsulation method using the less toxic solvent EtAc can be used successfully to produce IgG:PLGA MS. The experimentally designed study led to the identification of the critical parameters for the process. By selecting the values of these parameters, it is possible to produce IgG:PLGA MS with reproducible physico-chemical properties (e.g. particle size, stability, EE%, drug loading, and release profile). The formation of agglomerated MS will be evaluated further by controlling the precipitation of the polymer and adding a drying step after the recovery of the MS. The impact on the release profile and on the stability of the different entrapped Ab will be studied using PLGA with different inherent viscosities and hydrophilicities. The selected s/o/w encapsulation process will be used for MAbs and fragments, whose activity will be confirmed after encapsulation and during the release of the drug.

## **APPLICATION AND EVALUATION OF THE SPRAY-DRYING PROCESS TO A FULL LENGTH ANTIBODY (ANTI-TNF ALPHA) IN ORDER TO PREPARE SUBSEQUENT ENCAPSULATION**

### **1 INTRODUCTION**

The first step of the project was performed with the IgG as a model molecule to demonstrate the feasibility of Ab encapsulation into PLGA MS. However, due to the absence of specificity of such model, it was impossible to evaluate a potential loss of activity of the IgG during the spray-drying process, the encapsulation process or dissolution. Therefore, a humanized anti-TNF alpha full-length Ab (CDP571) was selected as suitable molecule for spray-drying and encapsulation evaluations.

This chapter described the application of the developed spray-drying process to the anti-TNF alpha MAb and the selection of the suitable formulations.

### **2 SPRAY-DRIED FORMULATION DEVELOPMENT FOR ANTI-TNF-ALPHA ANTIBODY**

The purpose of this study was to evaluate the effects of the formulation parameters on the physico-chemical properties of the produced SD microparticles. Different stabilizers (mannitol, trehalose and sucrose) used alone or in combination were evaluated at different ratios [107]. Two buffers (histidine pH 6.0 and glutamate pH 5.0) were also used to set different pH ([Table 23 and table 41 in appendix](#)). These excipients were selected based on the knowledge gained in the laboratory of biological formulation from UCB-Pharma. Indeed, it was proved that the selected formulations were typically those that allow a better stabilization during the drying process. The spray-drying process parameters were set as follows: liquid flow rate, 3 mL/min; inlet T°, 130°C, outlet T°, 70°C; atomization flow rate, 800 L/h; aspiration setting, 85 %. The solid concentration was increased from 25 mg/mL to 50 mg/mL with a 70:30 MAb:stabilizers ratio. This increase was applied because it was demonstrated that a lower CDP571 concentration generated a higher quantity of sub-visible particles (2.9 % vs. 1.6 % w/w aggregates with size > 100 nm for 25 mg/mL vs. 50 mg/mL MAb, respectively). A higher MAb concentration might contribute to stabilize the formulation during the spray-drying process. This relationship was not observed

VIII. Application and evaluation of the spray-drying process to a full length antibody (anti-TNF alpha) in order to prepare subsequent encapsulation

using the IgG as model molecule (page 100). It may be explained by the quality of the material. The initial level of HMWS was much higher for the IgG (20 % w/w) compared to that of the CDP571 (0.3 % w/w).

An additional formulation (SD CDP571-11, Table 23) was added to study the spray-drying process without addition of any stabilizer.

**Table 23: Evaluated formulations for the spray-drying process of anti-TNF alpha MAb**

Formulation	IgG:Mannitol:stabilizer ratio	20 mM Buffer	Stabilizer
SD CDP571-1	70:30:0	Histidine pH 6.0	-
SD CDP571-2	70:15:15	Histidine pH 6.0	Trehalose
SD CDP571-3	70:0:30	Histidine pH 6.0	Trehalose
SD CDP571-4	70:15:15	Histidine pH 6.0	Sucrose
SD CDP571-5	70:0:30	Histidine pH 6.0	Sucrose
SD CDP571-6	70:30:0	Glutamate pH 5.0	-
SD CDP571-7	70:15:15	Glutamate pH 5.0	Trehalose
SD CDP571-8	70:0:30	Glutamate pH 5.0	Trehalose
SD CDP571-9	70:15:15	Glutamate pH 5.0	Sucrose
SD CDP571-10	70:0:30	Glutamate pH 5.0	Sucrose
SD CDP571-11	100:0:0	Histidine pH 6.0	-

## 2.1 Results and discussion

The process yields were higher than 50 % ranging between 52.7 and 66.0 %. All the produced SD powders (SD CDP571-1 to -11) were characterized by a similar particle size distribution (Figure 34), with a median diameter  $d(0,5)$  ranging between 5.7 and 6.8  $\mu\text{m}$ , which was similar to that obtained with the bovine IgG.

VIII. Application and evaluation of the spray-drying process to a full length antibody (anti-TNF alpha) in order to prepare subsequent encapsulation

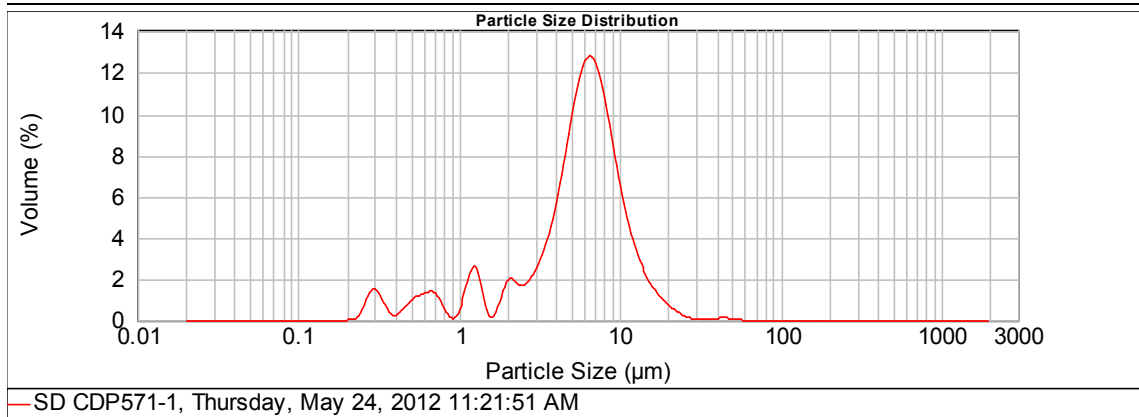


**Figure 34: Particle size distribution of spray-dried SD-CDP571-1**

The SD CDP571 microparticles were spherical, with some irregular torus-shaped particles (donut-like) (Figure 35).

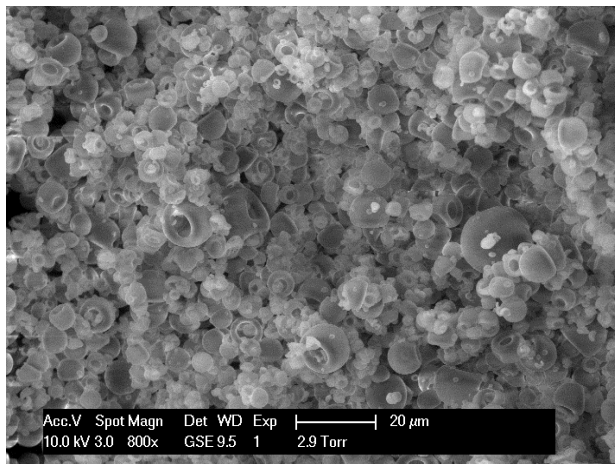


**Figure 35: SEM picture of the SD CDP571-1 microparticles**

The XRPD evaluation confirmed that the SD material was amorphous. The residual moisture ranged between 4.6 and 6.0 % w/w. The three highest water contents were observed with formulations SD CDP571-3 (6.0 %), 7 (6.0 %) and 8 (5.9 %) containing trehalose. Trehalose interacts more strongly with water. It is described that in amorphous trehalose, local pockets of crystalline dihydrate exist, which trap residual water molecules, immobilizing them when water is scarce [107].

The MAb concentration was evaluated after reconstitution (solubilization) of the SD powder in a known volume of water. The lowest recovery values, which were attributed to an incomplete dissolution of the CDP571 during the reconstitution, were observed for formulations SD CDP571-6 (77.3 % w/w) and 11 (82.9 % w/w). These latter were produced in glutamate buffer

VIII. Application and evaluation of the spray-drying process to a full length antibody (anti-TNF alpha) in order to prepare subsequent encapsulation

without addition of stabilizer or mannitol, respectively. In addition, incomplete dissolution of the SD powder, which led to a cloudy solution, was observed for formulations SD CDP571-4, 5, 9, and 10, all containing sucrose, and for formulation SD CDP571-6 and 11, both produced without stabilizer. This incomplete dissolution was explained by the formation of insoluble aggregates generated during the drying process where stabilizers were not incorporated.

The HMWS and LMWS levels were evaluated before and after the drying step (Table 24).

**Table 24: HMWS and LMWS (SEC) levels (%) measured before and after spray-drying of the SD CDP571 formulations (SD CDP571-1 to 11)**

Formulation	HMWS (%)		LMWS (%)	
	solution	spray-drying	solution	spray-drying
SD CDP571-1	0.32	0.37	0.54	0.56
SD CDP571-2	0.26	0.44	0.55	0.63
SD CDP571-3	0.24	0.29	0.57	0.66
SD CDP571-4	0.23	0.53	0.54	0.56
SD CDP571-5	0.24	0.69	0.54	0.56
SD CDP571-6	0.23	0.83	0.55	0.56
SD CDP571-7	0.21	0.62	0.56	0.63
SD CDP571-8	0.2	0.28	0.56	0.66
SD CDP571-9	0.2	0.56	0.55	0.56
SD CDP571-10	0.27	0.72	0.56	0.57
SD CDP571-11	0.28	0.94	0.62	0.64

The HMWS levels (Figure 36; in blue) were increased after spray-drying and were statistically higher than those measured for the solutions ( $p < 0.0001$ , paired t Test). The highest increase in HMWS (0.66%) was observed for formulation SD CDP571-11, produced without addition of stabilizer. This result confirmed the need for stabilizer to avoid Ab agglomeration during the spray-drying process. However, when comparing the increase in HMWS for formulations SD CDP571-2 (0.18 %) and 3 (0.05 %) to those for formulations 4 (0.3 %) and 5 (0.45 %), it appeared that sucrose did not present the same protective effect as trehalose [91]. In addition, the buffer agent might affect the Ab stability. In general, the formulations in histidine buffer (formulations SD CDP571-1 to 5) seemed to lead to lower levels of HMWS than formulations in glutamate (formulations SD CDP571-6 to 10). The LMWS increased to a maximum value of 0.1

% after spray-drying. They were statistically higher than those measured for the solutions ( $p < 0.01$ , t Test)

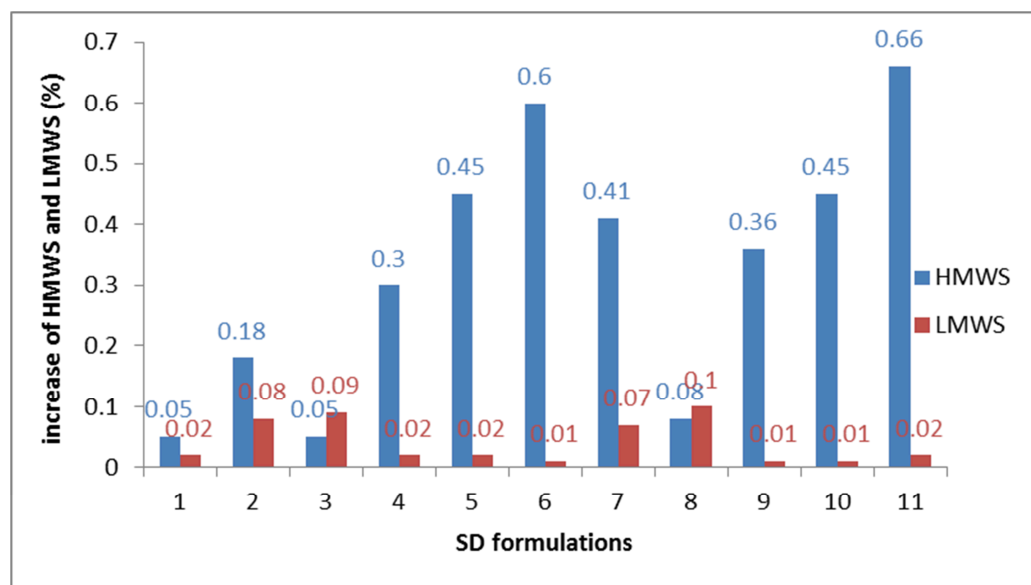


**Figure 36: Comparison of the increase of HMWS and LMWS after the spray-drying process measured by SEC for SD CDP571-1 to -11**

In addition to SEC, which is a method that is able to detect particles sized from 1 nm to 100 nm, which correspond to protein monomer and soluble aggregates (5 – 1000 KDa), DLS analysis was performed to evaluate the sub-visible particles. The presence of sub-visible particles was not reported before the spray-drying process (Table 25). The highest levels of aggregation (4.1 and 5.2 % > 100 nm) were observed for formulations SD CDP571-1 and 6 (Table 25). This observation confirmed that mannitol led to the formation of HMWS.

It was previously demonstrated that a lower CDP571 concentration generated a higher quantity of sub-visible particles (2.9 % vs. 1.6 % w/w aggregates with size > 100 nm for 25 mg/mL vs. 50 mg/mL MAb, respectively). A higher MAb concentration might contribute to stabilizing the formulation during the spray-drying process.

The particles characterized by a mean diameter higher than 5  $\mu\text{m}$  was evaluated by turbidity at 350 nm.

VIII. Application and evaluation of the spray-drying process to a full length antibody (anti-TNF alpha) in order to prepare subsequent encapsulation

**Table 25: Turbidity measurements at 350 nm ( $A_{350}$ ) and % aggregates >100 nm (DLS)**

Formulation	After spray-drying			
	After buffer exchange		Reconstituted solution	
	$A_{350}$	DLS - > 100 nm (%)	$A_{350}$	DLS - > 100 nm (%)
SD CDP571-1	0.08	0	0.19	4.1
SD CDP571-2	0.07	0	0.15	2.8
SD CDP571-3	0.07	0	0.15	3.0
SD CDP571-4	0.07	0	0.18	3.2
SD CDP571-5	0.08	0	0.19	2.5
SD CDP571-6	0.07	0	0.28	5.2
SD CDP571-7	0.07	0	0.14	1.2
SD CDP571-8	0.06	0	0.14	2.6
SD CDP571-9	0.06	0	0.19	2.9
SD CDP571-10	0.08	0.3	0.27	2.4
SD CDP571-11	0.07	0	0.15	2.3

An absorbance higher than 0.1 measured for the reconstituted solution indicated the presence of insoluble aggregates. The absorbance values after spray-drying were statistically higher than those measured for the solutions ( $p < 0.0001$ , paired t Test). It was expected, based on the macroscopic observation. The highest optical density ( $A_{350}$ ) were obtained with formulations SD CDP571-4, 5, 9 and 10, each containing sucrose, and formulations SD CDP571-1 and 6, both containing mannitol (Table 25). The addition of either mannitol (SD CDP571-1 and 6) or sucrose (SD CDP571-5 and 10) seemed to be less effective at preventing the formation of insoluble aggregates than trehalose, especially in the glutamate buffer.

The binding capacity was evaluated for each formulation by ELISA. All the evaluated formulations presented a relative binding capacity higher than 70 % (Figure 37). The level of increase of either the soluble aggregates (HMWS (SEC) and > 100 nm (DLS)) (SEC) or the insoluble aggregates ( $A_{350}$ ) observed after the spray-drying process did not seem to affect the binding capacity of the MAb.

VIII. Application and evaluation of the spray-drying process to a full length antibody (anti-TNF alpha) in order to prepare subsequent encapsulation

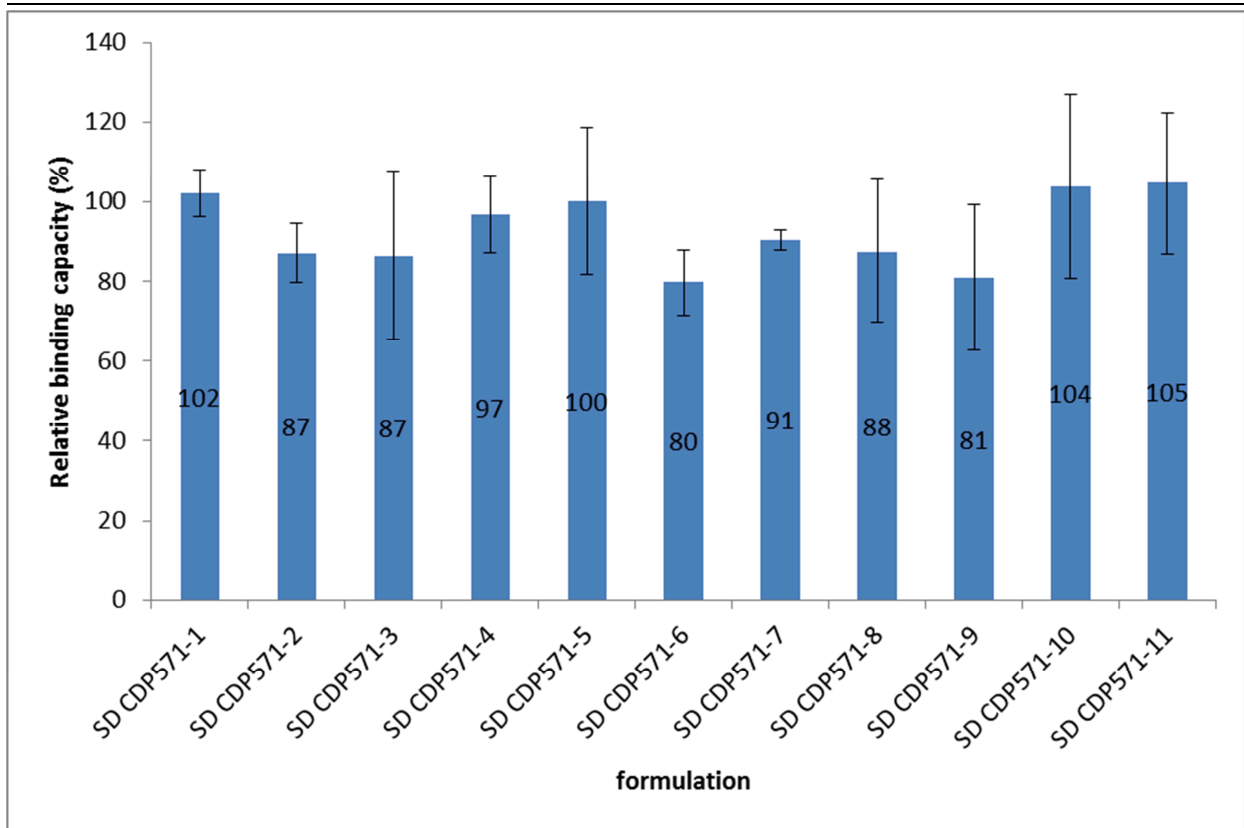


**Figure 37: Comparison of formulations SD CDP571-1 to 11 relative binding capacity (%), determined by ELISA; (mean (s), n = 4).**

Reporter gene bioassays were performed on formulations SD CDP571-3, 8 and 10 and confirmed the TNF activity of the CDP571 after the spray-drying process (Figure 38). However, the estimated relative potency of the CDP571 after spray-drying (from 40 to 55 %) suggested a lower potency compared to the CDP571 standard reference.

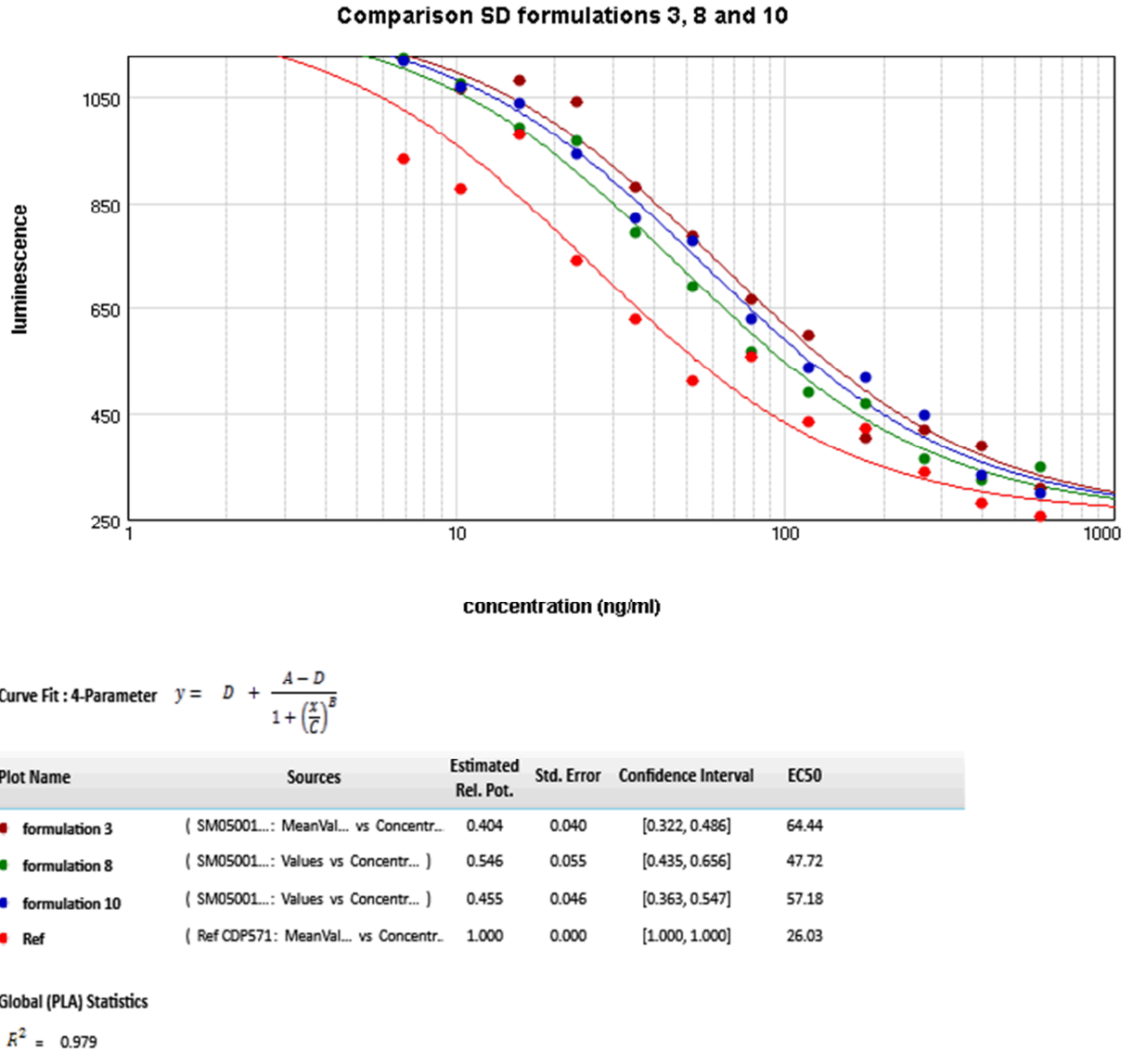


**Figure 38:** Graph of luminescence vs. concentration (ng / mL) plots of SD formulations 3 (●), 8 (●) and 10 (●) and CDP571 reference solution (●); calculated EC<sub>50</sub> and estimated relative potency vs. CDP571 reference standard based on a 4-parameter curve fitting

### **3 CONCLUSION**

It was confirmed that the spray-drying process was able to produce Ab microparticles characterized by an appropriate particle size with a mean diameter  $d(0.5)$  around 6  $\mu\text{m}$ . The binding capacity of the Ab were conserved after spray-drying.

During the screening study, insoluble aggregates were observed for formulations containing sucrose as a stabilizer and formulations containing only mannitol, especially when using a glutamate buffer compared to histidine. In contrast, the trehalose used as a stabilizer seemed to decrease the formation of insoluble aggregates.

The level of soluble aggregates (HMWS) measured by SEC was acceptable ( $< 3\%$  w/w). Indeed, an increase of maximum 0.66 % was measured after spray-drying for solutions formulated without stabilizer. The formulations without stabilizer or containing sucrose or mannitol in glutamate buffer were more affected by the spray-drying (increase in the HMWS fraction). It seemed that formulations in histidine buffer were characterized by a lower level of HWMS. However, formulations containing histidine showed higher amounts of sub-visible microparticles ( $> 100\text{ nm}$ ).

It was concluded that adding trehalose as a stabilizer positively affected the production of CDP571 SD microparticles. Therefore, the preferred formulation for the spray-drying was a CDP571 solution containing trehalose with an Ab:stabilizer ratio set at 70:30 in 20 mM histidine pH 6.0 (formulation SD CDP571-3). The stabilization effect of this preferred formulation on the CDP571 was also confirmed further during the encapsulation process.

## **DEVELOPMENT OF FULL LENGTH ANTIBODY (ANTI-TNF ALPHA) LOADED PLGA MICROSPHERES USING THE SOLID-IN-OIL-IN-WATER ENCAPSULATION METHOD**

### **1 INTRODUCTION**

It has been demonstrated that it was possible to encapsulate IgG in PLGA MS. This chapter will describe the development of such technique for the encapsulation of anti-TNF- $\alpha$  MAb.

### **2 SELECTIONS OF FORMULATIONS**

The encapsulation evaluation of CDP571 was carried out using the ten SD microparticle formulations (SD CDP571-1 to 10; [Table 41](#) in appendix). A 10 % w/v PLGA (Resomer<sup>®</sup> RG504) EtAc solution was used as the organic solution. The amount of SD CDP571 to be dispersed in this organic solution was set at 150 mg (15 % w/w theoretical drug loading). Indeed, a pre-test demonstrated that the EE% for the CDP571 (70 % w/w) was higher than that obtained for the bovine IgG (50 % w/w) using the same process (data not shown). Moreover, when increasing the theoretical loading from 8.7 % to 16 % w/w, the CDP571 content increased from 6.9 to 11.5 % without loss of EE %. Ten formulations of CDP571-loaded RG504 MS were produced ([Table 42](#) in appendix; formulations MS CDP571-1 to -10), using the s/o/w process.

#### **2.1 Results and discussion**

Except for formulation MS CDP571-5, which presented a larger particle size distribution with a median diameter  $d(0,5)$  of 62  $\mu\text{m}$  and a  $d(0,9)$  of 275  $\mu\text{m}$ , which was unexpected, the particle size distribution was relatively similar from one formulation to another. They were characterized by a  $d(0,5)$  ranging from 34 to 45  $\mu\text{m}$  and by a  $d(0,9)$  that reached a maximal value of 136  $\mu\text{m}$  ([Table 26](#)). Therefore, the particle size of the produced MS was suitable for injection.

IX. Development of a full length antibody (anti-TNF alpha) loaded PLGA microspheres using the solid-in-oil-in-water encapsulation method

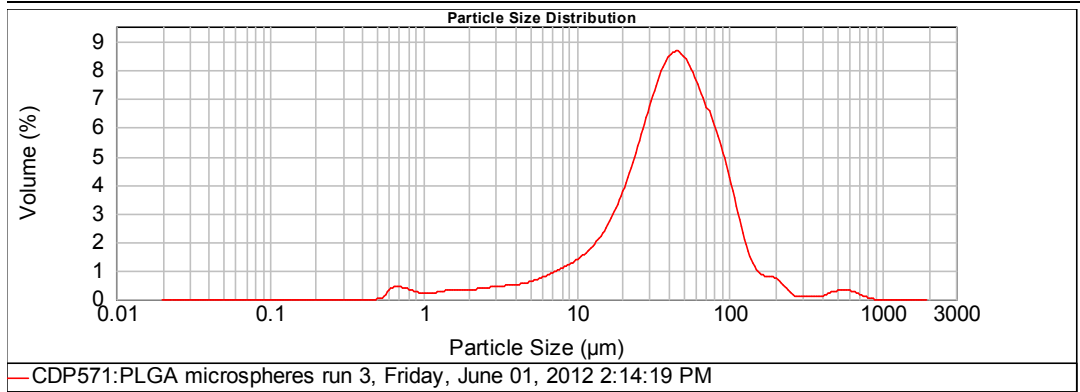


**Figure 39: Particle size distribution – CDP571: PLGA formulation 3**

Both the surface morphology and the internal porosity were evaluated by SEM for the CDP571:PLGA MS. As previously observed (page 104), spherical CDP571:PLGA MS characterized by a low porosity at the surface and a large internal porosity were produced (Figure 40 and Figure 41).

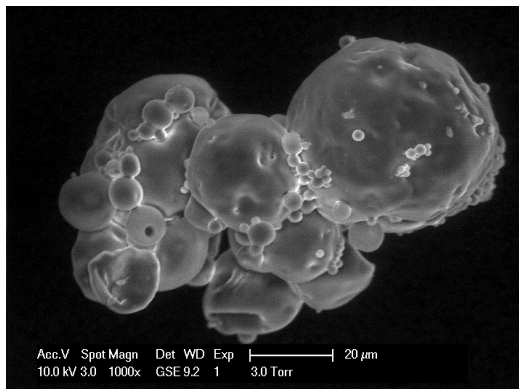


**Figure 40: SEM picture – surface morphology of MS CDP571-10**

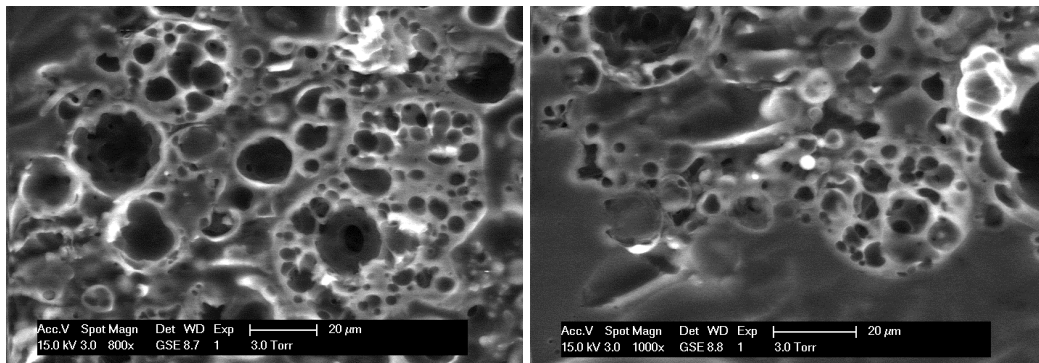


**Figure 41: SEM pictures – internal porosity of MS CDP571 Sectional views and the internal porosity after coating in an epoxy resin and polishing with a diamond knife microtome -10**

The encapsulation efficiency was tested for the ten MS CDP571 formulations (Table 26).

**Table 26: Encapsulation evaluation and particle size (d(0.5) of the MS CDP571-1 to -10**

Formulation	Theoretical loading (%)	EE (%)	Loading (%)	d(0.5) (µm)	d(0.9) (µm)
MS CDP571-1	15.4	27.4	4.2	41.3	104.8
MS CDP571-2	15.0	54.6	8.2	34.5	91.0
MS CDP571-3	15.5	75.0	11.6	41.9	98.9
MS CDP571-4	15.3	75.4	11.6	34.9	77.9
MS CDP571-5	15.4	72.0	11.1	62.2	274.5
MS CDP571-6	15.0	73.6	11.0	44.6	136.3
MS CDP571-7	15.5	75.0	11.6	37.1	99.2
MS CDP571-8	15.6	82.7	12.9	42.6	102.7
MS CDP571-9	15.4	74.4	11.5	39.1	95.6
MS CDP571-10	15.2	73.8	11.2	37.5	96.0

The lowest loading capacity (4.2 %) and EE% (27.4 %) were observed for formulation MS CDP571-1, which was produced without the addition of a stabilizer in the SD formulation. The increased protein loading achieved by co-encapsulation of trehalose or sucrose might be attributed to preferential hydration of the protein [108]. This indicated that H-bonds and polar interactions played an important role in protein encapsulation in PLGA MS, as the hydrophilic additive increased the encapsulation efficiency of the protein. The addition of sugars might decrease the interactions between the protein and the organic solvent, reducing the leakage of protein to the aqueous phase [109].

The loss of monomer (% monomer after spray-drying - % monomer after s/o/w) evaluated by SEC during the encapsulation evaluation ranged between 0.3 % and 4.4 % w/w. The highest losses were observed for formulations MS CDP571-10 (1.8 %) and 6 (1.3 %). The loss of monomer observed after the encapsulation process was attributed to an increase in the HMWS level (Figure 42).

IX. Development of a full length antibody (anti-TNF alpha) loaded PLGA microspheres using the solid-in-oil-in-water encapsulation method

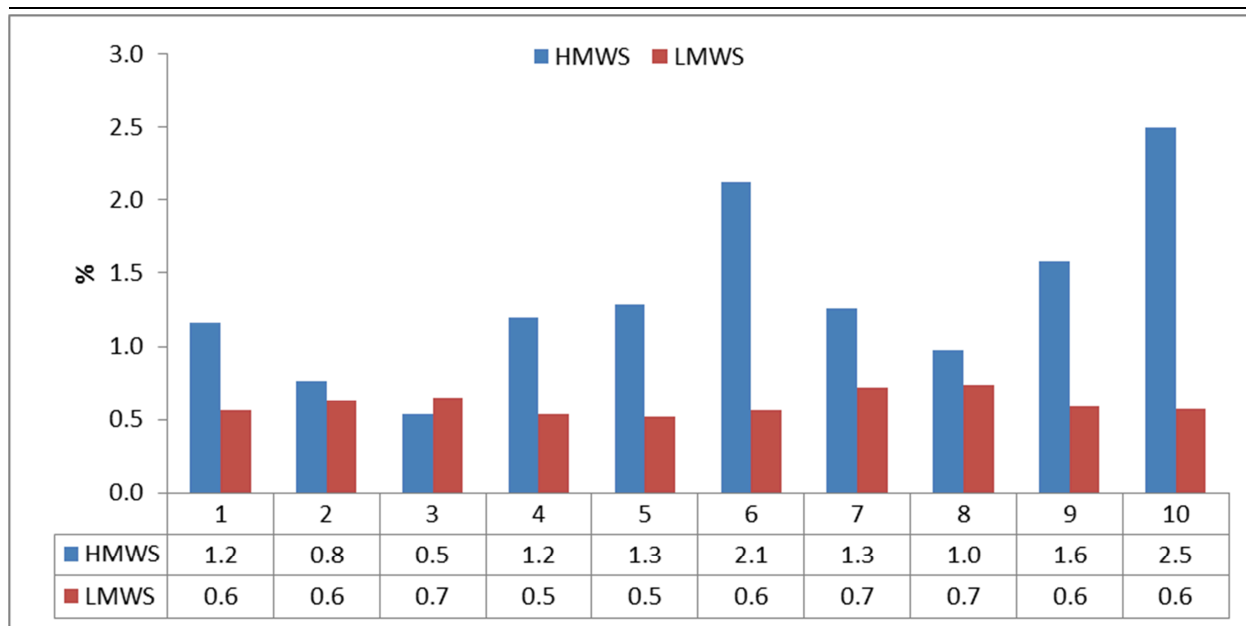


**Figure 42: Comparison of HMWS and LMWS level of Ab for formulations MS CDP571-1 to 10**

The addition of trehalose (formulations MS CDP571-2, 3, 7 and 8) and the use of histidine (formulations MS CDP571-1 to 5) decreased the formation of soluble aggregates (Figure 42). Indeed, the lowest percentage of HMWS (0.5 % w/w) was measured for formulation MS CDP571-3, which contained trehalose and an histidine buffer. It was confirmed that solid CDP571 microparticles used in the *s/o/w* method were protected by the addition of a hydrophilic component [60, 110]. Previous studies indicated that the sugars' stabilization might be explained by preferential hydration or by reduction of the flexibility and mobility of the proteins in the glassy matrix formed by the excipients [63]. The limitations of co-encapsulated water-soluble additives may be their limited residence time within the hydrated MS resulting in a limited stabilizing effect during the release [52].

It was also observed that a greater amount of SD powder (150 vs. 100 mg) dispersed in the organic phase contributed to stabilizing the CDP571 in terms of HMWS, which decreased from 3.5 % to 1.4 % w/w (data not shown).

The LMWS level (maximum 0.7 % w/w) was not affected by the encapsulation process, as similar percentages were measured on the SD samples.

The binding capacity was evaluated by ELISA on the samples used for evaluating the encapsulation efficiency (Figure 43).

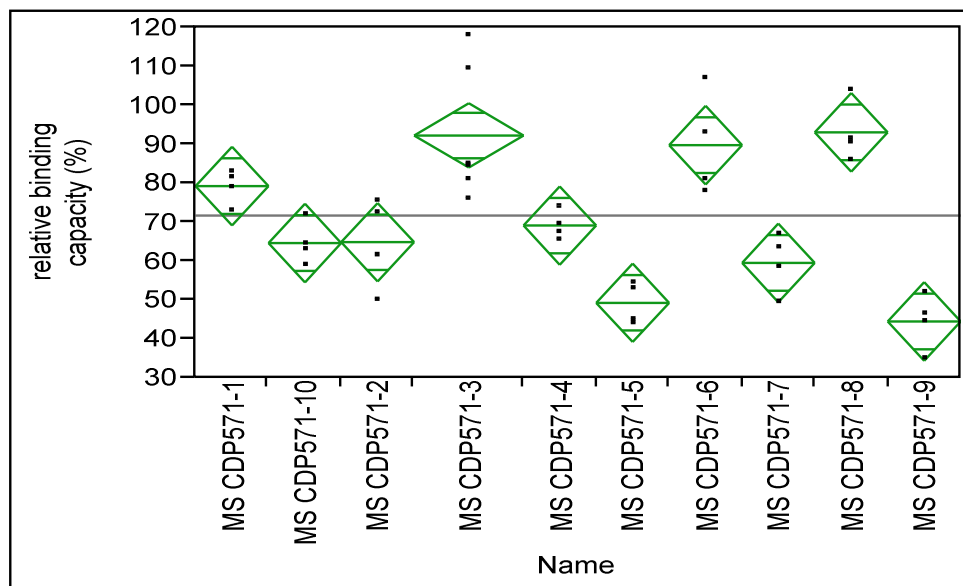
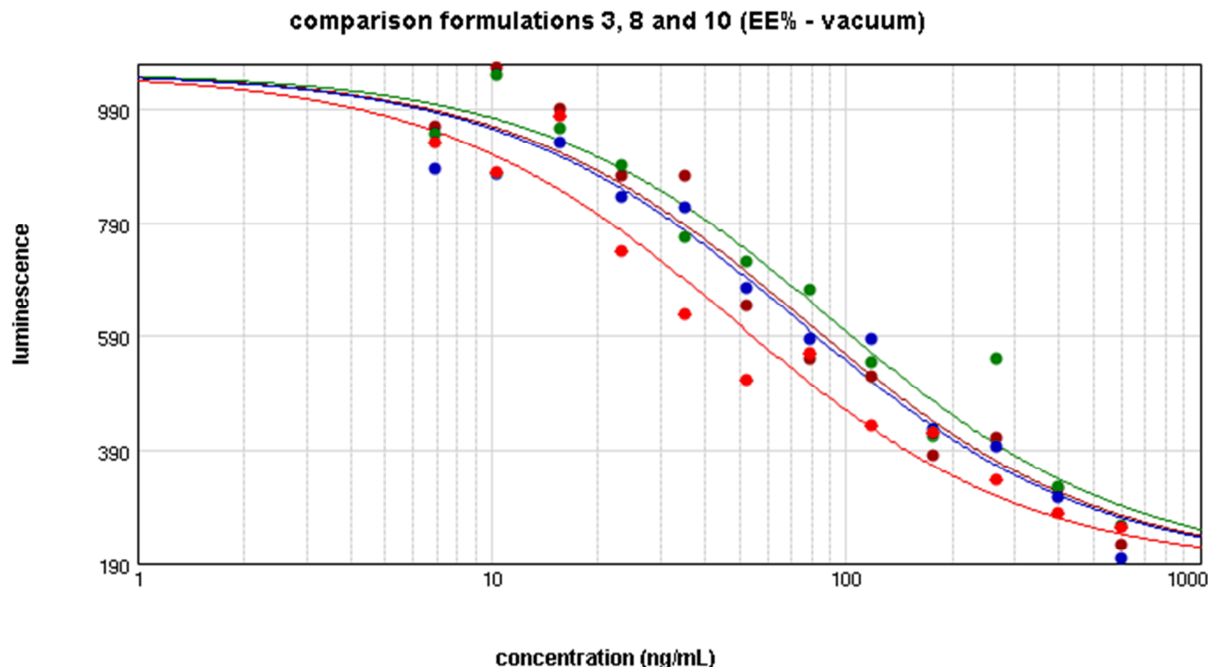


**Figure 43:** ELISA – Oneway ANOVA of relative binding capacity (%) by formulation MS CDP571-1 to 10 calculated vs. CDP571 reference standard; in green the mean diamonds (group mean and 95 % confidence interval) (n = 4)

While the binding capacity observed in formulations SD CDP571 - 1 up to 10 was about > 70 % (Figure 37 section VIII), the s/o/w process seemed to decrease the binding capacity of the MAb. The relative binding capacity of formulations (mean of response) was calculated to be 71.6 %. Some formulations (MS CDP571-5, -7 and -9) appeared to be lower ( $p < 0.001$ ). However, there was no loss of binding capacity with formulation MS CDP571-3, which contained trehalose in histidine buffer pH 6.0.

The TNF activity was evaluated by reporter gene bioassay on formulations MS CDP571-3, 8 and 10. It was confirmed that the anti-TNF activity of the CDP571 was preserved after the encapsulation process (Figure 44). In the same way than the MAb standard, the increasing concentrations of anti-TNF alpha MAb (samples from EE% assay) completely suppressed the luciferase activity (linked to the TNF- $\alpha$  activity) in a dose-dependent manner as reflected by the decrease of the luminescence signal.

IX. Development of a full length antibody (anti-TNF alpha) loaded PLGA microspheres using the solid-in-oil-in-water encapsulation method



Curve Fit : 4-Parameter  $y = D + \frac{A - D}{1 + \left(\frac{x}{C}\right)^B}$

Plot Name	Sources	Estimated Rel. Pot.	Std. Error	Confidence Interval	EC50
● formulation 3	( SM05001...: Values vs Concentr... )	0.628	0.096	[0.434, 0.822]	76.76
● formulation 8	( SM05001...: Values vs Concentr... )	0.523	0.080	[0.361, 0.685]	92.07
● formulation 10	( SM05001...: Values vs Concentr... )	0.661	0.101	[0.457, 0.865]	72.92
● Ref.	( Ref CDP571: MeanVal... vs Concentr... )	1.000	0.000	[1.000, 1.000]	48.17

**Figure 44:** Luminescence vs. concentration (ng/mL) plots of formulations MS CDP571 3 (●), 8 (●) and 10 (●) and the CDP571 reference solution (●).

The dissolution profiles were evaluated for formulations MS CDP571-1 to 10 and plotted in the [Figure 45](#) as the averages of the MS formulations containing trehalose (MS CDP571-2, 3, 7 and 8) and sucrose (MS CDP571-4, 5, 9 and 10).

IX. Development of a full length antibody (anti-TNF alpha) loaded PLGA microspheres using the solid-in-oil-in-water encapsulation method

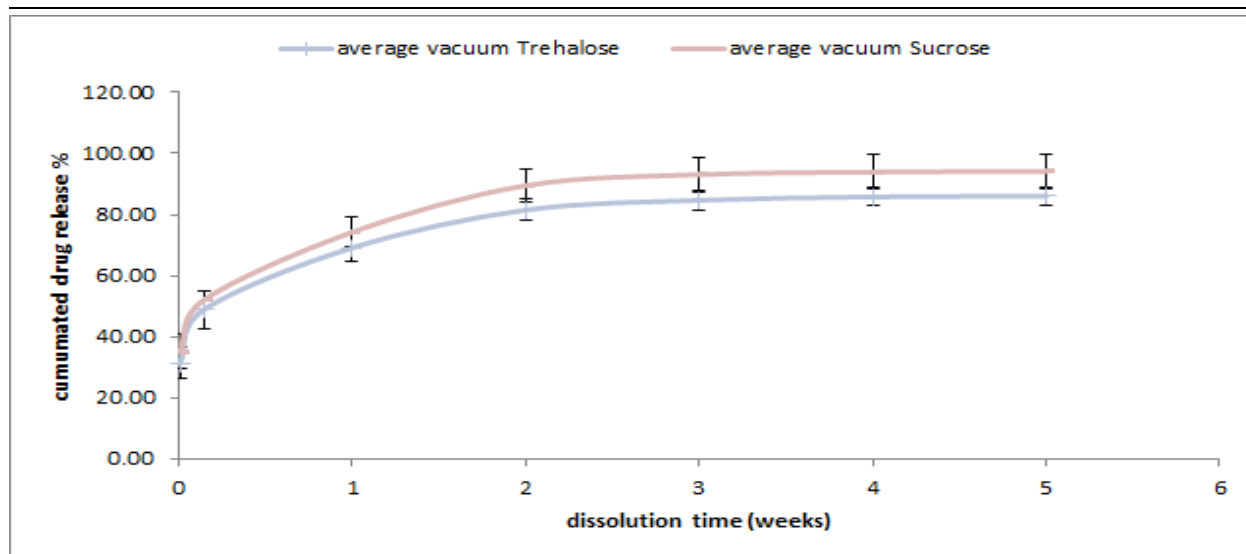


**Figure 45:** Mean and standard deviation of dissolution profiles measured for the 4 MS CDP571 formulations containing trehalose (in blue) and the 4 MS CDP571 formulations containing sucrose (in red).

A reproducible release profile characterized by a burst effect ranging between 40.6 and 55.7 % was obtained. The dissolution patterns appeared equivalent whatever the tested formulations (Figure 45). The nature of both the stabilizer and the buffering agent used in the MS formulations as well as the small variations of the physic-chemical characteristics of the produced MS did not seem to influence the release profile.

An increase in LMWS was observed over dissolution time for each formulation (Figure 46 B). After 2 - 3 weeks of dissolution in phosphate buffer, a deformation of the monomer peak, characterized by a shoulder, was observed on the SEC chromatograms for formulations 2, 3 and 8, containing trehalose (Figure 47). After 4 weeks, a complete shift of the main peak was observed for all the evaluated formulations. The degradation issues were attributed to the acidic degradation of the polymer, which is known to start after 3 - 4 weeks of dissolution [111].

IX. Development of a full length antibody (anti-TNF alpha) loaded PLGA microspheres using the solid-in-oil-in-water encapsulation method

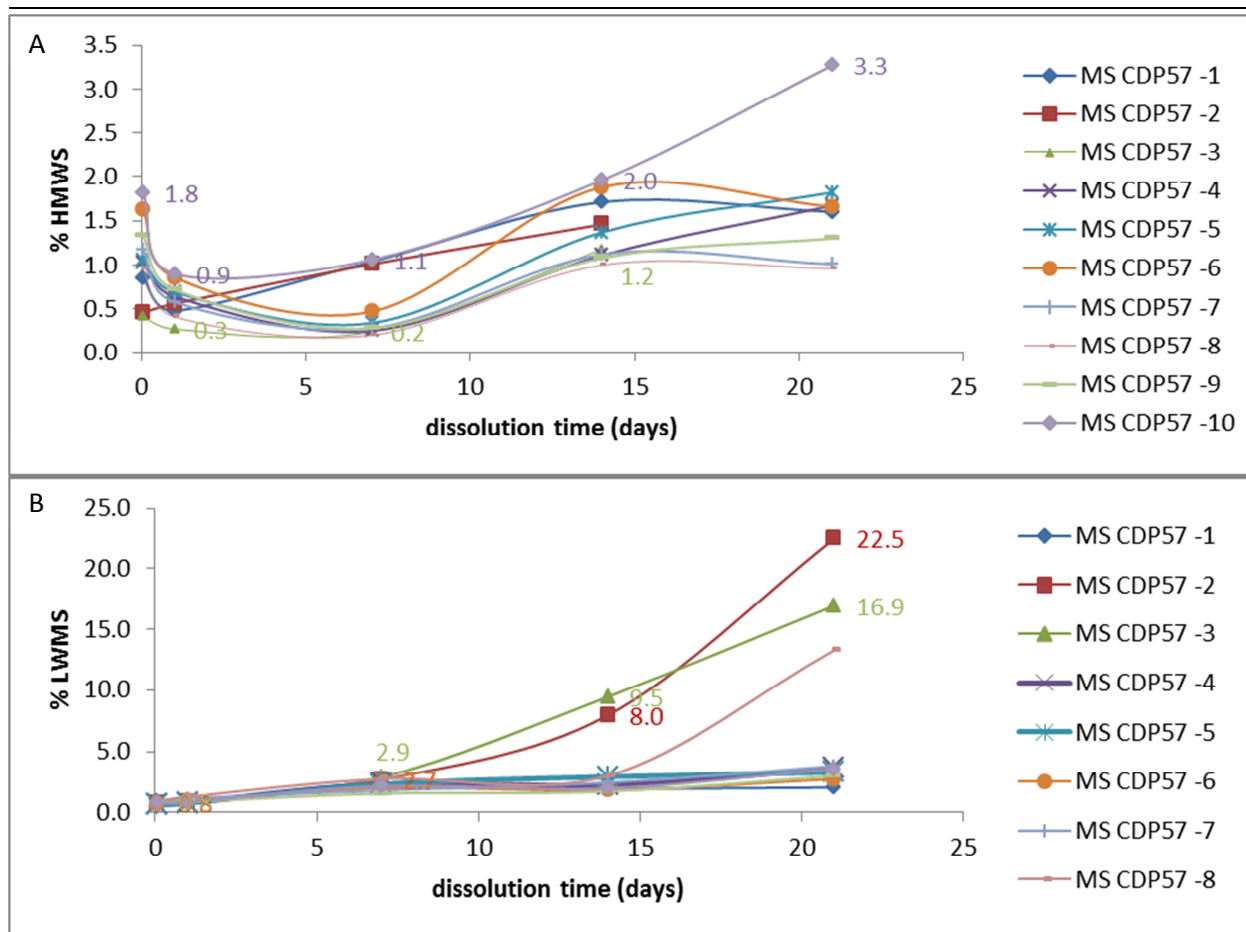


**Figure 46:** Comparison of % HMWS (A) and LMWS (B) over dissolution time (days) for MS CDP571-1 to 10.

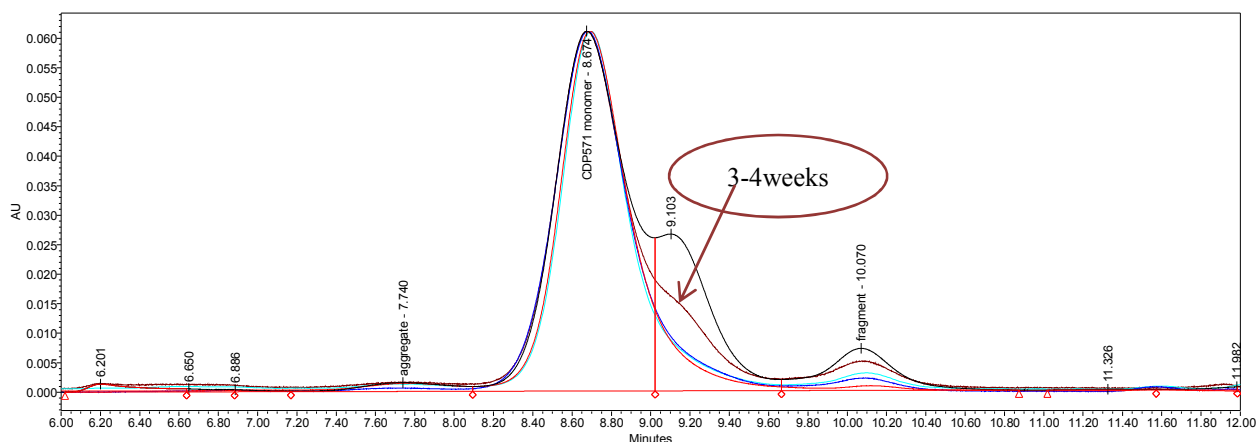


**Figure 47:** Chromatograms of formulation MS CDP571-3 over dissolution time: 24h in red, 1 week in dark blue, 2 weeks in clear blue, 3 weeks in brown and 4 weeks in black.

An increase in the HMWS up to a maximum of 3.3 % (MS CDP571-10) was also observed over time during the dissolution test (Figure 46 A). This degradation might also be linked to the acidic degradation of the polymer over the dissolution.

## 2.2 CONCLUSION

Based on the data obtained for the PLGA MS, trehalose and histidine were preferred as stabilizer and buffer (pH 6.0), respectively (formulation MS CDP571-3). Indeed, after modeling using a standard least square regression, it appeared that the histidine buffer led to a decrease in the loss of monomer, avoiding the formation of soluble aggregates ( $p = 0.0374$ ). On the other hand, the trehalose seemed to prevent the loss of monomer during the encapsulation process better than the sucrose, which tended to increase the level of HMWS after encapsulation ( $p = 0.0674$ ). Moreover, as previously observed, trehalose stabilized the Ab during the spray-drying

It was observed that after 4 weeks of dissolution, a complete loss of monomer appeared for all the evaluated formulations. This effect was correlated to the acidic degradation of the polymer. Different grades of PLGA were then evaluated to increase further the Ab stability during the dissolution.

## 3 SELECTION OF PLGA POLYMER

Both the degradation profile and the cross linkage density of the polymer influence the drug diffusion through the matrix. These properties depend on the molecular weight, the copolymer ratios, the glass transition temperature, the crystallinity and the hydrophilicity of the polymer. Different PLGA derivatives, which were characterized by different lactide:glycolide ratios and rheological behavior, were evaluated for the impact of the type of polymer (e.g. PLGA RG502, RG504, RG505 and RG755S) on the encapsulation efficiency, the dissolution profile and the stability of the Ab over the release. In addition, co-polymers of PEG-PLGA (e.g. RGPd5055, RGPd50105 and RGPd50155) were also evaluated. Indeed, highest protein activity was reported when the copolymer contained 10 – 30 % PEG, compared to that resulting from MS produced using PLGA [106]. It might be correlated to a reduce adsorption onto the polymer explained by the hydrophilic environment created by PEG chains [52].

150 mg of SD CDP571 powder produced from a 35 mg/mL CDP571 solution in 20 mM histidine (pH 6.0) containing 30 % w/w trehalose (formulation SD CDP571-3) were dispersed in 5 mL EtAc solution containing 10 % w/v PLGA or PEG-PLGA. The MAb-loaded polymer MS were produced using the s/o/w process. The MS were then dried under 1 mBar vacuum for 2 hours at 20°C.

### 3.1 Results and discussion

The type of polymer influenced the particle size distribution of the produced MS (Table 27). Comparing the formulations MS CDP571-11, -3 and -12 produced with PLGA characterized by a 50:50 lactide:glycolide ratio (RG502, RG504 and RG505), it was observed that the d(0.5) was increased from 26.1 µm to 51.1 µm. This increase was attributed to the increase in the rheological behavior of the polymer in solution. Indeed, the apparent viscosity increased with the molecular weight of the polymer (12 kDa, 46 kDa and 61.5 kDa as mean Mw for the RG502, RG504 and the RG505, respectively) (Table 6).

**Table 27: Particle size (d (0.5)), actual drug loading content, EE% and burst effect of PLGA and PEG-PLGA MS**

Formulation	PLGA	d(0.5) (µm)	Actual drug loading (%)	drug content	EE%	Burst effect (%)
MS CDP571-11	RG502	26.1	10.2		66.5	98.7
MS CDP571-3	RG504	44.6	9.3		61.1	52.8
MS CDP571-12	RG505	51.1	8.9		58.9	32.6
MS CDP571-13	RG755S	36.2	10.9		71.5	50.2
MS CDP571-14	RGPd5055	71.4	1.0		6.6	54.4
MS CDP571-15	RGPd50105	81.2	1.8		12.0	66.9
MS CDP571-16	RGPd50155	42.3	0.3		2.2	98.8

PEG-PLGA did not seem to be appropriate for CDP571 encapsulation. Indeed, PEG-PLGA provided a maximal loading of 2 % w/w (Table 27). In contrast, PLGA without PEG led to the production of MS characterized by a higher drug loading, from 9.0 to 11.0 % w/w. The RG755S provided the highest EE% (> 70 % w/w). The PEG could promote the diffusion of MAb from the inside of the premature MS to the continuous aqueous phase due to its property to form pores resulting to the lower EE% observed for formulations produced with PEG-PLGA [112]. In addition, during the precipitation step, the PEG branches of the diblock copolymer orientated

toward the aqueous phase. MAb, having a hydrophilic nature, might attach to hydrophilic moieties like PEG. The higher EE% (71.5 % w/w) observed for the MS CDP571-13 produced with the RG755S could be explained by the higher content in lactic acid (75 % vs. 50 % for the other tested Resomer) conducting to a faster precipitation of the polymer.

The binding capacity was evaluated on formulations MS CDP571-12 and 13. It was found to be higher than 85 % which confirmed the preservation of the binding capacity after encapsulation by s/o/w process.

The TNF activity was evaluated by reporter gene bioassay on the same formulations (MS CDP571-12 and 13). The anti-TNF activity was maintained during the encapsulation process, with a relative potency higher than 70% (Figure 48). Compared to the anti-TNF activity observed for formulation MS CDP571-3, containing RG504 (63 %), the MS CDP571-12 with RG505 (108 %) and MS CDP571-13 with RG755S (72 %) seemed to preserve better the TNF activity of the MAb during the encapsulation process. It might be explained by the faster precipitation of the polymer resulting to a faster entrapment of the MAb into the MS. For the RG505, the faster solidification was explained by a higher Mw (61.5 kDa) resulting to a lower solubility in the EtAc than the RG502 (Mw = 12 Kka) and the RG504 (Mw = 46 kDa). For the RG755S, it was linked to the higher lactic / glycolic ratio (75 / 25 vs. 50 /50 for the other tested Resomer).

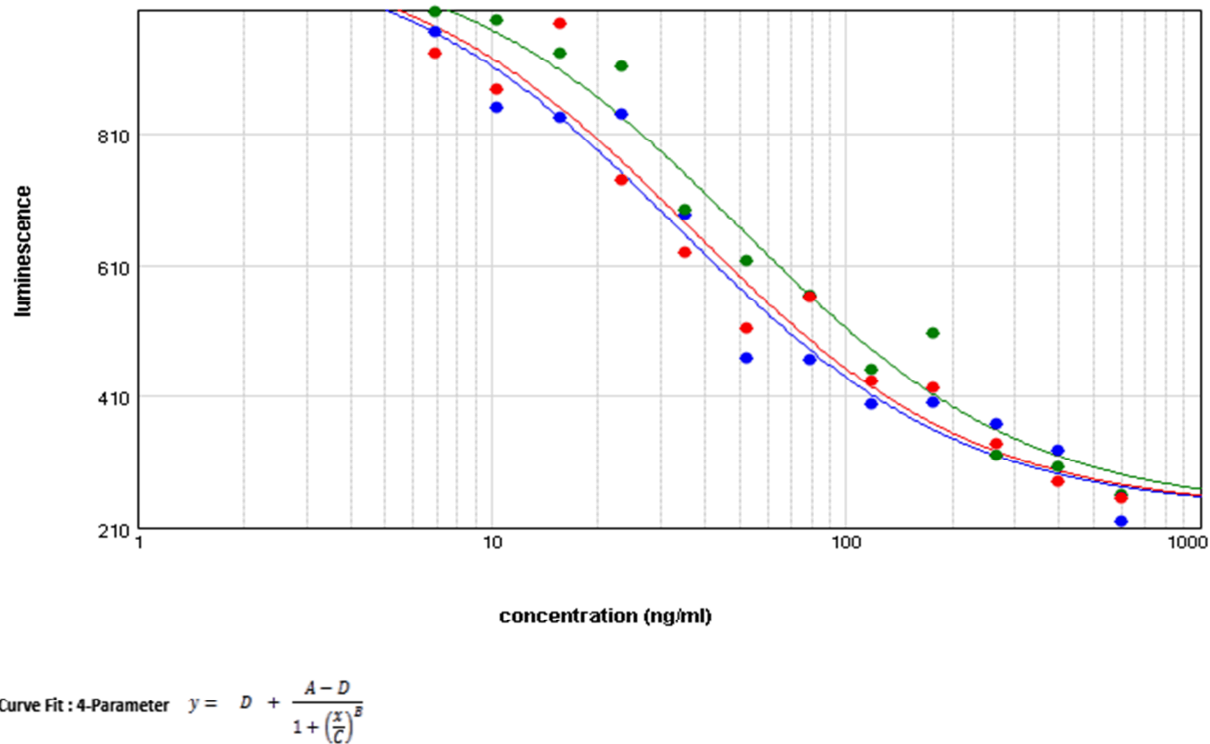


**Figure 48:** Luminescence vs. concentration (ng/mL) plots of encapsulated CDP571 formulations MS CDP571-12 (●) and 13 (●) and the CDP571 reference solution (●)

During the dissolution test, it was observed that the burst effect increased with the PEG content of the copolymer (from 5 to 10 and 15 % PEG for the RGPd5055 (MS CDP571-14), RGPd50105 (MS CDP571-15) and RGP d 50155 (MS CDP571-16), respectively) (Table 27). The release of MAb from microparticles containing PEG-PLGA was faster than comparable formulations without PEG. It was observed that erosion of microparticles containing PEG was faster at the beginning of release than formulations without PEG. It was explained by the hydrophilic and pore former properties of the PEG. In addition, it was demonstrated that PEG chains were predominantly located at the surface of particles based on poly-(lactic acid) (PLA) and PEG compositions, which facilitated the infiltration of water and resulted in a fast release of MAb [112].

IX. Development of a full length antibody (anti-TNF alpha) loaded PLGA microspheres using the solid-in-oil-in-water encapsulation method

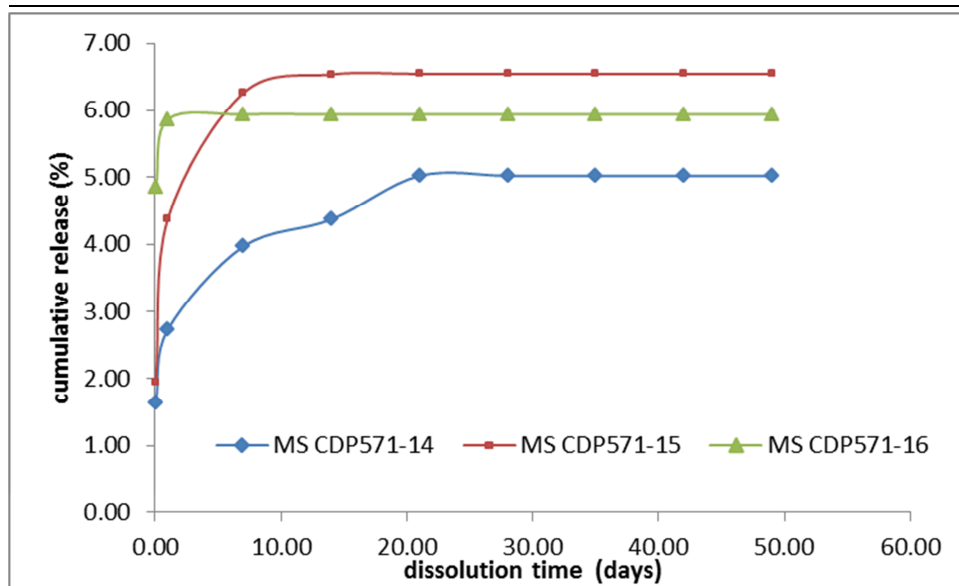


**Figure 49:** Cumulated release of CDP571 (% w/w) vs. dissolution time (days) of PEG-PLGA MS (formulations MS CDP571-14 in blue, 15 in red and 16 in green) (mean, n = 2)

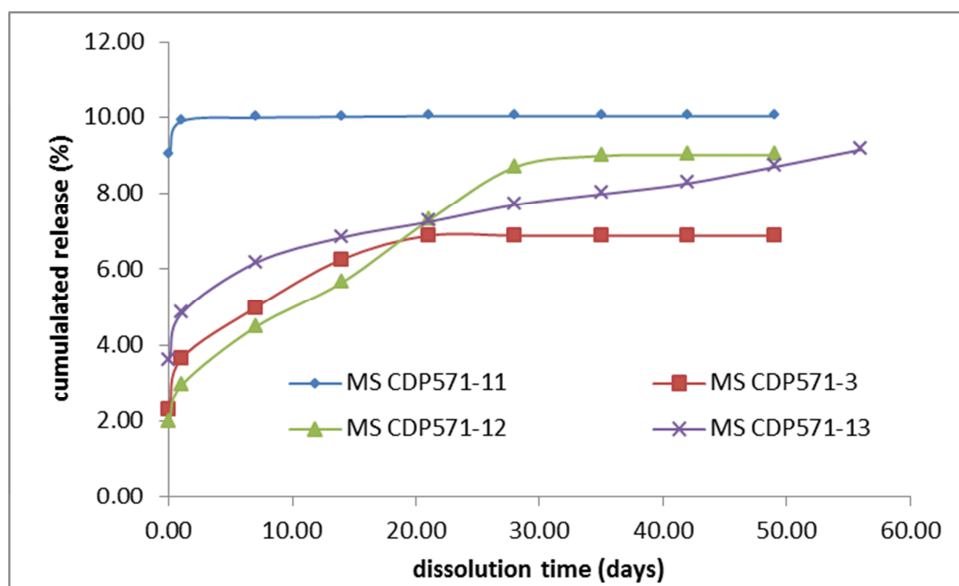


**Figure 50:** Cumulated release of CDP571 (% w/w) vs. dissolution time (days) of PLGA MS (formulations MS CDP571-11 in blue, 3 in red, 12 in green and 13 in purple) (mean, n = 2)

The release profile of the Ab from the PLGA MS was modulated by the type of polymer (Figure 50). The slowest release was observed for the RG755S MS (MS CDP571-13), characterized by a 75:25 lactide:glycolide ratio resulting in a slower degradation rate than the 50:50 Resomer such as RG502, RG504 and RG505. The MS CDP571-11 produced with the

IX. Development of a full length antibody (anti-TNF alpha) loaded PLGA microspheres using the solid-in-oil-in-water encapsulation method

RG502 presented the faster release. It was explained by its low Mw (12 kDa). It was observed that the Mw of the polymer was an important factor for the release profile. It appeared that the percentage of release after 24 h dissolution was inversely proportional to the Mw of the polymer, and subsequently to its inherent viscosity (0.2, 0.525 and 0.675 dL/g as mean inherent viscosity for the RG502, RG504 and RG505) (Figure 51) ( $r^2 = 0.9999$ ).

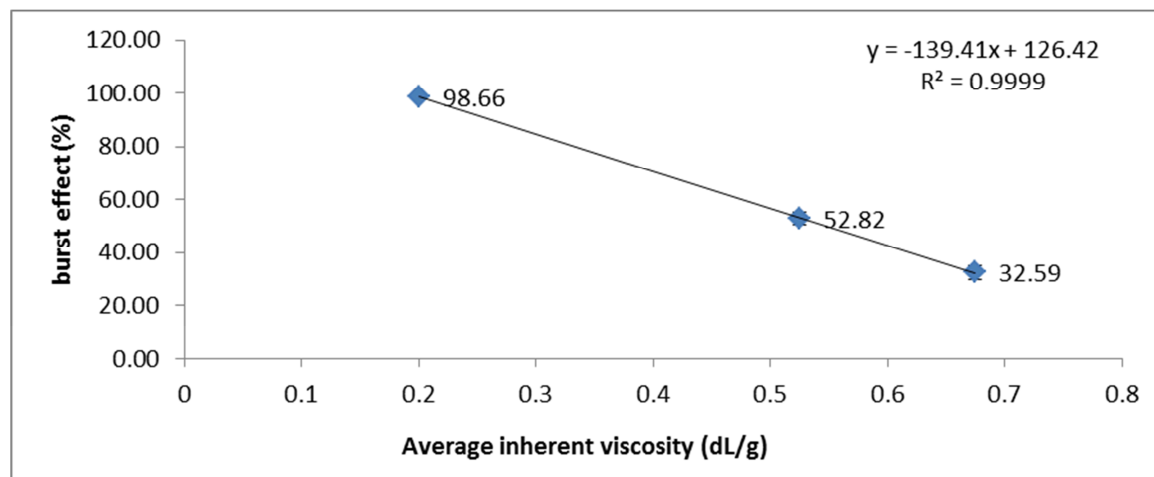


**Figure 51:** Linear regression of the burst effect (%) vs. the inherent viscosity (dL/g) of PLGA 50:50 polymers used for the preparation CDP571 MS formulations (MS CDP571-11, 3 and 12)

The evaluation of the LMWS levels evaluated during the dissolution test also differed according to the type of the polymer (Figure 52). The increase of LWMS over the dissolution was correlated to the Mw of the PLGA. The appearance of the LMWS was faster from the MS produced with the lower Mw polymer (RG502 (MS CDP571-11) > RG504 (MS CDP571-3) > RG505 (MS CDP571-12)). This resulted from a faster degradation of the PLGA with the lower Mw which conducted to a faster acidification inside the MS. For the RG755S MS (MS CDP571-13), the LMWS were generated at a later time of dissolution than the other evaluated polymers (e.g. 42 days for the MS CDP571-13 vs. 28 days for the MS CDP571-3). This difference might be explained by its slower degradation, explained by the higher level of lactic acid, leading to a less acidic microenvironment. With regard to its lower dissolution profiles and the lower appearance of the LMWS, the MS CDP571-12 (RG505) and -13 (RG755S) appeared to be good candidates.



IX. Development of a full length antibody (anti-TNF alpha) loaded PLGA microspheres using the solid-in-oil-in-water encapsulation method

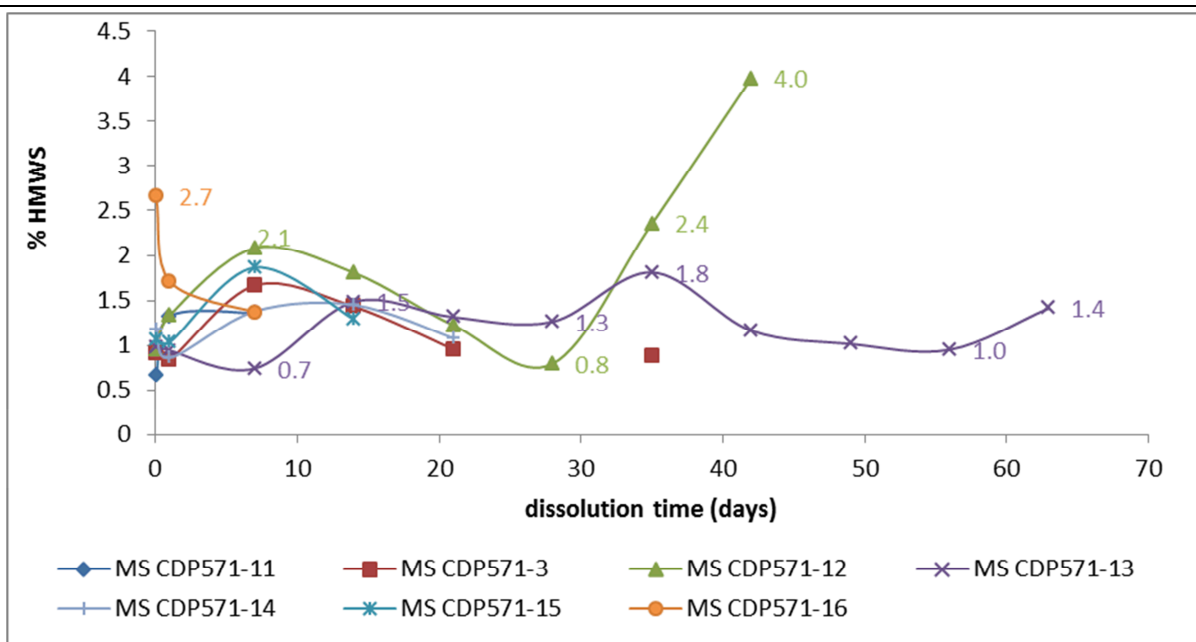


**Figure 53: Comparison of Ab HMWS levels (%) (SEC) for MS CDP571-11 to 16 over dissolution time (days)**

ELISA was performed on each formulation (MS CDP571-11 to 16) after 1 h contact time with the dissolution medium during the dissolution test. Additional ELISA tests were performed on MS CDP571-3, 12, 13 and 14 formulations, which continued to release the drug, after 4 weeks of dissolution, and on MS CDP571-13, after 7 weeks and 8 weeks. It was observed that the binding capacity was preserved for each formulation after 1 h dissolution, with a relative binding capacity ranging from 74% to 94% (Figure 54). After 4 weeks' dissolution, the binding capacity of MS CDP571-3 (0 %) and 14 (2 %) was completely lost, probably due to the increase in LMWS (Figure 52). In contrast, both MS CDP571-12 and 13 preserved their binding capacities (93 % and 68 % respectively). Additionally, the binding capacity of MS CDP571-13 was preserved for up to 8 weeks of dissolution (94 %).

IX. Development of a full length antibody (anti-TNF alpha) loaded PLGA microspheres using the solid-in-oil-in-water encapsulation method

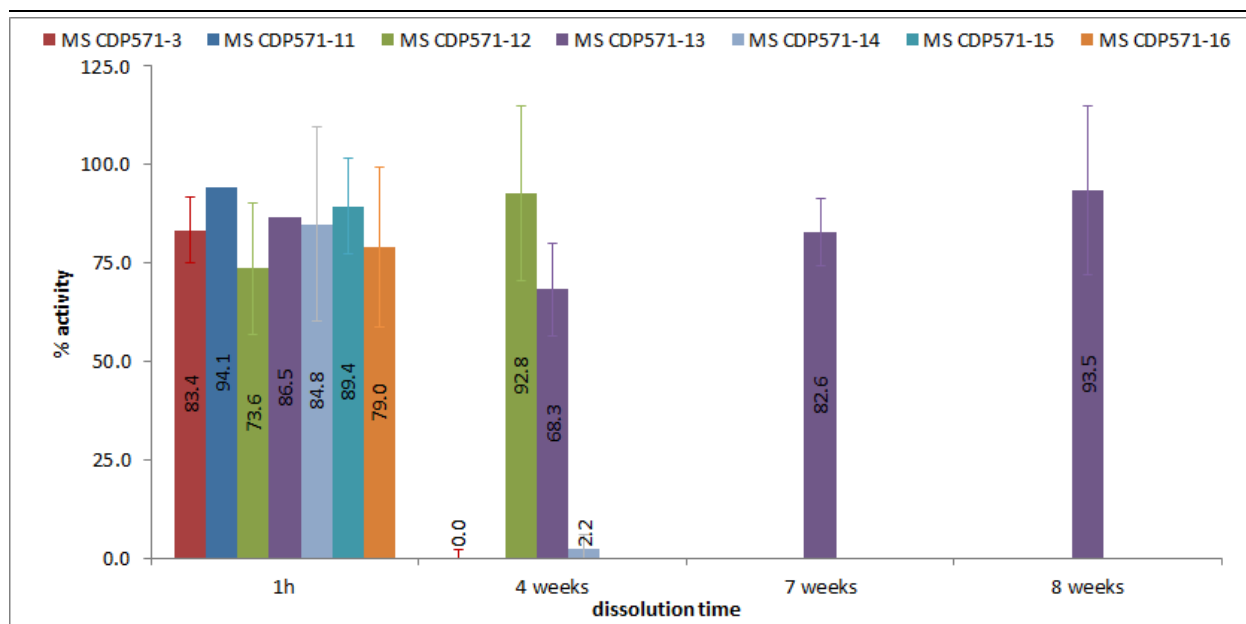


**Figure 54:** Comparison of relative binding capacities (ELISA) of released MAb after 1h of dissolution from MS formulations MS CDP571-3, 11, 12, 13, 14, 15 and 16, after 4 weeks from MS CDP571-3, 12, 13 and 14, and after 7 weeks and 8 weeks from MS CDP571-13. (mean (s), n = 4)

The anti-TNF alpha activity was confirmed for both MS CDP571-12 and 13 formulations during the dissolution test, with their relative potency from 89 % to 65 % and 83 % to 80 % after 1 h and 4 weeks of dissolution, respectively.

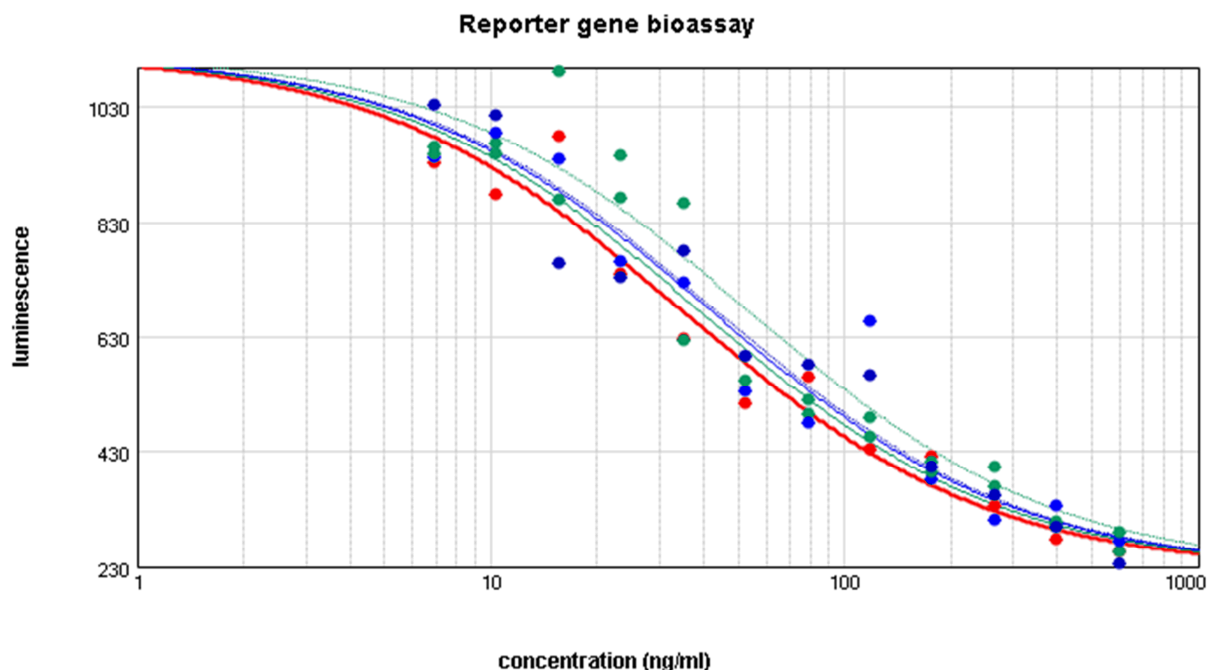


**Figure 55:** Reporter gene bioassay plot – luminescence vs. concentration of MAb for MS CDP571-12 (in green) and MS CDP571-1 3 (in blue) after 1 h and 4 weeks of dissolution and for the MAb reference (in red).

### 3.2 Conclusion

It was observed that the release profile could be modulated by selection of the type of polymer. PLGA presenting a higher inherent viscosity (e.g. RG505) and PLGA with a higher lactic acid ratio (e.g. RG755S) slowed down the release rate of the CDP571.

In addition, polymers with a slower degradation rate such as the RG505 (high MW) and the RG755S (75:25 lactid:glycolic ratio) , led to limiting the increase in fragmentation which could appear during the dissolution due to the acid degradation of the PLGA. The selection of the more appropriate PLGA led to maintain the TNF activity of the Ab, both during the encapsulation process and over the release of the drug from the PLGA MS.

## 4 EVALUATION OF ADDITION OF BASIC ADDITIVES

An acidic microenvironment induced by the formation of acidic degradation products and carboxylic acid end groups of PLGA might lead to irreversible inactivation of proteins encapsulated in PLGA matrices [113]. Therefore, it was shown that the co-encapsulation of additional additives such as basic compounds might result in enhanced protein stability,

IX. Development of a full length antibody (anti-TNF alpha) loaded PLGA microspheres using the solid-in-oil-in-water encapsulation method

minimizing acid-induced degradation during the release [49, 106]. Basic compounds were added to evaluate the fragmentation of the incorporated TNF-alpha during the dissolution test. Calcium carbonate, magnesium hydroxide and zinc carbonate are usually used in such formulations [29]. In order to characterize the protein stabilization mechanism in PLGA, the effect of (a) basicity of the salt additive and (b) base salt content, were studied for the protein stability and the release kinetics [114]. Two poorly water-soluble inorganic bases were evaluated ( $Mg(OH)_2$  pKa = 12.72 and  $CaCO_3$  pKa = 8.55) at two different concentrations (1.5 and 3 % (w/w)), using the RG505 Resomer [47, 114]. (Table 28)

**Table 28: Evaluated CDP571: PLGA MS formulations**

<b>Formulation (n=2)</b>	<b>PLGA</b>	<b>Additive</b>	<b>Additive content<sup>a</sup> (% w/w)</b>	<b>Theoretical drug loading (%)</b>	<b>d(0.5) (µm)</b>	<b>Actual loading content (%)</b>
MS CDP571-12	RG505	NA	0	15.2	51.2	8.61
MS CDP571-17	RG505	$Mg(OH)_2$	1.5	15.0	54.9	11.14
MS CDP571-18	RG505	$Mg(OH)_2$	3	14.8	56.7	10.01
MS CDP571-19	RG505	$CaCO_3$	1.5	15.0	61.9	10.00
MS CDP571-20	RG505	$CaCO_3$	3	14.8		9.73

<sup>a</sup> The additive content (% (w/w)) was calculated as a percentage of the total quantity of PLGA and CDP571.

## 4.1 Results and discussion

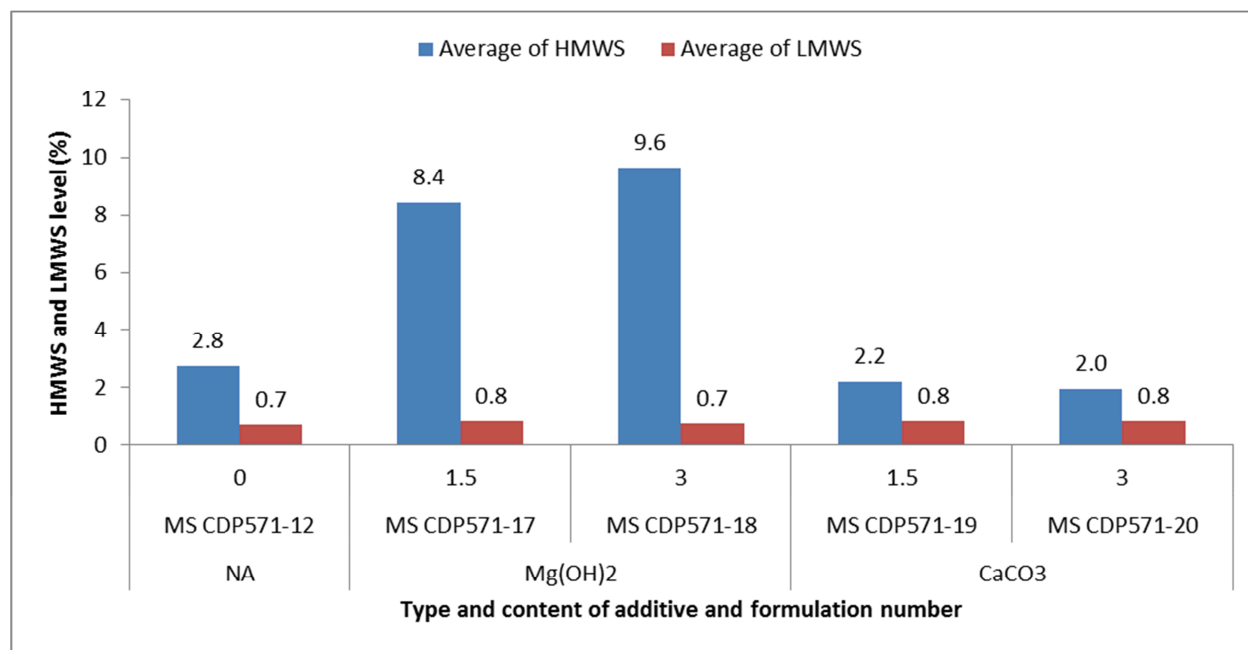


**Figure 56: Comparison of HMWS and LMWS levels for MAb co-encapsulated without and with Mg (OH)<sub>2</sub> or CaCO<sub>3</sub> (mean, n=2)**

Compared to the formulation MS CDP571-12 without basic additive (HMWS = 2.8 %), the addition of Mg(OH)<sub>2</sub> led to an increase in the level of HMWS, which was higher with a higher content of basic additive (8.4 % for 1.5 % Mg(OH)<sub>2</sub> vs. 9.6 % for 3.0 % Mg(OH)<sub>2</sub>) (Figure 56). Addition of CaCO<sub>3</sub> did not seem to increase the HMWS (2.2 – 2.0 %). The fragmentation (0.7 – 0.8 % LMWS) was not affected by the addition of basic additive. The increase in HMWS observed for the formulations containing Mg(OH)<sub>2</sub> (MS CDP571-17 and 18) could be explained by a heterogeneous pH distribution, which might create an alkaline microenvironment [113]. The creation of a basic environment (linked to highly dissociate hydroxide salts) might lead to an alkaline degradation of protein such as a deamidation reaction [29].

In order to evaluate the formation of acid or basic species which could be generated during the encapsulation process of the MAb, and especially in presence of basic additive, SAX analysis was performed on the formulations.

IX. Development of a full length antibody (anti-TNF alpha) loaded PLGA microspheres using the solid-in-oil-in-water encapsulation method

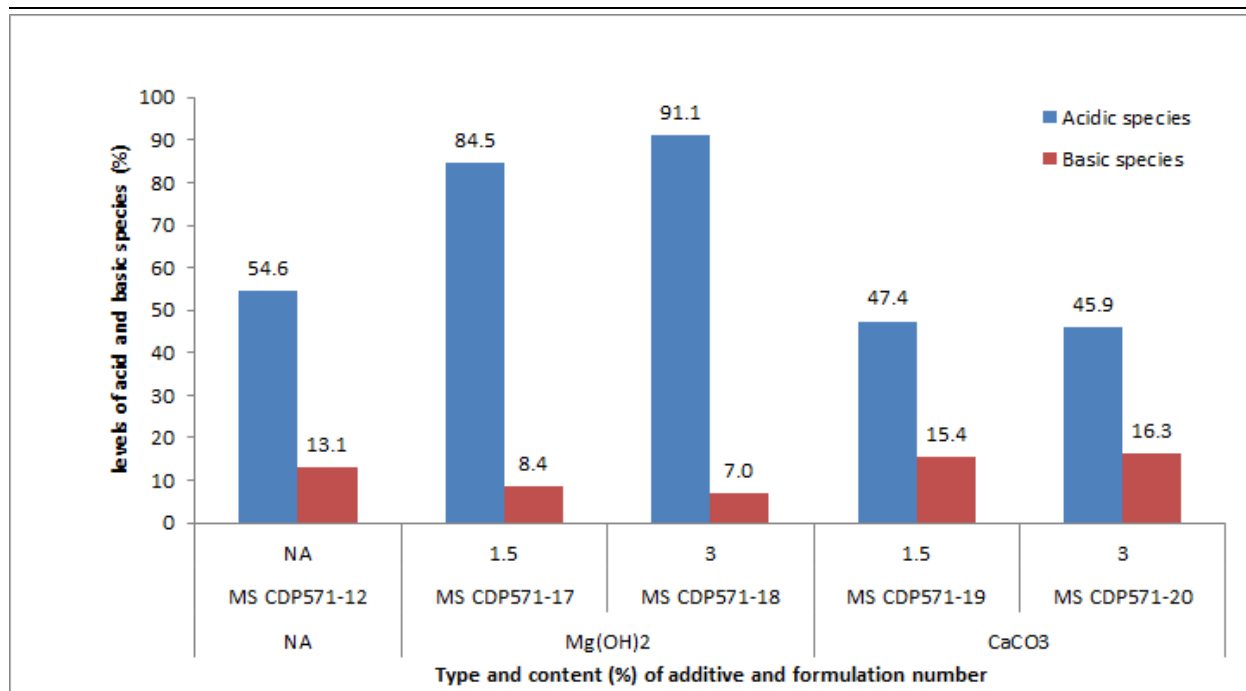


**Figure 57: Comparison of SAX data for the determination of acidic and basic species in MAb formulations co-encapsulated with Mg (OH)<sub>2</sub> and with CaCO<sub>3</sub>**

The amount of acidic species ranged between 45.9 and 91.1 % (Figure 57). In comparison, 37.7% of acidic species was measured after the spray-drying process (formulation SD CDP571-3). The addition of Mg(OH)<sub>2</sub> as basic additive seemed to have a detrimental effect on the CDP571 in regards to the level of acidic species measured on the formulations MS CDP571-17 and 18 (84.5 and 91.1 %, respectively). This increase might be related to the alkaline catalyzed deamidation which produced iso-aspartic acid.

Formulations MS CDP571-18 and 20, which were produced with the addition of 3 % basic additive, were characterized by a significantly lower relative binding capacity ( $p < 0.0001$ , oneway ANOVA) than that observed for either formulations MS CDP571-17 and 19, containing 1.5 % additive or the formulation MS CDP571-12 without basic additive (Figure 58).

IX. Development of a full length antibody (anti-TNF alpha) loaded PLGA microspheres using the solid-in-oil-in-water encapsulation method

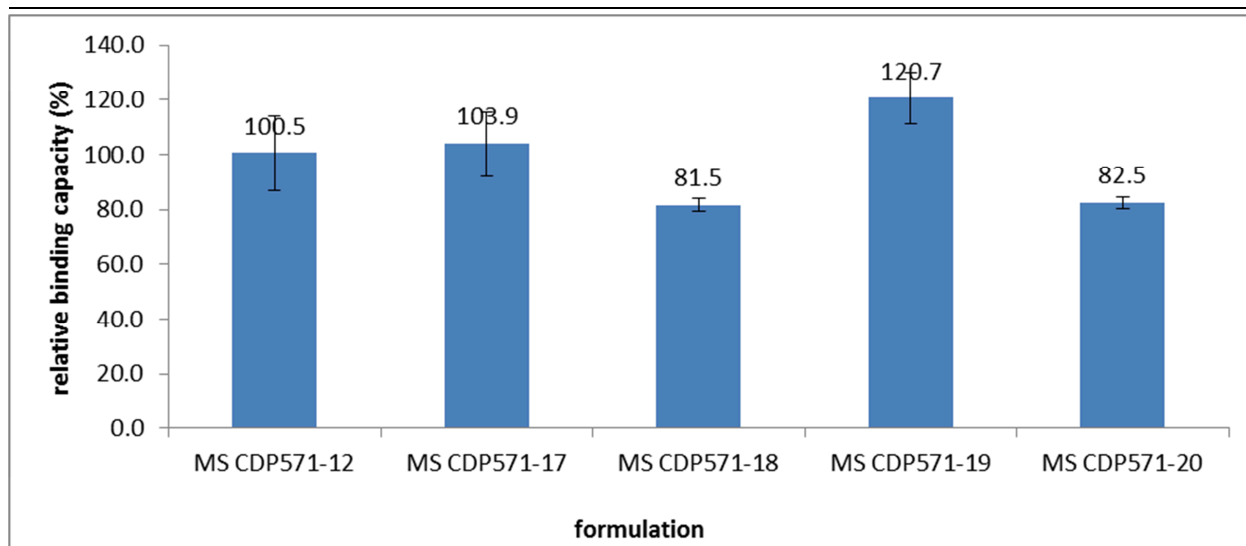


Figure 58: Relative binding capacity (ELISA) of MAb for MS CDP571-12, 17, 18, 19 and 20 (mean (s), n = 4)

The dissolution profiles were evaluated for the CDP571:PLGA MS.

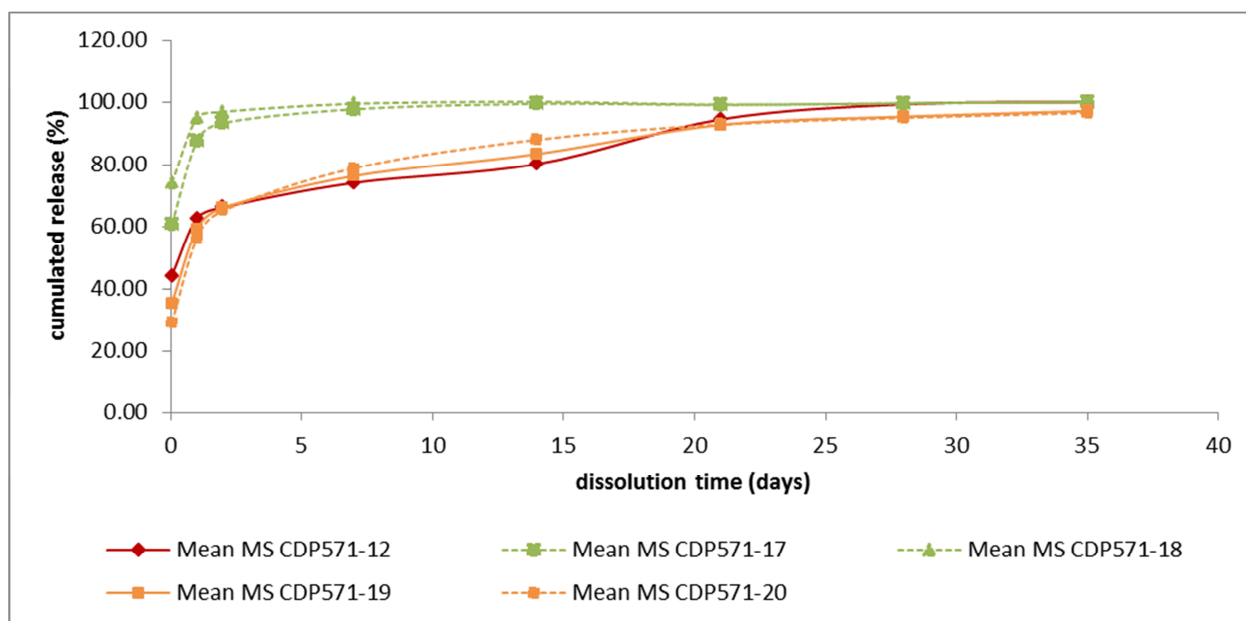


Figure 59: Cumulated MAb release (%) vs. dissolution time for MS CDP571-12 (in red), MS CDP571-17/18 (in green) and MS CDP571 19/20 (in orange) (mean, n=2)

The release of the MAb and the burst effect increased when  $Mg(OH)_2$  was added as a basic compound (Figure 59). This increase was not observed with  $CaCO_3$ , which led to a release profile similar to that without a basic salt. Mingli et al. explained that when water-insoluble alkaline substances, such as  $MgCO_3$ ,  $ZnCO_3$  and  $Mg(OH)_2$ , were incorporated into MS, they

built up osmotic pressure due to the neutralization effect of water-soluble acidic products of polymer degradation. The high osmotic pressure resulted in a fast protein release from MS [60]. Moreover, the presence of  $Mg(OH)_2$  might increase the microenvironment pH in the polymer matrix, which caused the dissociation of the end groups of PLGA (e.g.,  $-COOH$ , with a  $pK_a$  of 3.83 for both glycolic and lactic acids) and ionization of the monomers/oligomers. Therefore, both the ionization of the polymer end groups and the increase in the osmotic pressure were the driving forces for the diffusion of hydrophilic molecules into the polymer matrix, resulting in higher water content inside the MS [114]. In contrast, a higher content of  $CaCO_3$  led to a lower burst effect. Ara and co-workers studied the effect of addition of calcium salts on the hydrolytic degradation of PLGA [115]. They observed that the mass loss pattern for calcium carbonate specimens (composite material containing 70 % (w/w) PLGA 50:50 and 30 % (w/w) calcium carbonate) was significantly different from the others. Mass loss of calcium carbonate specimens was slower. Mass loss in the blend specimens occurred by dissolution of both the inorganic salts and oligomeric degradation products into the buffer solution. The solubility of  $CaCO_3$  in water is quite limited (0.002 % w/v). Therefore, the mass loss observed for  $CaCO_3$  specimens could be mainly attributed to the release of oligomers produced by the degradation of PLGA. The  $M_w$  of PLGA for  $CaCO_3$  specimens decreased significantly more slowly compared with that of the specimens prepared with other inorganic salts. The degradation constant of PLGA decreased with increasing pH or basicity of the calcium compounds blended with PLGA. The degradation-delaying effect of  $CaCO_3$  was understandable because of its buffering effect, achieved by neutralizing the carboxyl end groups of the degradation products.

The fragmentation and the aggregation levels of CDP571 were measured by SEC during the dissolution test at different times of dissolution.

IX. Development of a full length antibody (anti-TNF alpha) loaded PLGA microspheres using the solid-in-oil-in-water encapsulation method

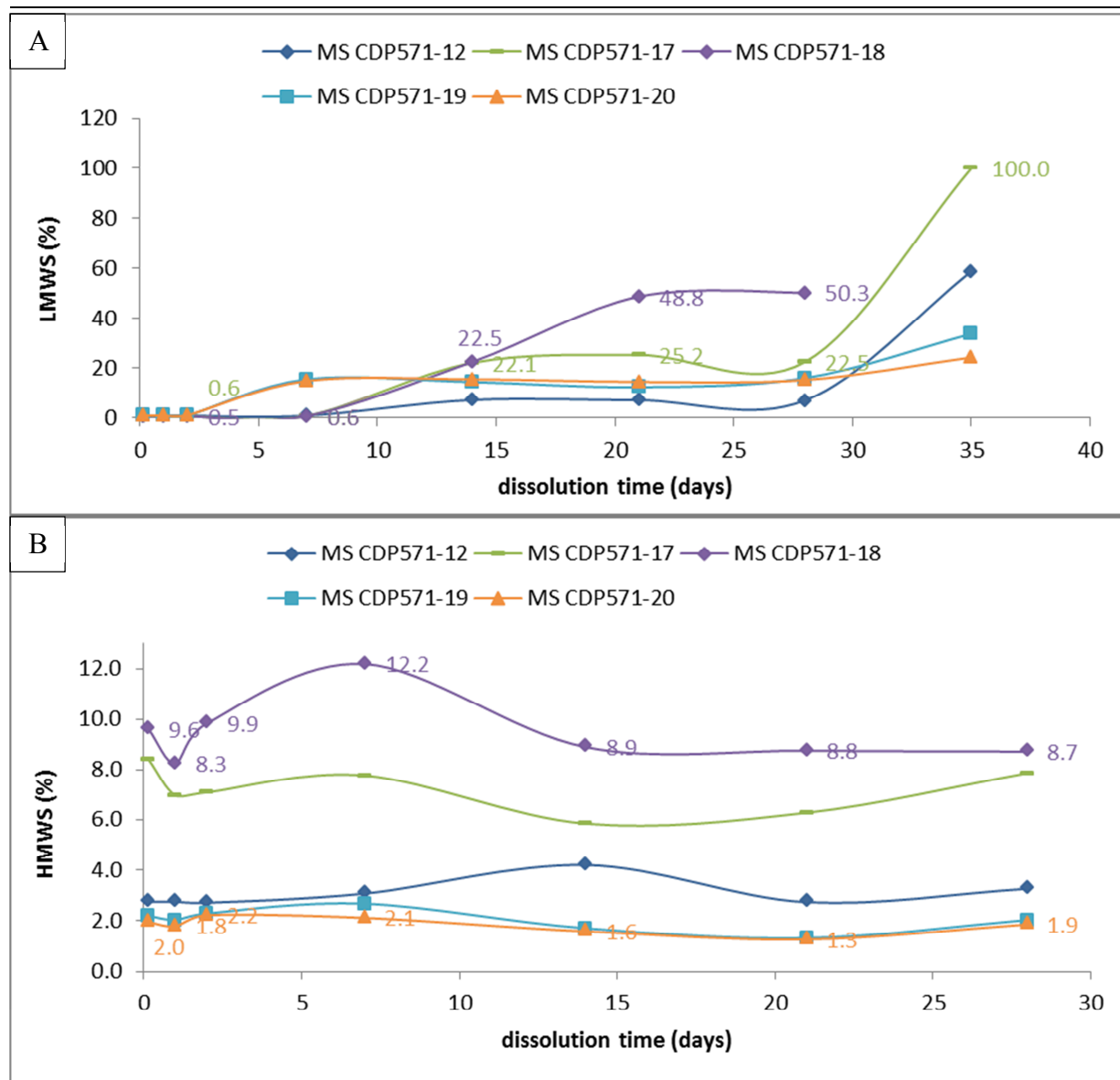
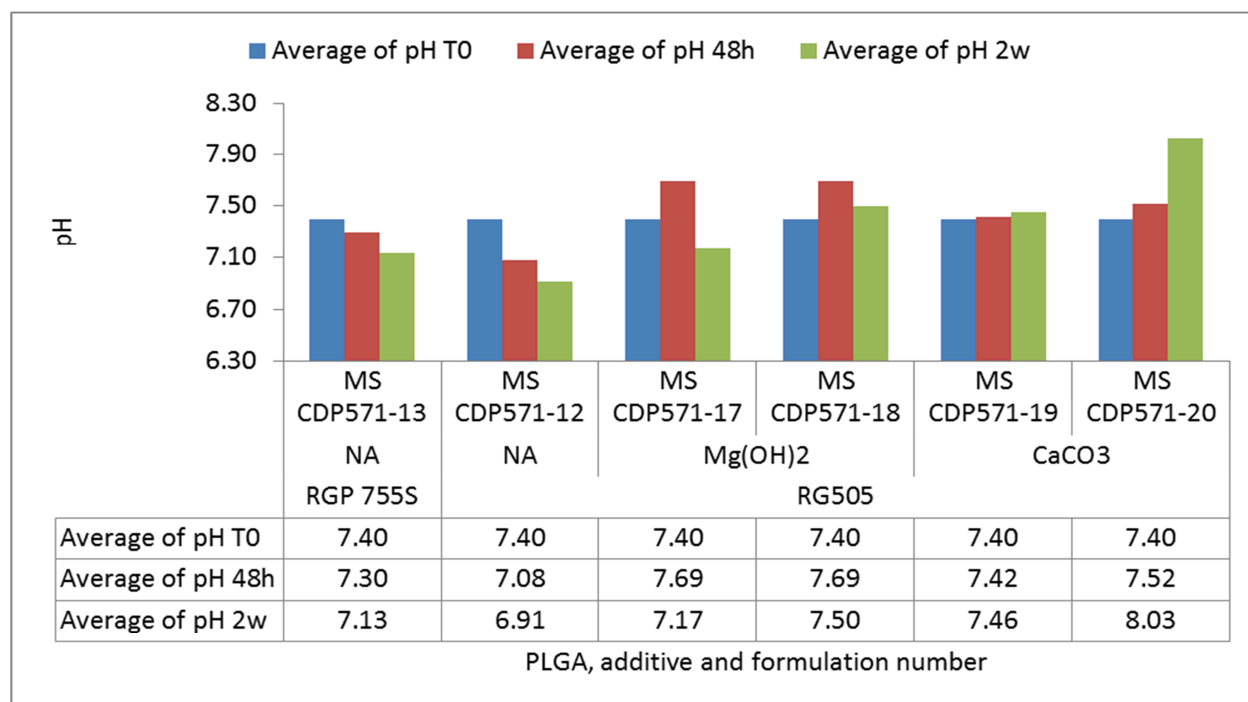


Figure 60: LMWS (A) and HMWS (B) levels vs. dissolution time of MAb from MS CDP571-12, 17, 18, 19 and 20

The decrease in fragmentation, which was expected when basic salts were added, was not observed in our study (Figure 60 A). In contrast, compared to formulation MS CDP571-12, which did not contain a basic additive, a higher increase in LMWS was observed with formulation MS CDP571-17 and 18, produced with  $Mg(OH)_2$ . This increase was higher with a higher content of additive. With formulations 19 and 20, which contained  $CaCO_3$ , the fragmentation increased to 14 – 15 % after 1 week of dissolution. Between 1 and 4 weeks, this

percentage remained constant. The addition of basic salts might increase hydrolytic protein degradation, which was linked to the increase in water uptake in PLGA matrices, as described previously [48]. This phenomena was greater when using the  $Mg(OH)_2$ .

It was observed that the addition of  $CaCO_3$  led to protecting CDP571 against aggregation issues (Figure 60 B). No increase in aggregation was observed for formulation 20, which contained 3 %  $CaCO_3$ , until 28 days of dissolution. In contrast, addition of  $Mg(OH)_2$  led to high percentages of aggregation, which increased with higher amounts of salt. The maximal value of aggregation was observed after 7 days of dissolution (8.4 % and 12.5 % for formulations MS CDP571-17 and -18, respectively).



**Figure 61: pH evolution measured during the dissolution test for MS CDP571-12 and -13 not containing basic additive, MS CDP571- 17 and -18 containing 1.5 % and 3 % of  $Mg(OH)_2$  respectively and MS CDP571- 19 and -20 containing 1.5 % and 3 %  $CaCO_3$  respectively (mean, n = 2)**

After 48 h and 2 weeks of dissolution, the pH values decreased in formulations MS CDP571-12 and 13, which did not contain alkaline additive (Figure 61). The pH in the dissolution medium for formulation MS CDP571-13, formulated with RG755S remained constant around 7.1-7.2. It might be explained by a slower degradation rate of the RG755S compared to the RG505, resulting in a slower acidification. With formulations containing alkaline additive (formulations MS CDP571-17 to 20), the pH increased after 48 h of dissolution up to 7.7. This increase was

higher when using  $\text{Mg}(\text{OH})_2$  ( $\text{pH} = 7.7$ ), compared to  $\text{CaCO}_3$  (max  $\text{pH} = 7.52$ ). After 2 weeks of dissolution, the  $\text{pH}$  of formulations MS CDP571-17 and 18 decreased. This decrease was higher when using lower concentration of  $\text{Mg}(\text{OH})_2$ , suggesting insufficient neutralization capacity. Shenderova and co-workers also observed that the  $\text{pH}$  of the media for MS containing  $\text{Mg}(\text{OH})_2$  increased after 3 days of dissolution. When 1 %  $\text{Mg}(\text{OH})_2$  was added, the  $\text{pH}$  decreased after 2 weeks upon polymer degradation. In contrast, for  $\geq 3$  %  $\text{Mg}(\text{OH})_2$ , the  $\text{pH}$  did not change between 3 and 14 days [47]. This suggests that at a loading higher than 3%, the polymer degradation may be significantly slowed down. In contrast, the  $\text{pH}$  of formulations 19 and 20 tended to increase, especially with higher concentrations of additive.  $\text{CaCO}_3$  seemed to lead to a better neutralization effect than  $\text{Mg}(\text{OH})_2$ .

## 4.2 Conclusion

Addition of  $\text{Mg}(\text{OH})_2$  led to negative effects on the CDP571-loaded PLGA MS. Indeed, its co-encapsulation led to an increase in the aggregation level and to increase the drug release. In contrast, the addition of  $\text{CaCO}_3$  seemed to provide appropriate properties to the CDP571 loaded PLGA MS but did not show any improvement in terms of the fragmentation level during dissolution.

## 5 DEVELOPMENT OF A FREEZE-DRIED PRODUCT

The major issues that may appear during the development of Ab containing microparticles include both physical instabilities (agglomeration/particle fusion) and chemical instabilities (hydrolysis of polymer materials, drug leakage and chemical reactivity of drug during the storage) [116]. In order to avoid such degradation, water has to be removed from the system. In the previous parts of this work, vacuum drying was used as the drying process, although agglomeration issues were observed during the resuspension of the dried MS.

The most commonly-used process in the pharmaceutical field for converting solutions or suspensions into solids with sufficient stability for distribution and storage is freeze-drying [117, 118, 119]. Freeze-drying may generate many stresses that could destabilize the MS suspension, especially the stress of freezing and dehydration. The critical formulation properties include the  $T_g'$  of the frozen sample, the  $T_c$ , the stability of the particles and the encapsulated drug and also the properties of the excipients used. The  $T_c$  is the maximum allowable product temperature during the primary drying.  $T_c$  is usually about  $2^\circ\text{C}$  higher than  $T_g'$ , or equal to the  $T_{cu}$ . To ensure

the total solidification of a frozen sample, the particle phase should be cooled to below the  $T_g'$  of the formulation, if it amorphous, or below  $T_{eu}$ , if it is in the crystalline state, to ensure the total solidification of the sample. Fast supercooling in liquid nitrogen was preferred to assure fast solidification of the suspension. The frozen particles samples have to be kept at the set freezing temperature for sufficient time to transform all the suspension into solid [38, 116].

During the freezing step, the high concentration of particulate system may induce agglomeration or sedimentation, and in some cases irreversible fusion, of particles. Furthermore, the crystallization of ice may exercise a mechanical stress on particles, leading to their destabilization. For these reasons, specific excipients have to be added to the particle suspension before freezing. These excipients are usually added to protect the product from freezing stress (cryoprotectant) or drying stress (lyoprotectant) and also increase its stability upon storage [116, 120]. The immobilization of particles within a glassy matrix of cryoprotectant can prevent their agglomeration and protect them against the mechanical stress of ice crystals. Mannitol can also separate from a frozen solution in the form of crystalline phases [121]. According to Chacon et al [120], the presence of at least 5 % cryoprotectant is essential to maintain the initial particle size. Moreover, a concentration of 5 % (w/v) of the different sugars employed provides isotonic particle dispersion after reconstitution of the freeze-dried powder with the required amount of sterile vehicle.

The objectives of this study were to: (1) produce a suitable lyophilizate (“cake”) which may be rapidly reconstituted, (2) preserve the physico-chemical properties of the freeze-dried product, with a small or unmodified particle size and drug entrapment, (3) obtain a low residual moisture (< 2 % w/w) and (4) assure good stability of the formulation [116].

Three cryoprotectants (mannitol, sucrose and trehalose) were evaluated at two levels of concentration (0.5 and 5 % w/v) for the selected MS formulation MS CDP571-13 (theoretical 15 % w/w CDP571-loaded RG755S MS produced with the SD CDP571-3 containing histidine and trehalose with a 70/30 MAb/trehalose ratio; [Table 43](#) in appendix). Seven freeze-dried formulations (lyo MS CDP571-1 to 7) were evaluated for the freeze-drying process ([Table 29](#)). Based on the data collected from this first evaluation, two cryoprotectants (sucrose and trehalose) were selected and evaluated again in triplicate at two levels of concentration (0.5 and 2 % w/v) (Lyo MS CDP571-8 and 9). Before freeze-drying, the MS CDP571-13 MS were reconstituted

- IX. Development of a full length antibody (anti-TNF alpha) loaded PLGA microspheres using the solid-in-oil-in-water encapsulation method

with 1 mL of the cryoprotectant solutions described in the [Table 29](#) to give a 15 % w/v suspension of MS.

**Table 29: Evaluated lyophilization formulation solutions for the freeze-drying of 15 % w/v suspension of the MS CDP571-13 formulation**

Formulation	Stabilizer (cryoprotectant)	Stabilizer concentration % (w/v)
Lyo MS CDP571-1	Mannitol	0.5
Lyo MS CDP571-2	Sucrose	0.5
Lyo MS CDP571-3	Trehalose	0.5
Lyo MS CDP571-4	Mannitol	5
Lyo MS CDP571-5	Sucrose	5
Lyo MS CDP571-6	Trehalose	5
Lyo MS CDP571-7	NA	0
Lyo MS CDP571-8	Sucrose	2
Lyo MS CDP571-9	Trehalose	2

It should be noted that formulations Lyo MS CDP571-1 to 7 underwent two lyophilization cycles (page [60](#), Freeze-drying in section Material and methods).

## 5.1 Results and discussion

### 5.1.1 Formulation solutions and suspensions before freeze-drying

In order to design an optimum freeze-drying process, critical properties of the formulation need to be known. The critical parameters ( $T_g'$  and  $T_c$ ) were established using DSC and FDM ([Figure 62](#)) for the 5 % w/v cryoprotectant solutions (mannitol, sucrose and trehalose) and for the evaluated suspensions (Lyo MS CDP571-1 to 6).

As measured by DSC, a  $T_g'$  was determined for formulations containing trehalose (- 32°C to - 30°C) or sucrose (- 34°C), which formed an amorphous mass when they were frozen. For the mannitol solution, both a  $T_g'$  (- 29°C) and a  $T_m$  (- 23°C) were observed, which was attributed to the partial crystallization of the mannitol, in accordance with the paper of Anhorn et al. [122].

The highest  $T_c$  (- 29°C) was measured for the suspensions containing sucrose.

IX. Development of a full length antibody (anti-TNF alpha) loaded PLGA microspheres using the solid-in-oil-in-water encapsulation method

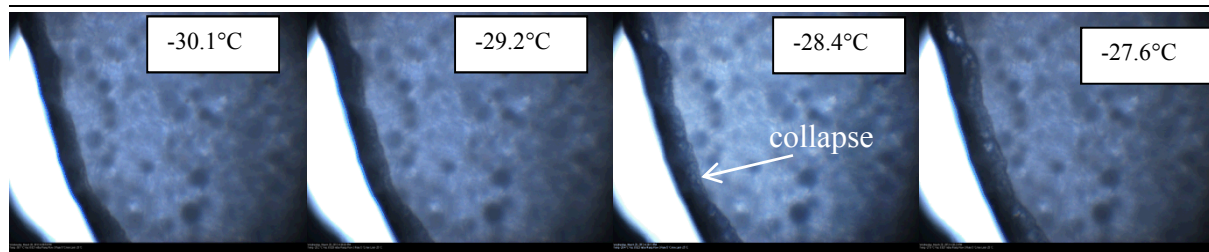


**Figure 62:** Pictures of freeze-drying microscopy (FDM) on 20 % w/v MS suspension, containing 5 % w/v sucrose (Lyo MS CDP571-5)

Therefore, the primary drying was realized at - 35°C (shelf temperature) to assure sublimation at temperatures lower than either the  $T_g'$  or the  $T_c$ .

### 5.1.2 Freeze-dried MS

The lyophilized cakes presented a pharmaceutically elegant structure. Macroscopic observation did not show any sign of collapse or shrinkage after the freeze-drying process, except on few formulations which had undergone two cycles of lyophilization (Lyo MS CDP571-2 and 6) (Figure 63). All the cakes were brittle and easy to reconstitute.



**Figure 63:** Pictures of cakes of freeze-dried MS for formulations Lyo MS CDP571-1 and 2.

The particle size of the MS was measured before and after freeze-drying (Figure 64). The MS CDP571-13 formulation withdrawn before filtration during the encapsulation process was characterized by a  $D [4,3]$  of  $42 \pm 26 \mu\text{m}$ . The Lyo MS CDP571-7 formulation dried without cryoprotectant provided the highest particle size ( $D [4,3] = 192 \mu\text{m}$ ). All the other evaluated freeze-dried formulations (Lyo MS CDP571-1 to 6), containing cryoprotectant, were characterized by a  $D [4,3]$  (ranging between 34.6 to 51.0  $\mu\text{m}$ ) that was similar to that of the MS CDP571-13 formulation. The highest  $D [4,3]$  (51.0  $\mu\text{m}$ ) was found for the Lyo MS CDP571-1

containing 0.5 % w/v mannitol. It was suggested that the different stereochemical conformations of the mannitol might modify interaction between the cryoprotectant and the frozen mass, leading to a lower protective effect [65]. Therefore, it was suggested that the mannitol had to remain molecularly dispersed in the amorphous particle phase to stabilize the MS properly. Nevertheless, with regard to the particle size evaluation, the cryoprotective effect of mannitol, trehalose or sucrose was confirmed. The cryoprotective agents provided mechanical protection to the MS as they avoided the agglomeration or the alteration of the particles due to the pressure developed by the growth of crystals. Another explanation of the mechanism of particle stabilization by cryoprotectants during freeze-drying (in particular the freezing step) is the particle isolation hypothesis. It was proposed that sugars isolate individual particles in the unfrozen fraction, thereby preventing agglomeration during freezing above  $T_g'$ . In this case, vitrification is not required for this effect and the spatial separation of particles within the unfrozen fraction is sufficient to prevent agglomeration.

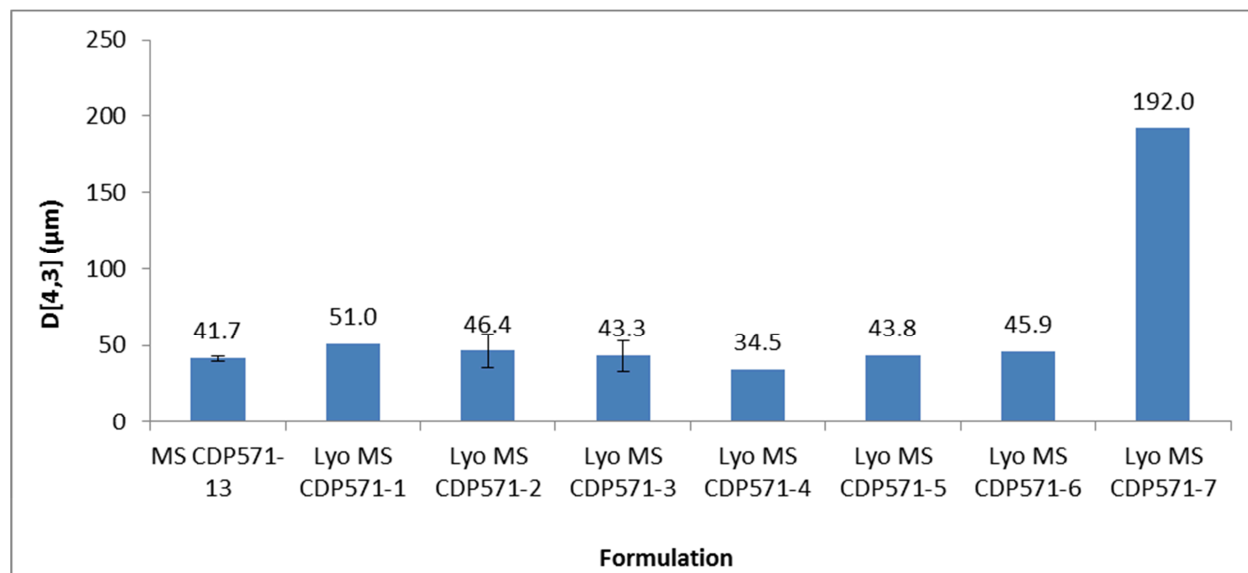


**Figure 64:** Comparison of the D[4.3] data measured by laser diffraction after dispersion of the MS in water for the freeze-dried MS (formulations Lyo MS CDP571-1to -7) and for formulation MS CDP571-13 before freeze-drying (mean (s), n = 3)

After the lyophilized cake's reconstitution in water, visually acceptable suspensions with no agglomeration were achieved. The MS were visually observed by optical microscopy in dispersion in water prior and after freeze-drying (Figure 65). The MS appeared spherical and isolated.

IX. Development of a full length antibody (anti-TNF alpha) loaded PLGA microspheres using the solid-in-oil-in-water encapsulation method

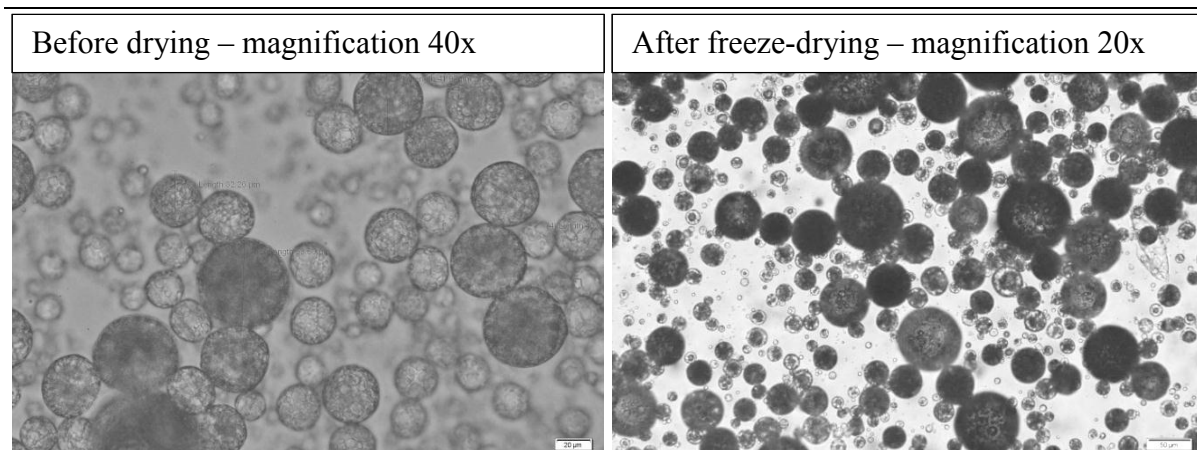


**Figure 65:** Optical microscopy pictures of MS suspensions of formulation Lyo MS CDP571-3 before drying and after freeze-drying (MS resuspended in water)

SEM was performed to evaluate the morphology of the freeze-dried MS (Figure 66). The freeze-dried MS appeared spherical without evidence of agglomeration. However, SEM observations become more difficult when the protectant concentration was 5 % w/v. In this case, a continuous matrix was observed with some particles (Figure 66 D, E and F) [116]. Cracking was observed on MS freeze-dried without cryoprotectant (Figure 66 G). The presence of pores was detected at the surface of the freeze-dried MS.

IX. Development of a full length antibody (anti-TNF alpha) loaded PLGA microspheres using the solid-in-oil-in-water encapsulation method

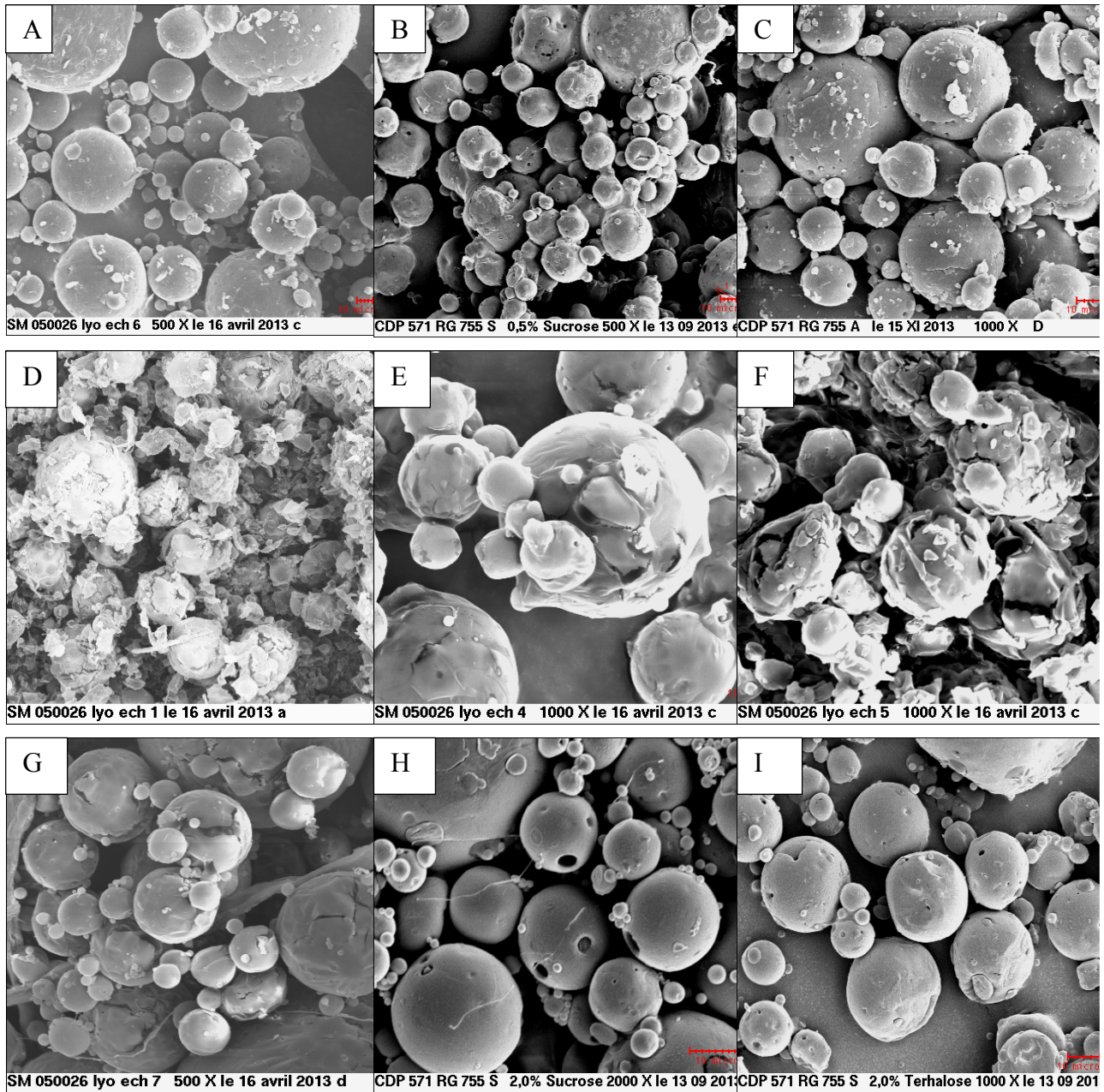


Figure 66: SEM pictures of the freeze-dried MS (Lyo MS CDP571-1 (A), 2 (B), 3 (C), 4 (D), 5 (E), 6 (F), 7 (G) -8 (H) and 9 (I))

IX. Development of a full length antibody (anti-TNF alpha) loaded PLGA microspheres using the solid-in-oil-in-water encapsulation method

A syringeability study was performed on the freeze-dried formulations (Lyo MS CDP571-1 to 7), which were suspended in 1 mL of water for injection and injected through 23 G needles (Table 30).

**Table 30: Syringeability data for the freeze-dried MS (formulations Lyo MS CDP571-1 to 7) (n = 1)**

Formulations	F max (N)
Lyo MS CDP571-4	29.3
Lyo MS CDP571-2	21.6
Lyo MS CDP571-3	28.4 <sup>a</sup>
Lyo MS CDP571-5	19.7
Lyo MS CDP571-6	27.0
Lyo MS CDP571-1	40.5
Lyo MS CDP571-7	36.7

<sup>a</sup> The test Lyo MS CDP571-3 was repeated due to ejection of the needle during the first trial.

Both formulations Lyo MS CDP571-1, containing 0.5 % w/v mannitol, and Lyo MS CDP571-7, with no cryoprotectant, provided the highest Fmax (40.5 N and 36.7 N, respectively). In contrast, formulations Lyo MS CDP571-2 and 5, containing sucrose, led to the lowest Fmax (21.6 N and 19.7 N, respectively). These observations could be related to the particle size distribution, as the formulations containing sucrose or trehalose provided particles characterized by the lowest mean diameter and a narrower size distribution (e.g.  $d(0.9) < 90 \mu\text{m}$ ). This confirmed the protective effect of trehalose and sucrose in preventing the particles from sticking together during removal of water.

An additional MS formulation (MS CDP571-13) dried by vacuum was also evaluated. The injection of the suspension through a 23 G syringe was impossible. This was due to the formation of agglomerated MS and inhomogeneous redispersion. This might be explained by the vacuum-drying temperature (at RT), which was in the range of the  $T_g$  of the wet MS [123].

The thermal events of the freeze-dried MS (formulations Lyo MS CDP571-1 to 7) were evaluated by DSC (Table 31).

**Table 31: DSC data for the freeze-dried MS (formulations Lyo MS CDP571-1 to 7) – Summary of thermal events**

Formulation	PLGA T <sub>g</sub> (°C)	Thermal event 1	Thermal event 2
Lyo MS CDP571-1	45.2	129 = solid-solid transition from $\delta$ to $\beta$ polymorph of mannitol	157 = melting of mannitol ( $\delta$ polymorph)
Lyo MS CDP571-2	37.4	-	178.6
Lyo MS CDP571-3	40.4	-	165.1
Lyo MS CDP571-4	38.2	154 = melting of mannitol ( $\delta$ polymorph)	166 = melting of mannitol ( $\beta$ polymorph)
Lyo MS CDP571-5	33.6	-	178.2
Lyo MS CDP571-6	40.2	121.9 = trehalose T <sub>g</sub>	169.1
Lyo MS CDP571-7	36.0	-	182.2

The T<sub>g</sub> of the PLGA were found to be ranged between 33.6 and 45.2°C on the thermograms of the freeze-dried MS. It was noted that the lowest T<sub>g</sub> was observed for formulations Lyo MS CDP571-2 and 5, containing sucrose (37.4 and 33.6°C) and Lyo MS CDP571-7, without cryoprotectant (36.0°C).

Moreover, a large endotherm was detected around 70°C in each of the thermograms of the freeze-dried MS, which represented the evaporation of the residual EtAc content (boiling point = 77.1°C) [124].

Mannitol is an excipient broadly used in the freeze-drying process [125]. The freeze-drying process can produce a partially amorphous and partially crystalline material. The crystallization of mannitol during this process can lead to different anhydrous polymorphs ( $\alpha$ ,  $\beta$ , and  $\delta$  mannitol) [126]. The melting points (166°C, 166.5°C, and 150-158°C respectively) of these polymorphic forms differ only slightly. In the thermogram of formulation Lyo MS CDP571-4, containing mannitol, endothermic peaks around 154°C and 166°C were detected, corresponding, respectively, to the melting point of the  $\beta$  and  $\delta$  (= delta) polymorphic forms. These peaks were related to the polymorphism of the mannitol and its tendency to crystallize during the freezing

step. Formulation Lyo MS CDP571-1, containing a lower amount of mannitol, showed two small endothermic events which were related to the transition of  $\delta$  polymorph into  $\beta$  polymorph ( $\sim 130^{\circ}\text{C}$ ) and the melting point of the  $\delta$  polymorph ( $157^{\circ}\text{C}$ ). The  $T_g$  of the sucrose, which is reported to be  $\sim 75^{\circ}\text{C}$  was not detected (Lyo MS CDP571-2 and 5), suggesting the existence of strong interactions between the different compounds in the formulation [127]. The thermogram of formulation Lyo MS CDP571-6 showed a  $T_g$  around  $120^{\circ}\text{C}$ , corresponding to the  $T_g$  of the trehalose [106].

The x-ray diffraction patterns of the freeze-dried MS (Lyo MS CDP571-2, 3, 5, 6 and 7) showed no peak for crystallinity, confirming the completely amorphous state of the formulations. The formulation Lyo MS CDP571-4 presented some peaks of crystallinity corresponding to the delta-mannitol polymorph. Sucrose and trehalose were preferred as they did not show any tendency to crystallization, which can limit the formation of hydrogen bonds. The amorphous state of the particles and a lyoprotectant allows maximal H-bonding between particles and stabilizer molecules. Moreover, other properties of these sugars are considered to be advantageous, including their marginal hygroscopicity and the absence of internal hydrogen bonds, which allow more flexible formation of hydrogen bonds with particles during freeze-drying and very low chemical reactivity [116, 128].

The level of encapsulation was evaluated for freeze-dried MS ([Figure 67](#)).

IX. Development of a full length antibody (anti-TNF alpha) loaded PLGA microspheres using the solid-in-oil-in-water encapsulation method

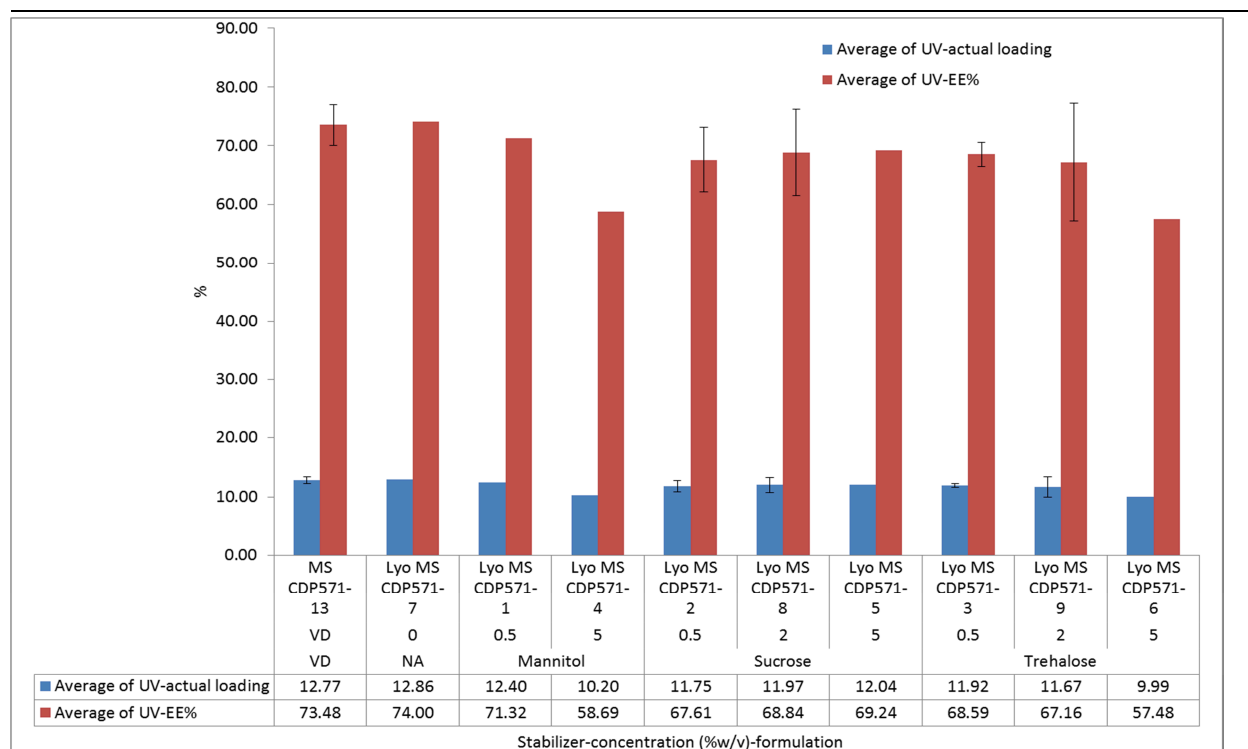


**Figure 67: Comparison of MAb loading and EE% for vacuum-dried (VA) (MS CDP571-13) and freeze-dried RG755S MS containing mannitol, sucrose or trehalose and not containing stabilizer (NA) (formulations MS CDP571-2, -3, -8, -9: mean (s), n = 3; formulations MS CDP571-1, -4, -5, -6, -7: n = 1)**

The MAb loading (from 10.0 % to 12.9 %) for freeze-dried MS (Lyo MS CDP571-1 to 7) were comparable to results measured on vacuum-dried MS (MS CDP571-13) ( $12.8 \pm 0.6$  % w/w drug loading). These results were in accordance with the work of Bozdag et al. who observed no effect of freeze-drying on the drug loading of PLGA particles with ciprofloxacin HCl [129]. The level of soluble aggregate and fragment was evaluated by SEC. As can be seen in Figure 68, the percentage of aggregation (HMWS) was significantly lower ( $p < 0.001$ ) with the Lyo MS CDP571 MS dried by freeze drying ( $< 0.1$  %) than by vacuum drying (MS CDP571-13) (2.8 %).

IX. Development of a full length antibody (anti-TNF alpha) loaded PLGA microspheres using the solid-in-oil-in-water encapsulation method

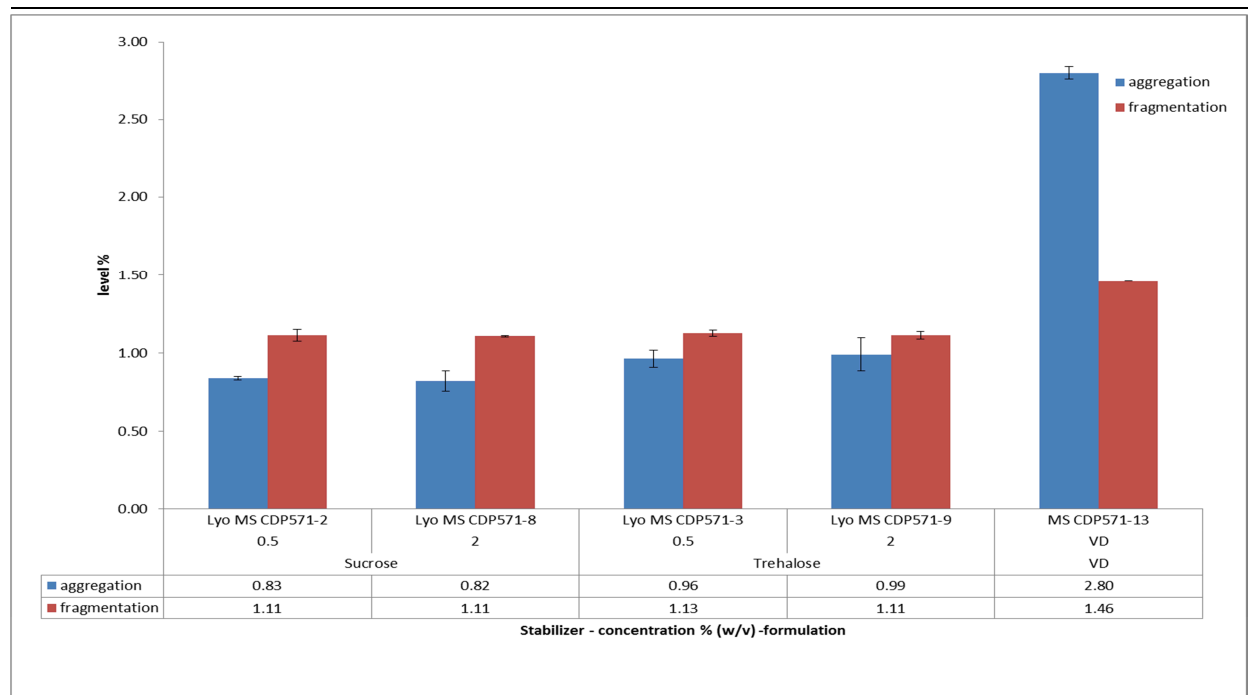


**Figure 68:** Comparison of aggregation (HMWS) and fragmentation (LMWS) levels of the freeze-dried MS (formulations Lyo MS CDP571-2, 3, 8 and 9) and the vacuum-dried MS (MS CDP571-13) (mean (s), n = 3)

The fragmentation level evaluated for the freeze-dried MS (< 1.1 %) was also significantly lower ( $p < 0.001$ ) than that for the vacuum dried MS (1.5 %).

It was concluded that the freeze-drying process, including addition of cryoprotectant, led to a better stabilization of the encapsulated CDP571 than vacuum drying. This might be explained by a faster inactivation of the residual water when the MS were freeze-dried, avoiding the degradation reactions of the MAb.

The release profiles of the freeze-dried MS (Lyo MS CDP571-2, 3, 8 and 9) were evaluated. Their dissolution profiles were compared to those obtained with the MS dried under vacuum (MS CDP571-13) (Figure 69). The release was faster, with an increased burst-effect after the freeze-drying process than after vacuum drying. It was already observed that the addition of a protein stabilizer such as trehalose can facilitate the release of protein from MS by generating a porous matrix after fast dissolution [60]. Moreover, compared to vacuum drying, the freeze-drying process might generate more porous MS, with water escaping via inter-connected microporous channels from the inner aqueous droplets to the outer surface. Indeed, the freezing process induced the formation of ice-crystals of free water molecules, which were then sublimed

[123]. The water removal process might generate further micro-channel pores from the loci of ice crystals to the surface.

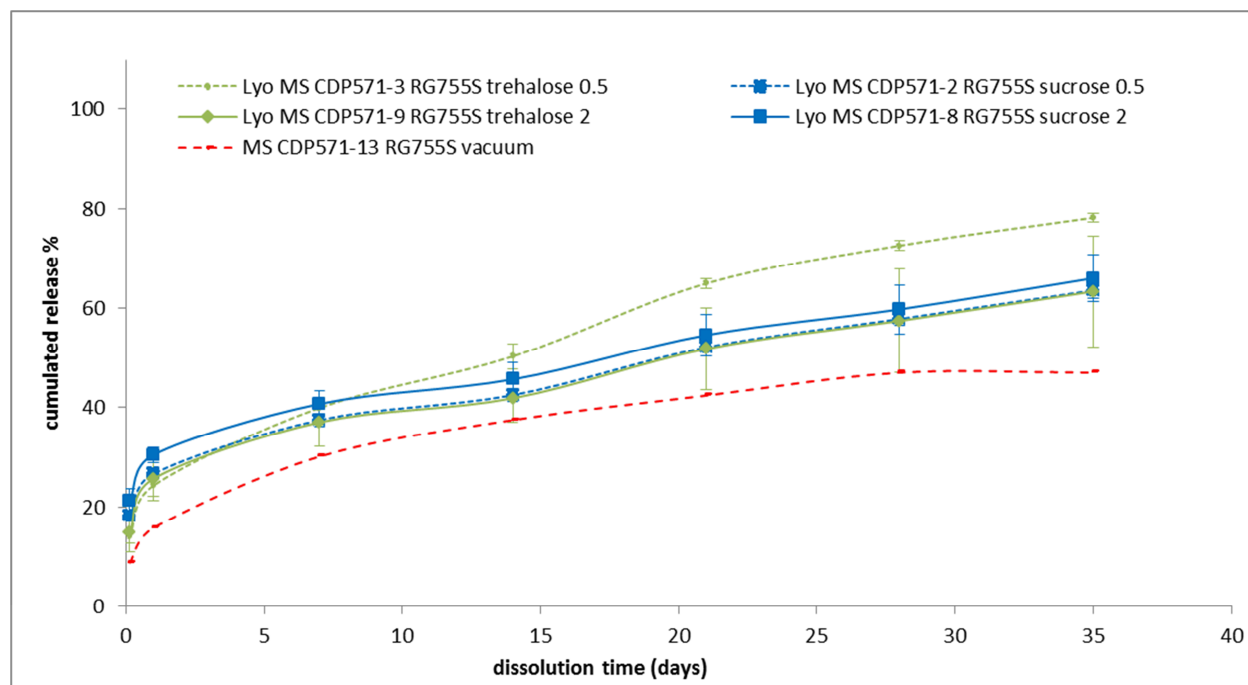


**Figure 69:** Comparison of the release profiles of the MS after freeze drying (in blue with sucrose, in green with trehalose) and vacuum drying (in red) (mean (s), n = 3)

The MAb HMWS and LMWS levels from MS were evaluated at different times of dissolution. The level of LMWS for the freeze-dried MS tended to increase over time during the dissolution test, as was already observed for the vacuum dried formulation (up to maximum 8.7 % and 7.0 % after 4 weeks of dissolution from the MS CDP571-13 and the freeze-dried MS, respectively) (Figure 71).

The freeze-drying process led to a lower initial percentage of HMWS (0.60 - 0.81 %) than vacuum drying (1.21 %) (Figure 70). Cryoprotectant played a major role in the protection of the CDP571 during the drying step. However, its protection seemed to be limited during the drug release, as the HMWS level increased over the dissolution period (up to 1.8 %) [106]. The limitation of co-encapsulated water-soluble additives may be their limited residence time within the hydrated MS [52].

IX. Development of a full length antibody (anti-TNF alpha) loaded PLGA microspheres using the solid-in-oil-in-water encapsulation method

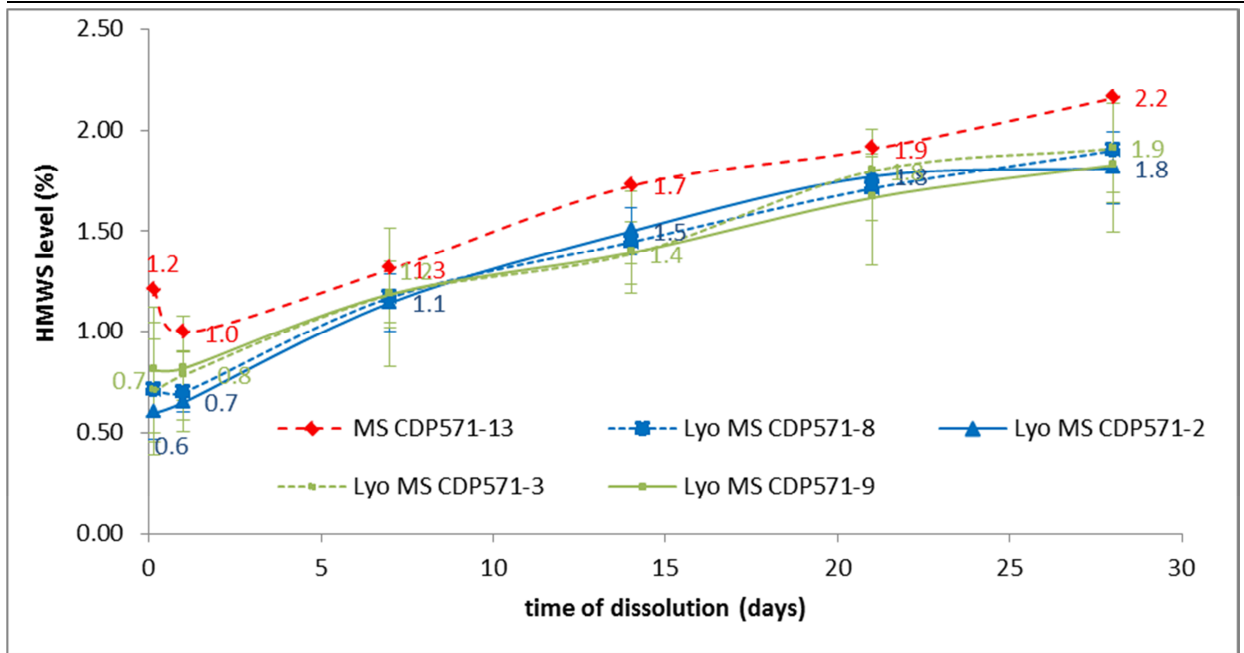


**Figure 70:** Evaluation of the HMWS (%) measured after 1 h, 24 h, 168 h, 336 h, 504 h and 672 h of dissolution from the MS after freeze-drying with sucrose (in blue, Lyo MS CDP571-2 and 8), with trehalose (in green, Lyo MS CDP571-3 and 9) and vacuum drying (in red, MS CDP571-13). (mean (s), n = 3)

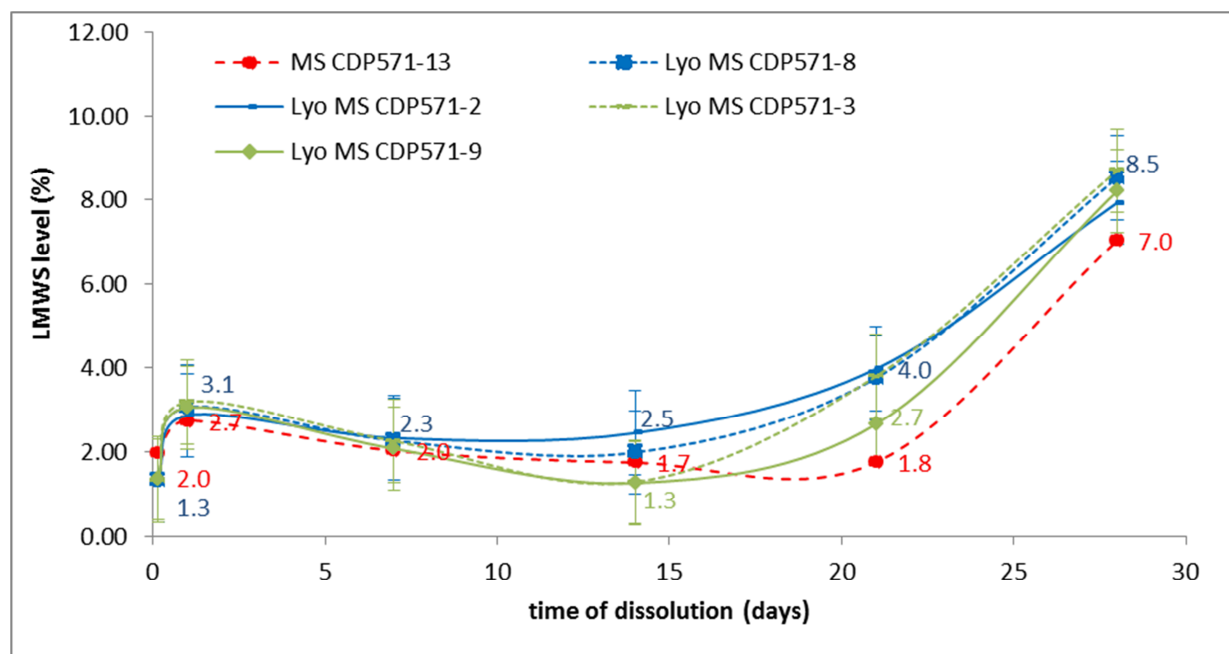


**Figure 71:** Evaluation of the LMWS (%) measured after 1 h, 24 h, 168 h, 336 h, 504 h and 672 h of dissolution from the MS after freeze-drying with sucrose (in blue, Lyo MS CDP571-2 and 8), with trehalose (in green, Lyo MS CDP571-3 and 9) and vacuum drying (in red) (MS CDP571-13) (mean (s), n = 3)

The residual water content was evaluated for the freeze-dried MS (formulations Lyo MS CDP571-1 to 7). All the evaluated formulations showed residual moisture lower than 1 % w/w (from 0.34 to 0.77 % w/w). For pharmaceutical dosage forms, it appears that a residual moisture content of 1 % or less is the most desirable [130].

The residual solvent content, evaluated by GC, was higher than the values recommended by the ICH Q3C (5000 ppm [131]) (Figure 72). The residual solvent content detected on the freeze-dried MS tended to be higher than that measured on the vacuum-dried MS.

IX. Development of a full length antibody (anti-TNF alpha) loaded PLGA microspheres using the solid-in-oil-in-water encapsulation method

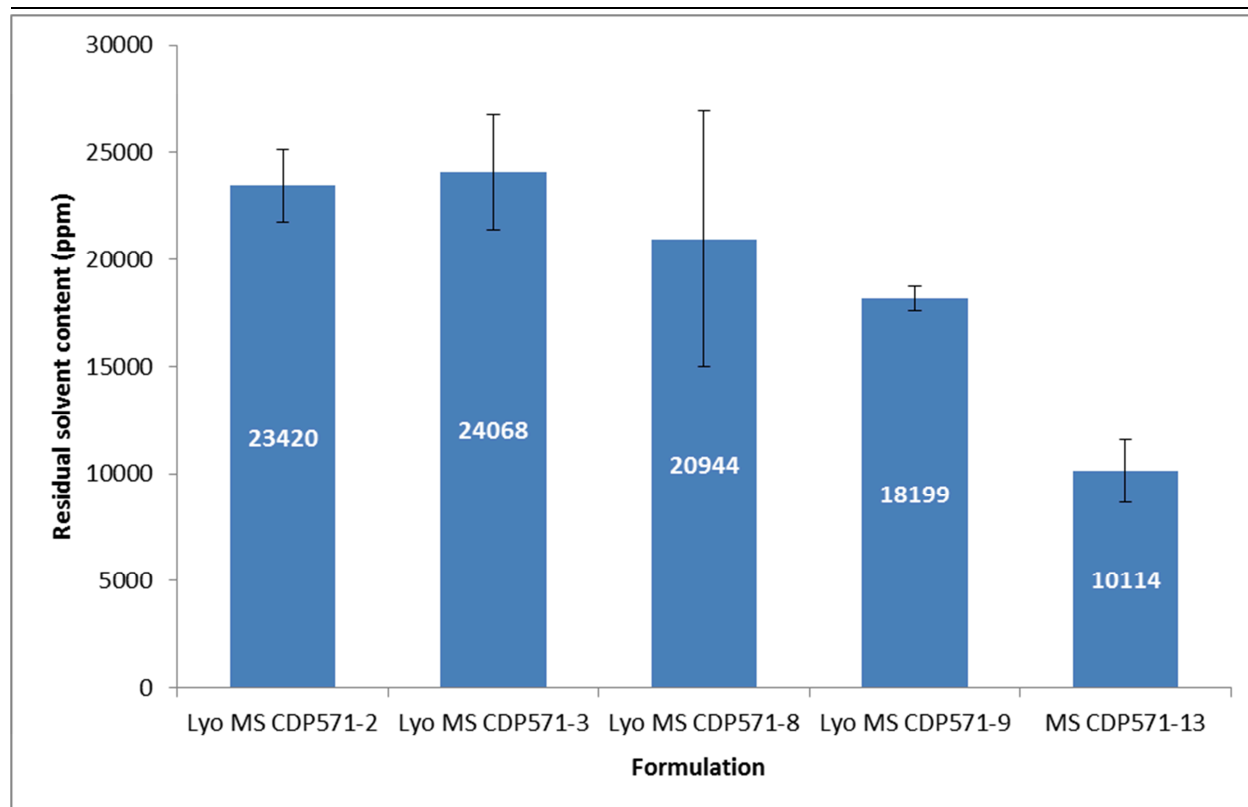


**Figure 72:** Comparison of the residual solvent content (ppm) measured on the freeze-dried MS (Lyo MS CDP571-2, 3, 8 and 9) and the vacuum-dried MS (MS CDP571-13) (mean (s), n = 3)

Most of the organic solvents, such as EtAc (Freezing point =  $-84^{\circ}\text{C}$ , boiling point =  $77.1^{\circ}\text{C}$ , solubility in water = 8.7 %), do not freeze in typical commercial freeze-dryers but remain as liquid residues within the frozen matrix. Samples dried with organic solvents that do not completely freeze may produce a product that is heterogeneous with respect to residual solvent [132]. A longer secondary drying in vacuum could help to decrease the level of residual solvent content.

## 5.2 CONCLUSION

It was concluded that the freeze-drying process led to improving the dispersion of the MS, resulting in better injectability compared to MS produced with vacuum drying. Addition of cryoprotectant was needed to maintain the integrity of the CDP571-loaded PLGA MS during freeze drying in terms of particle size and SEC profile. Both sucrose and trehalose were preferred to mannitol, which could present crystallization and polymorphisms. Moreover, the lower the concentration of the cryoprotectant, the lower was the burst effect. The Lyo MS CDP571-3,

IX. Development of a full length antibody (anti-TNF alpha) loaded PLGA microspheres using the solid-in-oil-in-water encapsulation method

---

containing a 0.5 % w/v trehalose solution, was preferred for freeze-drying the RG755S MS. This formulation was confirmed to be applicable to the RG505 MS (data not shown) (formulation Lyo MS CDP571-10). The current freeze-drying process was not effective at reaching the ICH specification regarding residual solvent content. It should be mentioned that the MS' suspension concentration, which is an important parameter, was not taken into account in this study.

## **STABILITY STUDY OF A FULL-LENGTH ANTIBODY (ANTI-TNF ALPHA) LOADED PLGA MICROSPHERES \***

\* adapted from [133]

### **1 INTRODUCTION**

Formulation stability is one of the most critical aspects of drug development in the pharmaceutical industry. Although systems based on polymer microparticles are extensively described in the literature, to our knowledge no data are available on the storage stability of Abs encapsulated in such systems.

In order to perform the stability study, around 200 mg of formulations MS CDP571-12 and 13 of anti-TNF alpha MAb-containing MS (theoretical 15 % w/w CDP571-loaded RG505 and RG755S vacuum dried MS produced with the SD CDP571-3 containing histidine and trehalose with a 70/30 MAb/trehalose ratio; table 42 in appendix) (e.g. PLGA RG505 and RG755S Resomer<sup>®</sup>) were each placed, in triplicate, in 3 mL Fiolax<sup>®</sup> clear glass vials (Schott, Müllheim, Germany) closed (not hermetically sealed) with a Flurotec<sup>®</sup> stopper (West Pharmaceutical services, Exton USA) at  $5 \pm 3^{\circ}\text{C}$ ,  $25 \pm 2^{\circ}\text{C}/60\% \text{ RH}$  and  $40 \pm 2^{\circ}\text{C}/75\% \text{ relative humidity (RH)}$  for up to 12 weeks. This study aimed to evaluate the effect of the storage temperature and relative humidity on the physico-chemical properties of the MAb-loaded PLGA MS, such as the drug loading, the dissolution profile, the particle size distribution and the morphology. The biological activity of the MAb within the MS was also investigated for the drug formulations stored in a dried state as well as during a dissolution test. This kind of stability study could validate a proof of concept for the encapsulation of MAb into a stabilizing formulation of biodegradable PLGA MS that have high encapsulation efficiency.

### **2 RESULTS AND DISCUSSION**

#### **2.1 Particle size and morphology of the MS**

The particle size distribution of the MS was evaluated before filtration during the manufacturing process and at the end of the stability study.

The MS' volumetric mean diameter seemed to be stable when the MS were stored at 5°C and 25°C for 12 weeks (Table 32). In contrast, after 6 weeks at 40 °C, the D[4.3] drastically increased, especially when the MS were based on RG505 polymer (from 69 µm to 291 µm). Indeed, when the MS were made of RG755S polymer, their mean diameter only increased from about 38 µm to 60 µm.

**Table 32: D[4.3] (µm) of MAb-loaded RG505 and RG755S MS before and after storage at 5, 25 and 40°C (mean, n = 3)**

Formulation	T0w	5°C ± 3°C - T12w	25°C ± 2°C - T12w	40°C ± 2°C - T6w
1-RG505	69.3	NR	67.6	291.1
2-RG755S	37.9	42.6	40.3	60.2

NR: not performed

SEM was used to visualize hypothetical modification within the morphology of the PLGA MS (e.g. agglomeration, coalescence) during storage. The MS were observed after 2 and 12 weeks at 5°C and after 2 and 6 weeks at 40°C.

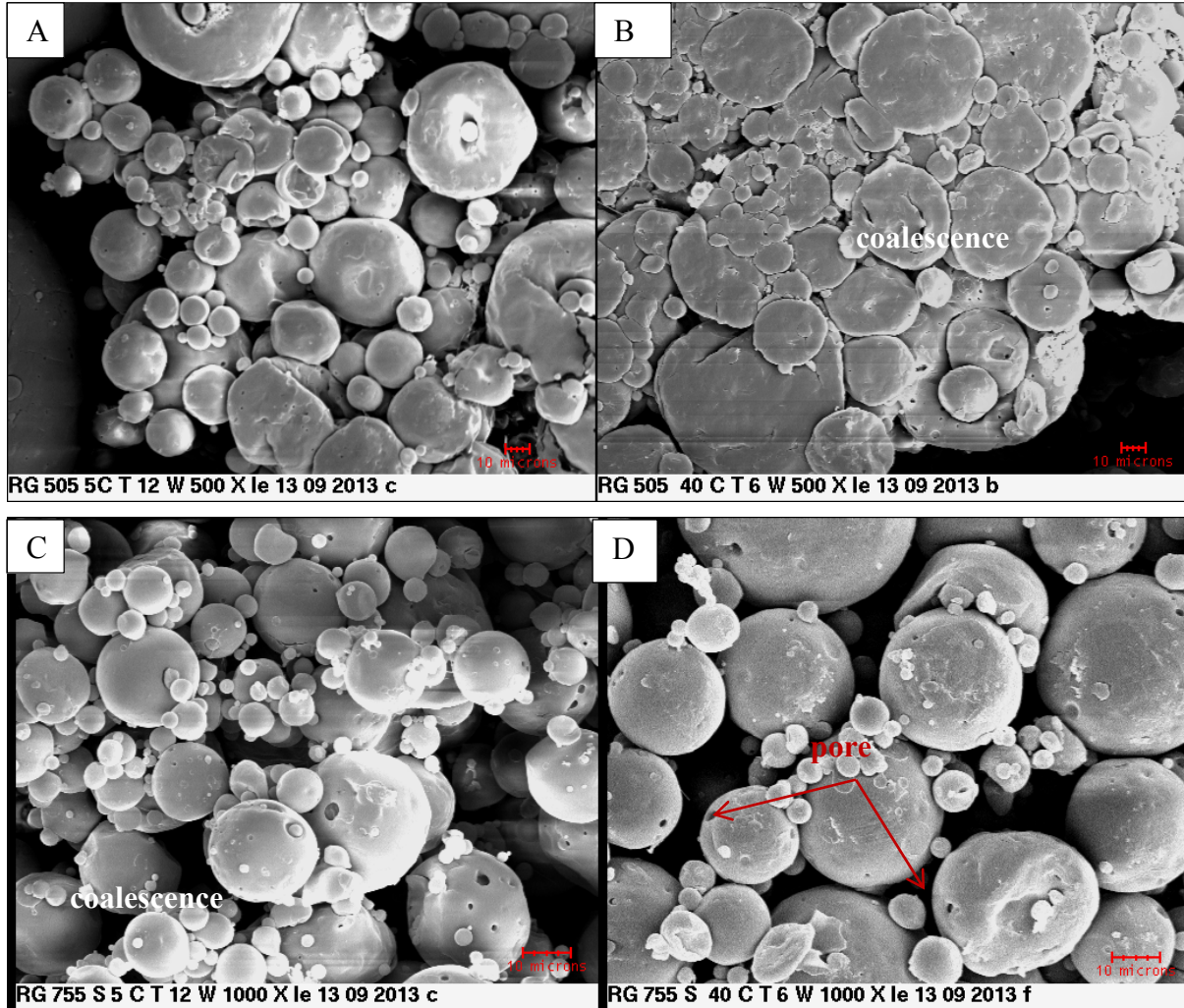


**Figure 73** Scanning electron micrographs of MAb-loaded RG505 MS at: (A) 12 weeks' storage at 5°C, magnification 500x and (B) 6 weeks' storage at 40°C, magnification 500x; and of MAb-loaded RG755S MS at: (C) 12 weeks' storage at 5°C, magnification 1 000x and (D) 6 weeks' storage at 40°C, magnification 1000x.

No agglomeration issues were observed for either RG505 or RG755S MS stored at 5°C for 12 weeks (Figure 73 A, C). Moreover, the RG755S MS were characterized by a spherical shape, and the photomicrograph revealed a smooth surface topography. The RG505 MS revealed a less spherical shape, with a few deformed spheres.

In contrast, at 40°C, RG505 MS presented deformations on their surface, their shape was irregular and collapsed MS were observed (Figure 73 B). This observation seemed to confirm the data obtained by laser diffraction. Indeed, the evaluated MS were characterized by a larger diameter after storage of 6 weeks at 40°C (Table 32). However, no agglomeration issue was observed with RG755S MS after storage, either at 5°C or at 40°C, but a small increase in the D

[4.3] was shown by laser diffraction for the RG755S MS after storage at 40°C for 6 weeks (from 37.9  $\mu\text{m}$  to 60.2  $\mu\text{m}$ ) (Table 32). It should be mentioned that some cracking and pores were observed on the surface of the RG755S MS stored at 40°C.

These modifications might have been caused by hydrolytic degradation of PLGA [134]. Sayin and co-authors explained that the apparent modification of the appearance and the variations of spherical shape were considered to be caused by hydrolytic degradation of PLGA polymer after storage under accelerated conditions at 40°C. As a consequence, they observed that the particle size of the MS increased [134]. It was shown that the degradation rate of the PLGA was affected by several physical and chemical factors, such as the initial pH, the ionic strength, the temperature of the external medium, the copolymer ratio, the molecular weight of the PLGA and the crystallinity. De and co-workers observed that the extent of aggregation decreased as the lactic acid content of the copolymer increased [135]. This statement was also observed in our study, and the agglomerates were visualized by SEM. Moreover, the increase in the D[4.3] measured by laser diffraction was lower for the RG755S MS compared to the RG505 MS, which were characterized by a lactic acid level of 75 % (w/w) and 50 % (w/w), respectively. GPC measurements showed that the Mw of the raw RG505 powder decreased faster than that of RG755S when stored for 6 weeks at 40°C (from 75.6 kDa to 24.0 kDa and from 60.8 kDa to 54.1 kDa respectively for the RG505 and the RG755S). It was confirmed for the MAb loaded PLGA MS. Indeed, after 6 weeks storage at 40°C, the Mw of the RG505 and the RG755S MS were decreased from 75.4 kDa to 38.3 kDa and from 61.5 kDa to 58.1 kDa, respectively (Table 33 and Table 34). It was concluded that the s/o/w process itself did not lead to PLGA degradation.

**Table 33: Residual water and solvent contents,  $T_g$  and enthalpy of relaxation and PLGA Mw of RG505 MS containing or not containing MAb before and after storage at 40°C for up to 6 weeks (mean (s), n = 3)**

Form	Time point	EtAc (ppm)	Water content (%)	$T_g$ (°C)	Enthalpy of relaxation (J/g)	PLGA Mw (kDa)
Ab MS	T0	24 641 ± 1 693	1.3 ± 0.1	34.4 ± 2.8	0.01 ± 0.02	75.4 ± 0.3
	T1 d	9 243 ± 1 016	1.6 ± 0.1	42.3 ± 0.3	0.66 ± 0.03	72.9 ± 1.9
	T3 d	2 087 ± 145	2.1 ± 0.1	48.8 ± 0.5	1.7 ± 0.7	65.9 ± 4.7
	T1 w	74 ± 66	2.3 ± 0.1	50.9 ± 0.1	2.4 ± 0.1	69.1 ± 0.9
	T6 w	0	3.6 ± 0.3	49.8 ± 0.2	4.3 ± 0.3	38.3 ± 1.4
Placebo MS	T0	36 400 ± 1 651	0.2 ± 0.1	37.2 ± 0.9	0.0	73.0 ± 1.1
	T1 d	12 414 ± 237	0.47 ± 0.03	41.7 ± 0.2	2.0 ± 0.1	76.9 ± 1.2
	T3 d	3 100 ± 740	0.6 3± 0.02	49.7 ± 0.7	1.8 ± 0.4	71.2 ± 0.1
	T1 w	461 ± 35	0.4 ± 0.1	51.8 ± 0.2	3.4 ± 0.1	66.8 ± 0.8
	T6 w	0	1.1 ± 0.1	45.3 ± 0.4	5.3 0 ± 0.4	26.6 ± 2.5

**Table 34: Residual water and solvent contents,  $T_g$  and enthalpy of relaxation and PLGA Mw of RG755S MS containing or not containing MAb before and after storage at 40°C for up to 6 weeks (mean (s), n = 3)**

Form	Time point	EtAc (ppm)	Water content (%)	$T_g$ (°C)	Enthalpy of relaxation (J/g)	PLGA Mw (kDa)
Ab MS	T0	10 114± 1 926	1.52 ± 0.04	44.6 ± 0.7	1.5 ± 0.4	61.5 ± 0.3
	T1 d	3 677 ± 2 840	2.2 ± 0.9	49.2 ± 0.4	0.9 ± 0.7	61.2 ± 0.2
	T3 d	939 ± 224	2.7 ± 0.6	52.4 ± 0.6	1.8 ± 0.4	61.6 ± 0.3
	T1 w	0	2.6 ± 0.3	52.6 ± 0.2	1.8 ± 0.1	59.4 ± 0.2
	T6 w	0	3.8 ± 0.1	53.1 ± 0.5	3.7 ± 0.1	58.1 ± 1.2
Placebo MS	T0	29 113 ± 1 458	0.22 ± 0.03	33.8 ± 4.1	0.2 ± 0.3	60.8 ± 0.9
	T1 d	9 443 ± 1 589	0.34 ± 0.04	48.1 ± 0.3	0.9 ± 0.2	63.1 ± 0.5
	T3 d	1 471 ± 310	0.62 ± 0.06	52.2 ± 0.3	2.4	58.3 ± 1.7
	T1 w	244 ± 91	0.24 ± 0.03	53.3 ± 0.2	2.4 ± 0.4	59.2 ± 0.6
	T6 w	0	0.86 ± 0.03	52.7 ± 1.1	4.6 ± 0.1	56.8 ± 1.1

The high difference in agglomeration tendency of the PLGA MS when stored at 40°C might also be attributed to the difference in  $T_g$  of the polymers. It was shown that the  $T_g$  of freshly prepared RG505 MS (34°C) was lower than that of RG755S MS (44.6°C) (Table 33 and Table 34). Above the  $T_g$ , the polymer became sticky and rubbery, which led to a higher tendency to agglomeration and collapse. It was demonstrated that the  $T_g$  value of the PLGA should be higher than 40°C to achieve long-term stability [128].

Both the residual water and EtAc contents (Table 33 and Table 34) might also be involved in the agglomeration issues, especially if they contributed to lowering the  $T_g$  of the polymer by acting as plasticizers. Indeed, Holzer and co-workers suggested that humidity could accelerate the agglomeration of MS by decreasing their apparent  $T_g$  [128].

It appeared that the amount of residual water at T<sub>0</sub> was similar for MS made of both types of polymer (1.3 % (w/w) vs. 1.52 % (w/w) for RG505 and RG755S, respectively) but it tended to increase when stored at 40°C/75 % RH (Table 33 and Table 34). However, this increase was not linked to any decrease in  $T_g$ . In addition, the amount of residual EtAc, which was evaluated in the RG505 MS (from 24641 ppm to < 50 ppm at T<sub>0</sub> and after 6 weeks' storage at 40°C, respectively) was higher compared to the RG755S MS (from 10114 ppm to < 50 ppm at T<sub>0</sub> and after 6 weeks' storage at 40°C, respectively). The decrease in residual solvent content observed on the MS stored at 40°C suggested the migration of the solvent to the surface of the MS and its evaporation. This decrease was higher with the RG505, which might also explain the difference in agglomeration tendency observed between the two tested PLGA. At 5°C, the amount of residual solvent content seemed to be more stable (16584 ppm and 7004 ppm after 12 weeks' storage at 5°C for RG505 and RG755S MS, respectively). According to Puthli, the agglomeration might be attributed to residual solvent migration and partial dissolution of PLGA on the superficial layers leading to coalescence [136]. De and co-workers suggested that during storage at higher temperatures, the residual solvent migrated to the surface of the spheres and dissolved the PLGA on the superficial layers, causing coalescence of the MS [135].

## **2.2 Polymorphic state – glass transition temperature and enthalpy of relaxation**

The X-ray diffraction pattern of the RG505 and RG755S MS showed no peak corresponding to crystalline structure, regardless of both the period of storage and the temperature or relative

humidity (data not shown). The polymer preserved its initial amorphous state during storage and the encapsulation process [137].

Amorphous solids tend to relax towards the thermodynamic equilibrium state due to molecular mobility. This structural relaxation could affect product performance such as the rate of degradation of the polymer and release of the drug. As suggested by Rawat and al, the PLGA MS solidification by solvent removal in the s/o/w encapsulation process was similar to the thermal quenching of an amorphous polymer from the molten state [138]. Rapid solvent removal by evaporation might result in polymer matrices characterized by high structural energy.

A  $T_g$  around 50°C was measured on the raw RG505 ( $T_g = 53.9^\circ\text{C}$ ) and RG755S ( $T_g = 53.3^\circ\text{C}$ ) PLGA powders, which corresponded to the literature [139]. These values were much higher than the  $T_g$  obtained on the freshly prepared MS (MAB:RG505 MS'  $T_g = 34.4^\circ\text{C}$  and MAB:RG755S MS'  $T_g = 44.6^\circ\text{C}$ ) (Table 33 and Table 34). After 12 weeks' storage at 5°C and 6 weeks' storage at 40°C, the  $T_g$  increased by 10°C and 15°C for the RG505 MS and by 5°C and 8°C for the RG755S MS, respectively. The  $T_g$  measured after 6 weeks' storage was close to the  $T_g$  observed after 1 week. The  $T_g$  rapidly went back to the  $T_g$  of the raw polymer when stored at 40°C. Indeed, after 3 days' storage, values of 48.8°C and 52.4°C were observed for the RG505 and the RG755S MS, respectively. This increase in the  $T_g$  was statistically related to the decrease in the residual solvent content that was observed at 40°C ( $p < 0.0001$ ). Indeed, the residual EtAc content decreased from 24641 ppm to 2087 ppm for the MAB-loaded RG505 MS and from 10114 ppm to 939 ppm for the MAB-loaded RG755S MS when stored for 3 days at 40°C (Table 33 and Table 34). As previously mentioned, the residual organic solvent led to a decrease in the  $T_g$  as it acted as a plasticizer. The residual water content of the MAB MS, which could also act as plasticizer, tended to increase when stored at 40°C/75 % RH (Table 33 and Table 34). However, the  $T_g$  values did not increase. It should be noted that the moisture content of the MS not containing MAB (placebo MS in Table 33 and Table 34) and the PLGA raw material (from 0.3 % to 1.0 % for RG505 and from 0.3 % to 0.8 % for RG755S) was lower and more stable than that of the MS containing MAB. The MAB might lead to absorption of water. An increase in the enthalpy of relaxation was found for the RG505 and RG755S MS at 5°C and 40°C (Table 33 and Table 34). This increase was faster when stored at 40°C, which might be explained by a higher mobility of the polymeric chains at higher temperatures (data not shown). The enthalpy of relaxation measured on the RG505 MS increased from 0 J/g to 2.7 J/g and 4.3 J/g after 12 weeks

at 5°C and 6 weeks at 40°C, respectively. No enthalpy of relaxation was observed for freshly prepared RG505 MS in contrast to the RG755S MS, which were already characterized by an enthalpy of 1.5 J/g. However, the enthalpies of relaxation observed for the placebo RG755S MS (0.2 J/g) were much lower than that obtained for the MAb MS. The presence of amorphous antibody at a level of around 12 % w/w in the MS might lead to a more structured state, resulting in a lower quenching effect. The significant increase in the enthalpy of relaxation observed after storage at 5°C and 40°C was a result of structural relaxation of the polymer chains.

The extent to which the PLGA MS were affected by physical ageing was likely to depend on the type of PLGA and the storage temperature [135]. It was observed that the storage of MS led to an increase in  $T_g$  and enthalpy of relaxation. However, the relationship between these physical changes and the modifications of the properties of the MS was difficult to establish, especially at 5°C. At this temperature, no specific change in the properties of the MAb MS, such as the release profile of the MAb from the MS or the morphology, was noticed. However, it was observed that the RG505 MS seemed to be more affected by the s/o/w process than the RG755S MS. This was shown by a lower  $T_g$  and a lack of enthalpy of relaxation measured for freshly prepared RG505 MS. That might explain the higher tendency of agglomeration for the RG505 MS.

### 2.3 Drug content

The drug content of the MAb-loaded PLGA MS was measured during the storage.

The antibody content (%) appeared much more stable in the RG755S MS (Figure 74).

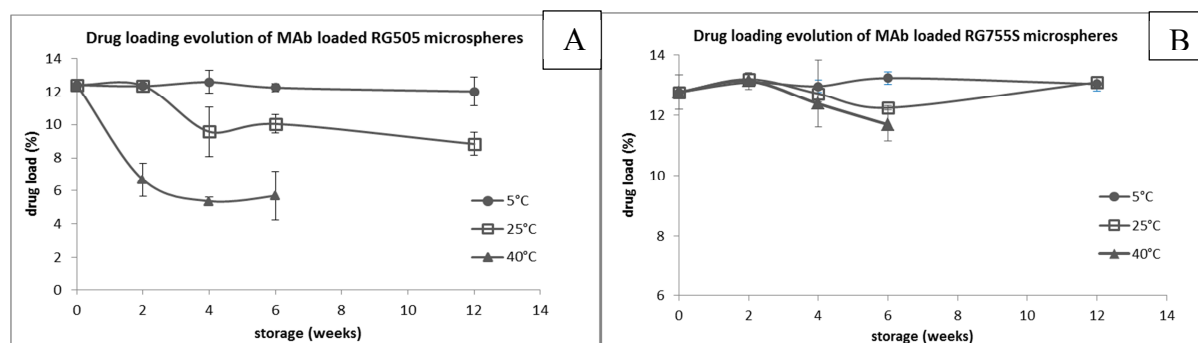


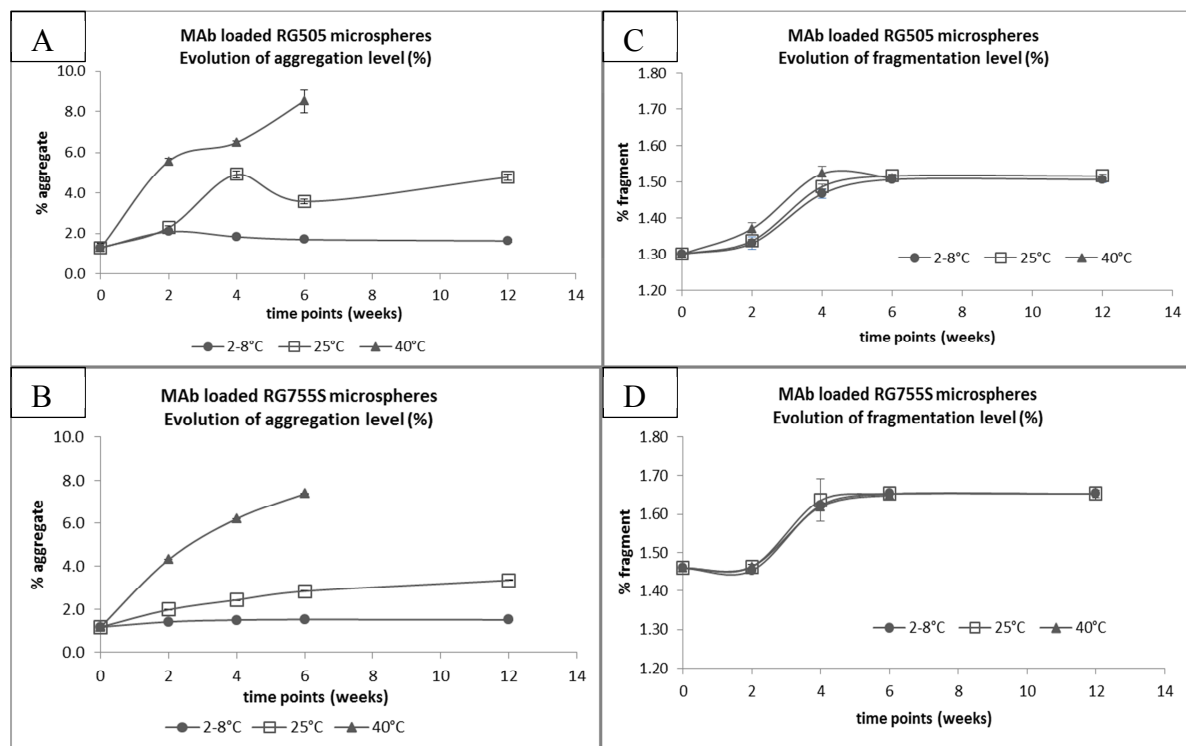
**Figure 74** Comparison of the drug loading evolution of the MAb-loaded (A) RG505 and (B) RG755S MS stored at 5, 25 and 40°C for up to 12 weeks (mean (s), n = 3)

After 12 weeks at 5°C and 25°C/60 % RH, the drug loading remained similar when the RG755S polymer was used. After 4 weeks at 40°C, the MAb content appeared to decrease from 12.4 % to

5.7 % and from 12.8 % to only 11.7 % (w/w) for the RG505 and RG755S MS, respectively. This decrease might be attributed to the diffusion of the drug from the polymeric matrix, leading to a greater exposure of the MAb to environmental stress. It might result in the formation of undetectable (unquantifiable) insoluble aggregates of MAb [120]. Indeed, the amount of MAb reduced less when RG755S was used because this polymer was characterized by a higher lactide:glycolide ratio and thus a slower degradation rate. This slower degradation rate might decrease the diffusion of the incorporated MAb and slow down acidification into the MS and the resulting degradation of the MAb.

## 2.4 HMWS/LMWS and activity evaluation

Several chemical reactions between PLGA and the incorporated Ab could occur, leading to accelerated Ab degradation [140]. Evolution of the HMWS and LMWS levels of MAb encapsulated into the RG505 and RG755S MS was evaluated over storage on the samples collected during the drug loading and the dissolution evaluations.



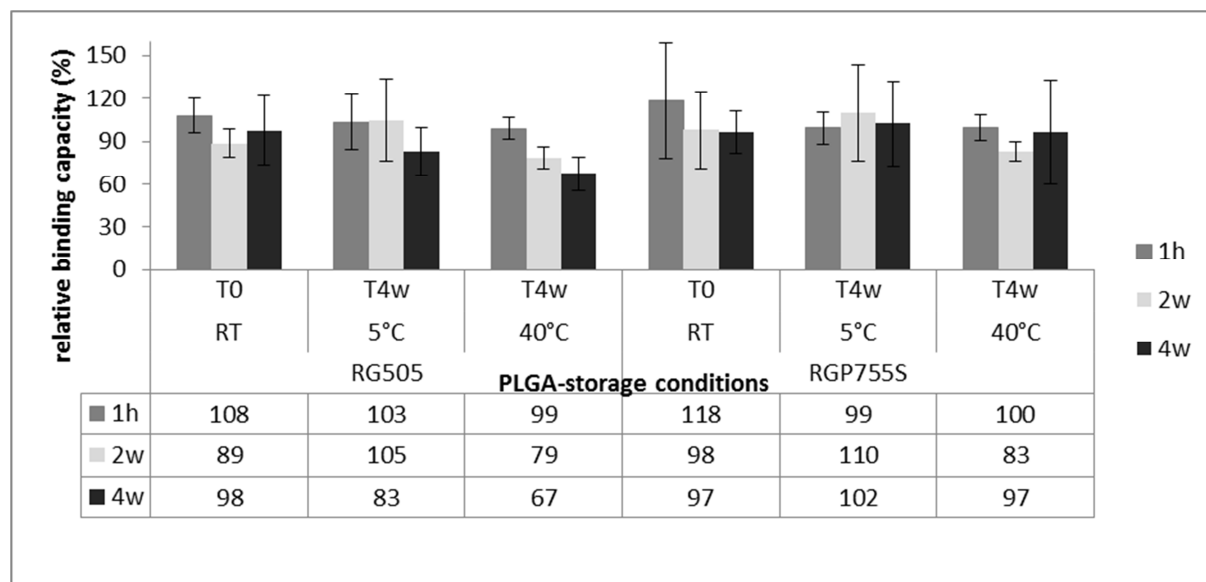
**Figure 75** Comparison of the evolution of the aggregation (A and B) and fragmentation (C and D) levels measured on MS after 0, 2, 4, 6 and 12 weeks' storage at 5, 25 and 40°C. (mean (s), n = 3)

Figure 75 (A, B) shows the evaluation of the HMWS level of the MAb after 0, 2, 4, 6 and 12 weeks at 5, 25 and 40°C. The HMWS content increased over time when MS were stored for 6 weeks at 25°C (2.3 % increase) and even faster at 40°C (7.2 % increase). At 5°C, the HMWS level seemed to be stable until 12 weeks for both formulations (0.4 % increase). However, it should be noted that, at these conditions, the HMWS level was higher for the RG505 MS (3.4 % vs. 2.8 % for the RG505 and the RG755S MS, respectively). This should be attributed to the lower  $T_g$  and to the higher degradation rate of the RG505 polymer, which led to a higher mobility of the polymer and a faster aggregation of the MAb [141].

The evaluation of the LMWS level of the MAb encapsulated inside the MS after 0, 2, 4, 6 and 12 weeks at 5, 25 and 40°C is illustrated in Figure 75 (C, D). After 4 weeks, a small increase in LMWS (maximum 0.2 %) was observed, regardless of either the storage conditions or the type of PLGA.

The percentage of HMWS and LMWS was also evaluated on samples collected during the dissolution test from MS stored for 6 weeks at 5, 25 and 40°C. No modification of the HMWS level was observed during the dissolution test (data not shown). In contrast, the LMWS level increased with the dissolution time and even more so with the RG505 MS. Before storage, an increase of  $5.1 \pm 0.2$  % LMWS was found after 4 weeks of dissolution with the RG755S MS, against  $7.1 \pm 0.1$  % for the RG505 MS. Moreover, the time and the storage temperature increased the level of LMWS of the RG505 MS. After 2 weeks of storage at 5°C, 25°C and 40°C of the RG505 MS, the percentage of LMWS measured after 4 weeks of dissolution increased by  $8.1 \pm 0.1$  %,  $9.3 \pm 0.4$  % and  $10.3 \pm 1.2$  %, respectively, compared to the  $7.1 \pm 0.1$  % measured at  $T_0$ . Neither the time nor the storage conditions seemed to have an impact on the level of LMWS for the RG755S MS (data not shown). The faster degradation of the RG505 might lead to a more acidic microenvironment inside the MS, which could explain the difference in terms of Ab fragmentation over the dissolution test.

ELISA tests were also performed to evaluate the binding capacity of the MAb released during the dissolution test after 1 h, 2 weeks and 4 weeks. This evaluation was performed on PLGA MS before and after 4 weeks' storage at 5, 25 and 40°C (Figure 76).



**Figure 76** Comparison of the relative binding capacity of MAb released after 1 h, 2 weeks and 4 weeks of dissolution from RG505 and RG755S MS before storage and after 4 weeks' storage at 5°C and 40°C. (mean (s), n = 3)

The binding capacity of MAb did not change upon storage or during dissolution when encapsulated in RG755S MS. Before storage of the RG755S MS, relative binding capacities of  $118 \pm 40\%$  and  $97 \pm 15\%$  were calculated after 1 h and 4 weeks of dissolution. After a 4 weeks' storage, the relative binding capacities measured after 4 weeks of dissolution did not decrease, either at 5°C ( $102 \pm 29\%$ ) or at 40°C ( $97 \pm 36\%$ ). In contrast, the MAb released after 4 weeks' dissolution from RG505 MS stored for 4 weeks at 40°C presented a relative binding capacity of  $67 \pm 12\%$  compared to the  $108 \pm 12\%$  measured at T0 after 1 h of dissolution, which was statistically lower ( $p < 0.0001$ , oneway analysis of binding capacity by dissolution time, ANOVA). This decrease was not observed for the MAb released after 1 h of dissolution.

A bioassay was performed to evaluate the biological activity of the MAb released from RG505 and RG755S MS. The potency of MAb released from RG505 and RG755S MS stored for 6 weeks at 5°C and 40°C and collected after 1 h and 4 weeks' dissolution was evaluated. The activity of the MAb released from the RG505 and the RG755S MS was preserved over the storage as no significant change was observed between  $EC_{50}$  values of samples tested before or after 6 weeks' storage, both at 5°C and 40°C (Table 35).

**Table 35: TNF-alpha cytotoxicity neutralization bioassay - EC<sub>50</sub> (ng/mL) of MAb released after 1 h and 4 weeks of dissolution from RG505 and RG755S MS before (T0) and after 6 weeks' storage (T6 w) at 5°C and 40°C (mean (s), n = 3)**

	RG505 MS			RG755S MS		
	T0	T6 w		T0	T6 w	
Dissolution time	NA	5°C	40°C	NA	5°C	40°C
1h	64 ± 21	46 ± 8	64 ± 27	43 ± 3	49 ± 4	50
4w	62 ± 14	58 ± 21	57	53 ± 12	50	51 ± 24

In addition, it should be mentioned that no loss of potency was observed after MAb encapsulation as the EC<sub>50</sub> of the reference MAb was similar (71 ± 18 ng/mL).

It should be mentioned that the data on binding capacity and TNF-alpha potency did not systematically relate to the SEC measurements. Indeed, no loss of potency was observed for the MAb that was released after 1 h of dissolution from RG505 MS stored for 4 weeks at 40°C, although they presented an increase of 5 % in their level of aggregation. Similarly, the increase in the level of LMWS which was observed after 4 weeks of dissolution was not related to a decrease in potency, regardless of the sample.

## 2.5 Dissolution test

The dissolution profiles of the MAb encapsulated in the RG505 and RG755S MS were evaluated at T<sub>0</sub> and over 6 weeks of storage at 40°C/75 % RH and 12 weeks at 5°C and 25°C/60 % RH (Figure 77).

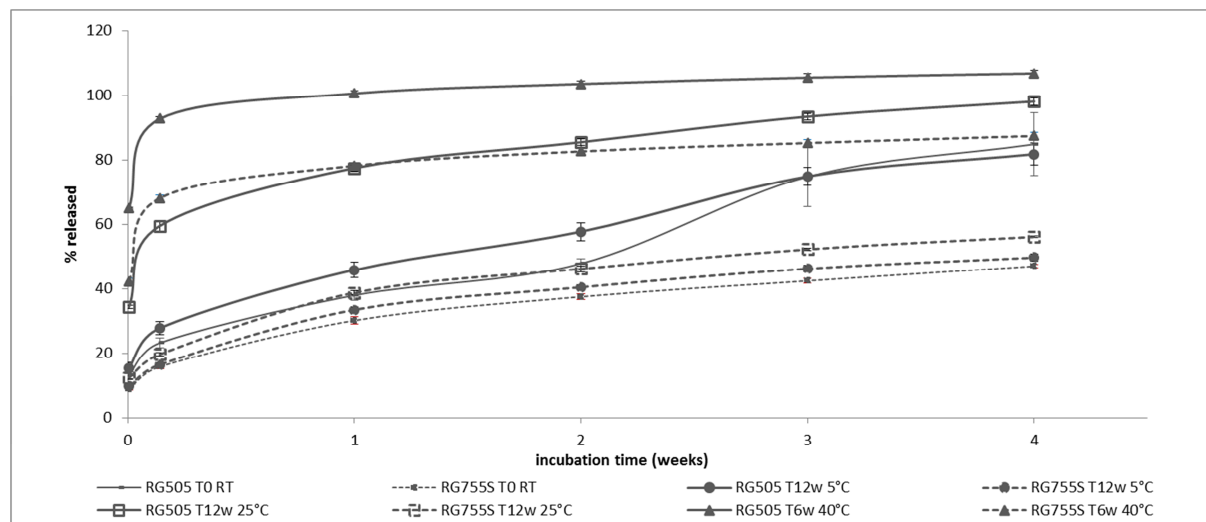


**Figure 77** Dissolution profile of RG505 (-) and RG755S (...) MS before (-) and after 12 weeks' storage at 5°C (●), 25°C (□) and 40°C (▲): cumulated released MAb (% w/w) vs. time of dissolution (weeks)(mean (s), n = 3)

At T<sub>0</sub>, the pattern of the drug release from the PLGA MS appeared steady and slower for the RG755S MS than for the RG505 MS. After 4 weeks of dissolution, the total amount of MAb that was released from freshly prepared MS was higher with RG505 (84.9 ± 9.8 %) than with RG755S MS (47.0 ± 0.6 %). This difference was related to the difference in terms of degradation rates of the tested polymers and confirmed the slower degradation of the 75:25 PLGA. The burst effect was quite limited for both of the tested formulations (23 % and 16 % for the RG505 and RG755S MS, respectively). When stored at 5°C, no difference was observed between the dissolution profiles for either type of MS, before and after 12 weeks ( $f_2 > 50$ ) (Table 36).

**Table 36: Calculated similarity factors ( $f_2$ ) of dissolution profiles of MAb-loaded RG505 and RG755S MS before and after storage at 5, 25 and 40°C**

Formulation	T12 w – 5°C	T12 w – 25°C	T6 w – 40°C
RG505 MS	58 ± 10	25 ±	12.7 ± 0.1
RG755S MS	78 ± 10	56 ± 2	17.4 ± 0.6

When stored at 40°C, the  $f_2$  values below 50 suggesting that the release profiles of both evaluated formulations were not similar to those obtained before storage. This difference was related to the increase in the burst effect. At 25°C, only the release profile of the RG755S formulation remained equivalent, with an  $f_2$  value of 56. As shown by Lewis and co-workers, the burst effect increased with duration and temperature of storage [142]. Indeed, the highest burst effects were observed for the MS stored at 40°C for 6 weeks (69.5 % and 33.4 % for the RG505 and the RG755S MS, respectively).

The kinetic model used to characterize the release of the MAb was modified according to the time and conditions of storage. Before storage, the RG755S formulation seemed to follow the Higuchi kinetic model ( $r^2 = 0.99$ ), based on the Fickian diffusion model, which was stable when stored at 5°C ( $r^2 = 0.99$ ) and 25°C ( $r^2 = 0.99$ ) for up to 12 weeks. We noted that the slope and the intercept of the calculated linear regression for the Higuchi models were higher at 25°C, indicating, respectively, a faster release and a higher initial release (data not shown). When stored at 40°C, the release profile changed and fitted better with the Korsmeyer model ( $r^2 = 0.97$ ). This change was related to the increase in the burst effect. This increase might be explained by the faster degradation of the polymer stored at 40°C, facilitating the diffusion of the drug through the polymeric matrix. Compared to the RG755S formulation, the release profile of the RG505 formulation also fitted to the Higuchi model prior to storage and when stored at 5°C ( $r^2 = 0.99$ ). However, it had a higher slope value, linked to a faster release rate. After storage at 25 or 40°C, the release kinetic fitted to the Korsmeyer model (respectively,  $r^2 = 1.00$  and  $r^2 = 0.95$ ). It was noted that the slope values of the Korsmeyer model were  $< 0.45$ , which corresponded to a Fickian diffusion mechanism of drug release. The release profile, following a diffusion model, was confirmed to be stable with a limited burst effect when the MS were stored at 5°C and much more stable for the RG755S MS, which could be stored at 25°C without modification of the dissolution profile. Moreover, the RG755S might be more appropriate for delivering the MAb for a long period of time ( $> 4$  weeks).

### 3 CONCLUSION

During this stability study, it was demonstrated that the MAb-loaded PLGA MS were stable when stored at 5°C and that the selection of the appropriate type of PLGA was critical to assuring the stability of the system. In our study, the RG755S, characterized by a 75:25 lactic-glycolic ratio, appeared to be more appropriate for stabilizing the encapsulated MAb and for delivering the MAb for a long period of time (> 4 weeks). The storage temperature was a key parameter in terms of stability and particle size. Indeed, storage at temperatures higher than 5°C could lead to stability problems for the antibody, such as aggregation, fragmentation and loss of activity. The incorporation of the MAb into a polymeric matrix allowed the integrity of the MAb to be preserved when stored at 5°C. As mentioned previously, some stability issues might be attributed to the presence of residual water and solvent, which might lead to polymeric hydrolysis, causing an acidic microenvironment. The antibody release profile could also be altered. Improvement of the drying step of the produced MS, including vacuum drying or freeze drying, could lead to an increase in the stability of the system at room temperature. In addition, storage at higher temperatures (40°C) led to modifications of the particle size and morphology of the MS. Lyophilized PLGA MS, in combination with cryoprotectives changing the  $T_g$  values, could prevent coalescence issues. In combination with proteins, it was previously described that the higher  $T_g$  of sucrose and trehalose were at least partially due to the formation of sucrose- or trehalose-protein-water micro crystals, thus preventing water from acting as plasticizer of the amorphous phase. Other properties of sucrose and trehalose were also considered to be advantageous, including marginal hygroscopicity, an absence of internal hydrogen bonds, which allowed more flexible formations, and very low chemical reactivity [128].

Physical ageing of the system associated with changes in the glass transition temperature and enthalpy of relaxation were noted during the storage of the MAb-loaded PLGA MS. However, no clear relationships between these effects and modifications of the performance of the system were established.

## **PK STUDY IN RATS OF FULL-LENGTH ANTIBODY (ANTI-TNF ALPHA) LOADED PLGA MICROSPHERES**

### **1 INTRODUCTION**

The aim of this study was to investigate the *in vivo* release profile and kinetic parameters of the CDP571 from the PLGA MS system. Two selected controlled release formations (Lyo MS CDP571-3 and 10, [Table 43 in appendix](#)) were compared to an immediate-release solution of CDP571 ([Table 11](#) in Material and Methods section). The evaluated formulations were subcutaneously injected into a Sprague Dawley rat model. The inflammation reaction at the injection site was evaluated by an histological study. The *in vivo* bioactivity of the CDP571 was verified by TNF bioassay realized on the plasmatic samples.

As the CDP571 was a humanized antibody, a preliminary pK study was performed with CDP571 solutions to confirm the absence of a neutralization effect of the drug after administration in rat ([Table 10](#) in Material and Methods section).

### **2 RESULTS AND DISCUSSION**

#### **2.1 pK data of the anti-TNF alpha MAb *in vivo* studies**

The CDP571 plasmatic concentration was determined after both IV and SC administration of the MAb at different time points ([Table 44](#), [Table 45](#), [Table 46](#) and [Table 47 in appendix](#)). The mean plasma levels of the MAb after IV and SC administration of MAb aqueous solution and MS were shown in [Figure 78](#) and [Figure 79](#) .

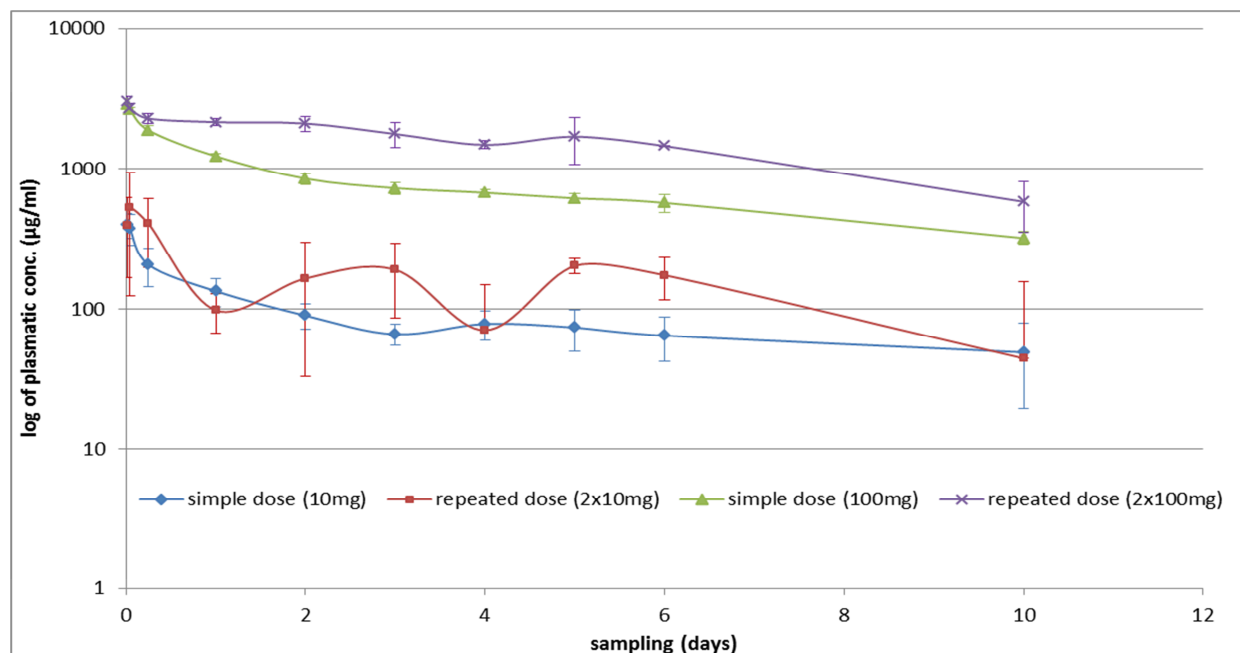


**Figure 78** Log of mean MAb plasmatic concentrations ( $\mu\text{g/mL}$ ) vs. time (h) after intravenous administration of 10 mg single dose (in blue); 2 x 10 mg, repeated dose 10 days after first administration (in red); 100 mg single dose (in green) and 2 x 100 mg, repeated dose 10 days after first administration (in purple), CDP571 in aqueous solution. (mean (s),  $n = 3$ )

After IV administration of the CDP571 in aqueous solution, the MAb plasmatic concentration, measured by ELISA, slowly decreased over time, regardless of the dose (10 mg vs. 100 mg single or repeated dose) (Figure 78). No immunogenicity issue appeared after administration of humanized CDP571 to the rats. Indeed, no neutralization of the antibody was observed over time and especially during the administration of the repeated dose. Therefore, the *in vivo* evaluation of the PLGA MS was conducted in rats using the humanized anti-TNF alpha MAb as the model. The characteristics of the MAb-produced MS administered in this pK study are summarized in Table 50 and Table 51 in appendix.

During the administration of the suspensions of MS using a 1 mL syringe with a 22 G needle, syringeability issues were observed. This problem was observed both with placebo and CDP571 MS but was smaller with the RG755S MS containing the MAb (Lyo MS CDP571-3). It might be explained by the higher particle size ( $d(0.9)$ ) observed for the RG505 MS (Lyo MS CDP571-10). Indeed, the  $d(0.9)$  was  $145 \mu\text{m}$  vs.  $75 \mu\text{m}$  for the CDP571-loaded RG505 and RG755S MS, and  $134 \mu\text{m}$  vs.  $70 \mu\text{m}$  for the placebo RG505 and RG755S MS, respectively (Table 48).

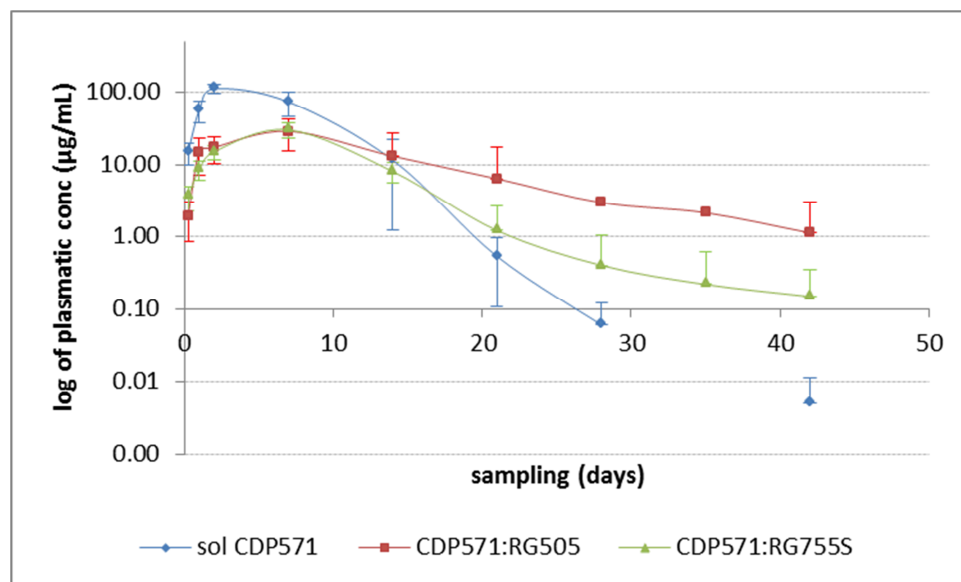


**Figure 79** Log of mean plasmatic CDP571 concentrations ( $\mu\text{g/mL}$ ) vs. time (days) after subcutaneous administration of the CDP571 solution (in blue), the MAb:RG505 MS (Lyo MS CDP571-10) (in red) and the MAb:RG755S MS (Lyo MS CDP571-3) (in green). (mean (s), n = 4)

The profile of the plasma CDP571 concentration, measured by ELISA, vs. time obtained from the *in vivo* SC study clearly showed that the MS were able to maintain a greater plasmatic level over 7 weeks compared to the solution (Figure 79). The feature of the plasma level profiles of the PLGA MS was an initial increase within 6 h to 1 week followed by a slow decrease to the lower limit set at 1 ng/mL, between 1 week and 6 weeks, regardless of the formulation (Figure 79). After subcutaneous administration of the CDP571 solution, the plasmatic concentration increased until it reached a maximal level after 48 h. After this point, the CDP571 plasmatic concentration decreased over time. When the CDP571 was administered from the MS formulations, the increase in the plasmatic concentration appeared to be slow and reached its maximum level after 1 week. In addition, the decrease in the plasmatic concentration appeared to be slow for the MS formulations in comparison to the solution formulation. The rat SC7 which received the RG505 formulation (Lyo MS CDP571-10) presented a good controlled release profile for up to 6 weeks (Table 46 and Table 47 in appendix). The residence time of the MAb administered in solution was relatively long, as expected by the data measured during the IV pK study (Table 44 and Table 45 in appendix). The intergroup variability was quite high especially in the group 2 (RG505 MS). It was then difficult to highlight a significant effect of the PLGA controlled-release formulations. The  $T_{1/2}$  calculated for the CDP571 solution and the CDP571-

loaded RG755S MS administered subcutaneously ( $63 \pm 21$  h vs.  $130 \pm 52$  h, respectively) appeared to be significantly different ( $p = 0.03$ , nonparametric multiple comparisons using the Wilcoxon each pair test). However, both the mean  $T_{1/2}$  calculated for the RG505 (166 h) and the RG755S (130 h) MS were higher than the one calculated for the solution (63 h).

The  $T_{max}$  measured after subcutaneous administration (48 h – 168 h) were higher than that after IV injection (15 min – 1 h) (Table 50 and Table 51 in appendix). The slow-release effect of the PLGA MS formulations was demonstrated. Indeed, it was shown that the  $T_{max}$  of the PLGA MS were higher (168 h) compared to that of the solution (48 h).

Both PLGA formulations were characterized by a similar  $C_{max}$  ( $29.0 \pm 13.4$  and  $30.3 \pm 6.9$   $\mu\text{g/mL}$  for the RG505 and the RG755S MS, respectively), which was lower than the  $C_{max}$  calculated for the CDP571 solution ( $112 \pm 14$   $\mu\text{g/mL}$ ) (Table 51 in appendix).

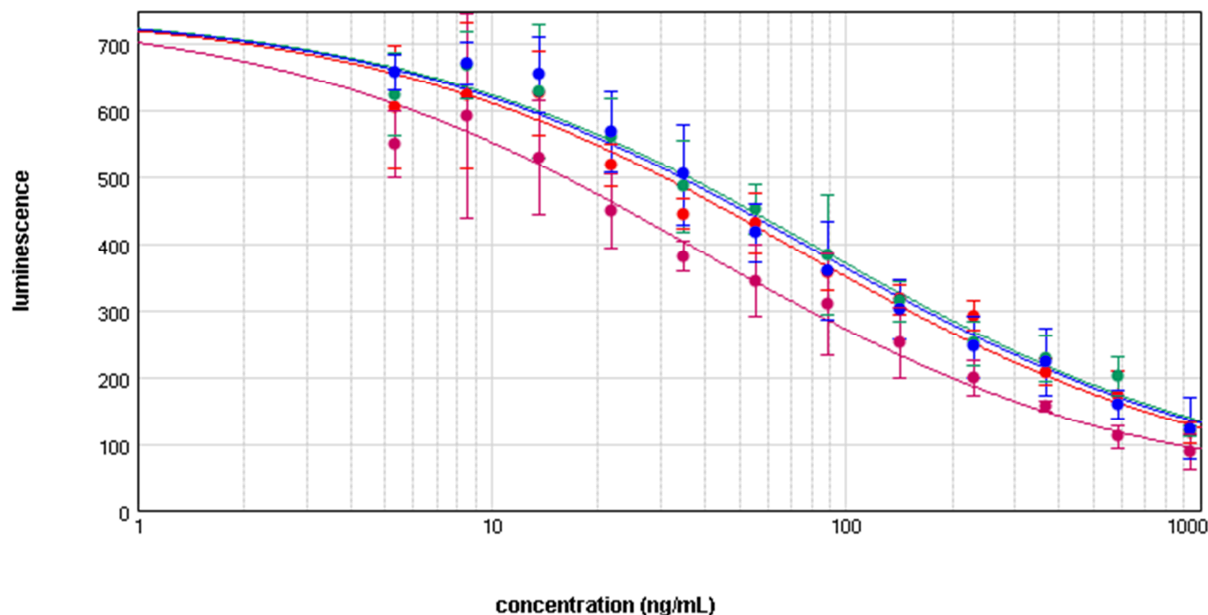
The estimated absolute bioavailability showed low values (20.9 %, 11.3 % and 8.4 % for the CDP571 solution, and the CDP571-loaded RG505 and RG755S MS, respectively) (Table 51 in appendix). The controlled-release formulations showed similar values but the variability of the RG755S was lower. The low bioavailability of the MAbs from the MS might be explained by an incomplete release of the antibody from the formulations [143]. The kinetics and pathways of degradation, protein binding and other clearance processes (e.g. lymphatic, re-adsorption to the polymer) might differ between drug released from MS injected intramuscularly and drug injected in solution [144]. Moreover, other factors independent of the system might affect the release of the drug and then the bioavailability such as the drug uptake into fatty acid and the fluid volume available at the site to dissolve the drug [82].

The major differences between the *in vivo* and *in vitro* release from the PLGA MS formulations are the lack of lag phase and the faster release kinetics for the apparent zero-order release phase of the *in vivo* data. The faster release *in vivo* might be a result of enhanced polymer degradation due to the presence of enzymes as well as other *in vivo* factors such as interstitial fluid volume and local pH. Accelerated enzymatic PLGA degradation *in vivo* was reported by other researchers [82, 145]. However, there was some controversy in the literature with respect to the role of enzymes in PLGA degradation [46].

The release kinetic from the RG505 formulation was faster both *in vivo* and *in vitro* compared to the RG755S formulation due to more rapid degradation of the higher lactide ratio PLGA.

## **2.2 Anti-TNF alpha activity evaluation**

The anti-TNF activity of the CDP571 was evaluated on the plasmatic samples withdrawn after 48 h and 1 week from administration of the group 1 (CDP571 solution), 2 (RG505 MS) and 3 (RG755S MS) formulations ([Table 11](#) in Material & Methods) using both the TNF-alpha cytotoxicity bioassay and the reporter gene bioassay. Both for the TNF-alpha cytotoxicity bioassay and for the reporter gene bioassay, the EC<sub>50</sub> values were calculated from the dose-response curves (absorbance / luminescence vs. concentration) (e.g. [Figure 80](#) ). These dose-response curves were constructed following serial dilutions of the plasmatic samples and the CDP571 reference standard and using the plasmatic concentrations measured by ELISA for the plasma samples. The EC<sub>50</sub> values were calculated using a 4-parameter curve fitting and compared to the standard solution stored at -80°C.



Curve Fit : 4-Parameter  $y = D + \frac{A - D}{1 + \left(\frac{x}{C}\right)^B}$

Plot Name	Sources	Estimated Rel. Pot.	Std. Error	Confidence Interval	EC50
● Ref.	( Ref CDP571: MeanVal... vs Concentr...	1.000	0.000	[1.000, 1.000]	74.04
● group 1 - 168 h	( Group1 -: MeanVal... vs Concentr...	0.854	0.090	[0.673, 1.035]	86.72
● group 2 - 168 h	( Group2 -: MeanVal... vs Concentr...	0.897	0.094	[0.707, 1.088]	82.50
● group 3 - 168 h	( Group3 -: MeanVal... vs Concentr...	1.906	0.202	[1.498, 2.313]	38.85

Global (PLA) Statistics

$R^2 = 0.982$

**Figure 80** Dose-response curves generated using the reporter gene bioassay for the MAb plasmatic samples 1 week after administration of the MAb solution (group 1 in green), the RG505 MS (group 2 in blue) and the RG755S MS (group 3 in pink) and for the standard reference (in red).

The EC<sub>50</sub> were calculated from the dose - response curves generated using the reporter gene bioassay for the MAb plasmatic samples 1 week after the SC administration of the different tested groups. The relative potencies were estimated based on the CDP571 reference standard. In regards to the calculated relative potencies (0.854 and 0.897 for the group 1 and the group 2 respectively, Figure 80), the groups 1 and 2 did not appear different than the reference in term of anti-TNF activity. For the group 3, the relative potency (1.906) was abnormally higher than that of the reference. It was explained by the high variability. Additional testing should be performed to confirm the data.

The means of EC<sub>50</sub> calculated from the dose-response curves generated using the cytotoxicity bioassay for the MAb plasmatic samples 48 h after administration of the MAb solution, the RG505 MS and the RG755S MS and for the standard reference (Ref.) were not significantly different from each other's (p = 0.17, oneway ANOVA; [Figure 81](#) ).

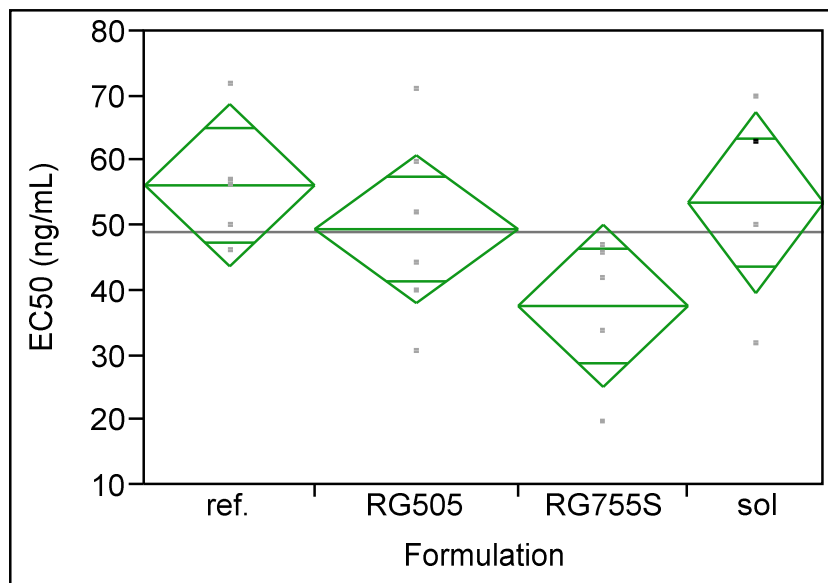


**Figure 81** TNF-alpha cytotoxicity bioassay – Oneway ANOVA of EC<sub>50</sub> (ng/mL) by formulation at 48 h time point; in green the mean diamonds (group mean and 95 % confidence interval) (n = min 4)

It was concluded that the MAb released from the MS preserved its bioactivity *in vivo*.

### 2.3 Histological studies

PLGA degradation could result in an inflammatory response, explained by the release of acidic oligomeric units in the immediate vicinity of the MS. Histological studies were performed to evaluate a possible inflammation effect at the injection site. Hematoxylin-eosin stains the nuclear material of cells in purple, while collagen of dermis is pink [82].

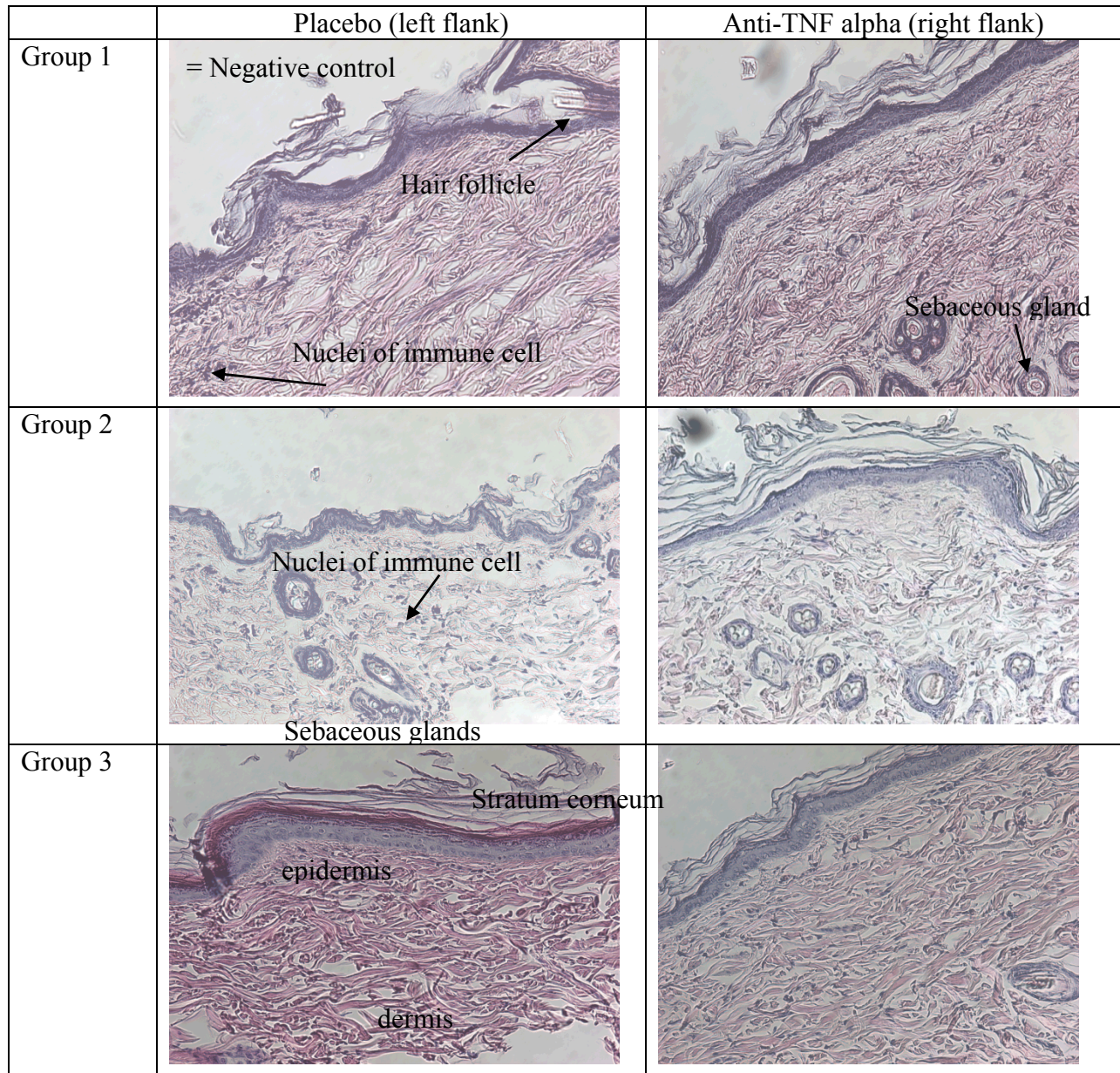


**Figure 82** Skin biopsies of rats from groups 1, 2 and 3 at the injection site (right and left flank) – histological examination using hematoxylin and eosin staining

After administration of either the polymeric MS (groups 2 and 3) or the biological compound (right flank), there was no evidence of massive leukocytes infiltration in the dermis surrounding the injection site. The number of immune cells did not seem to be affected, either by the administration of the polymeric MS (groups 2 and 3) or the control (group 1). The same profile was observed on both the treated and the control rats. It would have been interesting to add a positive control in this study. As an example, the histological examinations observed after injection of IL-12 or IL-23 were added to show the effect of inflammation and the inflammatory cellular infiltration [146].

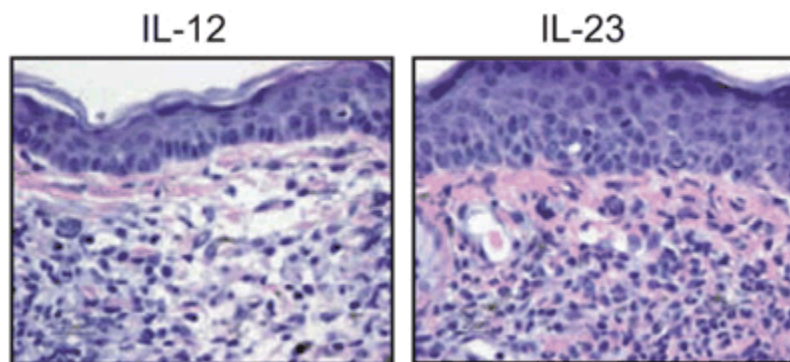


**Figure 83** Ears from C57Bl/6 mice (n = 5 for each group) were each injected intradermally very day with 500 ng of IL-12 or 500 ng of IL-23 in a total volume of 20  $\mu$ L. On day 6, ears were collected for staining with hematoxylin and eosin [146]

Moreover, there was no evidence of modification of the skin structure, e.g. the thickness of the epidermis was not altered (Figure 82). Macroscopically, no significant evidence of inflammation, such as redness, oedema or increased local heat, had been observed at the injection site on any of the tested rats, regardless of the administered formulation. It was therefore concluded in our study that the PLGA MS did not lead to an inflammatory response in the immediate vicinity of the MS.

### 3 CONCLUSION

During this SC pK study, it was demonstrated that MAb administration through polymeric MS effectively led to an *in vivo* sustained-release profile. Both the  $T_{max}$  and the  $T_{1/2}$  were increased and the  $C_{max}$  was decreased compared to the MAb administration in an aqueous solution. It was also confirmed that the MAb in the MS preserved its *in vivo* bioactivity. The low bioavailability of the MAb when SC administrated should be mentioned. During an upcoming *in vivo* study, the

complete release of the drug from the MS could be studied in order to understand this low value. A better understanding of the kinetics and pathways of degradation, protein binding and other clearance processes could also be interesting. Indeed, this can differ between drug released from MS and drug injected in solution. No sign of inflammation was observed at the injection site of the MS.

## GENERAL CONCLUSION AND PERSPECTIVES

This work aimed at building a drug delivery system able to enhance the stability and the residence time *in vivo* of MAbs delivered by the subcutaneous route. The microparticulate polymer-based formulations were selected as the preferred technical approach. As a reminder, the encapsulation method should maintain the native structure of the biological compound and so preserve its biological activity. Furthermore, the process should achieve sufficient drug loading (> 20 % w/w) into the MS to allow the administration of the therapeutic doses (> 100 mg/mL). The target release profile should reach a time greater than that observed with typical biological formulations in solution (> 1 month). Thus, the effects of peaks and valleys in plasma curves should be avoided *in vivo* by providing a continuous and regular supply of drug. Finally, the delivery system should be administered subcutaneously through accepted needles (> 22 G).

During the first part of the project which consisted to screen the encapsulation processes and optimize the related process parameters, a bovine polyclonal IgG was used as model for an economic point-of-view. Indeed, this material was cheaper and easily available compared to a MAb or a Fab' Ab. Different encapsulation methods such as the w/o/w and s/o/w methods were investigated. The encapsulation of Ab in solid state (s/o/w) was demonstrated to be more appropriate regarding stability and encapsulation efficiency. This method avoided the water / oil interfaces which could lead to aggregation and denaturation of the Ab.

DoEs were realized in order to define the critical process parameters during the production of both the SD Ab microparticles and the Ab-loaded PLGA MS.

The optimized spray-drying process, with the atomization air flow set at highest value (800 L/h), the inlet T° at 130°C and the liquid flow rate at 3 mL/min, allowed us to produce SD IgG microparticles characterized by a median diameter of 6 µm without loss of monomer (SEC). A further reduction of the particle size might be beneficial for the subsequent encapsulation into the polymeric MS. It should be mentioned that the HMWS starting level was very high. This may have masked possible degradation during the drying process.

During the DoE performed for the s/o/w process, the PLGA concentration appeared to be one of the most critical factors for encapsulating SD IgG inside PLGA MS. PLGA concentration effected the particle size distribution of the produced MS but also, the EE%, the release profile

and the stability of the IgG during both the encapsulation process and its release. Both the better EE% and IgG stability were explained by a faster precipitation of the polymer when the PLGA concentration was set at higher values (10 % w/v). Faster precipitation of the PLGA might be also related to the better encapsulation results measured with the EtAc than those observed with the MC. It should be interesting in the next step to study the effect of both the miscibility of the organic solvent (e.g. addition of ethanol as co-solvent) in the aqueous solution and the solubility of the polymer to see if the characteristics of the MS should still be improved.

Both the selected spray-drying and the *s/o/w* processes were applied to a monoclonal full-size anti-TNF alpha Ab.

An increase of the aggregation, especially at the sub-visible (DLS) and visible levels (turbidity,  $A_{350}$ ), was measured during the spray-drying process which was limited by the addition of the appropriate stabilizer. However, the binding capacity was maintained. A 50 mg/mL formulation containing trehalose at a 70:30 Ab : stabilizer ratio in 20 mM histidine pH 6.0 was preferred. It was assumed that the trehalose stabilized the MAb by water replacement; a protective layer was formed around the surface of the Ab.

The *s/o/w* method allowed us to produce appropriate MAb-loaded PLGA MS in terms of release profile and MAb stability. In order to guarantee maintenance of the MAb's activity, during both the encapsulation and the dissolution, the addition of a stabilizer such trehalose appeared to be crucial, as was the selection of the type of PLGA. Due to a slower degradation rate, the PLGA characterized by a higher Mw (e.g. RG505) or a higher percentage of lactide (e.g. RG755S) was preferred because they decreased both the release rate of the MAb from the MS and the level of LMWS appearing during the dissolution. E.g. it was demonstrated that the use of a PLGA characterized by a 75:25 lactide:glycolide ratio decreased the formation of LMWS during the dissolution, which led to preserving the MAb's activity throughout its release from the delivery system. The formation of LMWS was explained by the micro acidic environment induced by the degradation of the PLGA. The release profile was adjusted according to the type of polymer and its concentration. E.g. 10 % w/v RG755S allowed MAb MS with a release time of 6 weeks to be obtained.

During a stability study, it was demonstrated that the MAb-loaded PLGA MS were stable when stored at 5°C and that the selection of the appropriate type of PLGA was critical to assuring the

stability of the system. The better stability observed when using a PLGA characterized by a 75:25 lactide:glycolide ratio (e.g. RG755S) was attributed to its slower degradation rate. The temperature was a key parameter in terms of stability and particle size. Indeed, storage at temperatures higher than 5°C could lead to stability problems for the antibody, such as aggregation, fragmentation and loss of activity. The antibody release profile could be altered. In addition, higher temperatures led to modifications of the particle size and morphology of the MS. Some stability issues might be attributed to the presence of residual water and organic solvent, which exceeded the ICH recommendations (< 5000 ppm). Improvement of the drying step could lead to the system stabilizing.

A freeze-drying process was developed for the PLGA MS. It was demonstrated that the freeze-drying process led to improving the dispersion of the PLGA MS, resulting in better injectability compared to the MS produced with vacuum drying. Addition of stabilizer was needed to maintain the integrity of the PLGA MS during freeze drying in terms of particle size and MAb stability (SEC profile). E.g. trehalose, forming an amorphous matrix around the MS were preferred to mannitol, which could present crystallization and polymorphisms. The concentration of the hydrophilic stabilizer was fixed at 0.5 % w/v because higher concentration tended to increase the burst effect. The current freeze-drying process was not effective at reaching the ICH specification regarding residual solvent content. A longer secondary drying under vacuum could lead to improve this parameter. The decrease of the residual solvent content could also lead to a better stability over storage. The EtAc could be involved in the agglomeration issues observed during the stability study. It should be mentioned that the MS' suspension concentration, which is an important parameter, was not taken into account in this study.

Finally, a pharmacokinetic study was realized in rats with the two preferred MS formulations of anti-TNF alpha MAb and compared to a standard formulation solution. It was confirmed *in vivo* that the polymer MS presented a sustained release. Indeed, in comparison to the solution, the MS achieved lower  $C_{max}$  and higher  $T_{max}$ . The apparent half-life was higher. However, the low bioavailability of the MAb observed when SC administrated should be the subject of a further *in vivo* study. During an upcoming *in vivo* study, the complete release of the drug from the MS could be study to understand this low value. A better understanding of the kinetics and pathways of degradation, protein binding and other clearance processes could also be interesting. Indeed, this can differ between drug released from MS and drug injected in solution. The MS should be

recovered at the last time point in order to measure the residual content of the MAb inside the MS. A dosage and a characterization of the Ab present in the skin tissue could also help to understand the low bioavailability observed during this study. In parallel, a dissolution test in “parenteral lipid emulsion” could mimic the conditions of the sub-cutaneous tissue.

The selected process was applied with success to an anti-TNF alpha Fab’ Ab (data not shown). The produced MS presented properties equivalent to those obtained for the anti-TNF alpha full-length MAb. A pK study should be performed to compare the pK profiles of a Fab’, a PEGylated Fab’ and a full-size Ab administrated subcutaneously in solution or in polymeric MS. It might be demonstrated that the apparent half-live of a Fab’ could be increased either by PEGylation process or by encapsulation into polymeric MS. The controlled release formulations could be then a good alternative to the PEGylation of Fab’ which is an expensive process. Compared to the PEGylation, the polymeric formulations might offer the advantage to fine-tune the release profile.

However, in the present work, it was not possible to reach the target drug loading (> 20 % w/w). The optimization of both the formulation and the encapsulation process allowed a maximum of 13 % w/w MAb-loaded MS to be produced. Further development should be done to improve this parameter. The addition of lipids, such as phospholipids, in combination with the current polymers should help by increasing the MAb’s affinity for the polymer matrix. Another technical approach could be the extrusion process, which is less limited in terms of loading and which does not require the use of solvents. Finally, the dispersion of the MAb into the polymer liquefied in a supercritical fluid (CO<sub>2</sub>) could also be a good alternative as the use of solvent is not required for this.

In conclusion, the application of the concept of entrapment into a polymer matrix for stabilization and sustained release of biological compounds was demonstrated through this work. Indeed, anti-TNF alpha full-length antibody MS were developed and showed increased plasmatic residence time without apparent loss of activity. However, as mentioned before, further improvements are needed, especially regarding the drug loading content to be able to reach the therapeutic doses of the Abs.

---

**REFERENCES**

- [1] S. Kobsa and all, "Bioengineering approaches to controlled protein delivery," *Pediatric Research*, vol. 63 (5), 2008.
- [2] J. Beals and all., "Enhancing exposure of protein therapeutics," *Drug Discovery Today*, vol. 3 (1), 2006.
- [3] H. Luessen and E. van Winden, "Particulate and hydrogel-based protein delivery systems for parenteral administration," in *Protein Pharmaceuticals*, Aulendorf, Editio Cantor Verlag, 2010, pp. 369-392.
- [4] L. Jorgensen, E. Moeller, M. van de Weert, H. Nielsen and S. Frokjaer, "Preparing and evaluating delivery systems for proteins," *Eur. J. Pharm. Sciences*, vol. 29 (3), pp. 174-182, 2006.
- [5] "Therapeutic monoclonal antibodies approved or in review in the European Union or United State," 28 July 2014. [Online]. Available: [http://www.antibodysociety.org/news/approved\\_mabs.php](http://www.antibodysociety.org/news/approved_mabs.php).
- [6] T. T. Hansel, H. Kropshofer, T. Singer, J. A. Mitchell et A. J. T. George, «The safety and side effects of,» *Nature reviews / Drug Discovery*, vol. 9, pp. 325-338, 2010.
- [7] E. D. Lobo, R. J. Hansen and J. P. Balthasar, "Antibody Pharmacokinetics and Pharmacodynamics," *J. Pharm. Sci.*, vol. 93 (11), 2004.
- [8] Wei Wang, Staich Singh, David L. Zeng, Kevi King and Sandeep Nema, "Antibody Structure, Instability and Formulation," *J. Pharm. Sci.*, vol. 96 (1), January 2007.
- [9] A. Daugherty and J. Randall , "Formulation and delivery issues for monoclonal antibody therapeutics," *Adv. Drug Delivery Rev.*, vol. 58, pp. 686-706, 2006.
- [10] A. L. Nelson, «Antibody fragments: Hope and hype,» chez *mAbs 2:1*, 2010 Landes Bioscience, 2010, pp. 77-83.
- [11] S. Jevševar , M. Kusterle et M. Kenig , «PEGylation of antibody fragments for half-life extension,» *Methods Mol Biol.* , vol. 901, pp. 233-246, 2012.
- [12] P. Chames, M. Van Regenmortel, E. Weiss et D. Baty, «Therapeutic antibodies: successes, limitations and hopes for the future,» *Br J Pharmacol*, vol. 157(2), pp. 220-233, 2009.
- [13] T. Kissel, S. Maretschek, C. Packhauser, J. Schnieders and N. Seidel, "Microencapsulation Techniques for Parenteral Depot Systems and Their Application in the Pharmaceutical Industry," in *Microencapsulation, Methods and Industrial Applications, Second Edition*, vol. 99–122, Edited by Simon Benita, Informa Healthcare, 2005.
- [14] Jain R.A., "The manufacturing techniques of various drug loaded biodegradable poly(lactide-co-glycolide) (PLGA) devices," *Biomaterials*, vol. 21, pp. 2475-2490, 2000.
- [15] T. P. W. M. e. a. Janeway CA Jr, *Immunobiology: The Immune System in Health and Disease*. 5th edition, New York: Garland Science, 2001.
- [16] A. McPherson and L. Harris, *Nature*, vol. 360, pp. 369-372, 1992.
- [17] I. Roitt, J. Brostoff and D. Male, *Immunologie - 4ème édition*, Bruxelles: De Boeck -

- Université, 1997.
- [18] J. Bradley , «TNF-mediated inflammatory disease,» *J Pathol.*, vol. 214 (2), p. 149–160, 2008.
- [19] M. Capelle, R. Gurny and A. Tudor, "High throughput screening of protein formulation stability: Practical considerations," *Eur. J. Pharm. Biopharm.*, vol. 65, pp. 131-148, 2007.
- [20] C. Kirchhoff, "Introduction to protein chemistry," in *Protein Pharmaceuticals*, H. Mahler, G. Borchard and H. Luessen, Eds., Aulendorf, Cantor Verlag, 2010, pp. 18-43.
- [21] H.-C. Mahler, W. Friess, U. Grauschopf and S. Kiese, "Protein aggregation: Pathways, induction factors and analysis," *J. Pharm. Sci.*, vol. 98 (9), 2009.
- [22] M. Cromwell, "Protein aggregation," in *Protein Pharmaceuticals*, H. Mahler, G. Borchard and H. Luessen, Eds., Aulendorf, Cantor Verlag, 2010, pp. 111-141.
- [23] J. Laurence and R. Middaugh, "Fundamental structures and behaviors of proteins," in *Aggregation of Therapeutic Proteins*, W. Wang and C. Roberts, Eds., New Jersey, Wiley, 2010, pp. 1-62.
- [24] W. Wang, "Protein aggregation and its inhibition in biopharmaceutics," *Int. J. Pharm.*, vol. 289 (1), p. 1–30, 2005.
- [25] U. Lashmar UT, M. Vanderburgh M and S. Little SJ, "Bulk freeze–thawing of macromolecules. Effects of cryoconcentration on their formulation and stability," *BioProcess International*, pp. 44-54, 2007.
- [26] A. Minton , "The influence of macromolecular crowding and macromolecular confinement on biochemical reactions in physiological media," *J. Biol. Chem.*, vol. 276 (14), p. 10577–10580, 2001.
- [27] Yaqiang Wang , Mohona Sarkar , Austin E. Smith , Alexander S. Krois and Gary J. Pielak, "Macromolecular Crowding and Protein Stability," *J. Am. Chem. Soc.*, vol. 134 (40), p. 16614–16618, 2012.
- [28] C. Mattos et D. Ringe, «Proteins in organic solvents,» *Current Opinion in Structural Biology* , vol. 11, p. 761–764, 2001.
- [29] M. Houchin and E. Topp, "Chemical degradation of peptides and proteins in PLGA: a review of reactions and mechanisms," *J. Pharm. Sci.*, vol. 97 (7), 2008.
- [30] W. Y. K. Chana, T. D. Chana and P. B. O'Connorb, "Electron Transfer Dissociation with Supplemental Activation to Differentiate Aspartic and Isoaspartic Residues in Doubly Charged Peptide Cations," *J. Am. Soc. Mass. Spectrom.*, vol. 21 (6), pp. 1012-1015, 2010.
- [31] M. Yuh-Fun and S. P. Sellers, "Solid-State protein formulation methodologies, stability and excipient effects," *Therapeutic proteins methods in molecular biology*, vol. 308, pp. 265-285, 2005.
- [32] H.-C. Mahler and A. Mekking, "Formulation development of therapeutic proteins," in *Protein Pharmaceuticals*, Aulendorf, Cantor Verlag, 2010, pp. 144-161.
- [33] W. Wang, "Instability, stabilization, and formulation of liquid protein," *Int. J. Pharm.*, vol. 185, pp. 129-188, 1999.
- [34] D. Parkins and U. Lashmar, "The formulation of biopharmaceutical products," *Pharm. Sc. Techn. Today*, vol. 3 (4), pp. 129-137, 2000.
- [35] S. Ohtake, Y. Kita and T. Arakawa, "Interactions of the formulation excipients with

- proteins in solution and in the dried state," *Adv. Drug Delivery Reviews*, vol. 63, pp. 1053-1073, 2011.
- [36] T. Kamerzell, R. Esfandiary, S. Joshi, R. Middaugh et D. Volkin, «Protein-excipient interactions: mechanisms and biophysical characterization applied to protein formulation development,» *Adv. Drug Delivery Reviews*, vol. 63, pp. 1118-1159, 2011.
- [37] T. Arakawa and S. N. Timasheff, "Stabilization of protein structure by sugars," *Biochemistry*, vol. 21 (25), pp. 6536-6544, 1982.
- [38] M. Wiggenhorn, I. Presser and G. Winter, "Drying methods for protein formulations," in *Protein Pharmaceuticals*, Aulendorf, Cantor Verlag, 2010, pp. 162-191.
- [39] A. Saez, M. Guzman, J. Molpeceres and M. Aberturas, "Freeze-drying of polycaprolactone and poly(D,L-lactic-glycolic) nanoparticles induce minor particle size changes affecting the oral pharmacokinetics of loaded drugs," *Eur. J. Pharm. Biopharm.*, vol. 50, pp. 379-387, 2000.
- [40] A. Almeida and all., "Solid lipid nanoparticles as a drug delivery system for peptides and proteins," *Adv. Drug Del. reviews*, vol. 59, pp. 478-490, 2007.
- [41] V. Sinha et A. Trehan, «Biodegradable microspheres for protein delivery,» *J Control Release*, vol. 90 (3), pp. 261-80, 2003.
- [42] R. Mudargi, V. Ramesh Babu, Vidhya Rangaswany, Pradip Patel and M. A. Tejjraj, "Nano/micro technologies for delivery macromolecular therapeutics using poly(D,L-lactide-co-glycolide) and its derivatives," *J. Controlled Release*, vol. 125, pp. 193-209, 2008.
- [43] M. temtem et J. L. Santos, «Controlled release technology: Sphere of influence,» May 2012. [En ligne]. Available: [http://www.hovione.com/h\\_press/press\\_rel/201205\\_Sphere\\_of\\_Influence\\_PMPS.pdf](http://www.hovione.com/h_press/press_rel/201205_Sphere_of_Influence_PMPS.pdf). [Accès le 26 August 2014].
- [44] H. Agraval, N. Thacku et A. Misra, «Parenteral delivery of peptides and proteins,» chez *Challenges in delivery of therapeutic genomics and proteomics*, Elsevier, 2011, p. 557.
- [45] M. Van de Weert, W. Hennink and W. Jiskoot, "Protein Instability in Poly(Lactic-co-Glycolic Acid) Microparticles," *Pharm. Res.*, vol. 17 (10), pp. 1159-1167, 2000.
- [46] F. Alexis, "Factors affecting the degradation and drug-release mechanism of poly(lactic acid) and poly(lactic acid)-co-(glycolic acid)," *Polym. Int.*, vol. 54, pp. 36-46, 2005.
- [47] A. Shenderova, T. Burke and S. Schwendeman, "The acidic microclimate in poly(lactide-co-glycolide) micropsheres stabilizes camptothecins," *Pham. Res.*, vol. 16 (2), 1999.
- [48] M. Houchin, S. Neuenswander and E. Topp, "Effect of excipients on PLGA film degradation and the stability of an incorporated peptide," *J. Control. Release*, vol. 117, pp. 413-420, 2007.
- [49] K. Fu, D. Pack, A. Klibanov and R. Langer, "Visual Evidence of Acidic Environment Within Degrading Poly(lactic-co-glycolic acid) (PLGA) Microspheres," *Pharm. Res.*, vol. 17 (1), 2000.
- [50] S. Stolnik and all, "Formulations for delivery of therapeutic proteins," *Biotechnolo. Lett*, vol. 31, pp. 1-11, 2009.
- [51] K. Tae-Kyoung and D. Burgess, "Pharmacokinetic characterization of <sup>14</sup>C-vascular endothelial growth factor controlled release microspheres using a rat model," *J. Pharm.*

- Pharmacol.*, vol. 54, pp. 897-905, 2002.
- [52] H. Tamber, P. Johansen, H. Merkle and B. Gander, "Formulation aspects of biodegradable polymeric microspheres for antigen delivery," *Adv. Drug Deliv. Rev.*, vol. 57, pp. 357-376, 2005.
- [53] E. Schacht and all, "Polyacetal and poly(ortho ester)-poly(ethylene glycol) graft copolymer thermogels: Preparation, hydrolysis and FITC-BSA release studies," *J. Controlled Release*, vol. 116, pp. 219-225, 2006.
- [54] M. Hamidi and all., "Hydrogel nanoparticles in drug delivery," *Adv. Drug Del. Reviews*, vol. 60, pp. 1638-1649, 2008.
- [55] T. R. Hoare et D. S. Kohane, «Hydrogels in drug delivery: Progress and challenges,» *Polymer*, vol. 49, pp. 1993-2007, 2008.
- [56] A. Vashist, A. Vashist, Y. K. Gupta et S. Ahmad, «Recent advances in hydrogel based drug delivery,» *J. Mater. Chem. B*, vol. 2, pp. 147-166, 2014.
- [57] "Polyscitech," Akina, [Online]. Available: <http://polyscitech.com/PLGA/PLGA.php>. [Accessed 15 January 2014].
- [58] S. Schwendeman, M. Cardamone, H. Bvandon, A. Klivanov and R. Langer, "Stability of proteins and their delivery from biodegradable polymer microspheres," New York, S. Cohen and H. Bernstein, 1996, pp. 1-49.
- [59] S. Kleinhans, C. Arpagaus and G. Schönenberger, "Spray-drying," in *The laboratory Assistant*, Switzerland, Büchi Labortechnik AG, 2007, pp. 68-87.
- [60] Y. Mingli, K. Sungwon and P. Kinam, "Issues in long-term protein delivery using biodegradable microparticles," *J. Control. Release*, vol. 146, pp. 241-260, 2010.
- [61] S. Freitas, H. P. Merkle and B. Gander, "Microencapsulation by solvent extraction/evaporation: reviewing the state of the art of microsphere preparation process technology," *J. Controlled Release*, vol. 102 (2), p. 313-332, 2005.
- [62] T. Morita, Y. Sakamura, Y. Horikiri, S. Takehiko and H. Yoshino, "Protein encapsulation into biodegradable microspheres by a novel S/O/W emulsion method using poly(ethylene glycol) as a protein micronization adjuvant," *J. Controlled Release*, vol. 69, pp. 435-444, 2000.
- [63] J. Wang, K. Ming Chua and C. Wang, "Stabilization and encapsulation of human immunoglobulin G into biodegradable microspheres," *J. Colloid Interface Sci.*, vol. 271, pp. 92-101, 2004.
- [64] S. Marquette, C. Peerboom, A. Yates, L. Denis, J. Goole and K. Amighi, "Encapsulation of IgG by s/o/w: effects of process parameters on microspheres properties," *Eur. J. Pharm. Biopharm.*, vol. doi: <http://dx.doi.org/10.1016/j.ejpb.2013.10.013>, 2013.
- [65] P. Biotechnology, "Pierce™ BCA Protein Assay Kit," [Online]. Available: <http://www.piercenet.com/instructions/2161296.pdf>. [Accessed 05 12 2013].
- [66] University of California, "Dynamic Light Scattering," UC Davis GeoWiki, [Online]. Available: [http://chemwiki.ucdavis.edu/Analytical\\_Chemistry/Instrumental\\_Analysis/Microscopy/Dynamic\\_Light\\_Scattering](http://chemwiki.ucdavis.edu/Analytical_Chemistry/Instrumental_Analysis/Microscopy/Dynamic_Light_Scattering). [Accessed 6 March 2014].
- [67] A. Giteau, V. Tran, O. Thomas, X. Garric, J. Coudane, S. Marchal, I. Chourpa, J.-P. Benoît, C. Montero-Menei and M.-C. Venier-Julienne, "Effect of various additives and

- polymers on lysozyme release from PLGA microspheres prepared by an s/o/w emulsion technique," *Eur. J. Pharm. Biopharm.*, vol. 75, pp. 128-136, 2010.
- [68] "Distance formula," [Online]. Available: <http://www.cut-the-knot.org/pythagoras/DistanceFormula.shtml>. [Accessed March 2014].
- [69] P. Qi, D. Volkin, H. Zhao, M. Nedved, R. Hughes, R. Bass, S. Yi, M. Panek, D. Wang, P. Dalmonte and M. Bond, "Characterization of the photodegradation of a human IgG1 monoclonal antibody formulated as a high-concentration liquid dosage form," *J. Pharm. Sci.*, vol. 98 (9), September 2009.
- [70] C. Lallemand, N. Kavrochorianou, C. Steenholdt, K. Bendtzen, M. Ainsworth, J.-F. Meritet, B. Blanchard, P. Lebon, P. Taylor, P. Charles, S. Alzabin et M. Tovey, «Reporter gene assay for the quantification of the activity and neutralizing antibody response to TNF alpha antagonists,» *J. Immunological Methods*, vol. 373, pp. 229-239, 2011.
- [71] Food and Drug Administration (FDA), "Guidance for Industry: Dissolution Testing of Immediate Release Solid Oral Dosage Forms," August 1997. [Online]. Available: <http://www.fda.gov/downloads/drugs/guidancecomplianceregulatoryinformation/guidances/ucm070237.pdf>.
- [72] P. Costa and J. Lobo, "Modeling and comparison of dissolution profiles," *Eur. J. Pharm. Sc.*, vol. 13, pp. 123-133, 2001.
- [73] S. Dash, P. Murthy, L. Nath and P. Chowdhury, "Kinetic modeling on drug release from controlled drug delivery systems," *Acta Poloniae Pharmaceutica - Drug research*, vol. 67, no. 3, pp. 217-223, 2010.
- [74] T. Ehtezazi, C. Washington and C. Melia, "Determination of the internal morphology of poly (D, L-lactide) microspheres using stereological methods," *J. Controlled Release*, vol. 57, pp. 301-314, 1999.
- [75] S. Mao, J. Xu, C. Cai, O. Germershaus, A. Schapper and T. Kissel, "Effect of w/w process parameters on morphology and burst release of FITC-dextran loaded PLGA microspheres," *Int. J. Pharm.*, vol. 334, pp. 137-148, 2007.
- [76] G. Höhne, W. Hemminger and H. -J. Flammersheim, *Differential scanning calorimetry*, Berlin: Springer, 2003.
- [77] "Differential scanning calorimetry (DSC)," PerkinElmer, 2013.
- [78] L. Al Hausley, M. Bozinger, C. Bordes, J. Gauvrit and S. Briançon, "Improvement of bovine serum albumin microencapsulation process by screening design," *Int. J. Pharm.*, vol. 344, pp. 16-25, 2007.
- [79] T. Feczko, J. Toth, G. Dosa and J. Gyenis, "Influence of process conditions on the mean size of PLGA nanoparticles," *Chem. Eng. Process.*, vol. 50, pp. 846-853, 2011.
- [80] W. D. A. a. S. K. Humphrey, "VMD - Visual Molecular Dynamics," *J. Molec. Graphics*, vol. 14, pp. 33-38, 1996.
- [81] C. E. Ophardt, "Virtual ChemBook," Elmhurst College, 2003. [Online]. Available: <http://www.elmhurst.edu/~chm/vchembook/567tertprotein.html>. [Accessed 12 November 2013].
- [82] B. Zolnik and D. Burgess, "Evaluation of in vivo-in vitro release of dexamethasone from PLGA microspheres," *J. Control Release*, vol. 127, pp. 137-145, 2008.
- [83] S. Sejin, R. L. Woo, K. J. Yoon, H. K. Myung, S. K. Yong and D. P. Ki, "Optimized

- stability retention of a monoclonal antibody in the PLGA nanoparticles," *Int. J. Pharm.*, vol. 368, pp. 178-185, 2009.
- [84] F. Lagarce, E. Garcion, N. Faisant, O. Thomas, P. Kanaujia, P. Menei and J. Benoit, "Development and characterization of interleukin-18-loaded biodegradable microspheres," *Int. J. Pharm.*, vol. 314, pp. 179-188, 2006.
- [85] I. Castellanos, K. Carrasquillo, J. López, M. Alvarez and K. Griebenow, "Encapsulation of bovine serum albumin in poly(lactide-co-glycolide) microspheres by the solid-in-oil-in-water technique," *J. Pharm. Pharmacol.*, vol. 53(2), pp. 167-78, 2001.
- [86] F. Quaglia, G. De Rosa, E. Granata, F. Ungaro, E. Fattal and M. Immacolata La Rotonda, "Feeding liquid, non-ionic surfactant and cyclodextrin affect the properties of insulin-loaded poly(lactide-co-glycolide) microspheres prepared by spray-drying," *J. Control Release*, pp. 267-278, 2003.
- [87] Y. Maa, H. Costantino, P. Nguyen et C. Hsu, «The effect of operating and formulation variables on the morphology of spray-dried protein particles,» *Pharm Dev Technol*, vol. 2 (3), pp. 213-23, 1997.
- [88] S. Schüle, T. Schulz-Fademrecht, P. Garidel, K. Bechtold-Peters and W. Fries, "Stabilization of IgG1 in spray-dried powders for inhalation," *Eur. J. Pharm. Biopharm.*, vol. 69, pp. 793-807, 2008.
- [89] K. Prinn, H. Costantino et M. Tracy, «Statistical modeling of protein spray-drying at the lab scale,» *AAPS PharmSciTech*, vol. 3 (1), p. article 4, 2002 3.
- [90] S. Schüle, W. Friesb, K. Bechtol-Peters et P. Gabriele, «Conformational analysis of protein secondary structure during spray-drying of antibody/mannitol formulations,» *Eur. J. Pharm. Biopharm.*, vol. 65, pp. 1-9, 2007.
- [91] M. Maury and all, "Spray-drying of proteins: effects of sorbitol and trehalose on aggregation and FT-IR amide I spectrum of an immunoglobulin G," *Eur. J. Pharm. Biopharm.*, pp. 251-261, 2005.
- [92] M. Li, O. Rouaud and D. Poncelet, "Microencapsulation by solvent evaporation: state of the art for process engineering approaches," *Int. J. Pharm.*, vol. 363, pp. 26-39, 2008.
- [93] Z. Rahman, A. Zidan, M. Habib and M. Khan, "Understanding the quality of protein loaded PLGA nanoparticles variability by Plackette-Burman design," *Int. J. Pharm.*, vol. 389, pp. 186-194, 2012.
- [94] Yang Yi-Yan, Tai-Shung Chung and Ngee Ping Ng, "Morphology, drug distribution, and in vitro release profiles of biodegradable polymeric microspheres containing protein fabricated by double-emulsion solvent extraction/evaporation method," *Biomaterials*, vol. 22, pp. 231-241, 2001.
- [95] T. Feczko, J. Toth and J. Gyenis, "Comparison of the preparation of PLGA-BSA nano- and microparticles by PVA, poloxamer and PVP," *Colloids and Surfaces A: Physicochem. Eng. Aspects*, vol. 319, pp. 188-195, 2008.
- [96] Li Wen-I, K. W. Anderson, C. Mehta Rahul and P. Deluca, "Prediction of solvent removal profile and effect on properties for peptide-loaded PLGA microspheres prepared by solvent extraction/evaporation method," *J. Controlled Release*, vol. 37, pp. 199-214, 1995.
- [97] H. Sah, "Microencapsulation techniques using ethyl acetate as a dispersed solvent: effects

- of its extraction rate on the characteristics of PLGA microspheres," *J. Controlled Release*, vol. 47, pp. 233-245, 1997.
- [98] T. Feckó, J. Tóth, G. Dósa and J. Gyenis, "Optimization of protein encapsulation in PLGA nanoparticles," *Chem. Eng. Process.*, vol. 50, pp. 757-765, 2011.
- [99] R. Ghaderi and J. Carfors, "Biological activity of lysozyme after entrapment in poly(D, L-lactide-co-glycolide)-microspheres," *Pharm. Res.*, vol. 14 (11), 1997.
- [100] N. Venkata and N. Jyothi, "Microencapsulation techniques, factors influencing encapsulation efficiency: a review," *The internet journal of nanotechnology*, vol. 3 (1), 2009.
- [101] N. Jyothi, M. Prasanna, S. Prabha, S. Ramaiah, G. Srawan and S. Sakarkar, "Microencapsulation techniques, factors influencing encapsulation efficiency," *The internet journal of nanotechnology*, vol. 3 (1), 2009.
- [102] Y. Yang, T. Chung, X. Bai and W. Chan, "Effect of preparation conditions on morphology and release profiles of biodegradable polymeric microspheres containing protein fabricated by double-emulsion method," *Chem. Eng. Sci.*, vol. 55, pp. 2223-2236, 2000.
- [103] B. Gander, P. Johansen, H. Nam-Trân and H. Merkle, "Thermodynamic approach of protein microencapsulation into poly(D,L)lactide) by spray-drying," *Int. J. Pharm.*, vol. 129, pp. 51-61, 1996.
- [104] X. Luan, M. Skupin, J. Siepmann and R. Bodmeier, "Key parameters affecting the initial release (burst) and encapsulation efficiency of peptide-containing poly(lactide-co-glycolide) microparticles," *Int. J. Pharm.*, vol. 324, pp. 168-175, 2006.
- [105] A. Giteau, M.-C. Venier-Julienne, A. Aubert-Pouëssel and J.-P. Benoît, "How to achieve sustained and complete protein release from PLGA-based microparticles?," *Int. J. Pharm.*, vol. 350, pp. 14-26, 2008.
- [106] U. Bilati, E. Alleman and E. Doelker, "Strategic approaches for overcoming peptide and protein instability within biodegradable nano- and microparticles," *Eur. J. Pharm. Biopharm.*, 59, pp. 375-388, 2005.
- [107] N. Kumar Jain et I. Roy, «Effect of trehalose on protein structure, *Protein Sci.* Jan 2009; 18(1): 24–36,» *Protein Sci. Jan 2009*, vol. 18 (1), p. 24–36, 2009.
- [108] P. Johansen, Y. Men, R. Audran, G. Corradin, H. Merkle and B. Gander, "Improving stability and release kinetics of microencapsulated tetanus toxoid by co-encapsulation of additives," *Pharm. Res.*, vol. 15 (7), 1998.
- [109] C. Stureson and J. Carlfors, "Incorporation of protein in PLG-microspheres with retention of bioactivity," *J. Controlled Release*, vol. 67, pp. 171-178, 2000.
- [110] J. L. Cleland and A. J. Jones, "Stable formulations of recombinant human growth hormone and interferon for microencapsulation in biodegradable microspheres," *Pharm. Res.*, vol. 13, no. 10, 1996.
- [111] B. Zolnik and D. Burgess, "Effect of acidic pH on PLGA microsphere degradation and release," *J. Controlled Release*, vol. 122 (3), pp. 338-344, 2007.
- [112] J. Buskea, C. König, S. Bassarabb, A. Lamprecht, S. Mühlau et K. Wagner, «Influence of PEG in PEG–PLGA microspheres on particle properties and protein release,» *Eur. J. Pharm. Biopharm.*, vol. 81, p. 57–63, 2012.

- [113] G. Zhu, S. Mallery and S. Schwendeman, "Stabilization of Proteins encapsulated in injectable poly(lactide-co-glycolide)," *Nature Biotechnology*, vol. 18, 2000.
- [114] G. Zhu and S. Schwendeman, "Stabilization of Proteins Encapsulated in Cylindrical Poly(lactide-co-glycolide) Implants: Mechanism of Stabilization by Basic Additives," *Pharm. Res.*, vol. 17 (3), 2000.
- [115] M. Ara, M. Watanabe and Y. Imai, "Effect of blending calcium compounds on hydrolytic degradation of poly(DL-lactic acid-co-glycolic acid)," *Biomaterials*, vol. 23, pp. 2479-2483, 2002.
- [116] W. Abdelwahed, G. Degobert, S. Stainmesse and H. Fessi, "Freeze-drying of nanoparticles: Formulation, process and storage considerations," *Adv. Drug Delivery Rev.*, vol. 58, pp. 1688-1713, 2006.
- [117] S. Schaffazick, A. Pohlmann, T. Dalla-Costa and S. Guterres, "Freeze-drying polymeric colloidal suspensions: nanocapsules, nanospheres and nanodispersion. A comparative study," *Eur. J. Pharm. Biopharm.*, vol. 56, pp. 501-505, 2003.
- [118] S. de Chasteigner, G. Cavé, H. Fessi, J.-P. Devissaguet and F. Puisieux, "Freeze-drying of itraconazole-loaded nanosphere suspensions: a feasibility study," *Drug Develop. Res.*, vol. 38, pp. 116-124, 1996.
- [119] M. Lane, F. Brennan and O. Corrigan, "Influence of post-emulsification drying processes on the microencapsulation of human serum albumin," *Int. J. Pharm.*, vol. 307, pp. 16-22, 2006.
- [120] M. Chacon, J. Molpeceres, M. Guzman and M. Aberturas, "Stability and freeze-drying of cyclosporine loaded poly(D,L lactide-glycolide) carriers," *Eur. J. Pharm. Biopharm.*, vol. 8, pp. 99-107, 1999.
- [121] F. Franks, "Freeze-drying of bioproducts: putting principles into practice," *Eur. J. Pharm. Biopharm.*, vol. 45, pp. 221-229, 1998.
- [122] M. Anhorn, H.-C. Mahler and K. Langer, "Freeze drying of human serum albumin (HSA) nanoparticles," *Int. J. Pharm.*, vol. 363, pp. 162-169, 2008.
- [123] T. H. Kim and T. G. Park, "Critical effect of freezing/freeze-drying on sustained release of FITC-dextran encapsulated within PLGA microspheres," *Int. J. Pharm.*, vol. 271, pp. 207-214, 2004.
- [124] Wikipedia, "Ethyl acetate," 11 10 2013. [Online]. Available: [http://en.wikipedia.org/wiki/Ethyl\\_acetate](http://en.wikipedia.org/wiki/Ethyl_acetate).
- [125] S. TORRADO et S. TORRADO, «Characterization of Physical State of Mannitol after Freeze-Drying: Effect of Acetylsalicylic Acid as a Second Crystalline Cosolute,» *Chem. Pharm. Bull.*, vol. 50 (5), pp. 567-570, 2002.
- [126] A. Burger, J.-O. Henck, S. Hetz, J. Rollinger et A. Weissnicht, «Energy / Temperature diagram and compression behavior of the polymorphs of D/mannitol,» *J. Pharm. Sciences*, vol. 89 (4), pp. 457-468, 2000.
- [127] A. Simperler, A. Kornherr, R. Chopra, A. Bonnet, W. Jones, S. Motherwell and G. Zifferer, "Glass Transition Temperature of Glucose, Sucrose, and Trehalose: An Experimental and in," *J. Phys. Chem.*, vol. 110, pp. 19678-19684, 2006.
- [128] M. Holzer, V. Vogel, W. Mäntele, D. Schwartz, D. Haase and K. Langer, "Physico-chemical characterization of PLGA nanoparticles after freeze-drying and storage," *Eur. J.*

- Pharm. Biopharm.*, vol. 72, pp. 428-437, 2009.
- [129] S. Bozdag, K. Dillen, J. Vandervoort and A. Ludwig, "The effect of freeze-drying with different cryoprotectants and gamma-irradiation sterilization on the characteristics of ciprofloxacin HCl-loaded poly(D,L-lactide-glycolide) nanoparticles," *J. Pharm. Pharmacol.*, vol. 57, pp. 699-707, 2005.
- [130] Food and Drug Administration (FDA), "Guideline for the determination of residual moisture in dried biological products," 1990. [Online]. Available: <http://www.fda.gov/ohrms/dockets/dockets/05d0047/05d-0047-bkg0001-Tab-11.pdf>. [Accessed April 2014].
- [131] E. M. Agency, "ICH Topics Q3C (R4) - Impurities: guideline for residual solvents," February 2009. [Online]. Available: <http://www.ema.europa.eu>.
- [132] L. Rey and J. May, *Freeze-drying/Lyophilization of pharmaceutical and biological products*, Informa Healthcare, 2010.
- [133] S. Marquette, C. Peerboom, A. Yates, L. Denis, I. Langer, K. Amighi et J. Goole, «Stability study of full-length antibody (anti-TNF alpha) loaded PLGA microspheres,» *Int J Pharm.*, Vols. %1 sur %2470 (1-2), pp. 41-50, 2014.
- [134] B. Sayin and S. Calis, "Influence of accelerated storage conditions on the stability of vancomycin-loaded poly(D,L-lactide-co-glycolide) microspheres," *FABAD J. Pharm. Sci.*, vol. 29, pp. 111-116, 2004.
- [135] S. De and D. Robinson, "Particle size and temperature effect on the physical stability of PLGA nanospheres and microspheres containing bodipy," *AAPS Pharm.Sci.Tech.*, vol. 5 (4), 2004.
- [136] S. Puthli and P. Vavia, "Stability Studies of Microparticulate System with Piroxicam as Model Drug," *AAPS Pharm. Sci. Tech.*, vol. 10 (3), pp. 872-880, 2009.
- [137] R. Parikh and R. Dubey, "Pharmaceutical Technology Europe: Studies of PLGA microspheres," 1 May 2004. [Online]. Available: <http://pharmtech.com>.
- [138] A. Rawat and D. Burgess, "Effect of physical ageing on the performance of dexamethasone loaded PLGA microspheres," *Int. J. Pharma.* 415, pp. 164-168, 2011.
- [139] Evonik, "RESOMER® Product Table," [Online]. Available: <http://www.sigmaaldrich.com/materials-science/polymer-science/resomer.html#a4>. [Accessed April 2014].
- [140] A. Rudra, K. Santra and B. Mukherjee, "Poly(D,L-lactide-co-glycolide) microspheres as a delivery system of protein ovalbumin used as a model protein drug," *Trends in applied sciences research*, vol. 6 (1), pp. 47-56, 2011.
- [141] P. Shao and L. Bailey, "Porcine Insulin Biodegradable Polyester Microspheres: Stability and in vitro release characteristics," *Pharm. Dev. Techn.*, vol. 5 (1), pp. 1-9, 2000.
- [142] L. Lewis, R. Boni and C. Adeyeye, "The physical and chemical stability of suspension of sustained-release diclofenac microspheres," *J. Microencapsulation*, vol. 15 (5), pp. 555-567, 1998.
- [143] Jiming Xuan, Yaling Lin, Jingbin Huang, Fei Yuan, Xiaoqing Li, Ying Lu, He Zhang, Junjie Liu, Zhiguo Sun, Hao Zou, Yan Chen, Jing Gao and Yanqiang Zhong, "Exenatide-loaded PLGA microspheres with improved glycemic control: In vitro biactivity and in vivo pharmacokinetic profiles after subcutaneous administration to SD rats," *Peptides*,

- vol. 46, pp. 172-179, 2013.
- [144] M. Blanco-Prieto, M. Campanero, K. Besseghir, F. Heimgatner and B. Gander, "Importance of single or blended polymer types for controlled in vitro release and plasma levels of somatostatin analogue entrapped in PLA/PLGA microspheres," *J. Controlled Release*, vol. 96, pp. 437-448, 2004.
- [145] B. Clark, P. Dickinson and I. Pyrah, "Case study: in vitro/in vivo release from injectable microspheres," in *Injectable dispersed systems: formulations, processing and performance*, vol. 149, D. Burgess, Ed., Taylor & Francis, 2005, pp. 543-570.
- [146] Y. Zheng, D. M. Danilenko, P. Valdez, I. Kasman, J. Eastham-Anderson, J. Wu et W. Ouyang, «Interleukin-22, a TH17 cytokine, mediates IL-23-induced dermal inflammation and acanthosis,» *Nature*, vol. 445, pp. 648-651, 2007.

## APPENDIX

**Table 37: Summary of the tested IgG formulations (solutions)**

Formulation of the tested IgG solution	IgG concentration (mg/mL)	Buffering agent	Stabilizers - Type and concentration				
sol IgG 1	12	25 mM histidine pH 6.0	mannitol - 10 mg/mL	arginine - 2 mg/mL	Tween 20 - 2.5 mg/mL	PEG 4000 - 5 mg/mL	NaCl - 250 mM
sol IgG 2	47.5	25 mM histidine pH 6.0	mannitol - 55 mg/mL	serine - 26 mg/mL	Tween 20 - 1.375 mg/mL	PEG 4000 - 2.6 mg/mL	NaCl - 150 mM
sol IgG 3	83	25 mM histidine pH 6.0	mannitol - 10 mg/mL	serine - 2 mg/mL	Tween 20 - 0.25 mg/mL	PEG 4000 - 5 mg/mL	NaCl - 50 mM
sol IgG 4	83	25 mM histidine pH 6.0	mannitol - 100 mg/mL	proline - 2 mg/mL	Pluronic F68 - 2.5 mg/mL	PEG 4000 - 0.2 mg/mL	NaCl - 50 mM
sol IgG 5	12	50 mM phosphate pH 7.2	mannitol - 100 mg/mL	serine - 2 mg/mL	Tween 20 - 2.5 mg/mL	0.2 mg/mL PEG4000	NaCl - 50 mM
sol IgG 6	12	50 mM phosphate pH 7.2	mannitol - 100 mg/mL	arginine - 50 mg/mL	Pluronic F68 - 0.25 mg/mL	PEG 4000 - 5 mg/mL	NaCl - 50 mM
sol IgG 7	83	50 mM phosphate pH 7.2	mannitol - 10 mg/mL	serine - 50 mg/mL	Pluronic F68 - 2.5 mg/mL	PEG 4000 - 0.2 mg/mL	NaCl - 250 mM
sol IgG 8	83	50 mM phosphate pH 7.2	mannitol - 10 mg/mL	proline - 50 mg/mL	Tween 20 - 2.5 mg/mL	PEG 4000 - 5 mg/mL	NaCl - 50 mM
sol IgG 9	12	25 mM histidine pH 6.0	mannitol - 10 mg/mL	arginine - 50 mg/mL	Pluronic F68 - 0.25 mg/mL	PEG 4000 - 0.2 mg/mL	NaCl - 50 mM
sol IgG 10	83	50 mM phosphate pH 7.2	mannitol - 100 mg/mL	arginine - 2 mg/mL	Tween 20 - 0.25 mg/mL	PEG 4000 - 0.2 mg/mL	NaCl - 250 mM
sol IgG 11	47.5	25 mM histidine pH 6.0	mannitol - 55 mg/mL	serine - 26 mg/mL	Pluronic F68 - 1.375 mg/mL	PEG4000 - 2.6 mg/mL	NaCl - 150 mM
sol IgG 12	12	50 mM phosphate pH 7.2	mannitol - 10 mg/mL	proline - 2 mg/mL	Pluronic F68 - 0.25 mg/mL	PEG 4000 - 5 mg/mL	NaCl - 250 mM
sol IgG 13	83	25 mM histidine pH 6.0	mannitol - 100 mg/mL	serine - 50 mg/mL	Pluronic F68 - 2.5 mg/mL	PEG 4000 - 5 mg/mL	NaCl - 250 mM
sol IgG 14	12	25 mM histidine pH 6.0	mannitol - 100 mg/mL	proline - 50 mg/mL	Tween 20 - 0.25 mg/mL	PEG 4000 - 0.2 mg/mL	NaCl - 250 mM
sol IgG 15	80	50 mM phosphate pH 7.2	mannitol - 55 mg/mL	proline - 25 mg/mL	-	PEG 4000 - 0.25 mg/mL	NaCl - 50 mM
sol IgG 16	80	50 mM phosphate pH 7.2	-	proline - 25 mg/mL	Tween 20 - 2.5 mg/mL	PEG 4000 - 0.25 mg/mL	NaCl - 50 mM

XIV. Appendix

sol IgG 17	80	50 mM phosphate pH 7.2	-	proline - 25 mg/mL	Tween 20 - 2.5 mg/mL	PEG 4000 - 0.25 mg/mL	NaCl - 50 mM
sol IgG 18	80 mg/mL IgG	50 mM phosphate pH 7.2	mannitol - 55 mg/mL	proline - 25 mg/mL	-	PEG 4000 - 0.25 mg/mL	NaCl - 50 mM
sol IgG 19	80 mg/mL IgG	25 mM histidine pH 6.0	-	proline - 25 mg/mL	Tween 20 - 2.5 mg/mL	-	-

**Table 38: Summary of the tested SD IgG formulations**

Formulation of the tested SD IgG	total solid concentration (mg/mL)	Buffering agent	Type of stabilizer	IgG : stabilizer ratio
SD IgG 1	15	20 mM Histidine pH 6.0	Mannitol	70:30
SD IgG 2	27.5	20 mM Histidine pH 6.0	Mannitol	70:30
SD IgG 3	40	20 mM Histidine pH 6.0	Mannitol	70:30
SD IgG 4	25	20 mM Histidine pH 6.0	Mannitol	70:30

**Table 39: Summary of the IgG tested MS formulations and process parameters (screening design); (a) concentration of PLGA solution (RG504), (b) concentration of stabilizer (PVA / PVP), (c) volume of external phase, (d) emulsification time, (e) emulsification rate, (f) volume of extraction phase, (g) type of stabilizer and (h) quantity of SD IgG (SD IgG 3 – Table 42)**

Formulation of the tested IgG MS	a (%w/v)	b (%w/v)	c (mL)	d (min)	e (rpm)	f (mL)	g	h (mg)
MS IgG-1	5.5	1.05	65	3	7025	250	PVA	30
MS IgG-2	1	2	30	5	3400	400	PVA	30
MS IgG-3	5.5	1.05	65	3	7025	250	PVA	30
MS IgG-4	10	0.1	30	5	13500	100	PVA	30
MS IgG-5	10	2	100	5	13500	400	PVP	30
MS IgG-6	10	2	30	1	3400	100	PVP	30
MS IgG-7	5.5	1.05	65	3	7025	250	PVA	30
MS IgG-8	10	0.1	100	1	3400	400	PVA	30
MS IgG-9	1	2	100	1	13500	100	PVA	30
MS IgG-10	1	0.1	30	1	13500	400	PVP	30
MS IgG-11	1	0.1	100	5	3400	100	PVP	30
MS IgG-12	1	1	100	5	3400	400	PVA	60
MS IgG-13	10	1	100	1	13500	400	PVA	30
MS IgG-14	1	1	100	5	13500	400	PVA	30
MS IgG-15	10	1	100	5	3400	400	PVA	60
MS IgG-16	10	1	100	1	3400	400	PVA	60
MS IgG-17	15	1	100	3	7500	400	PVA	100
MS IgG-18	15	1	100	5	7500	400	PVA	50
MS IgG-19	10	1	100	1	13500	400	PVA	100
MS IgG-20	15	1	100	1	10500	400	PVA	75
MS IgG-21	10	1	100	3	13500	400	PVA	75
MS IgG-22	15	1	100	5	13500	400	PVA	100
MS IgG-23	10	1	100	5	10500	400	PVA	75

XIV. Appendix

<b>Formulation of the tested IgG MS</b>	<b>a (%w/v)</b>	<b>b (%w/v)</b>	<b>c (mL)</b>	<b>d (min)</b>	<b>e (rpm)</b>	<b>f (mL)</b>	<b>g</b>	<b>h (mg)</b>
MS IgG-24	15	1	100	3	13500	400	PVA	75
MS IgG-25	10	1	100	1	13500	400	PVA	100
MS IgG-26	10	1	100	1	13500	400	PVA	100
MS IgG-27	10	1	100	1	10500	400	PVA	75
MS IgG-28	10	1	100	5	13500	400	PVA	75
MS IgG-29	10	1	100	1	10500	400	PVA	100
MS IgG-30	15	1	100	1	13500	400	PVA	100
MS IgG-31	15	1	100	5	10500	400	PVA	100
MS IgG-32	15	1	100	1	13500	400	PVA	75
MS IgG-33	15	1	100	5	10500	400	PVA	75
MS IgG-34	10	1	100	5	13500	400	PVA	100

**Table 40: Summary of the s/o/w DoE results: d(0.5), d(0.9), drug loading content, quantity of released drug, EE%, loss of monomer measured both during the EE% evaluation and dissolution (SEC) – tested MS IgG-1 to -34 (Table 39)**

Formulation (Table 39)	d(0.5) ( $\mu\text{m}$ ) <sup>a</sup>	d(0.9) ( $\mu\text{m}$ )	Drug loading (%)	Total quantity of released drug (%) <sup>b</sup>	EE (%)	Burst effect (%) <sup>c</sup>	Monomer loss EE% test (%) <sup>d</sup>	Monomer loss 1h disso test (%)
MS IgG-1	37.0	65.9	4.0	3.7	55.4	88.8	-5.4	0.2
MS IgG-2	28.9	56.6	1.4	3.9	5.4	94.0	5.5	24.3
MS IgG-3	34.9	74.2	2.1	1.9	28.8	79.1	-5.7	-1.2
MS IgG-4	23.4	42.2	0.6	0.3	15.9	86.9	-2.0	26.2
MS IgG-5	15.7	51.4	2.4	1.9	64.7	68.9	-12.4	-9.1
MS IgG-6	255.1	794.3	2.0	1.8	52.6	44.1	-7.6	-4.5
MS IgG-7	38.5	65.6	2.4	2.1	35.0	85.6	-8.4	-1.0
MS IgG-8	193.0	387.2	3.8	2.7	98.8	30.2	-8.3	-9.1
MS IgG-9	15.6	28.2	2.9	6.4	11.4	96.6	3.4	9.9
MS IgG-10	8.9	45.6	0.8	2.3	11.8	96.5	33.9	29.8
MS IgG-11	95.6	215.9	1.5	4.6	3.4	90.9	-8.1	10.1
MS IgG-12	64.3	365.6	1.8	5.2	5.0	88.7	4.3	28.5
MS IgG-13	37.2	92.9	3.0	2.2	77.7	41.4	-2.7	-5.7
MS IgG-14	13.6	144.7	1.8	5.6	7.1	89.4	0.3	17.4
MS IgG-15	246.8	625.0	6.0	6.7	81.8	50.8	-3.7	-4.8
MS IgG-16	159.1	356.9	4.3	4.5	60.8	65.5	-1.3	-5.2
MS IgG-17	96.8	235.2	5.0	5.1	62.4	30.3	-2.5	-7.0
MS IgG-18	93.1	221.2	3.0	2.6	60.5	28.2	-3.8	-6.4
MS IgG-19	43.5	118.2	4.6	4.7	50.1	58.8	0.4	-3.3
MS IgG-20	65.7	144.6	2.9	3.2	41.9	28.3	-1.7	-11.1
MS IgG-21	38.7	120.3	3.2	3.6	37.5	40.1	-0.3	-3.5
MS IgG-22	58.7	164.0	2.9	3.0	37.8	37.9	-1.2	-4.8
MS IgG-23	53.2	128.6	3.1	3.3	36.0	42.1	-1.7	-5.8
MS IgG-24	60.3	184.9	2.7	2.9	45.1	28.2	-2.4	-6.2

XIV. Appendix

<b>Formulation (Table 39)</b>	<b>d(0.5) (µm)<sup>a</sup></b>	<b>d(0.9) (µm)</b>	<b>Drug loading (%)</b>	<b>Total quantity of released drug (%)<sup>b</sup></b>	<b>EE (%)</b>	<b>Burst effect (%)<sup>c</sup></b>	<b>Monomer loss EE% test (%)<sup>d</sup></b>	<b>Monomer loss 1h disso test (%)</b>
MS IgG-25	34.1	86.5	5.5	6.4	50.8	50.7	-2.5	-3.5
MS IgG-26	33.9	90.4	5.1	5.8	46.4	50.9	-1.4	-3.6
MS IgG-27	55.1	110.9	5.4		63.8	39.5	-7.8	-12.0
MS IgG-28	55.8	110.3	5.1		59.9	38.4	-7.9	-11.2
MS IgG-29	54.6	113.8	6.6		59.9	49.2	-7.6	-10.2
MS IgG-30	58.8	141.2	6.1		78.1	32.5	-8.2	-12.3
MS IgG-31	66.7	145.0	5.3		69.7	32.6	-7.8	-18.2
MS IgG-32	54.0	132.8	5.0		84.8	27.7	-8.6	-12.5
MS IgG-33	76.2	180.9	3.4		56.8	16.6	-9.8	-4.0
MS IgG-34	42.1	94.1	5.2		47.4	48.8	-6.9	-10.6

<sup>a</sup> Except for the mean particle size, the data were average of two replicates,

<sup>b</sup> The maximum release drug load was the cumulated released loading calculated at the end of the dissolution test

<sup>c</sup> The corrected burst effect was calculated taken into account the maximum released drug load

<sup>d</sup> The negative monomer loss value meant that the percent of monomer was higher after encapsulation process

**Table 41: Summary of the CDP571 tested spray-dried**

<b>Formulation of the tested SD CDP571</b>	<b>Total solid concentration (mg/mL)</b>	<b>Buffering agent</b>	<b>Type of stabilizer(s)</b>	<b>Mab : mannitol : stabilizer ratio</b>
SD CDP571-1	50 mg/mL	20 mM histidine pH 6.0	Mannitol	70:30:0
SD CDP571-2	50 mg/mL	20 mM histidine pH 6.0	Mannitol + trehalose	70:15:15
SD CDP571-3	50 mg/mL	20 mM histidine pH 6.0	Trehalose	70:0:30
SD CDP571-4	50 mg/mL	20 mM histidine pH 6.0	Mannitol + sucrose	70:15:15
SD CDP571-5	50 mg/mL	20 mM histidine pH 6.0	Sucrose	70:0:30
SD CDP571-6	50 mg/mL	20 mM glutamate pH 5.0	Mannitol	70:30
SD CDP571-7	50 mg/mL	20 mM glutamate pH 5.0	Mannitol + trehalose	70:15:15
SD CDP571-8	50 mg/mL	20 mM glutamate pH 5.0	Trehalose	70:0:30
SD CDP571-9	50 mg/mL	20 mM glutamate pH 5.0	Mannitol + sucrose	70:15:15
SD CDP571-10	50 mg/mL	20 mM glutamate pH 5.0	Sucrose	70:0:30
SD CDP571-11	50 mg/mL	20 mM histidine pH 6.0	-	100:0:0

**Table 42: Summary of the CDP571 tested MS formulations**

Formulation of the tested CDP571 MS	SD CDP571 formulation (Table 41)	theo loading (% w/w)	SD CDP571 quantity (mg)	Type of co-polymer (10 % w/v sol)	Type of basic additive and concentration (% w/w vs PLGA)
MS CDP571-1	SD CDP571-1	15	150	RG504	-
MS CDP571-2	SD CDP571-2	15	150	RG504	-
MS CDP571-3	SD CDP571-3	15	150	RG504	-
MS CDP571-4	SD CDP571-4	15	150	RG504	-
MS CDP571-5	SD CDP571-5	15	150	RG504	-
MS CDP571-6	SD CDP571-6	15	150	RG504	-
MS CDP571-7	SD CDP571-7	15	150	RG504	-
MS CDP571-8	SD CDP571-8	15	150	RG504	-
MS CDP571-9	SD CDP571-9	15	150	RG504	-
MS CDP571-10	SD CDP571-10	15	150	RG504	-
MS CDP571-11	SD CDP571-11	15	150	RG502	-
MS CDP571-12	SD CDP571-3	15	150	RG505	-
MS CDP571-13	SD CDP571-3	15	150	RG755S	-
MS CDP571-14	SD CDP571-3	15	150	RGPd5055	-
MS CDP571-15	SD CDP571-3	15	150	RGPd50105	-
MS CDP571-16	SD CDP571-3	15	150	RGPd50155	-
MS CDP571-17	SD CDP571-3	15	150	RG505	Mg(OH) <sub>2</sub> - 1.5 % w/w
MS CDP571-18	SD CDP571-3	15	150	RG505	Mg(OH) <sub>2</sub> - 3 % w/w
MS CDP571-19	SD CDP571-3	15	150	RG505	CaCO <sub>3</sub> - 1.5 % w/w
MS CDP571-20	SD CDP571-3	15	150	RG505	CaCO <sub>3</sub> - 3 % w/w

**Table 43: Summary of the CDP571 tested freeze-dried MS formulations**

<b>Formulation of the tested freeze-dried MS</b>	<b>Type of MS in 15% w/v suspension (Table 42 )</b>	<b>Type of cryoprotectant and concentration in the reconstituted solution (% w/v)</b>
Lyo MS CDP571-1	MS CDP571-13	Mannitol - 0.5 % w/v
Lyo MS CDP571-2	MS CDP571-13	Sucrose - 0.5 % w/v
Lyo MS CDP571-3	MS CDP571-13	Trehalose - 0.5 % w/v
Lyo MS CDP571-4	MS CDP571-13	Mannitol - 5 % w/v
Lyo MS CDP571-5	MS CDP571-13	Sucrose - 5 % w/v
Lyo MS CDP571-6	MS CDP571-13	Trehalose - 5 % w/v
Lyo MS CDP571-7	MS CDP571-13	-
Lyo MS CDP571-8	MS CDP571-13	Sucrose - 2 % w/v
Lyo MS CDP571-9	MS CDP571-13	Trehalose - 2 % w/v
Lyo MS CDP571-10	MS CDP571-12	Trehalose - 0.5 % w/v

**Table 44: CDP571 plasmatic concentration ( $\mu\text{g/mL}$ ) – IV pK study (time points 0.25, 1, 6, 24 and 48 h)**

Time point (h)		0.25			1			6			24			48		
Group	rat ID	Conc.	StdDev	n												
group 1	rat 1	390	21	3	444	109	3	266	13	4	161	16	6	86	5	4
	rat 2	321	22	4	270	29	4	207	14	4	102	8	4	75	30	6
	rat 3	483	76	3	410	29	3	145	6	2	138	10	6	110	7	4
group 2	rat 4	3137	163	3	3134	412	4	2014	76	4	1266	63	6	699	26	4
	rat 5	2723	123	4	2468	215	4	1645	159	3	1206	88	4	919	394	5
	rat 6	2768	59	4	2402	163	4	1997	874	4	1225	242	6	933	62	4
group 3	rat 7	409	37	6	469	137	6	524	265	6	106	30	4	89	23	6
	rat 8	307	21	6	496	227	6	444	245	6	34	12	4	156	110	6
	rat 9	464	64	6	621	259	6	245	38	5	153	15	4	248	157	8
group 4	rat 10	3341	378	4	2848	161	4	2442	138	4	2171	625	6	2131	602	6
	rat 11	2773	81	4	2459	191	4	2347	98	4	2285	695	6	2366	532	6
	rat 12	2917	115	4	2799	223	4	2081	197	3	2027	498	6	1838	599	7

n=number of data

**Table 45: CDP571 plasmatic concentration ( $\mu\text{g/mL}$ ) – IV pK study (time points 72, 96, 120, 144 and 240 h)**

Time point (h)		72			96			120			144			240		
Group	rat ID	Conc.	StdDev	n	Conc.	StdDev	n	Conc.	StdDev	n	Conc.	StdDev	n	Conc.	StdDev	n
group 1	rat 1	78	5	6	98	34	6	82	6	4	88	51	8	43	18	10
	rat 2	55	4	6	61	9	5	47	3	5	44	5	5	23	10	7
	rat 3	66	3	6	77	4	6	93	11	4	63	38	8	82	65	9
group 2	rat 4	662	32	6	747	53	4	615	43	6	511	34	4	237	109	6
	rat 5	675	46	6	594	52	4	591	36	5	625	69	6	276	124	7
	rat 6	847	87	4	683	49	4	641	25	5	576	97	6	445	146	8
group 3	rat 7	251	174	8	112	103	6	238	200	9	216	229	8	20	14	5
	rat 8	205	179	8	38	9	4	143	180	10	225	236	8	84	NA	1
	rat 9	111	58	7	63	32	4	226	311	8	80	5	5	30	14	6
group 4	rat 10	2084	504	6	1539	632	8	2426	993	6	1455	580	8	457	53	5
	rat 11	1861	680	7	1553	880	8	1227	449	8	1475	573	8	851	179	5
	rat 12	1388	756	8	1371	661	8	1454	525	8	1448	1061	8	436	86	4

NA=not applicable

**Table 46: CDP571 plasmatic concentration (ng/mL) – SC pK study (time points 6, 24, 48, 168 and 336 h)**

Time point (h)		6			24			48			168			336		
Group	rat ID	Conc.	StdDev	n	Conc.	StdDev	n	Conc.	StdDev	n	Conc.	StdDev	n	Conc.	StdDev	n
group 1	rat 1	21678	5165	8	78558	25182	8	124435	29037	5	114740	13542	4	26155	11214	8
	rat 2	10905	3755	8	34254	13448	8	93903	41437	6	34479	33329	4	7457	2244	8
	rat 3	15172	3372	7	54345	12251	8	124164	54733	6	66546	21028	4	9561	4798	9
	rat 4	11498	5401	8	56972	15532	8	105669	54872	5	51959	24743	4	4900	5228	8
group 2	rat 5	1488	553	4	7431	1384	7	13623	3778	4	14555	4945	8	823	223	4
	rat 6	1135	292	4	14408	19193	7	12842	1454	4	31289	19960	10	17551	24079	8
	rat 7	3139	501	6	22998	17699	8	25468	12861	4	41150	13066	10	24460	11683	10
group 3	rat 9	5661	8882	6	6914	1014	4	14776	2909	4	21648	6578	9	6083	1535	7
	rat 10	3288	2745	7	12267	1749	4	10825	3278	4	37871	13231	10	11703	3926	8
	rat 11	2601	2074	7	7876	1315	4	18841	5512	4	33171	13132	10	6502	2749	8
	rat 12	3020	2448	6	7445	855	4	15899	2871	4	28439	13548	10	7881	2719	8

**Table 47: CDP571 plasmatic concentration (ng/mL) – SC pK study (time points 504, 672, 840 and 1008 h)**

Time point (h)		504			672			840			1008		
Group	rat ID	Conc.	StdDev	n	Conc.	StdDev	n	Conc.	StdDev	n	Conc.	StdDev	n
group 1	rat 1	344	199	9	16	3	2	<LOQ	NA	NA	<LOQ	NA	NA
	rat 2	<LOQ <sup>a</sup>	NA <sup>b</sup>		<LOQ	NA	NA	<LOQ	NA	NA	<LOQ	NA	NA
	rat 3	904	215	10	105	36	8	<LOQ	NA	NA	7	3	3
	rat 4	850	155	10	119	31	8	<LOQ	NA	NA	13	13	3
group 2	rat 5	137	NA	1	<LOQ	NA	NA	<LOQ	NA	NA	4	0	2
	rat 6	80	21	6		NA	NA	<LOQ	NA	NA	7	6	2
	rat 7	18920	6268	6	6300	3228	20	4157	1732	16	3379	621	12
group 3	rat 9	3272	855	11	1398	572	8	828	369	8	451	142	7
	rat 10	178	31	8	52	28	8	5	4	7	7	5	3
	rat 11	449	54	8	<LOQ	NA	NA	<LOQ	NA	NA	74	83	2
	rat 12	1421	1532	11	154	87	8	42	24	8	62	53	8

LOQ=limit of quantification

NA=not applicable

**Table 48: Particle size evaluation of PLGA MS produced for the SC pK study**

Batch	D[4.3] (µm)	d(0.1) (µm)	d(0.5) (µm)	d(0.9) (µm)
Freeze-dried CDP571:RG505	174.9	13.9	53.0	144.6
Freeze-dried CDP571:RG755S	37.7	9.4	32.4	74.8
Freeze-dried Placebo RG505	79.9	13.9	48.9	134.4
Freeze-dried Placebo RG755S	34.7	5.1	28.8	70.2

**Table 49: Drug loading and EE% data of the CDP571 freeze-dried MS produced for the SC pK study**

Formulation	Theo loading (%)	Drug loading (%)	EE% (%)
Freeze-dried CDP571:RG505	17.4	10.01 ± 0.03	57.6 ± 0.2
Freeze-dried CDP571:RG755S	17.4	12.5 ± 0.2	72.1 ± 1.1

**Table 50: pK parameters – IV pK study**

<b>Dose</b>	<b>Route</b>	<b>CDP571 Form</b>	<b>Regimen</b>	<b>Rat</b>	<b>HL_Lambda_z</b>	<b>Tmax</b>	<b>Cmax</b>	<b>Clast</b>	<b>AUClast</b>	<b>Cl_F_obs</b>
<b>(mg/kg)</b>					<b>(h)</b>	<b>(h)</b>	<b>(µg/mL)</b>	<b>(µg/mL)</b>	<b>(h*µg/mL)</b>	<b>(mL/h/kg)</b>
10.00	IV	solution	Single	IV1	121.45	1.00	444.32	42.98	23511.15	0.32
				IV2	113.79	0.25	321.22	23.09	14889.75	0.54
				IV3	143.59	0.25	482.83	81.50	21980.99	0.26
20.00	IV	solution	Repeat	IV7	31.68	6.00	523.70	19.84	40262.27	0.49
				IV8	112.79	1.00	496.06	83.60	37932.66	0.39
				IV9	46.66	1.00	621.03	30.26	29868.54	0.63
100.00	IV	solution	Single	IV4	86.95	0.25	3136.98	236.86	167727.23	0.51
				IV5	113.68	0.25	2723.01	276.17	170169.78	0.46
				IV6	232.09	0.25	2768.43	444.72	187376.21	0.30
200.00	IV	solution	Repeat	IV10	51.81	0.25	3340.50	457.17	389105.92	0.47
				IV11	152.30	0.25	2773.04	851.33	380945.16	0.35
				IV12	64.59	0.25	2916.77	436.43	329047.05	0.54

HL Lambda corresponding to T<sub>1/2</sub>

**Table 51: pK parameters – SC pK study**

Dose	Route	CDP571 Form	Regimen	Rat	HL_Lambda_z <sup>a</sup>	Tmax	Cmax	Clast	AUClast	Cl_F_obs	F
(mg/kg)					(h)	(h)	(µg/mL)	(µg/mL)	(h*µg/mL)	(mL/h/kg)	(%)
50.00	SC	solution	Single	SC1	32.46	48.00	124.44	0.02	31844.16	1.57	20.89
				SC2	78.64	48.00	93.90	7.46	13202.73	3.56	
				SC3	64.65	48.00	124.16	0.01	21630.27	2.31	
				SC4	75.19	48.00	105.67	0.01	17422.77	2.87	
50.00	SC	RG505 MS	Single	SC5	50.15	168.00	14.56	0.14	3400.71	14.66	11.32
				SC6	72.94	168.00	31.29	0.01	8724.33	5.73	
				SC7	374.03	168.00	41.15	3.38	17609.16	2.57	
50.00	SC	RG755S MS	Single	SC9	205.20	168.00	21.65	0.45	6378.03	7.68	8.43
				SC10	113.27	168.00	37.87	0.01	8536.23	5.86	
				SC11	114.79	168.00	33.17	0.07	7590.48	6.58	
				SC12	87.39	168.00	28.44	0.06	7032.21	7.10	

HL Lambda corresponding to T<sub>1/2</sub>

F= bioavailability



Contents lists available at ScienceDirect

European Journal of Pharmaceutics and Biopharmaceutics

journal homepage: [www.elsevier.com/locate/ejpb](http://www.elsevier.com/locate/ejpb)

Research paper

## Encapsulation of immunoglobulin G by solid-in-oil-in-water: Effect of process parameters on microsphere properties <sup>☆</sup>



Sarah Marquette <sup>a,b,\*</sup>, Claude Peerboom <sup>b</sup>, Andrew Yates <sup>b</sup>, Laurence Denis <sup>b</sup>, Jonathan Goole <sup>a</sup>, Karim Amighi <sup>a</sup>

<sup>a</sup> Laboratory of Pharmaceutics and Biopharmaceutics, Université Libre de Bruxelles (ULB), Brussels, Belgium

<sup>b</sup> Laboratory UCB Pharma S.A., Braine-l'Alleud, Belgium

### ARTICLE INFO

#### Article history:

Received 27 June 2013

Accepted in revised form 22 October 2013

Available online 31 October 2013

#### Keywords:

Microspheres

Solid-in-oil-in-water

Antibody

PLGA

Ethyl acetate

Design of experiment

### ABSTRACT

Antibodies (Abs) are prone to a variety of physical and chemical degradation pathways, which require the development of stable formulations and specific delivery strategies. In this study, injectable biodegradable and biocompatible polymeric particles were employed for controlled-release dosage forms and the encapsulation of antibodies into polylactide-co-glycolide (PLGA) based microspheres was explored. In order to avoid stability issues which are commonly described when water-in-oil (w/o) emulsion is used, a solid-in-oil-in-water (s/o/w) method was developed and optimized. The solid phase was made of IgG microparticles and the s/o/w process was evaluated as an encapsulation method using a model Ab molecule (polyclonal bovine immunoglobulin G (IgG)). The methylene chloride (MC) commonly used for an encapsulation process was replaced by ethyl acetate (EtAc), which was considered as a more suitable organic solvent in terms of both environmental and human safety. The effects of several processes and formulation factors were evaluated on IgG:PLGA microsphere properties such as: particle size distribution, drug loading, IgG stability, and encapsulation efficiency (EE%). Several formulations and processing parameters were also statistically identified as critical to get reproducible process (e.g. the PLGA concentration, the volume of the external phase, the emulsification rate, and the quantity of IgG microparticles). The optimized encapsulation method has shown a drug loading of up to 6% (w/w) and an encapsulation efficiency of up to 60% (w/w) while preserving the integrity of the encapsulated antibody. The produced microspheres were characterized by a  $d(0.5)$  lower than 110  $\mu\text{m}$  and showed burst effect lower than 50% (w/w).

© 2013 Published by Elsevier B.V.

### 1. Introduction

The number of therapeutic monoclonal antibodies (MAbs) which are currently in development has increased dramatically over the past few years. There are more than 34 therapeutic MAbs approved or under review in the European Union and United States [1]. Their pharmacological activity is highly specific and commonly

leads to minimal side effects. MAbs may be also conjugated to other therapeutic compounds or radioisotopes in order to increase the efficacy of a drug to a target site, thus reducing its potential systemic side effects, or for specific diagnostic purposes, respectively. Nowadays, less immunogenic human MAbs are available but they are still prone to a variety of physical and chemical degradation pathways, although MAbs, seem to be more stable than other proteins [2,3].

Antibodies are characterized by relatively high molecular weight (150,000 Da) but engineered antibody fragments are much smaller (50,000 Da) than intact full-length MAb and are characterized by different systemic distributions and plasmatic clearances [4].

Injectable biodegradable and biocompatible polymeric particles could be used both to protect MAbs from *in vivo* degradation and to control their release after administration. In the last two decades, synthetic biodegradable polymers have been increasingly used in drug delivery as they are more stable than natural polymers. Thermoplastic aliphatic poly(esters), such as poly-lactide (PLA), poly-glycolide (PGA), and especially PLGA, have generated tremendous

Abbreviations: (M)Ab(s), (monoclonal) antibody (antibodies); EE%, encapsulation efficiency; EtAc, ethyl acetate; IgG, immunoglobulin G; MC, methylene chloride; PGA, poly-glycolide; PLA, poly-lactide; PLGA, polylactide-co-glycolide; PVA, polyvinyl alcohol; PVP, polyvinylpyrrolidone; SEC, size exclusion chromatography; SEM, scanning electron microscopy; s/o/w, solid-in-oil-in-water; SD, spray-dried;  $T_{in}$ , inlet temperature;  $T_{out}$ , outlet temperature; w/o, water-in-oil.

<sup>☆</sup> This is an open-access article distributed under the terms of the Creative Commons Attribution-NonCommercial-No Derivative Works License, which permits non-commercial use, distribution, and reproduction in any medium, provided the original author and source are credited.

\* Corresponding author. UCB Pharma S.A., Chemin du Foriest, 1420 Braine-l'Alleud, Belgium. Tel.: +32 2 386 63 20.

E-mail address: [sarah.marquette@ucb.com](mailto:sarah.marquette@ucb.com) (S. Marquette).



## Stability study of full-length antibody (anti-TNF alpha) loaded PLGA microspheres



S. Marquette<sup>a,b,\*</sup>, C. Peerboom<sup>b</sup>, A. Yates<sup>b</sup>, L. Denis<sup>b</sup>, I. Langer<sup>c</sup>, K. Amighi<sup>a</sup>, J. Goole<sup>a</sup>

<sup>a</sup> Laboratory of Pharmaceutics and Biopharmaceutics, Université Libre de Bruxelles (ULB), Campus de la Plaine, CP 207, Boulevard du Triomphe, Brussels 1050, Belgium

<sup>b</sup> Laboratory UCB Pharma S.A., Chemin du Foriest, Braine-L'Alleud 1420, Belgium

<sup>c</sup> IRIBHM, Université Libre de Bruxelles (ULB), Campus Erasme, CP602, Route de Louvik 808, Bruxelles 1070, Belgium

### ARTICLE INFO

#### Article history:

Received 28 February 2014

Received in revised form 28 April 2014

Accepted 29 April 2014

Available online 2 May 2014

#### Keywords:

Microspheres

Encapsulation

Antibody

PLGA

Stability

### ABSTRACT

Antibodies (Abs) require the development of stable formulations and specific delivery strategies given their susceptibility to a variety of physical and chemical degradation pathways. In this study, the encapsulation of an antibody into polylactide-co-glycolide (PLGA) based microspheres was explored to obtain a controlled-release of the incorporated drug. In order to avoid stability issues, a solid-in-oil-in-water (s/o/w) method was preferred. The solid phase was made of anti-TNFalpha monoclonal antibody (MAb) spray-dried microparticles, and the PLGA microspheres were produced using two different polymers (i.e., Resomer<sup>®</sup> RG505 and Resomer<sup>®</sup> RG7555). The stability of the MAb incorporated into the microspheres was investigated under three conditions (5 ± 3 °C, 25 ± 2 °C/60% RH and 40 ± 2 °C/75% RH) for 12 weeks. During this stability study, it was demonstrated that the MAb loaded PLGA microspheres were stable when stored at 5 ± 3 °C and that the Resomer<sup>®</sup> RG7555, composed of 75% (w/w) lactic acid as PLGA, was preferred to preserve the stability of the system.

Storage at temperatures higher than 5 °C led to antibody stability issues such as aggregation, fragmentation and loss of activity. The release profiles were also altered. Physical ageing of the system associated with changes in the glass transition temperature and enthalpy of relaxation was noticed during the storage of the MAb loaded PLGA microspheres.

© 2014 Elsevier B.V. All rights reserved.

### 1. Introduction

The number of therapeutic MAbs currently in development has increased tremendously over the past few years. To our knowledge, 34 therapeutic MAbs have been approved or are under review in both the European Union and the United States of America (Anon, 2012). MAbs, like other biologic molecules, are susceptible to a variety of physical and chemical degradation pathways (Lobo et al., 2004; Wang et al., 2007). Degradation may occur at moderate

temperatures; however, the extent of these reactions is much more pronounced at high temperatures. Antibodies are generally stored at 2–8 °C. Storage at room temperature often leads to antibody degradation and/or inactivity. While liquid antibody formulations are less expensive, faster to develop and generally easier to prepare for administration than alternative formulation approaches, liquid antibody formulations are prone to oxidation, deamination, aggregation and fragmentation. Water mediated degradation pathways are a common problem when considering the stabilization of antibody-based drugs (Daugherty and Mersny, 2006). Introducing an antibody into a hydrophobic polymer system can reduce the impact of water on the antibody. Removal of water from antibody preparations provides a starting point for incorporating a dried material into a hydrophobic polymer matrix, such as PLGA, which can be made into microspheres generated through a solid-in-oil-in-water encapsulation process. Moreover, the controlled release they provide gives advantages for therapeutic antibodies: (a) reduced systemic Ab exposure and potential toxicity, (b) longer duration between dosing intervals, and (c) improved control over the release kinetic (Grainger, 2004). These alternative delivery approaches for antibodies reduce the number of parenteral

Abbreviations: (M)Ab(s), (monoclonal) antibody (antibodies); DMF, dimethyl formamide; EE%, encapsulation efficiency; EtAc, ethyl acetate; GPC, gel permeation chromatography; HMWS, high molecular weight species; LOD, limit of detection; LMWS, low molecular weight species; MC, methylene chloride; Mw, molecular weight; PBS, phosphate buffer saline; PGA, poly-glycolide; PLA, poly-lactide; PLGA, polylactide-co-glycolide; PVA, polyvinyl alcohol; SEC, size exclusion chromatography; SEM, scanning electron microscopy; s/o/w, solid-in-oil-in-water; SD, spray-dried; THF, tetrahydrofuran; T<sub>g</sub>, glass transition temperature; T(x)w, time after (x) week(s) storage; w/o, water-in-oil.

\* Corresponding author at: UCB Pharma S.A., Chemin du Foriest, Braine-L'Alleud 1420, Belgium. Tel.: +32 2 386 63 20.

E-mail address: [sarah.marquette@ucb.com](mailto:sarah.marquette@ucb.com) (S. Marquette).

<http://dx.doi.org/10.1016/j.ijpharm.2014.04.053>

0378-5173/© 2014 Elsevier B.V. All rights reserved.